Polycyclic propargylamine derivatives as multifunctional neuroprotective agents

Frank T. Zindo

B.Pharm.
(UWC)

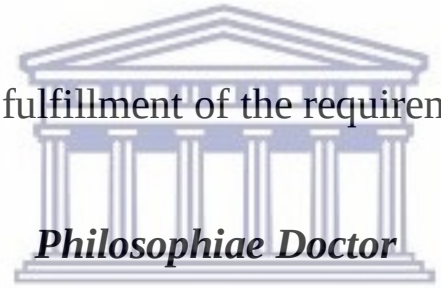

Thesis submitted in fulfillment of the requirements for the degree

Philosophiae Doctor

in Pharmaceutical Chemistry at the School of Pharmacy of the University of the Western Cape

Supervisor: Prof. J. Joubert
Co-supervisor: Prof. S.F Malan

UWC
2018

Dedicated to my late parents, Patrick Frank Zindo and Tsitsi Betty Gonorenda

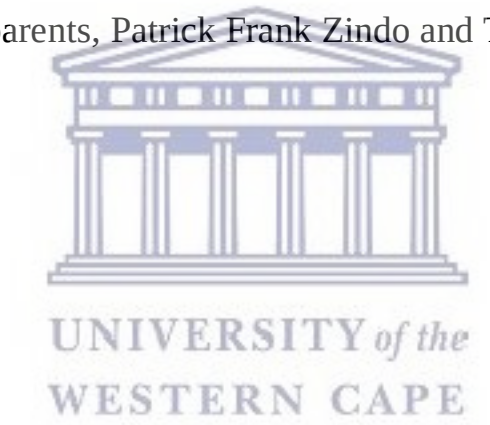

DECLARATION

I declare that *Polycyclic propargylamine derivatives as multifunctional neuroprotective agents* is my own work, that it has not been submitted for any degree or examination in any other university, and that all sources I have used or quoted have been indicated and acknowledged by complete references.

Frank Tapiwa Zindo

Signed……...

Date: 20/11/2018

AUTHOR'S CONTRIBUTIONS

First and second authored papers

1. **Propargylamine as functional moiety in the design of multifunctional drugs for neurodegenerative disorders: MAO inhibition and beyond**

   F.T.Z performed the literature review and drafted the manuscript. J.J. and S.F.M. contributed to the final version of the manuscript.

2. **Polycyclic propargylamine and acetylene derivatives as multifunctional neuroprotective agents**

   F.T.Z., J.J. and S.F.M. conceived of the presented idea. F.T.Z. designed and performed the calcium modulation assays and computer modelling studies, processed the experimental data, performed the analysis and drafted the manuscript. Q.R.B. synthesised and characterized the compounds. S.F.M. and J.J. supervised the findings of this work. All authors discussed the results and contributed to the final manuscript.

3. **Design, synthesis and evaluation of pentacycloundecane and hexacycloundecane propargylamine derivatives as multifunctional neuroprotective agents**

   F.T.Z. and J.J. conceived of the presented idea. F.T.Z. designed, synthesised and characterized the compounds and performed all biological and *in silico* evaluations, processed the experimental data, performed the analysis and drafted the manuscript. F.T.Z., S.I.O., A.B.E. and O.E.E. performed cytotoxicity and neuroprotection assays. S.F.M. and J.J. supervised the findings of this work. All authors discussed the results and contributed to the final manuscript.

4. **Adamantane amine derivatives as dual acting NMDA receptor and voltagegated calcium channel inhibitors for neuroprotection**

   Y.E.K., F.T.Z. and J.J. conceived of the presented idea. Y.E.K. and F.T.Z. designed, synthesised and characterized the compounds. F.T.Z. and Y.E.K. performed the calcium modulation assays, processed the experimental data and performed the analysis. S.F.M. and J.J. supervised the findings of this work. All authors discussed the results and contributed to the final manuscript.

Additional papers

1. **Design, synthesis and evaluation of indole derivatives as multifunctional agents against Alzheimer's disease**

   I.D. and J.J. conceived of the presented idea. I.D. took the lead in writing the manuscript. I.D. performed the ChE and MAO inhibition assays. I.D. and J.J. performed the *in-silico* studies. F.T.Z., S.I.O., A.B.E. and O.E.E. planned and carried out the cytotoxicity and neuroprotection assays. S.F.M. and J.J. supervised the findings of this work. All authors discussed the results and contributed to the final manuscript.

2. **Versatility of 7-substituted coumarin molecules as antimycobacterial agents, neuronal enzyme inhibitors and neuroprotective agents**

   E.K., S.L.S., E.M.S., H.V., D.F.W., S.I.O., A.B.E., S.F.M., F.T.Z., O.E.E. and J.J. conceived and designed the experiments; G.B.F. and J.J. synthesized the compounds; H.V., J.J., F.T.Z., D.F.W., G.B.F., S.I.O. and A.B.E. performed the experiments and analysis; E.K. and J.J. wrote the paper.

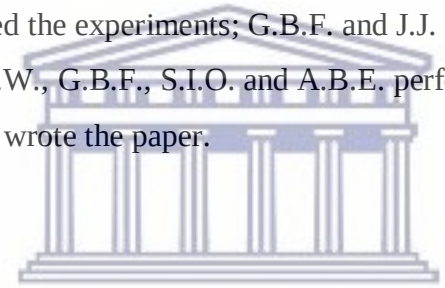

Abstract

The abnormal death of neurons in the central nervous system of individuals suffering from neurodegenerative diseases such as Parkinson's disease, Alzheimer's disease, Huntington's disease and amyotrophic lateral sclerosis, takes place by an intrinsic cell suicide programme known as apoptosis. This process is triggered by several stimuli, and consists of numerous pathways and cascades which lead to the death of neuronal cells. It is this multifactorial nature of neurodegenerative diseases that has over the years seen many researchers develop compounds that may serve as multi-target directed ligands (MTDLs) which could potentially confer neuroprotection by acting simultaneously on different receptors and target sites implicated in neurodegeneration.

This study was aimed at developing MTDLs that may serve as neuroprotective agents by simultaneously (a) inhibiting *N*-methyl D-aspartate receptors (NMDAR) and blocking *L*-type voltage gated calcium channels (VGCC) thus regulating the Ca^{2+} influx mediated excitotoxic process; (b) inhibiting the monoamine oxidase enzymes A and -B (MAO-A/B) thus allowing increase in dopamine levels in the central nervous system and reducing the levels of the highly oxidative products produced by the activity of these enzymes; (c) possessing anti-apoptotic activity to halt the neuronal cell death process.

In designing the compounds we focused on the structures of rasagiline and selegiline, two well-known MAO-B inhibitors and proposed neuroprotective agents, and of NGP1-01, a known VGCC blocker and NMDAR antagonist. The first series of compounds (reported in research article 1, Chapter 3), comprised polycyclic propargylamine and acetylene derivatives. Compounds **12**, **15** and **16** from this series showed promising VGCC and NMDA receptor channel inhibitory activity ranging from 18 % to 59 % in micromolar concentrations, and compared favourably to the reference compounds. In the MAO-B assay, compound **10** exhibited weak MAO-B inhibition of 73.32 % at 300 μM. The rest of the series showed little to no activity on these target sites, despite showing significant anti-apoptotic activity. This suggested the compounds in this series to be exhibiting their neuroprotective action through some other mechanism(s) unexplored in this study.

Follow up work on these compounds yielded a second series of compounds which comprised pentacycloundecane and hexacycloundecane propargylamine derivatives (presented in research article 2, Chapter 4). These compounds showed the ability to significantly improve

the viability of SH-SY5Y neuroblastoma cells, by 31% and 61% at a 1 µM concentration. These compounds also showed dual calcium modulation activity by blocking VGCC's (26.6% to 51.3%, at 10 µM) and by blocking NMDAR (31.4% and 88.3%, at 10 µM). When assayed for MAO inhibition, most of the active compounds displayed selectivity to the MAO-B isoenzyme with IC_{50} values ranging from 1.70 µM to 36.31 µM and appeared to be reversible MAO inhibitors as defined by the time-dependency studies conducted. The inclusion of the propargylamine moiety in the structures of these compounds afforded them multi-mechanistic neuroprotective ability which most importantly included MAO-B inhibition.

The third series of compounds (presented in research article 3, Chapter 5) comprised adamantane-derived compounds, structurally similar to NGP1-01. From this series, compounds **1**, **2**, **5** and **10** displayed good inhibitory activity against both NMDAR channel (66.7 - 89.5 % at 100 µM) and VGCC (39.6 – 85.7 % at 100 µM)), and appeared to be superior calcium modulators to NGP1-01.

The results obtained in this study suggests these compounds to be promising leads to multi-mechanistic compounds that may be useful as drug agents for the treatment of neurodegenerative disorders. Further *in vitro* and *in vivo* studies, which may include mechanistic studies as well as elucidation of the actual binding mode of these compounds, their direct involvement in the anti-apoptotic cascade, dopamine transmission and blood-brain barrier permeability, would provide better insight on their drugability. Also, these analogues may be screened for potential neuroprotective activity on various other drug targets such as adenosine receptors, serotonin 1_A receptors and dopamine 3 (D_3) receptors, which have now emerged as potential targets for the treatment of neurodegenerative disorders.

Key terms

Neurodegeneration: Umbrella term for the progressive loss of structure or function of neurons, including death of neurons.

Apoptosis: Process of programed cell death in multicellular organisms.

Excitotoxicity: Pathological process by which nerve cells are damaged and killed by excessive stimulation by neurotransmitters such as glutamate and similar substances.

Neuroprotection: An effect that may result in salvage, recovery or regeneration of the nervous system, its cells, structure and function.

Multitarget-directed ligands: Single molecules that exert their pharmacological effect by interacting with two or more drug target sites – the term 'multifunctional drugs' is used synonymously for the purpose of this thesis.

Propargylamine derivatives: Molecules containing a 2-propynylamine moiety such as the MAO-B inhibitory compounds selegiline and rasagiline.

Polycyclic scaffold: Lipophilic scaffolds with more than one cyclic component such as amantadine and the Cookson's diketone.

Monoamine oxidase: an enzyme, present in most tissues, which catalyses the oxidation and inactivation of monoamine neurotransmitters.

NMDA receptors: A glutamate receptor and ion channel protein found in nerve cells.

Voltage gated calcium channels: A group of voltage-dependent ion channels found in the membrane of excitable cells such as muscles, glial cells and neurons.

Acknowledgements

I would like to express my deepest appreciation to the following people and institutions for their selfless support and assistance towards the completion of this thesis. Through their support and guidance, I successfully completed this milestone.

- Prof. Jacques Joubert
- Prof Sarel Malan
- Dr Rajan Sharma
- Erika Kapp
- Audrey Ramplin
- National Research Foundation, University of the Western Cape (UWC) for funding
- School of Pharmacy, UWC
- Pharmaceutical Chemisitry, UWC
- Department of Medical Biosciences, UWC
- My wife, Boitumelo Zindo and my sister Portia Madombwe for their continued support and encouragement

Table of Contents

Chapter 1

Introduction & Rational

1.1. Neurodegeneration

Neurodegenerative diseases (NDs) such as Alzheimer's (AD), Parkinson's (PD), and Huntington's diseases (HD) and amyotrophic lateral sclerosis (ALS) form part of a group of age related conditions characterized by progressive loss of structure or function of neurons, including death of neurons. Neurodegeneration has a mean onset of 55 years and is estimated to affect more than 100 million people worldwide [1]. Very few of these neurological conditions are curable, and many worsen over time as one ages, ultimately leading to death. They produce a range of symptoms and functional limitations that pose daily challenges to individuals and their families. Further to this, neurological conditions pose an economic burden to society and are estimated to cost the United States nearly $800 billion per year [1]. These costs are projected to increase even further over the coming years as the elderly segment of the population nearly doubles between 2011 and 2050 [1].

Though the pathogenesis of NDs is yet to be fully understood, it is known that several factors including toxins, endogenous-, environmental- and genetic factors are involved in the aetiology of these disorders [2]. While each disease state has its own specific molecular mechanism and clinical manifestations, some general pathways can be recognized in their different pathogenic cascades. Disturbances in neurotransmitter systems such as the monoaminergic system [3,4], mitochondrial dysfunction [5], cholinergic dysfunction [6], oxidative stress [6] and metal dyshomeostasis [7] are some of the common theories of causation widely explored in the literature. The complex pathogenesis of neurodegenerative diseases is now known to be the reason why drugs that target a single enzymatic system or receptor have failed to render sufficient neuroprotective and/or neurorestorative activity for their treatment [8–10]. It is now widely accepted that a more effective therapy would result from the use of multi-target directed ligands (MTDLs) able to intervene in the different pathological events implicated in the aetiology of NDs [11].

This thesis discusses a number of causation theories in greater detail in the relevant chapters, as well as potential drug agents that may serve as MTDLs to meet the curative needs of the respective NDs. It is however important to note that the core of the research herewith presented focused on designing MTDLs that may potentially halt the neuronal breakdown

process by addressing particularly the disturbances in the monoaminergic system, as well as the excitotoxicity resulting from excessive calcium influx into neuronal cells.

Monoaminergic system

Activated monoamine oxidase (MAO) have been reported to play a critical role in the pathogenesis of NDs. The enzymatic system, which comprises of two isoenzymes, MAO-A and MAO-B, catalyzes the oxidative deamination of biogenic and xenobiotic amines and has an important role in metabolism [12]. The enzymes preferentially degrade benzylamine and phenylethylamine and target a wide variety of specific neurotransmitters in the brain, including epinephrine, norepinephrine, dopamine, serotonin, and β-phenylethylamine [13,14]. The role of the MAO in modulating the function of a wide range of specific neurotransmitters is the reason the enzymatic system is associated with various conditions, including mood disorders [15], anxiety and depression [16,17], schizophrenia [18], attention deficit hyper-activity disorder [19-21], and NDs [22]. In neurodegeneration, particularly PD, the MAO-B enzyme, has been shown to exist in elevated levels in the brain of affected patients [23]. This enzyme has been shown to contribute to the neurodegenerative process through various mechanisms including, oxidative stress [24], neuroinflammation [25], triggering of apoptosis [26,27], failure of aggregated-protein clearance [28-30] and glial activation [31]. Significant attention has thus been duly directed to this enzymatic system as a therapeutic target in the design of neuroprotective agents, and as such, monoamine oxidase inhibitors (MAOI's) such as selegiline and rasagiline (Figure 1) remain the mainstay therapy for the management of NDs.

Calcium modulation

Aging neurons have also been shown to have reduced cytosolic calcium buffering capacity, increased calcium influx through *L*-type voltage-gated calcium channels (VGCCs) and via *N*-methyl D-aspartate receptor (NMDAR)-mediated calcium influx [32]. The resulting changes in neuronal calcium dynamics can cause the activation of calcium-dependent signals to enzymes such as phospholipases and proteases, as well as oxidative stress through reactive oxygen species (ROS) and reactive nitrogen species (RNS) leading to neuronal cell death [33-35]. This mechanism of apoptosis has led to the extensive development of calcium modulators due to the neuroprotective potential they may render [36]. Examples of drugs currently in use as calcium modulators include nimodipine (Figure 1), which is known to halt/retard neuronal cell death evoked by focal cerebral ischemia by blocking VGCC [37] and memantine (Figure 1), a noncompetitive and low-affinity NMDAR antagonist used in AD [38].

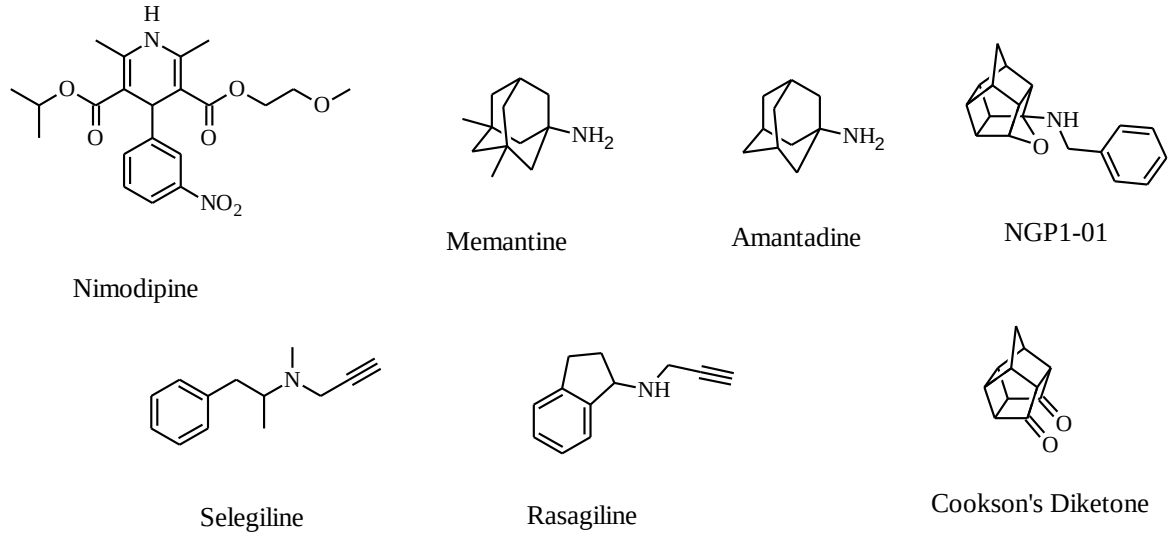

Figure 1 : Structures of nimodipine, memantine, amantadine, NGP1-01, selegiline, rasagiline and Cookson's diketone.

1.2. Polycyclic compounds

Heteroatom substituted polycyclic hydrocarbon 'cage' compounds are receiving attention from several research groups as potential scaffolds for the development of new drugs. Interest in these compounds stems from the discovery that amantadine (Figure 1), a 1-amino substituted polycyclic hydrocarbon, exhibit anti-parkinsonian activity [39] attributed to its action on the nigrostriatal doperminergic neurons in the brain. Amantadine is an FDA approved drug used in PD due to its rapid and strong voltage-dependent blocking kinetics of the NMDA receptor channel [40], as well as its ability to increase dopamine release and decrease dopamine reuptake in the CNS [41]. Similar to amantadine, NGP1–01 (Figure 1), a pentacycloundecaneamine synthetically derived from the polycyclic hydrocarbon scaffold commonly known as the Cookson's diketone (Figure 1) [42], has been shown to exhibit neuroprotective properties through VGCC blockade and NMDAR antagonistic activity [73]. NGP1-01, like amantadine, has also been shown to inhibit dopamine reuptake *in vivo*, with resulting neuroprotective activity [44–47]. It is apparent from the literature that amantadine and Cookson's diketone are polycyclic moieties that can be used to modify and improve the pharmacokinetic and pharmacodynamic properties of drugs, and are useful as both scaffolds for side-chain attachment as well as for improving a drug's lipophilicity [48]. Lipophilicity enhances a drug's transport across cellular membranes, including the selectively permeable blood–brain barrier, and increases the drug's affinity for lipophilic regions in target proteins [48,49]. The brain being the drug target site for treating NDs, the significance of these polycyclic moieties is clear. In addition polycyclic moieties could afford molecules with

metabolic stability, thereby prolonging the pharmacological effect of a drug, leading to a reduction in dosing frequency and improved patient compliance [50].

1.3. Propargylamine derivatives

The last few decades have seen increasing research interest and exploration of the neuroprotective ability of compounds bearing the propargylamine function seen in selegiline and rasagiline (Figure 1), two well known MAO-B inhibitors and proposed neuroprotective agents. The propargylamine moiety within these compounds' structures is now known to play an important role in providing the neuronal and mitochondrial protective properties inherent in these compounds [51–53]. Other reported activities ascribed to this moiety in the literature include anti-apoptotic activity [54–56] and amyloid-β (Aβ) aggregation inhibition [57]. These features of the propargylamine moiety have logically led to its incorporation into structures of many drug-like compounds designed for neuroprotection, with the aim of affording the resultant molecules with a broader therapeutic profile that may potentially meet the curative needs of NDs. This approach is discussed in greater detail in a review article included in this thesis (Chapter 2). The review describes various strategies adopted by researchers over the last decade in designing and evaluating drug-like molecules incorporating this moiety.

1.4. Study aim

This study was aimed at developing several multimechanistic polycyclic derivatives, represented by compounds **P1**, **P2**, **Y1** and **12**, (Figure 2) designed to serve as potential neuroprotective agents. By incorporating various functional groups with known biological activities into single molecules, we aimed to develop analogues that showed multiple mechanisms of action, as exhibited by their constituting moieties. Compounds that act on the various pathways involved in the apoptotic process of neuronal cells have great potential to serve as future analogues for the treatment and management of neurodegenerative disorders.

A main feature in the various compounds reported in this study was the polycyclic scaffold in the form of the Cookson's diketone or amantadine moiety (Figure 1). The influence of these polycyclic compounds on the NMDAR and VGCC's as well as their ability to impart desirable pharmacokinetic and pharmacodynamic properties on resultant molecules was the basis of their incorporation in the designed analogues. Further to the polycyclic scaffold, several compounds were designed to carry the propargylamine moiety, a deliberate strategy to impart the resultant molecules with MAO-B inhibitory activity, as well as providing them

with neuronal and mitochondrial protective properties, among other activities ascribed to this moiety.

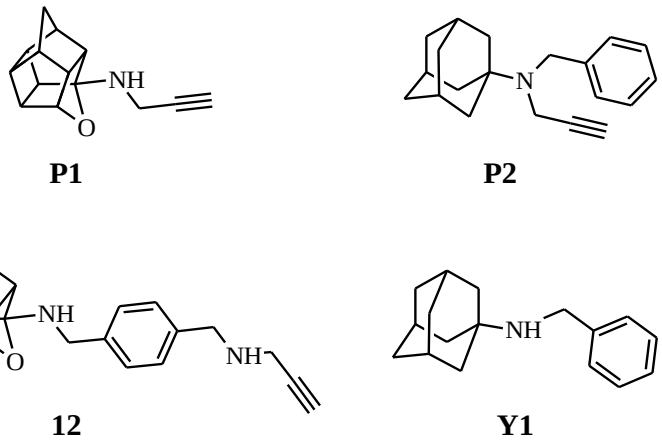

P1 **P2**

12 **Y1**

Figure 2 : Representative structures of the various compounds designed and synthesized in this study.

The primary objectives of this study were therefore to design and synthesize a series of polycyclic propargylamine derivatives and to evaluate these compounds as multimechanistic neuroprotective agents. The main approach was to develop multifunctional drugs which would halt the apoptotic neuronal breakdown process and eliminate some of the signs and symptoms of diseases such as AD and PD by: (a) Inhibiting NMDA receptors and blocking VGCC's thus regulating the Ca^{2+} influx mediated excitotoxic process; (b) Inhibiting the MAO-B enzyme thus allowing increase in dopamine levels in the CNS and reducing the levels of the highly oxidative products produced by the activity of this enzyme; (c) Possess anti-apoptotic activity to halt the natural neuronal cell death process.

The design of the various compounds was guided by preliminary *in silico* studies performed during the initial design phases. In these studies, the proposed compound structures were docked in computer-simulated target proteins in order to envisage their potential binding interaction with the proteins. This allowed for the development of analogues with the desirable receptor binding properties.

Following the *in-silico* studies, the next objective was to synthesize the best ranked compounds utilizing various synthetic strategies. Microwave assisted methods were often used as the preferred method of synthesis as they present several advantages which include; remarkable reduction of reaction time, improved yields, cleaner reactions and reduction or elimination of hazardous solvents compared to reactions performed under conventional

thermal heating conditions [58,59]. The successfully synthesized compounds were then evaluated *in vitro* for potential activity on the various target sites implicated in neurodegeneration.

The final findings from this study were compiled into two research articles published in peer-reviewed journals. The first article (Chapter 3) describes the design, synthesis and evaluation of polycyclic propargylamine and acetylene derivatives as multifunctional neuroprotective agents (represented by compounds **P1** and **P2**, Figure 2). These compounds were shown to possess significant neuroprotective properties, but however showed little to no activity on the intended target sites (MAO-B, VGCC and NMDAR). The second article (Chapter 4) describes the expansion on the initial series of compounds reported in chapter 3. This article describes the modifications performed to the compounds described in the first article in order to afford a new series of compounds (represented by compound **12**; Figure 2) which showed neuroprotective properties and most importantly, showed improved activity on the MAO-B, VGCC and NMDAR.

Research article 3 (Chapter 5) describes adamantane amine derivatives designed to serve as dual acting NMDA receptor and voltage-gated calcium channel inhibitors for neuroprotection. These compounds were designed and synthesized by Yakub Kadernani as part of his M.Sc. degree [60]. My input to this body of work included developing the synthetic pathways for the synthesis of these compounds and screening the compounds for calcium modulatory potential by conducting NMDA and VGCC assays using protocols I developed and standardized during the first year of my Ph.D. This series of compounds (represented by compound **Y1**; Figure 2) lacks the proparglyamine derivative and was therefore not assessed for MAO-B inhibition. The design strategy with this series was focused on producing derivatives that could potentially exhibit similar calcium modulatory activity as seen with NGP1-01. These adamantane derived compounds are potentially better neurotherapeutic options than amantadine and memantine as they were shown to inhibit both NMDAR and VGCC-mediated calcium influx, whereas the base adamantine structures only inhibit NMDAR-mediated calcium influx.

Additional research outputs include research articles 4 and 5 (Chapter 7), which describe the design, synthesis and evaluation of indole derivatives as multifunctional agents against Alzheimer's disease, and describe the versatility of 7-substituted coumarin molecules as antimycobacterial agents, neuronal enzyme inhibitors and neuroprotective agents,

respectively. The indole derivatives described in research article 4 were designed and synthesized by Ireen Denya as part of her M.Sc. degree [61]. The objective of this study was to improve the inhibitory, neuroprotective and stability profile and eliminate the stereochemistry associated with rasagline and ladostigil. The 7-substituted coumarin molecules described in research article 5 are compounds that were designed and synthesized by Germaine Foka as part of her M.Sc. degree [62]. These compounds were initially designed and synthesized to serve as multifunctional neuronal enzyme inhibitors. As part of a collaborative project, further evaluation of the structure-activity relationships for selectivity and specific characteristics of these compounds were performed in order to assess their viability as neuronal enzyme inhibitors and/or antimycobacterial clinical agents. My contribution to both these studies included conducting general cytotoxicity screening assays of the synthesized compounds and assessing them for potential neuroprotective ability *in vitro*. Though structurally dissimilar in that the compounds reported in this chapter lacked polycyclic scaffolds as well as propargylamine moieties, the compounds still showed promising neuroprotective potential. My contribution to this body of work as well as the potential these compounds may have in serving as neuroprotective agents is the reason for their inclusion in this thesis.

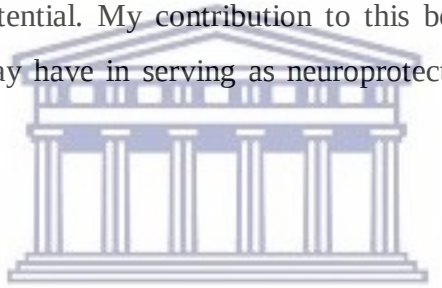

References

[1] Gooch C.L., Pracht E., Borenstein A.R. The burden of neurological disease in the United States: A summary report and call to action. *Ann. Neurol.* 81(4), 479-484 (2017).

[2] Spencer P.S., Schaumburg H.H., Ludolph A.C. *Experimental and Clinical Neurotoxicology.* (Eds). Oxford University Press, Oxford, UK (2000).

[3] Baker G.B., Reynolds G.P. Biogenic amines and their metabolites in Alzheimer's disease: noradrenaline, 5-hydroxytryptamine and 5-hydroxyindole-3-acetic acid are depleted in the hippocampus but not in substantia innominata. *Neurosci. Lett.* 100(1–3), 335–339 (1989).

[4] Cross A.J. Serotonin in Alzheimer type dementia and other dementing illnesses. *Ann. NY Acad. Sci.* 600, 405–415 (1990).

[5] Swerdlow R.H., Khan S.M. The Alzheimer's disease mitochondrial cascade hypotheses: an update. *Exp. Neurol.* 218(2), 308–315 (2009).

[6] Coyle J.T., Puttfarcken P. Oxidative stress, glutamate and neurodegenerative disorders. *Science* 262(5134), 689–695 (1993).

[7] Huang X., Moir R.D., Tanzi R.E., Bush A.I., Rogers J.T. Redoxactive metals, oxidative stress and Alzheimer's disease pathology. *Ann. NY Acad. Sci.* 1012, 153–163 (2004).

[8] Karolewicz B., Klimek V., Zhu H. *et al.* Effects of depression, cigarette smoking, and age on monoamine oxidase B in amygdaloid nuclei. *Brain Res.* 1043(1–2), 57–64 (2005).

[9] Finberg J.P. Pharmacology of rasagiline, a new MAO-B inhibitor drug for the treatment of Parkinson's disease with neuroprotective potential. *Rambam Maimonides Med. J.* 1(1), e0003 (2010).

[10] Strydom B., Bergh J.J., Petzer J.P. Inhibition of monoamine oxidase by phthalide analogues. *Bioorg Med. Chem. Lett.* 23(5), 1269–1273 (2013).

[11] Kristal B.S., Conway A.D., Brown A.M. *et al.* Selective dopaminergic vulnerability: 3,4-dihydroxyphenylacetaldehyde targets mitochondria. *Free Radic. Biol. Med.* 30(8), 924–931 (2001).

[12] Cia Z. Monoamine oxidase inhibitors: promising therapeutic agents for Alzheimer's disease (Review). *Mol Med Rep.* 9(5):1533-41, (2014).

[13] Said U.Z., Saada H.N., Abd-Alla M.S., Elsayed M.E., Amin A.M: Hesperidin attenuates brain biochemical changes of irradiated rats. *Int J Radiat Biol* 88(8), 613-618, (2012).

[14] Bodkin J.A., Cohen B.M., Salomon M.S., Cannon S.E., Zornberg G.L., Cole J.O: Treatment of negative symptoms in schizophrenia and schizoaffective disorder by selegiline augmentation of antipsychotic medication. A pilot study examining the role of dopamine. *J Nerv Ment Dis* 184(5), 295-301 (1996).

[15] Dunleavy D.L: Mood and sleep changes with monoamine-oxidase inhibitors. *Proc R Soc Med.* 66(9), 951 (1973).

[16] Shabbir F., Patel A., Mattison C., Bose S., Krishnamohan R., Sweeney E., Sandhu S., Nel W., Rais A., Sandhu R., Ngu N., Sharma S. Effect of diet on serotonergic neurotransmission in depression. *Neurochem Int* 62(3), 324-329 (2013).

[17] Merikangas K.R., Merikangas J.R. Combination monoamine oxidase inhibitor and beta-blocker treatment of migraine, with anxiety and depression. *Biol Psychiatry* 38(9), 603-610 (1995).

[18] Samson J.A., Gurrera R.J., Nisenson L., Schildkraut J.J. Platelet monoamine oxidase activity and deficit syndrome schizophrenia. *Psychiatry Res* 56(1), 25-31 (1995).

[19] Lawson D.C., Turic D., Langley K., Pay H.M., Govan C.F., Norton N., Hamshere M.L., Owen M.J., O'Donovan M.C., Thapar A. Association analysis of monoamine oxidase A and

attention deficit hyperactivity disorder. *Am J Med Genet B Neuropsychiatr Genet*. 116B(1), 84-89 (2003).

[20] Wargelius H.L., Malmberg K., Larsson J.O., Oreland L: Associations of MAOA-VNTR or 5HTT-LPR alleles with attention-deficit hyperactivity disorder symptoms are moderated by platelet monoamine oxidase B activity. *Psychiatr Genet.* 22(1), 42-45 (2012).

[21] Nedic G., Pivac N., Hercigonja D.K., Jovancevic M., Curkovic K.D., Muck-Seler D. Platelet monoamine oxidase activity in children with attention-deficit/hyperactivity disorder. *Psychiatry Res* 175(3), 252-255 (2010).

[22] Youdim M.B., Fridkin M., Zheng H. Novel bifunctional drugs targeting monoamine oxidase inhibition and iron chelation as an approach to neuroprotection in Parkinson's disease and other neurodegenerative diseases. *J Neural Transm* 111, 1455-1471 (2004).

[23] Youdim M.B., Weinstock M. Molecular basis of neuroprotective activities of rasagiline and the anti-Alzheimer drug TV3326 [(N-propargyl-(3R)aminoindan-5-YL)-ethyl methyl carbamate]. *Cell. Mol. Neurobiol.* 21(6), 555–573 (2002).

[24] Siddiqui A., Mallajosyula J.K., Rane A., Andersen J.K. Ability to delay neuropathological events associated with astrocytic MAO-B increase in a Parkinsonian mouse model: implications for early intervention on disease progression. *Neurobiol Dis* 43(2), 527-532 (2011).

[25] Bielecka A.M., Paul-Samojedny M., Obuchowicz E. Moclobemide exerts anti-inflammatory effect in lipopolysaccharide-activated primary mixed glial cell culture. Naunyn Schmiedebergs *Arch Pharmacol* 382(5-6), 409-417 (2010).

[26] Naoi M., Maruyama W., Akao Y., Yi H., Yamaoka Y. Involvement of type A monoamine oxidase in neurodegeneration: regulation of mitochondrial signaling leading to cell death or neuroprotection. *J Neural Transm Suppl:* (71), 67-77 (2006).

[27] Merad-Boudia M., Nicole A., Santiard-Baron D., Saillé C., Ceballos-Picot I. Mitochondrial impairment as an early event in the process of apoptosis induced by glutathione depletion in neuronal cells: relevance to Parkinson's disease. *Biochem Pharmacol* 56(5), 645-655 (1998).

[28] Hüll M., Berger M., Heneka M. Disease-modifying therapies in Alzheimer's disease: how far have we come? *Drugs* 66(16), 2075-2093 (2006).

[29] Rodríguez S., Ito T., He X.J., Uchida K., Nakayama H. Resistance of the golden hamster to 1-methyl-4-phenyl-1,2,3,6-tetrahydropyridine (MPTP)-neurotoxicity is not only related

with low levels of cerebral monoamine oxidase-B. *Exp Toxicol Pathol* 65(1-2), 127-133 (2013).

[30] Konradi C., Riederer P., Jellinger K., Denney R. Cellular action of MAO inhibitors. *J Neural Transm Suppl* 25: 15-25 (1987).

[31] Weinstock M., Luques L., Poltyrev T., Bejar C., Shoham S. Ladostigil prevents age-related glial activation and spatial memory deficits in rats. *Neurobiol Aging* 32(6), 1069-1078 (2011).

[32] Bezprozvanny I. Calcium signaling and neurodegenerative diseases. *Trends Mol Med.* 15(3),89-100 (2009).

[33] Alexi T., Borlongan C.V., Faull R.L., Williams C.E., Clark R.G., Gluckman P.D., Hughes P.E. Neuroprotective strategies for basal ganglia degeneration: Parkinson's and Huntington's diseases. *Prog Neurobiol.* 60(5), 409-70 (2000).

[34] Mattson M.P. Excitotoxic and excitoprotective mechanisms: abundant targets for the prevention and treatment of neurodegenerative disorders. *Neuromolecular Medicine*. 3(2), 65-94 (2003).

[35] Meldrum B., Garthwaite, J. Excitatory amino acid neurotoxicity and neurodegenerative disease. *Trends Pharmacol Sci.* 11(9), :379-387 (1990).

[36] Stone T.W., Addae J.I. The pharmacological manipulation of glutamate receptors and neuroprotection. *Eur. J. Pharmacol.* 447(2–3), 285–296 (2002).

[37] Sobrado M., López M.G., Carceller F., García A.G., Roda J.M. Combined nimodipine and citicoline reduce infarct size, attenuate apoptosis and increase bcl-2 expression after focal cerebral ischemia. *Neuroscience* 118(1), 107–113 (2003).

[38] Lipton S.A. Paradigm shift in neuroprotection by NMDA receptor blockade: memantine and beyond. *Nat. Rev. Drug Discov.* 5(2), 160–170 (2006).

[39] Schwab R.S., Poskanzer D.C., England A.C., Young R.R. Amantadine in Parkinson's disease. Review of more than two years' experience. *JAMA.* 222(7), 792-795 (1972).

[40] Greenamyre J.T., O'Brien C.F. N-methyl-d-aspartate antagonists in the treatment of Parkinson's disease. *Arch. Neurol.* 48(9), 977–981 (1991).

[41] Mizoguchi K., Yokoo H., Yoshida M., Tanaka T., Tanaka M.K. Amantadine increases the extracellular dopamine levels in the striatum by re-uptake inhibition and by N-methyl-D-aspartate antagonism. *Brain Res.* 662(1-2), 255-8 (1994).

[42] Cookson R.C., Grundwell E., Hude J. Synthesis of cage-like molecules by irradiation of Diels-Alder adducts. *Chem. Ind. (London)* 1003-1004 (1958).

[43] Geldenhuys W.J., Malan S.F., Murugesan T., van der Schyf C.J., Bloomquist J.R. Synthesis and biological evaluation of pentacyclo[5.4.0.02,6.03,10.05,9]undecane derivatives as potential therapeutic agents in Parkinson's disease. *Bioorg. Med. Chem.* 12(7), 1799–1806 (2004).

[44] Geldenhuys W. J., Malan S. F., Bloomquist J. R., Van der Schyf C. J. Structure-activity relationships of pentacycloundecylamines at the N-methyl-d-aspartate receptor. *Bioorg. Med. Chem*. 15(3), 1525-32 (2007).

[45] Kiewert C., Hartmann J., Stoll J., Thekkumkara T.J., Van der Schyf CJ, Klein J. NGP1-01 is a brain-permeable dual blocker of neuronal voltage- and ligand-operated calcium channels. *Neurochem. Res.* 31(3), 395-9 (2006).

[46] Mdzinarishvili A., Geldenhuys W.J., Abbruscato T.J., Bickel U., Klein J., Van der Schyf C.J. NGP1-01, a lipophilic polycyclic cage amine, is neuroprotective in focal ischemia. *Neurosci. Lett.* 383(1-2), 49-53 (2005).

[47] Geldenhuys W.J., Malan S.F., Murugesan T., Van der Schyf C.J., Bloomquist J.R. Synthesis and biological evaluation of pentacyclo[5.4.0.0(2,6).0(3,10).0(5,9)]undecane derivatives as potential therapeutic agents in Parkinson's disease. *Bioorg. Med. Chem*. 12(7), 1799-806 (2004).

[48] Joubert J., Geldenhuys W.J, Van der Schyf C.J. *et al.* Polycyclic cage structures as lipophilic scaffolds for neuroactive drugs. *ChemMedChem* 7(3), 375–84 (2012).

[49] Zah J., Terre'Blanche G., Erasmus E., Malan S.F. Physicochemical prediction of a brain-blood distribution profile in polycyclic amines. *Bioorg. Med. Chem.* 11(17), 3569–3578 (2003).

[50] Brookes K.B., Hickmott P.W., Jutle K.K., Schreyer C.A. Introduction of pharmacophoric groups into polycyclic systems 4. aziridine, oxiran, and tertiary betahydroxyethylamine derivatives of adamantine. *S. Afr. J. Chem.* 45, 8–11 (1992).

[51] Weinreb O., Amit T., Bar-Am O., Youdim M.B.H. Rasagiline: a novel anti-Parkinsonian monoamine oxidase-B inhibitor with neuroprotective activity. *Prog. Neurobiol.* 92(3), 330–344 (2010).

[52] Youdim M.B.H., Bar-Am O., Yogev-Falach M. *et al.* Rasagiline: neurodegeneration, neuroprotection, and mitochondrial permeability transition. *J. Neurosci. Res.* 79(1–2), 172–179 (2005).

[53] Maruyama W., Akao Y., Carrillo M.C., Kitani K., Youdium M.B.H., Naoi M. Neuroprotection by propargylamines in Parkinson's disease: suppression of apoptosis and induction of prosurvival genes. *Neurotoxicol. Teratol.* 24(5), 675–682 (2002).

[54] Sterling J., Herzig Y., Goren T. *et al.* Novel dual inhibitors of AChE and MAO derived from hydroxy aminoindan and phenethylamine as potential treatment for Alzheimer's disease. *J. Med. Chem.* 45(24), 5260–5279 (2002).

[55] Yogev-Falach M., Bar-Am O., Amit T., Weinreb O., Youdim M.B. A multifunctional, neuroprotective drug, ladostigil (TV3326), regulates holo-APP translation and processing. *FASEB J.* 20(12), 2177–2179 (2006).

[56] Youdim M.B., Weinstock M. Molecular basis of neuroprotective activities of rasagiline and the anti-Alzheimer drug TV3326 [(N-propargyl-(3R)aminoindan-5-YL)-ethyl methyl carbamate]. *Cell. Mol. Neurobiol.* 21(6), 555–573 (2002).

[57] Bar-Am O., Amit T., Weinreb O., Youdim M.B., Mandel S. Propargylamine containing compounds as modulators of proteolytic cleavage of amyloid-beta protein precursor: involvement of MAPK and PKC activation. *J. Alzheimers Dis.* 21(2), 361–371 (2010).

[58] Kappe C.O., Stadler A. Microwaves in Organic and Medicinal Chemistry. *Wiley-VCH*. Weinheim, 2005.

[59] Wathey B., Tierney J., Lidstrom P., Westman J. The impact of microwave-assisted organic chemistry on drug discovery. *Drug Discov. Today.* 7(6), 373-80 (2002).

[60] Kadernani Y. 'Polycyclic cage compounds as neuroprotective agents', M.Sc., University of the Western Cape, Bellville. (2014)

[61] Denya I. 'Design, Synthesis and Evaluation of Indole Derivatives as Multifunctional Agents against Alzheimer's Disease.', M.Sc., University of the Western Cape, Bellville. (2017)

[62] Foka G. 'Synthesis and evaluation of novel coumarin-donepezil derivatives as dual acting monoamine oxidase and cholinesterase inhibitors in Alzheimer's disease.', M.Sc., University of the Western Cape, Bellville. (2016)

Chapter 2

Review Article: Propargylamine as functional moiety in the design of multifunctional drugs for neurodegenerative disorders: MAO inhibition and beyond

Article published online on 29 April 2015

Future Med Chem. 2015;7(5):609-29. doi: 10.4155/fmc.15.12.

Propargylamine as functional moiety in the design of multifunctional drugs for neurodegenerative disorders: MAO inhibition and beyond

Frank T Zindo[1], Jacques Joubert[1] & Sarel F Malan*[,1]

[1]*Pharmaceutical Chemistry, School of Pharmacy, University of the Western Cape, Private Bag X17, Bellville 7535, South Africa*

*Author for correspondence: Tel.: +27 21 959 3190 Fax: +27 21 959 1588 sfmalan@uwc.ac.za

Abstract

Much progress has been made in designing analogues that can potentially confer neuroprotection against debilitating neurodegenerative disorders, yet the multifactorial pathogenesis of this cluster of diseases remains a stumbling block for the successful design of an 'ultimate' drug. However, with the growing popularity of the "one drug, multiple targets" paradigm, many researchers have successfully synthesized and evaluated drug-like molecules incorporating a propargylamine function that shows potential to serve as multifunctional drugs or multitarget-directed ligands. It is the aim of this review to highlight the reported activities of these propargylamine derivatives and their prospect to serve as drug candidates for the treatment of neurodegenerative disorders.

Key terms:

Apoptosis: Process of programed cell death in multicellular organisms.

Multitarget-directed ligands: Single molecules that exert their pharmacological effect by interacting with two or more drug target sites – term 'multifunctional drugs' used synonymously for the purpose of this review.

Neuroprotection: An effect that may result in salvage, recovery or regeneration of the nervous system, its cells, structure and function.

Neurodegeneration: Umbrella term for the progressive loss of structure or function of neurons, including death of neurons.

Excitotoxicity: Pathological process by which nerve cells are damaged and killed by excessive stimulation by neurotransmitters such as glutamate and similar substances.

Propargylamine derivatives: Molecules containing a 2-propynylamine moiety such as the MAO-B inhibitory compounds selegiline and rasagiline.

2.1. Introduction

Parkinson's disease (PD), Alzheimer's disease (AD) and Huntington's disease (HD) are conditions constituting part of the broad cluster of diseases commonly referred to as neurodegenerative disorders (ND). A classical feature of these diseases is the transient loss of neuronal cells in the brain due to apoptosis triggered by one of many factors including toxins, endogenous-, environmental- and genetic factors [1]. The lack of neurorestorative mechanisms in these neuronal cells is a dreadful fact to patients suffering from NDs as it allows for the transient worsening of these conditions over a period of 5–10 years, often resulting in death [2]. The cardinal symptoms associated with these diseases are mostly

dependent on the region of the brain and the specific neuronal cells affected. For example, symptoms of tremor, rigidity and postural instability seen in PD result from the loss of dopaminergic neurons in the substantia nigra pars compacta and its projections in the nigrostriatal tract [3]. Although not yet fully understood, the pathogenesis of NDs is known to be complex in nature. Currently established theories of causation include disturbances in neurotransmitter systems such as the monoaminergic system [4,5], mitochondrial dysfunction [6], cholinergic dysfunction [7], oxidative stress [7] and metal dyshomeostasis [8]. While not implicated in the pathogenesis of NDs, adenosine [9], serotonin 1_A [10,11] and dopamine 3 (D_3) [12] receptors have also now emerged as targets for the treatment of PD. These causation theories and treatment concepts are discussed in greater detail under the relevant sections of this paper as we discuss the recent findings reported in the field. It is important to note that the theories herewith discussed do not constitute the entirety of current knowledge and concepts, and other approaches not included are beyond the scope of this review. Acknowledging the multifactorial nature of NDs suggests that targeting any single mechanistic site will not result in successful retardation of the disease progression, and as such, many 'single-site-targeting' drugs have failed to render sufficient neuroprotective and/or neurorestorative activity. The use of 'magic bullets' targeting a single receptor or enzymatic system is thus insufficient for treatment of these multifactorial diseases [13–15]. Current treatment options include the use of monoamine oxidase inhibitors (MAOI's) like selegiline (**1**) and rasagiline (**2**) (Figure 1) in the treatment of PD.

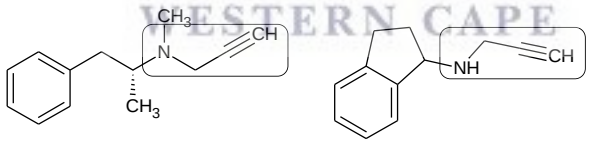

1

IC_{50} ± SEM
hMAO-A = 67.25 ± 1.02 µM
hMAO-B = 19.60 ± 0.86 nM[17]

2

IC_{50} ± SEM
hMAO-A = 16.44 ± 0.85 µM
hMAO-B = 69.00 ± 0.4 nM[18]

Figure 1. The MAO-B inhibitors. Selegiline (**1**) and rasagiline (**2**) with the propargylamine moiety indicated. h: Human; SEM: Standard error of the mean. Data taken from [17,18].

These drugs are aimed at correcting disturbances in the monoaminergic neurotransmitter system by virtue of inhibiting the MAO-B enzyme that is responsible for catalyzing the oxidative degradation of dopamine. The production of free radicals from this oxidative reaction, which could contribute to the degenerative process, is also attenuated by inhibition of this enzyme. The importance of MAO-B in the aetiology of PD is however challenged in

that MAO-B itself may not directly contribute to the cell death of dopamine neurons in PD [16] and that MAOI's may not necessarily depend on MAO-B inhibition to exert their clinical effects. Recently developed MAOI's are also not specific to the MAO-B enzyme. It is now widely accepted that a more effective therapy would result from the use of multitarget-directed ligands (MTDLs) able to intervene in the different pathological events underlying the aetiology of neuronal disorders [19]. This design strategy involves the incorporation of distinct pharmacophores of different drugs in the same structure to develop hybrid molecules. Each pharmacophore of the hybrid drug should essentially retain the ability to interact with its specific site(s) on the target, producing the consequent pharmacological response [19]. The advent of this MTDL approach has now seen many researchers develop a number of compounds that can potentially confer neuroprotection by acting simultaneously on different receptors and target sites implicated in NDs. This approach has yielded resultant molecules which combine MAO inhibition with cholinesterase inhibition and/or metal homeostasis, MAO inhibition with calcium homeostasis modulation, MAO inhibition with antioxidant and free radical scavenging activity, and MAO inhibition with adenosine receptor antagonism, among others. The last few decades have seen increasing research interest and exploration of the neuroprotective ability of compounds bearing propargylamine function seen in selegiline and rasagiline. The propargylamine moiety is now known to play an important role in providing the neuronal and mitochondrial protective properties inherent in these compounds [20–22] and other reported activities ascribed to this moiety in the literature include antiapoptotic [23–25] and amyloid-β (Aβ) aggregation inhibition [26]. These features of the propargylamine moiety have logically led to its incorporation into structures of many drug like compounds designed for neuroprotection to afford resultant molecules with broader therapeutic profiles that may potentially meet the curative needs of multifactorial NDs (Figure 2). It is the aim of this review to highlight the progress made in this field over the last decade in the quest to design the 'ideal' multifunctional neuroprotective agent.

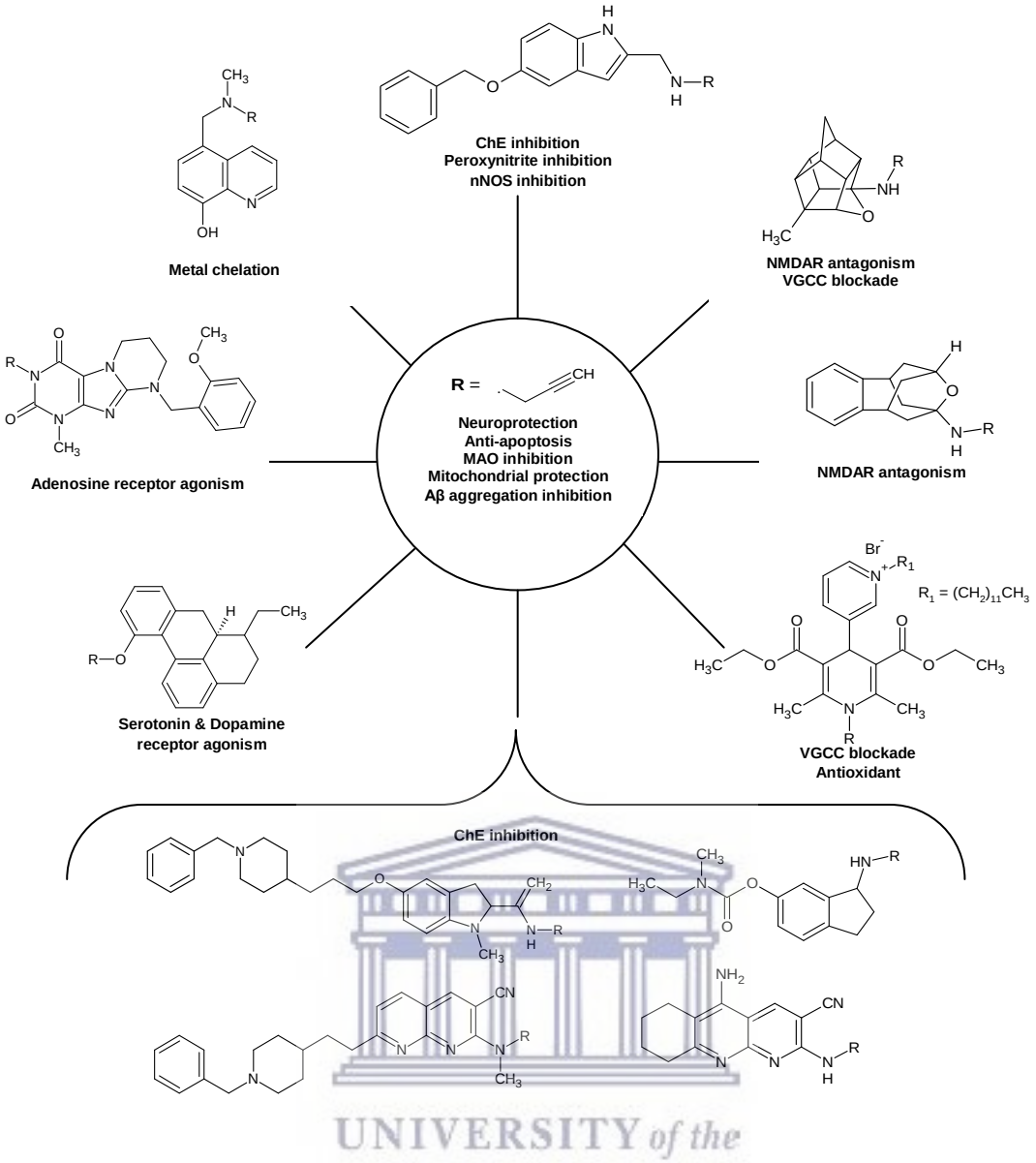

Figure 2. Various propargyl and propargylamine derivatives and their resultant activities.

Aβ: Amyloid-β; NMDAR: *N*-methyl-d-aspartate receptors; nNOS: Neuronal nitric oxide; VGCC: Voltage gated calcium channels.

2.2. Strategies involving MAO inhibition

2.2.1. MAO inhibition & cholinesterase inhibition

The MAO enzyme is responsible for the oxidative deamination of a wide range of biogenic and xenobiotic amines, including dopamine (DA), noradrenaline, adrenaline, tyramine, serotonin, β-phenylethylamine, *N*-methylhistamine, benzylamine and methoxy metabolites of the parent amines, such as metanephrine and normetanephrine [27]. This enzyme is known to exist in two isoforms, namely MAO-A and MAO-B, which show different selectivities for substrates and inhibitors [28]. Excessive oxidative deamination, due to the age-related elevated levels of MAO-B in patients affected by neurodegenerative disorders [29], sees the depletion of these vital neurotransmitters with the concomitant production of hydrogen

peroxide and other neuronal-cell-damaging free radicals. This excessive deamination does not only act indirectly as a trigger to the apoptotic process, but also gives rise to some of the signs and symptoms associated with these disorders [29–31]. Replenishing the depleted levels of DA in the nigro-striatal pathway to alleviate symptoms [32] has been a successful therapeutic strategy as seen in several currently available drugs such as rasagiline and selegiline. These drugs are aimed at increasing DA levels by inhibiting its oxidative breakdown by the MAO enzyme in the striatum. The inhibition of MAO enzymes, particularly MAO-B, may also exert neuroprotective effects by inhibiting the formation of toxic byproducts of MAO-B-catalyzedoxidation of neurotransmitters [33]. The latter may be beneficial in various NDs, particularly where neurotoxic product formation promotes the generation of reactive oxygen species (ROS), leading to oxidative stress and ultimately contributing to increased neuronal damage [34,35]. Though unquestionably beneficial, this strategy fails to meet the curative needs of the diverse cerebral mechanisms implicated in the control of NDs [36,37]. This shortfall has seen the exploration of a MTDL approach that combines inhibition of the MAO enzyme and the inhibition of cholinesterase, which are major enzymatic systems also implicated in NDs.

Low levels of acetylcholine are also thought to play a significant role in the pathophysiology of NDs [36]. During the progression of these diseases, there is loss of cholinergic neurons which results in a deficit of acetylcholine (ACh) in the specific brain regions that mediate learning and memory functions [37]. Consequently, acetylcholinesterase inhibitors (AChEI) such as tacrine (**3**), rivastigmine (**4**), donepezil (**5**) and galanthamine (**6**) form the mainstay of currently available treatment options for AD (Figure 3). These drugs are known to improve symptoms of AD by inhibiting AChE thereby raising the levels of ACh in the synaptic cleft [38]. AChE has also been implicated in accelerating the formation of amyloid fibrils in the brain and forming stable complexes with amyloid-β (Aβ) [39]. These complexes are thought to play a significant role in the pathology of NDs [38] and inhibiting the activity of AChE thus offers neuroprotective activity by retarding the formation of these amyloid fibrils and Aβ complexes [39]. In healthy human brain, AChE predominates over butyrylcholinesterase (BuChE) activity [40], but the activity of the latter seems to have been underestimated [41]. While AChE is localized mainly to neurons, BuChE is associated primarily with glial cells as well as endothelial cells [42] where it serves a possible role of supportive hydrolysis of ACh [43]. Augmenting cholinergic function by inhibiting both AChE and BuChE pathways may therefore be of clinical value. Clinical studies with the dual ChEI, rivastigmine (**4**), support the concept of centrally inhibiting BuChE in addition to AChE inhibition in AD therapy

based on the high correlation of the former with cognitive improvement [44]. A variety of MTDLs that possess cholinesterase inhibitory activity have therefore been designed and synthesized using these known inhibitors (**3–6**) as lead structures.

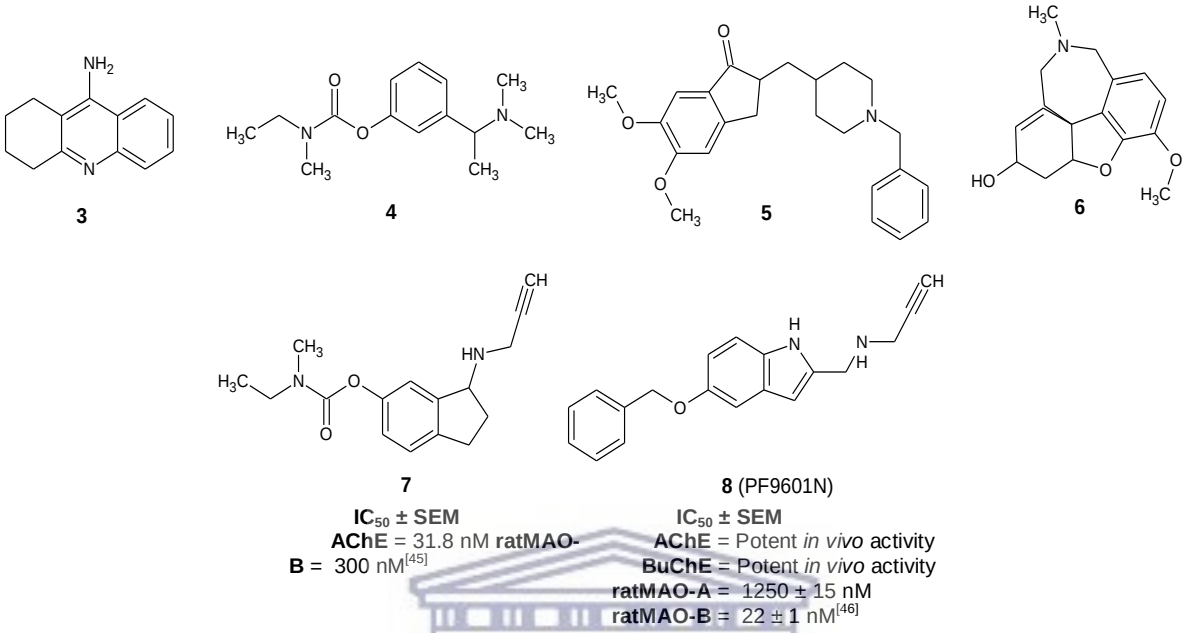

Figure 3. Acetylcholinesterase inhibitors. Tacrine (**3**), rivastigmine (**4**), donepezil (**5**) & galanthamine (**6**); the multifunctional monoamine oxidase and ChE inhibitors ladostigil (**7**) and PF9601N (**8**). SEM: Standard error of the mean. Data taken from [45,46].

Youdim and Weinstock (2001) designed and synthesized ladostigil (**7**) by incorporating the carbamate moiety of rivastigmine (**4**) into position 6 of the well-known MAO-I rasagiline (**2**) with the intention of yielding a molecule that could potentially exhibit inhibitory activity against cholinesterase (ChE) and MAO enzymes (Figure 3) [47]. This molecule was extensively evaluated using *in vitro* and *in vivo* models for ChE and MAO-A/B inhibitory activity and was shown to inhibit AChE and BuChE, and showed significant memory improvement in rats where memory impairment was induced by scopolamine [48]. Ladostigil was found to have the additional advantage of a therapeutic index larger than other ChE inhibitors currently in clinical use for the treatment of AD and seems to excert an improved neuroprotective effect by additional modes not discussed here [47,49,50]. Although reported to be 5 times less potent than rasagiline from *in vitro* findings, ladostigil was shown to be a brainselective MAO-A and MAO-B inhibitor at similar doses required for ChE inhibition following repeated oral and intraperitoneal (IP) administration to rats and mice [48,51–52]. A once daily administration of ladostigil (26 mg/kg) for 2 weeks inhibited brain MAO-A by 66% and MAO-B by 71%, with very little or no effect on the peripheral MAO enzymes in the

liver and intestine [48,52–53]. The time dependent effect observed is consistent with the irreversible inhibition of the MAO enzyme by ladostigil and its active metabolites. A school of thought support the notion of selectively targeting the MAO-B enzyme, based on the fact that the extrapyramidal region of the human brain has approximately 4-times more MAO-B than MAO-A [54]. However, it has been reported that unless both forms of the enzyme are inhibited, L-DOPA administration neither produces the rise of brain dopamine nor the behavioral changes seen after administration of a nonspecific inhibitor such as tranylcypromine [55]. This phenomenon is best explained by the fact that dopamine is a substrate for both MAO-A and MAO-B [56] and hence when one form of the enzyme is selectively inhibited, the other enzyme metabolizes the dopamine. This concept thus suggests nonselective brain specific MAOI's such as ladostigil to be superior to its selective counterparts in treating NDs characterized by dopamine depletion. Further to this approach, Samadi *et al.* (2011) designed multitarget-directed MAO and ChE inhibitors by connecting *N*-benzyl piperidine and the propargylamine moieties present in the AChEI donepezil (**4**) [57], and the well-known MAO-I PF9601N (**8**) [46], respectively, through an appropriate linker to a central naphthyridine moiety to afford compound **9** (Figure 4) [58]. PF9601N is also an effective neuroprotective agent in several *in vivo* models of PD by attenuating the MPTP-induced striatal dopamine depletion in young-adult and old-adult C57/BL mice, reducing the loss of tyrosine hydroxylase positive neurons after nigrostriatal injection of 6-hydroxydopamine (6-OHDA) in rats [59], and enhancing the duration of l-3,4-dihydroxyphenylalanine induced contralateral turning in 6-OHDA lesioned rats [60]. From their findings, Samadi and colleagues reported compound **9** to exhibit promising MAO and ChE inhibitory activity. *In vitro* analysis of compound **9** using Ellman's method [63] against *Electrophorus electricus* AChE (EeAChE) and horse serum butyrylcholinesterase (eqBuChE) with tacrine (**3**) and donepezil (**5**) as reference compounds led to its identification as a multifunctional drug-like molecule showing potent and selective AChE inhibitory activity (IC_{50} = 37 ±4 nM) and a moderate MAO-A inhibitory profile (IC_{50} = 41 ±7 μM) [58].

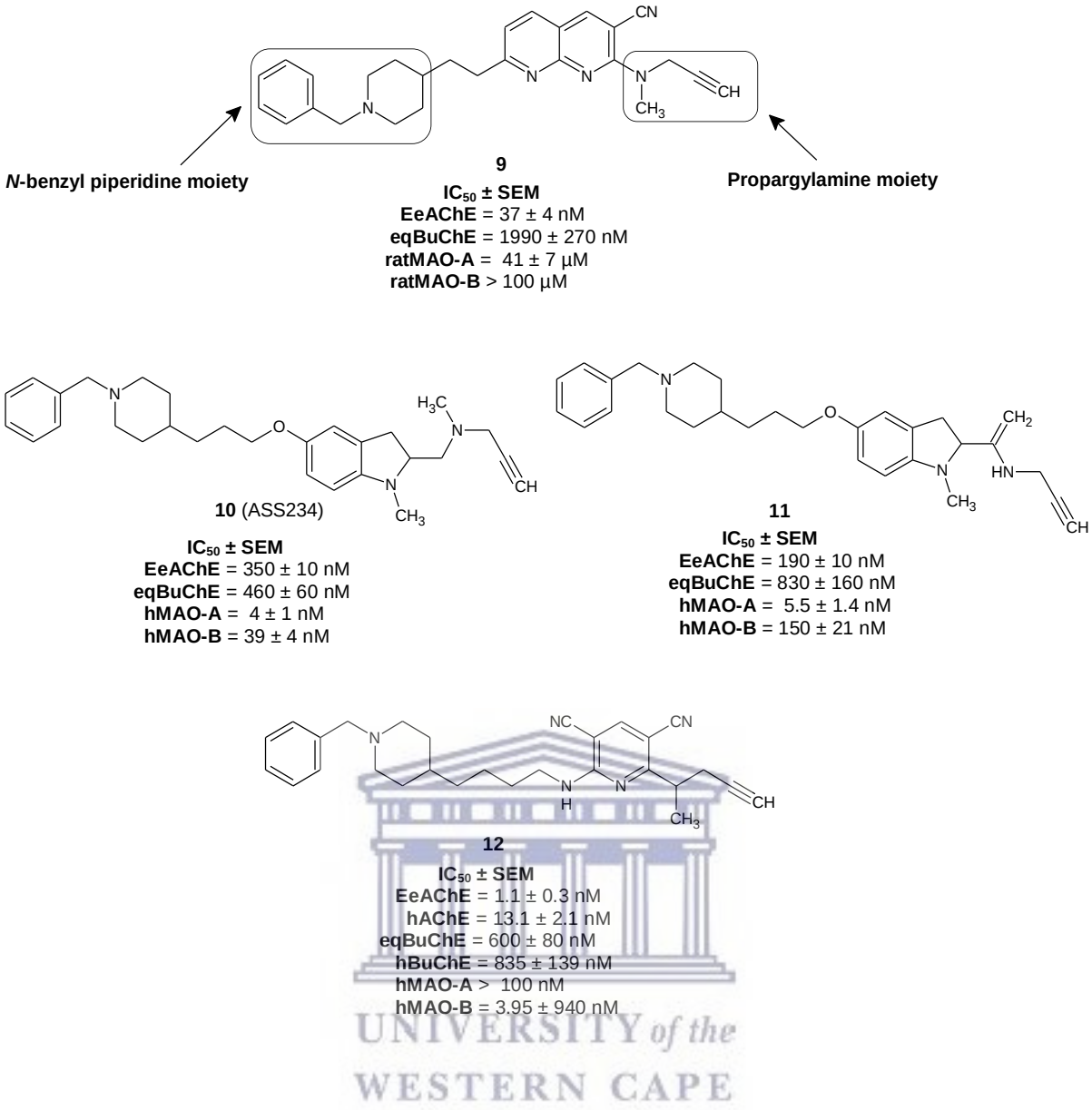

Figure 4. Compound 9 showing the *N*-benzyl piperidine and the propargylamine moieties as seen in donepezil (5) and PF9601N (8), respectively, and the structurally similar derivatives, 10 - 12. SEM: Standard error of the mean. Data taken from [58,61–62]

The group also noted the need for an appropriate length spacer between the *N*-benzyl piperidine and the propargylamine moieties to modulate AChE inhibition. The length of the spacer is reported to control the dual interaction of these moieties with both the catalytic active site (CAS) and peripheral anionic site (PAS) of the enzyme, improving inhibition when both binding sites are spatially targeted at the same time [58].

Using a similar approach, Bautista-Aguilera *et al.* (2014a) designed several hybrids of donepezil (**5**) and PF9601N (**8**) [64]. The hybrids are exemplified by ASS234 (**10**), which was shown to inhibit MAO A/B, AChE and BuChE enzymes (Figure 4) [61]. The IC_{50} values obtained after performing *in vitro* biological assays against EeAChE and eqBuChE using the Ellman method [63] and also against human MAO A/B following a fluorometric method [65]

indicated compound **11** to be a potent human MAO-A (hMAO-A, IC_{50} = 5.5 ±1.4 nM) and moderately potent hMAO-B (IC_{50} = 150 ±31 nM), EeAChE (IC_{50} = 190 ±10 nM), and eqBuChE (IC_{50} = 830 ±160 nM) inhibitor. Compared to **10**, the donepezileindolyl-based amine analog **11** was 1.8-fold more potent for the inhibition of AChE but 1.8-fold less active regarding BuChE inhibition, however their IC_{50} values were still comparable. To shed light on the orientation of the cholinesterase inhibitor **11** in both cholinesterases, molecular modeling studies were carried out using Autodock Vina® software [66] where a structure of EeAChE (PDB: 1C2B) was used for the *in silico* studies. Analysis of the intermolecular interactions indicated that the propargylamine group is likely an important feature for these derivatives to exhibit both AChE- and BuChE-inhibitory activities [64]. They also noted the linear conformation to be key in allowing compound **11** to span both the CAS and PAS sites, contributing to its superior binding affinity toward AChE. By virtue of theoretical studies using 3D-QSAR models, they noted the amine feature as imperative for activity as similar amides showed no activity [64]. The same was true for ChE inhibitory activity, as the amide derivatives had a less potent activity profile.

Bautista-Aguilera *et al.* (2014b) expanded on their series to afford a new series of donepezil and PF9601N hybrids connected through an appropriate linker [62]. When assayed for MAO inhibition against recombinant human MAO-A/B, compound **12** was shown to selectively inhibit hMAO-B (IC_{50} = 3.950 ±0.940 nM). The mechanism of hMAO-B inhibition by compound **12** was further characterized by employing dose-response curves (IC_{50}) with varied preincubation times. A time-dependent inhibition was observed and IC_{50} values were found to decrease in a time-dependent manner [62]. This observation and the failure to recover the initial inhibition of compound **12** after a 100-fold dilution in saturated-substrate concentration, suggested an irreversible MAO-B inhibition by compound **12**. Based on results obtained from performing inhibitory assays on EeAChE, human recombinant AChE (hAChE), eqBuChE and human recombinant BuChE (hBuChE), they reported compound **12** to be a highly active ChE inhibitor (EeAChE: IC_{50} = 1.1 ±0.3 nM; eqBuChE: IC_{50} = 600 ±80 nM; hAChE: IC_{50} = 13.1 ±2.1 nM; hBuChE: IC_{50} = 835 ±139 nM). Compared to the reference compound ASS234, compound **12** was 318-fold more potent for the inhibition of EeAChE, but 1.3-fold less active for the inhibition of eqBuChE. In comparison with donepezil, compound **12** was 11.8-fold and 11.5-fold more active at inhibiting EeAChE and eqBuChE, respectively [62]. Docking simulations of EeAChE (PDB: 1C2B) and compound **12** were performed and the ligand-enzyme binding interactions of this ChE inhibitor were investigated. From the docking study, Bautista-Aguilera and colleagues proposed two major binding modes at the enzyme-binding site (Figure 5). In both modes, compound **12** showed

an extended conformation and interacted simultaneously with both CAS and PAS sites of EeAChE.

Similar to observations made by Samadi *et al.* (2011), a linker of appropriate length was reported to facilitate the binding of both *N*-benzylpiperidine and indole-propargylamine moieties at CAS and PAS, respectively [62]. The approach of dually inhibiting the MAO and AChE enzymatic systems may find significant application in the treatment of NDs as compounds with such activity profiles may potentially serve as drugs for the treatment of PD and AD. While several authors seem to ascribe MAOI's to treating PD and AChEI's to AD, the last decade has seen the exploration of the use of MAO inhibitors as potential drugs for AD [14,67–69]. In fact, a clinical trial assessing the beneficial properties of selegiline, a MAO-B inhibitor, showed a cognition improving efficacy in subjects treated with donepezil, suggesting a synergistic effect [70]. This observation further suggests an interlink between the various patholological events implicated in NDs and the need for MTDLs as treatment strategies.

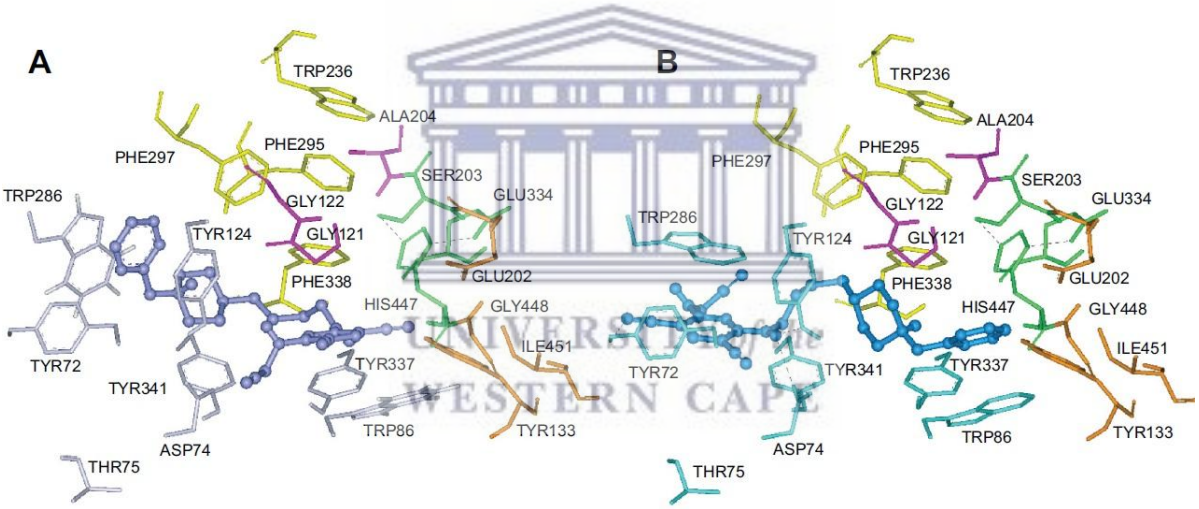

Figure 5. Binding modes A and B exhibited by compound 12. The compound is represented as violet and blue balls and sticks in the simulated binding mode **(A)** and **(B)**, respectively. Note that compound **12** interacts with both the peripheral anionic site site in both conformations (composed of amino acid residues shown in light violet in mode **(A)** and light blue in mode **(B)**) and catalytic active site site (composed of amino acid residues shown in green, pink and orange) of EeAChE from the Research Collaboratory for Structural Bioinformatics (Protein Data Bank: 1C2B). In yellow are amino acid residues making up the acyl binding pocket. Reproduced with permission from [62] © Dove Press Limited (2014).

For color images please see online www.future-science.com/doi/full/10.4155/FMC.15.12

2.2.2. MAO inhibition & calcium homeostasis modulation

Activation of the postsynaptic *N*-methyl-d-aspartate receptors (NMDAR), 2-amino-3-(3-hydroxy-5-methylisoxazol-4-yl)proprionate receptors and kainate receptors allows for opening of their associated ion channels to allow the influx of Ca^{2+} and Na^{+} ions. Calcium entry may also occur through *L*-type voltage gated calcium channels (VGCC) and result in both calcium overload and mitochondrial disruption [71]. Excessive influx of calcium can overwhelm Ca^{2+}-regulatory mechanisms and lead to excitotoxicity and cell death. This mechanism of apoptosis has led to the extensive development of NMDAR antagonists in the last few decades due to the neuroprotective potential such compounds may render [72]. While much progress has been made, the unfavorable side effect profiles of many lead compounds have seen them fail to surpass the clinical trials arena, leaving only a few to reach the market. Examples of drugs currently in use include nimodipine (**13**), which is known to halt/retard neuronal cell death evoked by focal cerebral ischemia [73], memantine (**14**), a noncompetitive and low-affinity NMDAR antagonist used in AD [74], and amantadine (**15**), a drug that is used in PD due to its beneficial effects on the NMDAR (Figure 6) [75]. Heteroatom substituted polycyclic cage amines are also receiving attention as potential scaffolds for the development of new drugs, with examples including NGP1–01 (**16**) that has been shown to have neuroprotective properties through VGCC blockade and NMDAR antagonistic activity [76]. The activity of these polycyclic compounds on the NMDAR and calcium channels is the basis of incorporating polycyclic moieties in analogues designed for neuroprotection [76]. A recent approach has seen the incorporation of the propargylamine moiety into the structures of such polycyclic compounds. As such, polycyclic propargylamine derivatives were synthesized and evaluated in an effort to potentially afford molecules with inherent MAO inhibitory capacity as well as calcium modulatory activity as exhibited by their parent polycyclic scaffolds [76,80–83].

In this regard, Duque *et al.* (2010) reported several polycyclic amines to have NMDAR antagonistic activity by measuring their effect on the increase in intracellular calcium evoked by glutamate or NMDA (both at 100 μM, in the presence of 10 μM of glycine) on rat cultured cerebellar granule neurons [77]. Although most compounds in their series of propargylamine derivatives were shown to be inactive, as seen with compound **17**, they reported compound **18** to have moderate NMDAR antagonism (IC_{50} = 34 ±2.3 μM, Figure 6). Following up on their work, the group synthesized a modified series, represented by compounds **19** and **20**, devoid of the hemiaminal unit seen in both compounds **17** and **18** [78]. The presence of a hemiaminal subunit in these compounds is anticipated to result in a compromised stability and therefore hinder the further development of such compounds as therapeutic agents [78].

This is derived from the knowledge that NGP1–01 (**16**), containing an hemiaminal unit [76], decomposes easily in aqueous medium [84,85]. Though compounds **19** and **20** were 12.9-fold and 18.3-fold less potent than memantine (**14**) for NMDAR antagonism, respectively, when compared with amantadine (**15**) they exhibited a 4.7-fold and 3.3-fold more potent activity, respectively.

Several interesting structure activity relationships can be deduced from these polycyclic compounds. For example comparison of the activity profile of compounds **17** and **18** seems to suggest that attaching an ethyl moiety to the polycyclic system of these compounds results in reduced Glutamate and NMDAR antagonism (Figure 6). In addition, compound **20**, which is devoid of the hemianimal unit but contains a methyl group on the polycyclic system, shows improved NMDAR antagonism (IC_{50} = 27.5 ±13.2 μM) when compared with the structurally similar compound **18** (IC_{50} = 34 ±2.3 μM). An interesting observation is that the inclusion of a propargyl moiety, as seen in compound **20**, might be responsible for the decreased NMDAR antagonism of this compound when compared with compound **19** (IC_{50} = 19.4 ±3.3 μM), which lacks this moiety.

Based on the same concept, Zindo *et al.* (2014) described polycyclic propargylamine derivatives represented by compounds **21** and **22** [79]. These compounds were assessed for calcium flux modulation by virtue of NMDAR antagonism and VGCC blockade in freshly prepared synaptoneurosomes [86] using the fluorescent ratiometric calcium indicator, FURA2-AM (Figure 6). Although their findings showed compound **21** to be inactive on both these sites when screened at 100 μM, they noticed the positive effect of having a methyl group directly attached to the polycyclic structure of **21** to afford **22**. This substitution rendered the methyl derivative **(22)** an improved inhibitory activity profile of 26 and 38% on the VGCC and NMDAR, respectively [79]. Similarly, amantadine (**15**) is about 60 times less active as an NMDAR antagonist than its dimethyl derivative, memantine (**14**) [77]. Although these compounds (**17–22**) were also designed to render MAO inhibitory activity by virtue of incorporating a propargylamine moiety, they showed minimal or no MAO-B inhibitory activity when tested at 10, 50 and 300 μM. The lack of MAO-B inhibitory activity of these compounds is most likely attributed to their failure to adequately occupy the MAO enzyme cavity and form productive interactions with the FAD (flavin adenine dinucleotide) co-factor as shown in Figure 7.

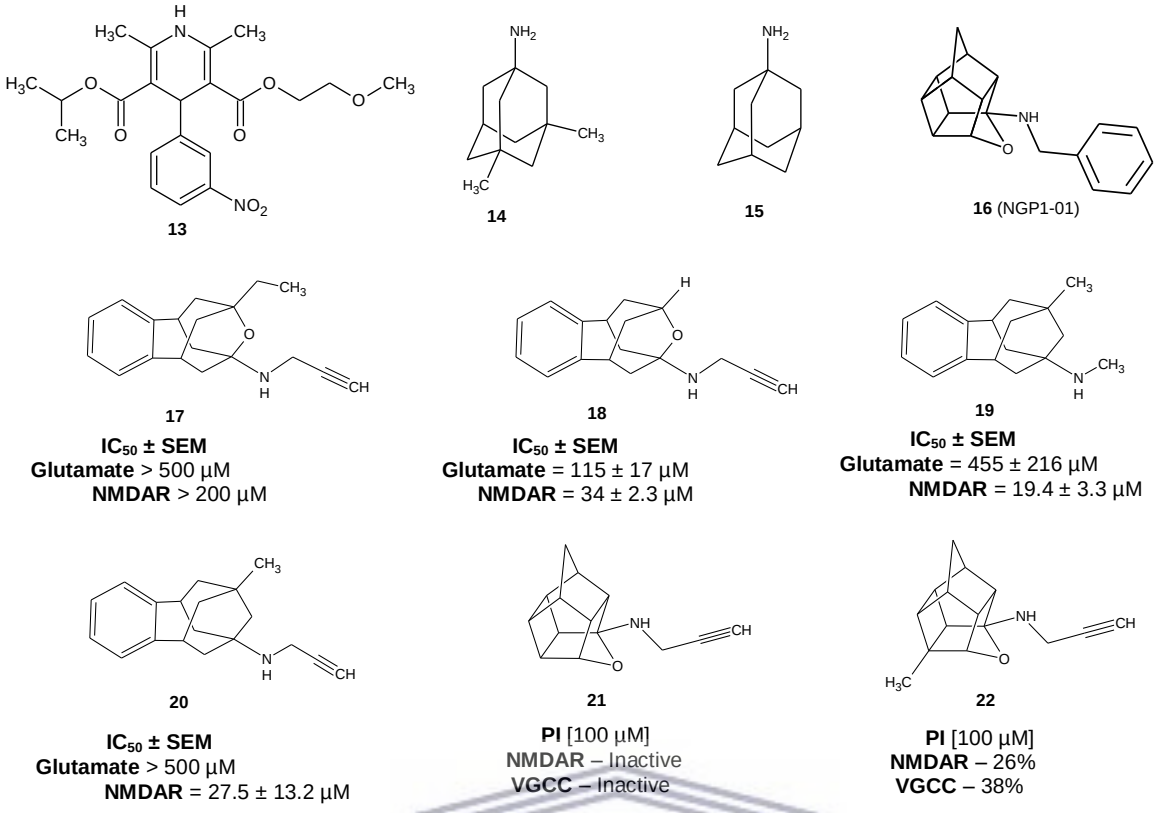

Figure 6. *N*-methyl-d-aspartate receptor and calcium channel modulators. Nimodipine (**13**), memantine (**14**), amantadine (**15**) and NGP1–01 (**16**); Polycyclic propargylamine derived compounds (**17**–**22**). NMDAR: *N*-methyl-d-aspartate receptors; PI: Percentage inhibition; SEM: Standard error of the mean; VGCC: Voltage gated calcium channels. Data taken from [77–79].

Research on such heteroatom substituted polycyclic cage amines is gradually receiving increasing attention. These compounds can be used to modify and improve the pharmacokinetic and pharmacodynamic properties of drugs and it is apparent from the literature that the polycyclic cage is useful as both a scaffold for side-chain attachment as well as for improving a drug's lipophilicity [88]. This lipophilicity enhances a drug's transport across cellular membranes, including the selectively permeable blood–brain barrier, and increases its affinity for lipophilic regions in target proteins [88,89]. The brain being the drug target site for treating NDs, the significance of these polycyclic moieties is clear. In addition polycyclic moieties could afford metabolic stability, thereby prolonging the pharmacological effect of a drug, leading to a reduction in dosing frequency and improved patient compliance [90].

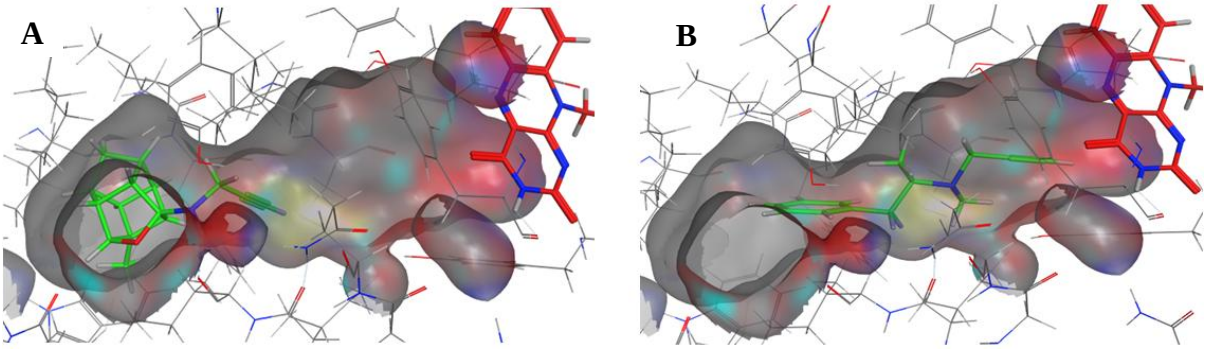

Figure 7. Inactive compound 22 and selegiline. (A) The inactive compound 22 and **(B)** selegiline a known irreversible and selective MAO-B inhibitor in a computer simulated MAO-B enzyme cavity (PDB: 2V5Z). Note that compound 22 merely occupies the entrance cavity of the enzyme, unlike selegiline, that traverses deeper into the enzyme cavity to proximate the flavin adenine dinucleotide co-factor and allow for binding interactions which result in MAO-B activity. The compounds are shown in green with the flavin adenine dinucleotide co-factor indicated in red. Generated from Molecular Operating Environment software [87] For color images please see online www.future-science.com/doi/full/10.4155/FMC.15.12

2.2.3. MAO inhibition & metal homeostasis

The increase in brain levels of copper, zinc and particularly iron is reported to actively contribute to the formation of senile plaques by generating more ROS through the Aβ1–42-metal complex [91]. Although iron is an essential element in the metabolism of all cells, its homeostasis is crucial in relation to PD. Beneficially, the metal acts as a co-factor that dose dependently stimulates tyrosine hydroxylase, the enzyme at the rate-limiting step in the synthesis of dopamine [92]. Disturbances in brain iron homeostasis, which is usually a tightly regulated process, play a significant role in the death of dopaminergic neurons [93]. This mechanism of apoptosis is further confirmed by the presence of accumulated iron in affected neurons and associated microglia in the substantia nigra of PD patients [94–96]. The additional free-iron has the capacity to generate ROS, promote the aggregation of α-synuclein protein and exacerbate or even cause neurodegeneration [93]. Iron chelators would therefore be beneficial in the attenuation of progression of PD and other neurodegenerative diseases, such as AD and HD [97]. The correlation between iron accumulation in the brain and progression of ND's has logically led to the exploration of iron chelators as possible neuroprotective agents that could help slow the development of the disease by scavenging unbound, free radical-enhancing iron in the brain [93]. Such an approach has been evidently successful in VK 28 (**23**, Figure 8), a potent BBB permeable iron chelator that exerts neuroprotective activity against 6-OHDA toxicity in rats, when given either by intravenous or intraperitoneal routes, without altering peripheral iron metabolism [98].

M30 (**24**) is a multitarget iron chelator designed by Zheng *et al.* (2005) (Figure 8) [106]. This molecule was designed by replacing the piperazine moiety of the known metal chelator, VK 28 (**23**), with a propargylamine moiety. In addition to its 'iron chelator radical scavenging' properties and *in vivo* brain selective inhibition of MAO-A and MAO-B [(IC_{50}, MAO-A = 0.037 ±0.02 μM; MAO-B = 0.057 ±0.01 μM)] [99,100], M30 showed significant dopaminergic neuroprotective and neurorestorative activities in the classical MPTP (1-methyl-4-phenyl-1,2,3,6-tetrahydropyridine) [99] and lactacystin [107] animal models. Among the many other unique properties demonstrated by M30, this compound has shown significant cognitive enhancement in double transgenic Swedish Mutation/PSI1 mice [101–103] suggesting potential benefits in AD. It also possesses antioxidant activities, reduces apoptosis and ameliorates the fall in mitochondrial membrane potential resulting from oxidative stress in neuronal cell cultures [101–103].

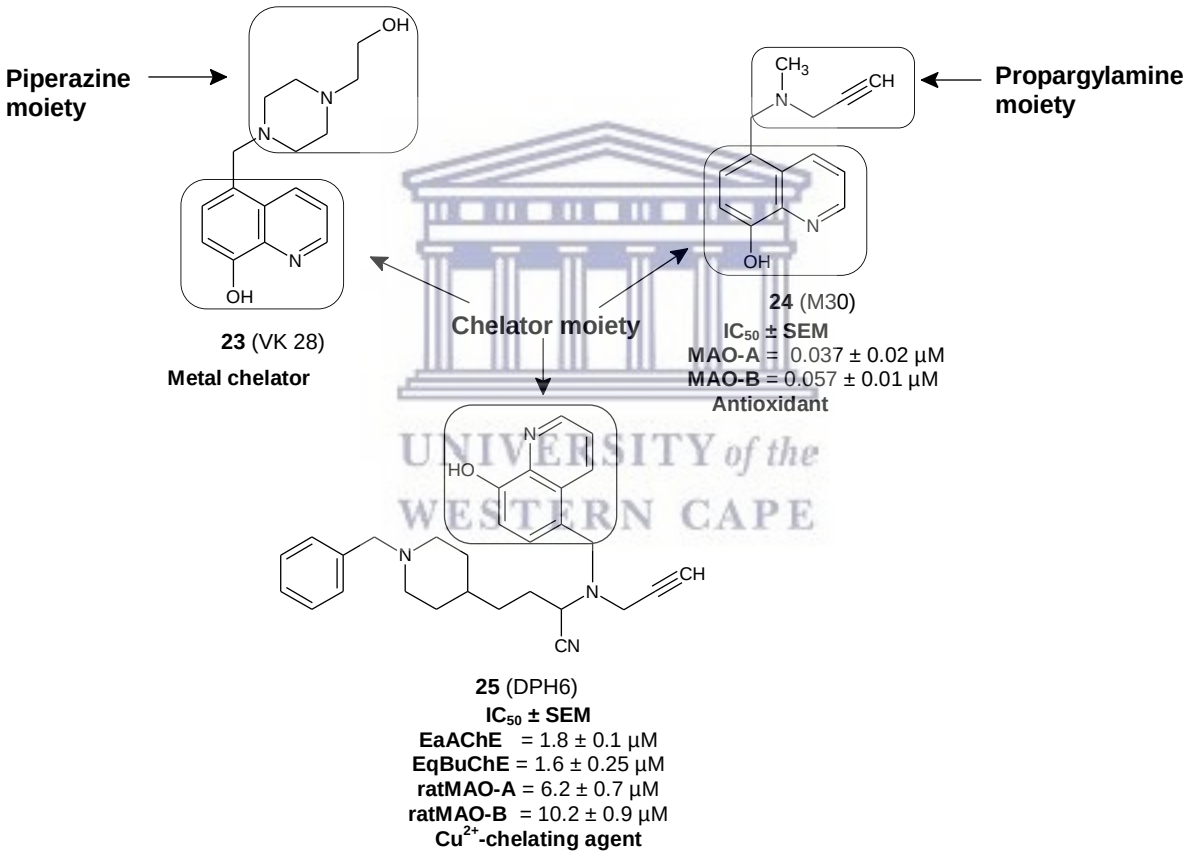

Figure 8. Metal chelator VK 28 (23) with the piperazine moiety replaced by a propargylamine moiety to afford M30 (24) and compound 25, a new multifunctional MAO-I, ChE-I and metal chelating agent. SEM: Standard error of the mean. Data taken from [99–105].

M30 also has antidepressant activity similar to that of amitriptyline and moclobemide but with an additional advantage of not causing clinically significant potentiation of the 'pressor

response' to oral tyramine [104], a common adverse effect associated with ingesting tyramine containing foods together with MAOI's.

2.2.4. MAO inhibition, metal homeostasis & cholinesterase inhibition

Following up on their work on ASS234 (**10**), which was shown to inhibit Aβ aggregation, possess antioxidant properties, protect from Aβ-induced apoptosis *in vitro* and to inhibit MAO A/B, AChE and BuChE enzymes [61], Wang *et al.* (2014) designed DPH6 (**25**), a multifunctional lead molecule with an improved therapeutic profile, for the potential treatment of AD (Figure 8) [105]. This donepezil, propargylamine and 8-hydroxyquinoline (DPH) hybrid was a result of the juxtaposition of donepezil (**5**) and M30 (**24**). DPH6 exhibited some MAO inhibitory effect on both enzyme isoforms (MAO-A IC_{50} = 6.2 ±0.7 μM; MAO-B IC_{50} = 10.2 ±0.9 μM) upon evaluation using [14C]-5HT and [14C]-phenylethylamine as substrates, respectively [108]. This activity however was 166- and 179-fold less potent, respectively, than M30 [109]. From dose-response curves, DPH6 showed nonselective MAO inhibition in comparison to standard selective MAO-A and MAO-B inhibitors clorgyline [110] and selegiline (**1**) [111], respectively. When assessed for *in vitro* cholinesterase inhibitory activity using the Ellman method [63] and Lineweaver-Burk reciprocal plots, DPH6 was suggested to be a mixed type reversible inhibitor (K_i = 1.21 ±0.25 μM) of EeAChE (IC_{50} = 1.8 ±0.1 μM) and eqBuChE (IC_{50} = 1.6 ±0.25 μM). The need for an appropriate chain length for connecting the *N*-benzyl-piperidin-4'-yl residue to the propargylamine moiety was evident in their series of compounds, with the three carbon spacer as in DPH6, being reported to confer the molecule the greatest cholinesterase inhibitory activity. This allows the compound to interact simultaneously with both catalytic and peripheral site of EeAChE. Although less active as an EeAChE inhibitor than donepezil (**5**), DPH6 exhibited a 4.5-fold greater activity at inhibiting eqBuChE and when compared with one of its lead compounds M30, it was 64-fold more potent at inhibiting both cholinesterases, a feature the lead metal chelator lacks. In addition, Wang and colleagues discovered an essential role for the cyano group in properly positioning the ligand by hydrogen bond formation with the amino acid residues of the binding sites of AChE, BuChE and MAO-A enzymes [105]. Compounds lacking this cyano motif in their series showed drastically lowered inhibitory activities. DPH6 was also assessed for metal-chelating properties toward the biometals Cu(II), Fe(III) and Zn(II) by UV-VIS spectrometry and significant variations on complexation times were observed depending on the metal. The observed DPH6-Cu(II) spectral differences occurring after only 5-min of incubation of DPH6

with Cu(II) indicated preferential and selective binding for Cu(II) salts compared with Zn(II) and Fe(II) which required an incubation time of at least 1 h for complex formation. By use of Job's method [112], a molar fraction of 0.65 for DPH6 complexing Cu(II) was established, revealing a 2:1 stoichiometry for the complex formation. While DPH6 failed to show closely comparable cholinesterase inhibitory activity to donepezil, it was shown to be less toxic than donepezil at high concentrations in an *in vitro* model of toxicity in HepG2 cells [105]. At these high concentrations donepezil is known to produce a wide assortment of side effects including bradycardia, nausea, diarrhea, loss of appetite and stomach pain [113]. Important to note is the similar cell viability profile displayed by DPH6 and donepezil at low concentrations [105]. DPH6's significant interaction in the two key enzymatic systems implicated in neurodegeneration combined with its reported metal chelating properties make this an attractive compound in neurodegenerative drug design.

2.2.5. MAO inhibition, antioxidant & free radical scavenging

Considerable evidence has shown oxidative stress and oxidative damage, mostly due to the actions of nitric oxide (NO), to be implicated in NDs [114]. Indirect evidence similarly implicates NO in the mechanisms underlying nigral cell degeneration as nitric oxide synthase (NOS) inhibitors protect against MPTP/MPP^+- induced experimental PD in mice and monkeys [115,116]. The toxicity associated with NO is due to its reactivity and its reaction with superoxide to form peroxynitrite ($ONOO^-$), a highly oxidizing agent that also degrades to form hydroxyl radicals, among other radical species [117]. This reactivity of NO and the subsequent oxidative stress are thought to be important contributors to neuronal damage in NDs as they initiate and promote the oxidation of different cellular components such as lipids, proteins and DNA, causing the loss of neurons in different brain areas [114]. In this regard, molecules with the capacity to reduce oxidative stress and thereby decrease the rate of neuronal degeneration may find potential as neuroprotective agents. As discussed under section 2.2.1., PF9601N (**8**) was shown to have neuroprotective effects in several experimental models of PD. Although designed as a MAO-B inhibitor [118,119], PF9601N has in the last decade been shown to protect nigrostriatal dopamine neurons against MPTP neurotoxicity in C57BL/6 adult mice [120], protect rat nigral neurons after 6-OHDA striatal lesion [121] and also demonstrated *in vitro* antioxidant neuroprotective effects in SHSY5Y dopaminergic cells [122]. Following from this established multiple activities of PF9601N, Bellik *et al.* (2010) investigated its protective effects on the NO system by measuring the compounds' effect on peroxynitritemediated oxidation and influence on both neuronal and

inducible NOS isoform activity [123]. From their findings, they postulated the presence of the two reactive nitrogen atoms in the structures of PF9601N and its CYP-dependent metabolite, FA72, to be imperative for reaction with $ONOO^-$. This notion emanated from the observation that selegiline (**1**), which lacks an indole nitrogen atom, showed approximately 3-fold less activity for peroxynitrite inhibition. In a similar manner, PF9601N and FA72 were more efficient than selegiline in inhibiting rat brain NOS. Although the presence of the propargylamine moiety seemed to be responsible for the decreased inducible NOS inhibitory effect observed for selegiline and PF9601N, its contribution to the MAO inhibitory capacity of these molecules remains a preferred feature. In addition to its more effective MAO-B inhibition and its antiapoptotic activity [124], PF9601N also undergoes CYP-dependent metabolism in the brain [125] affording its active metabolite FA72 which, like its precursor molecule, inhibits NOS and forms interactions with $ONOO^-$. These unique features therefore suggest PF9601N to be a better neuroprotective compound than selegiline.

2.2.6. MAO inhibition & adenosine receptor antagonism

Adenosine receptors (ARs) have emerged as potential targets for the treatment of PD in recent years [9]. An approach of dually antagonizing A_1- and A_{2A}ARs was found to be highly effective in different models of PD [126,127]. For example, Mihara *et al.* (2007) reported on a dual A_1/A_{2A}AR antagonist which decreased neuronal degeneration and improved motor impairment *via* A_{2A}AR blockade, and showed positive effects on cognitive impairment associated with the disease by blocking A_1ARs [128]. In Japan, the 8-styrylxanthine derivative istradefylline (Nouriast®) an adenosine A_{2A}AR antagonist, was recently approved for use as an adjunct treatment for PD [129]. Several other selective AR antagonists are being explored in the preclinical and clinical trials arena for potential use in NDs [9,130]. Petzer *et al.* (2009) also suggested a multitarget approach that entails inhibiting both ARs and the MAO-B enzyme which may be more advantageous for the treatment of PD [131]. This notion is supported by findings from preclinical studies that have shown A_1 and A_{2A}AR antagonists as well as MAO-B inhibitors to potentially exhibit neuroprotective effects [132–135]. While A_{2A} antagonism and MAO-B inhibition may confer anti-PD effects combined with neuroprotective properties, A_1 antagonism may ameliorate cognitive deficits associated with the disease [136]. Utilizing this strategy, Koch *et al.* (2013) synthesized and evaluated the tetrahydropyridione-based propargylamine derivatives **27** and **28** (Figure 9) [136]. These compounds were a result of structural modifications to **26**, a tricyclic compound they previously reported to be a relatively potent and highly selective rat A_{2A}AR antagonist [K_i-

value of 0.147 μM] [137], but with a lower affinity at human A_{2A}ARs. The resultant compounds **27** and **28** were evaluated in radioligand binding assays for their affinity at A_1AR in rat brain cortical membrane and at A_{2A}ARs in rat brain striatal membrane preparations, then further investigated at human A_1 and A_{2A}ARs recombinantly expressed in Chinese hamster ovary cells. Based on their findings, Koch *et al.*, reported compound **27** to be a potent dually active A_1/A_{2A} AR antagonist (K_i, human receptors, A_1: 0.249 μM, A2A: 0.253 μM), a significant improvement on the low affinity for human A_{2A}AR reported for the lead compound **26**.

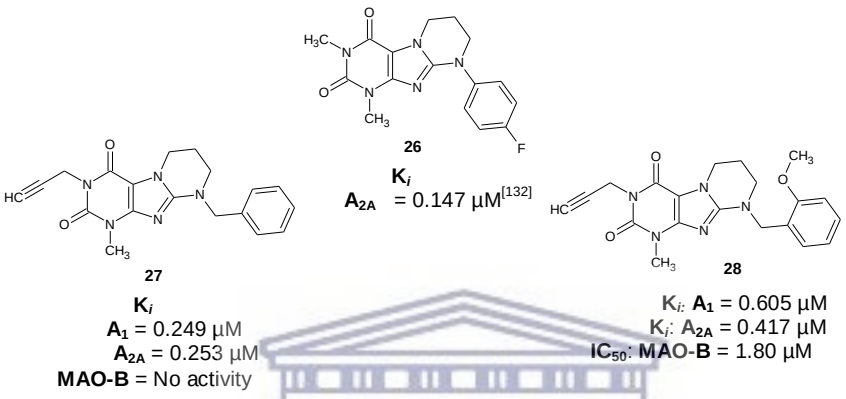

Figure 9: **Tetrahydropyridione based propargylamine derivatives 26 – 28**. Data taken from [136,137].

To ascertain selectivity for the various AR's, these compounds were additionally investigated in binding studies at human A_{2B} and A_3ARs expressed in Chinese hamster ovary cells. Among the structure activity relationships reported by Koch *et al.* for their series of propargyl tetrahydropyrimidione's, they noted the unsubstituted *N*9-benzyl derivative **27** to be a relatively potent dual human A_1/A_{2A}AR antagonist with only low affinity at the A_{2B}AR. The introduction of a methoxy group in the *ortho*-position of the benzyl ring (compound **28**) resulted in a decrease of A_1 and A_{2B}AR affinity, but in an increase in affinity for the A_3AR [136]. A more attractive activity profile was seen in compound **28** which showed triple-target inhibition (K_i A_1: 0.605 μM, K_i A_{2A}: 0.417 μM, IC_{50} MAO-B: 1.80 μM). By exhibiting dual (A_1/A_{2A}, **27**) or triple (A_1/A_{2A}/MAO-B, **28**) activity, which is expected to result in additive or even synergistic effect, these compounds may be relevant considerations for treatment of neurodegenerative diseases.

2.3. Other multifunctional strategies

2.3.1. Cholinesterase & apoptosis inhibition

Samadi *et al.* (2011) successfully synthesized compound **29** by a Friedländer-type reaction (Figure 10) [138]. This tacrine-based propargylamine derivative was assessed for its neuroprotective potential against an oxidative stress model in which the mitochondria in SH-SY5Y neuroblastoma cells were stressed with a mixture of oligomycin-A/rotenone [63]. The results showed compound **29** to have a modest neuroprotective effect against oxidative stress, in the same range of the well-known reference antioxidant *N*-acetylcysteine [139]. This molecule was also evaluated as an inhibitor of EeAChE, bovine erythrocytes AChE (beAChE), and eqBuChE. It was not surprising to note the ability of compound **29** to inhibit beAChE (IC_{50} = 1.53 ±0.04 μM), EeAChE (IC_{50} = 0.030 ±0.003 μM) and eqBuChE (IC_{50} = 2.6 ±0.3 μM) as it contains a pharmacophoric group resembling tacrine, a known AChE inhibitor. This finding suggests the structural modifications of the tacrine (**2**) molecule, specifically the inclusion of a propargylamine moiety, to be acceptable for retaining the inherent AChE inhibitory capacity and yet provide the resultant molecule with *in vitro* neuroprotection against oxidative stress.

2.3.2. Calcium homeostasis & antioxidant effects

The 1,4-dihydropyridine (1,4-DHP) functionality is a key scaffold used in drug design and a wide variety of pharmacological activities have been reported, such as cardioprotective [142,143], anti-inflammatory, anti-ischemic, neuroprotective and many other actions [144]. This may particularly be due to the calcium channel modulating properties of 1,4-DHP. Based on the above considerations, Rucinns *et al.* (2014) synthesized and evaluated a series of 1,4-DHP derivatives containing a cationic pyridine moiety at position 4, and a propargylamine group as a substituent at position 1 of the 1,4-DHP cycle as potential multifunctional ligands [140]. Among the novel derivatives reported in their work, compound **30** (Figure 10) demonstrated significant calcium antagonistic properties in neuroblastoma SH-SY5Y cell lines (IC_{50} = 14 μM) when compared with known calcium channel inhibitors amlodipine and nimodipine (**13**) (IC_{50} = 11 μM and IC_{50} = 53 μM, respectively). This compound also showed a slight total antioxidant effect, did not affect mitochondrial functioning and no toxicity was observed *in vivo*.

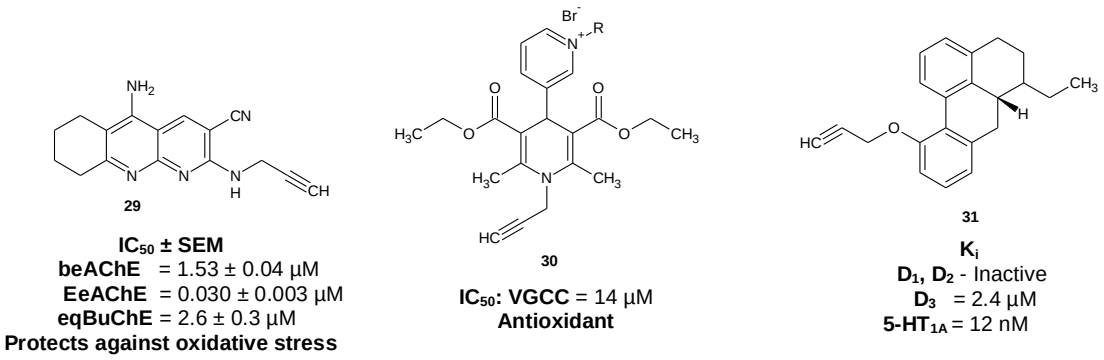

Figure 10. Compounds 29 – 31, each having distinct structural features and multiple activities.
5-HT: Serotonin receptor; D: Dopamine receptor; SEM: Standard error of the mean; VGCC: Voltage gated calcium channels. Data taken from [138,140–141].

2.3.3. Serotonin 1_A receptor & dopamine 3 receptor agonism

The D_3 receptor is implicated in a variety of brain functions and is a promising therapeutic target for a number of neurological disorders, including PD [145–150]. Therefore selective D_3 receptor agonists will be of therapeutic value for patients suffering from PD. For example, the well-known anti-PD drug pramipexole is a D_3 receptor agonist currently in use, but with limited dopamine receptor selectivity [12,151]. In addition, a number of studies have indicated the serotonin 1_A (5-HT_{1A}) receptor to be associated with neuroprotection [152,153], PD [154–156] and AD [157]. Agents selectively acting at both D_3 and 5-HT_{1A} receptors may thus hold significant therapeutic benefit in NDs. The 11-propargyloxyaporphine derivative (**31**) developed by Liu *et al.* (2010), displayed high affinity for the 5-HT_{1A} receptor with a K_i value of 14.0 nM (Figure 10) [141]. The [35S]GTPγS function assay indicated that this compound is a partial 5-HT_{1A} receptor agonist. Compared to its 11-hydroxylaporphine analogue, a fourfold increase in 5-HT_{1A} receptor activity was observed with the incorporation of the propargyl moiety at position 11. The propargyl moiety may also improve and add to the neuroprotective ability of this compound [20–22]. Compound **31** was also evaluated at the dopamine receptor and showed no affinity at either the D_1 or D_2 receptor. However, significant potency was observed at the D_3 receptor (K_i = 2.4 μM). In view of the promising role of the 5-HT_{1A} receptor and the D_3 receptor in NDs, such a D_3/5-HT_{1A} dual action propargyl-incorporated compound may find use in the treatment of NDs.

Although the compounds reported in sections 2.3.1 to 2.3.3 were not assessed for potential MAO inhibitory activity it will be interesting to investigate the MAO and antiapoptotic activity of these propargyl containing derivatives.

2.4. Conclusion

The complex pathogenesis and aetiology of neurodegenerative diseases make it clear that drugs targeting a single receptor or enzymatic system will not result in successful retardation and treatment of these multifactorial diseases. This is futher evident in that drugs used in the symptomatic treatment of these diseases fail to render sufficient neuroprotective and/or neurorestorative activity. The advent of the multitarget-directed ligand approach has however seen the development of compounds that combine symptomatic treatment and neuroprotection in one molecule by acting simultaneously on different receptors and target sites implicated in NDs. Compounds bearing the propargylamine function have received significant attention based on the neuroprotective ability observed for the MAO-B inhibitors selegiline and rasagiline. This has led to its incorporation into many drug-like compounds designed for neuroprotection and to afford molecules with broader therapeutic profiles to potentially meet the curative needs of the multifactorial NDs. The role of the propargylamine moiety in providing neuronal and mitochondrial protective properties [20–22] antiapoptosis activity [23–25] and Aβ aggregation inhibition [26] is clear in the literature. Its direct role in the discussed multifunctional compounds to target specific pathological sites however remains uncertain. This is partially due to the chemical diversity of the compounds as well as the molecular and conformational requirements for interaction with the diverse biological systems.

2.5. Future perspective

Much progress has been made in developing compounds that exhibit neurorestorative/neuroprotective activity for treatment of NDs and for some drug targets, the propargylamine moiety has proven to be a key feature. The propargylamine derivatives developed in the last few decades show promising potential for application in clinical use and further exploration of these compounds with a focus on the following aspects is anticipated:

- Despite the wide array of activities reported, the exact mechanisms in which most of these compounds exhibit their respective biological actions still remain speculative and mechanistic studies are becoming essential to define the role of the propargyl moiety in the activity of these compounds. Using x-ray crystallography to identify the molecular interactions of the ligand and receptor/enzyme should lead to better insight with regards to the binding of these structures to specific sites and bioisosteric

substitution of the propargylamine moiety may confirm the pharmacophoric value of this group in neuroprotective drug design;

- Pharmacokinetic studies to establish ADME properties of these structures are imperative for further development and blood–brain barrier permeation is an obvious requirement. Here lipophilicity and other characteristics determining the ability of these compounds to cross this barrier and reach their target sites in the brain would be essential;

- Though many of the discussed compounds have been reported to exhibit significant multifunctional activity based on *in vitro* and *in vivo* findings, not many have thus far progressed to the clinical trials arena. An exception being Ladostigil which is presently in year two of a three year Phase 2b clinical trial. Interim results from 200 patients diagnosed with mild cognitive impairment that have completed at least one year of treatment showed no serious or unexpected adverse events related to the drug, or safety issues preventing continuation of the trial. Interim results also point to a positive trend in the efficacy of the drug. This includes reduced loss of brain volume as determined by MRI, improved immune system parameters and trends in improvement of cognitive parameters [158];

- Establishing the exact pathophysiology of NDs is vital, yet remains a challenge. A well described disease pathophysiology will shed light on the 'ideal' combination of drug target sites to consider when designing the ultimate drug for each of the defined neurodegenerative diseases. With growing insight into the pathogenesis of neurodegeneration and with the use of computer simulation software, the ultimate MTDL could potentially be designed.

Normal rate of progress in biological and medicinal chemistry techniques and application of sound drug design strategies should therefore in the near future lead to the development of more specific and effective neuroprotective agents. The following decade will no doubt see the development of more tailored drug ligands that may confer the desired, or at least improved, therapeutic profile lacking in currently available treatments for neuronal diseases. This will include multifunctional drugs or multitarget-directed ligands to address the multifactorial aetiology of the neurodegenerative diseases.

2.6. Executive summary

Background: propargylamine in treatment of neurodegenerative diseases

• The multifactorial nature of neurodegenerative diseases (ND) suggests that targeting any single mechanism will not result in successful retardation of the disease progression and 'single-site-targeting' drugs have failed to render sufficient neuroprotective and/or neurorestorative activity.

• More effective therapy would result from the use of multifunctional compounds able to intervene in the different pathological events underlying the aetiology of neuronal disorders.

• The success of selegiline and rasagiline in the treatment of Parkinson's disease (PD) has led to growing research interest and exploration of the neuroprotective ability of compounds bearing the propargylamine function to serve as multitarget-directed ligands.

Propargylamine in MAO & cholinesterase inhibition

• Excessive deamination of neurotransmitters by MAO enzymes acts indirectly as a trigger to the apoptotic process and also gives rise to some of the signs and symptoms associated with these disorders.

• Low levels of acetylcholine and the activity of cholinerasterase enzymes play a significant role in the pathophysiology of NDs such as Alzheimer's disease (AD).

• Combining the structural features of donepezil and PF9601N provided a drug compound that was shown to selectively inhibit hMAO-B and to be a highly active ChE inhibitor. A linker of appropriate length was reported to facilitate the binding of both the *N*-benzylpiperidine and indole-propargylamine moieties of this compound at the CAS and PAS of AChE, respectively.

Propargylamine in MAO inhibition & calcium homeostasis modulation

• Activation of the postsynaptic NMDA receptors and kainate receptors allows for opening of the associated ion channels to allow the influx of Ca^{2+} and Na^{+} ions. Excessive influx of calcium may also occur through VGCC and can overwhelm Ca^{2+}-regulatory mechanisms leading to excitotoxicity and ultimately cell death.

• Polycyclic propargylamine derivatives showed promising inhibitory activity on the VGCC and NMDAR and inclusion of a methyl group directly attached to the polycyclic structure of the derivative rendered improved activity.

• The limited MAO-B inhibitory activity of the polycyclic propargylamine derivatives is attributed to their failure to adequately occupy the MAO enzyme cavity and form productive

interactions with the FAD cofactor.

Propargylamine in MAO inhibition, metal homeostasis & cholinesterase inhibition

• Disturbances in brain iron homeostasis, which is usually a tightly regulated process, play a significant role in the death of dopaminergic neurons.

• M30, a multitarget iron chelator showed *in vivo* brain selective inhibition of MAO-A and MAO-B in addition to its iron chelator radical scavenging properties without clinically significant potentiation of the pressor response to oral tyramine.

• DPH6, a multifunctional molecule with an improved therapeutic profile for the treatment of AD exhibited MAO inhibitory effect on both MAO isoforms and was suggested to be a mixed type reversible inhibitor of EeAChE and eqBuChE. It also exhibited Cu^{2+}-chelating properties and was found to be less toxic than donepezil at high concentrations in HepG2 cells.

Propargylamine in MAO inhibition & adenosine receptor antagonism

• The emergence of adenosine receptors (AR) as potential targets for the treatment of PD led to the synthesis of tetrahydropyridione based propargylamine derivatives which were found to be triple-target antagonist/inhibitors on A_{1AR}, A_{2A} and MAO-B.

Serotonin 1_A receptor & dopamine 3 receptor agonism

• The D_3 receptor and serotonin 1_A ($5\text{-}HT_{1A}$) receptor have been implicated in a variety of brain functions, and are promising therapeutic targets for a number of neurological disorders. The D_3/$5\text{-}HT_{1A}$ dual action shown by a propargyl-incorporated compound developed could find application in the treatment of NDs.

Financial & competing interests disclosure

The authors have no relevant affiliations or financial involvement with any organization or entity with a financial interest in or financial conflict with the subject matter or materials discussed in the manuscript. This includes employment, consultancies, honoraria, stock ownership or options, expert testimony, grants or patents received or pending, or royalties. No writing assistance was utilized in the production of this manuscript.

Author Contributions

F.T.Z performed the literature review and drafted the manuscript. J.J. and S.F.M. contributed to the final version of the manuscript.

References

Papers of special note have been highlighted as:

- **of interest**

[1] *Experimental and Clinical Neurotoxicology.* Spencer PS, Schaumburg HH, Ludolph AC (Eds). Oxford University Press, Oxford, UK (2000).

[2] Bayer A, Reban J. *Alzheimer's Disease and Relative Conditions.* MEDEA Press, Czech Republic, 192–208 (2004).

[3] Dauer W, Przedborski S. Parkinson's disease: mechanisms and models. *Neuron* 39(6), 889–909 (2003).

[4] Baker GB, Reynolds GP. Biogenic amines and their metabolites in Alzheimer's disease: noradrenaline, 5-hydroxytryptamine and 5-hydroxyindole-3-acetic acid are depleted in the hippocampus but not in substantia innominata. *Neurosci. Lett.* 100(1–3), 335–339 (1989).

[5] Cross AJ. Serotonin in Alzheimer type dementia and other dementing illnesses. *Ann. NY Acad. Sci.* 600, 405–415 (1990).

[6] Swerdlow RH, Khan SM. The Alzheimer's disease mitochondrial cascade hypotheses: an update. *Exp. Neurol.* 218(2), 308–315 (2009).

[7] Coyle JT, Puttfarcken P. Oxidative stress, glutamate and neurodegenerative disorders. *Science* 262(5134), 689–695 (1993).

[8] Huang X, Moir RD, Tanzi RE, Bush AI, Rogers JT. Redoxactive metals, oxidative stress and Alzheimer's disease pathology. *Ann. NY Acad. Sci.* 1012, 153–163 (2004).

- **Discusses the emergence of redox-active metals as key players in Alzheimer's disease (AD) pathogenesis.**

[9] Hauser RA. Future treatments for Parkinson's disease: surfing the PD pipeline. *Int. J. Neurosci.* 121(2), 53–62 (2011).

- **Review on selected new therapies in clinical development for motor features or treatment complications of Parkinson's disease (PD), and some that may slow disease progression.**

[10] Alessandri B, Tsuchida E, Bullock RM. The neuroprotective effect of a new serotonin receptor agonist, BAY X3702, upon focal ischemic brain damage caused by acute subdural hematoma in the rat. *Brain Res.* 845(2), 232–235 (1999).

[11] Kamei K, Maeda N, Ogino R *et al.* New 5-HT1A receptor agonists possessing 1,4-benzoxazepine scaffold exhibit highly potent anti-ischemic effects. *Bioorg. Med. Chem. Lett.* 11(4), 595–598 (2001).

[12] Collins GT, Witkin JM, Newman AH *et al.* Dopamine agonist-induced yawning in rats: a dopamine D3 receptormediated behavior. *J. Pharmacol. Exp. Ther.* 314(1), 310–319 (2005).

[13] León R, García AG, Marco-Contelles J. Recent advances in the multitarget-directed ligands approach for the treatment of Alzheimer's disease. *Med. Res. Rev.* 33(1), 139–189 (2013).

[14] Youdim MHB, Buccafusco JJ. CNS Targets for multifunctional drugs in the treatment of Alzheimer's and Parkinson's diseases. *J. Neural. Transm.* 112(4), 519–537 (2005).

[15] Sterling J, Herzig Y, Goren T *et al.* Novel dual inhibitors of AChE and MAO derived from hydroxy aminoindan and phenethylamine as potential treatment for Alzheimer's disease. *J. Med. Chem.* 45(24), 5260–5279 (2002).

[16] Damier P, Kastner A, Agid Y, Hirsch EC. Does monoamine oxidase type B play a role in dopaminergic nerve cell death in Parkinson's disease? *Neurology* 46(5), 1262–1269 (1996).

[17] Matos MJ, Santana L, Janeiro P. Design, Synthesis and pharmacological evaluation of new coumarin derivatives as monoamine oxidase A and B inhibitors. *ECSOC* 12, 1–30 (2008).

[18] Matos MJ, Vilar S, Gonzalez-Franco R *et al.* Novel (coumarin- 3-yl)carbamates as selective MAO-B inhibitors: synthesis, *in vitro* and *in vivo* assays, theoretical evaluation of ADME properties and docking study. *Eur. J. Med. Chem.* 63, 151–161 (2013).

[19] Bolea I, Gella A, Unzeta M. Propargylamine-derived multitarget-directed ligands: fighting Alzheimer's disease with monoamine oxidase inhibitors. *J. Neural. Transm.* 120(6), 893–902 (2013).

[20] Weinreb O, Amit T, Bar-Am O, Youdim MBH. Rasagiline: a novel anti-Parkinsonian monoamine oxidase-B inhibitor with neuroprotective activity. *Prog. Neurobiol.* 92(3), 330–344 (2010).

[21] Youdim MBH, Bar-Am O, Yogev-Falach M *et al.* Rasagiline: neurodegeneration, neuroprotection, and mitochondrial permeability transition. *J. Neurosci. Res.* 79(1–2), 172–179 (2005).

[22] Maruyama W, Akao Y, Carrillo MC, Kitani K, Youdium MBH, Naoi M. Neuroprotection by propargylamines in Parkinson's disease: suppression of apoptosis and induction of prosurvival genes. *Neurotoxicol. Teratol.* 24(5), 675–682 (2002).

[23] Sterling J, Herzig Y, Goren T *et al.* Novel dual inhibitors of AChE and MAO derived from hydroxy aminoindan and phenethylamine as potential treatment for Alzheimer's disease. *J. Med. Chem.* 45(24), 5260–5279 (2002).

[24] Yogev-Falach M, Bar-Am O, Amit T, Weinreb O, Youdim MB. A multifunctional, neuroprotective drug, ladostigil (TV3326), regulates holo-APP translation and processing. *FASEB J.* 20(12), 2177–2179 (2006).

[25] Youdim MB, Weinstock M. Molecular basis of neuroprotective activities of rasagiline and the anti-Alzheimer drug TV3326 [(N-propargyl-(3R)aminoindan-5-YL)-ethyl methyl carbamate]. *Cell. Mol. Neurobiol.* 21(6), 555–573 (2002).

[26] Bar-Am O, Amit T, Weinreb O, Youdim MB, Mandel S. Propargylamine containing compounds as modulators of proteolytic cleavage of amyloid-beta protein precursor: involvement of MAPK and PKC activation. *J. Alzheimers Dis.* 21(2), 361–371 (2010).

[27] Youdim MBH, Finberg JPM. Monoamine oxidase inhibitor antidepressants. In: *Preclinical Psychopharmacology (Part 1).* Grahame-Smith DG, Cowen PJ (Eds). Excerpta Medica, Amsterdam, 38–70 (1983).

[28] Youdim MBH, Finberg JPM, Tipton KF. Amine oxidases. In: *Handbook of Experimental Pharmacology.* Weiner N, Trendelenburg U (Eds). Springer-Verlag, Berlin, 119–92 (1988).

[29] Nicotra A, Pierucci F, Parvez H, Senatori O. Monoamine oxidase expression during development and aging. *Neurotoxicology* 25(1–2), 155–165 (2004).

[30] Fowler JS, Volkow ND, Wang GJ *et al.* Age-related increases in brain monoamine oxidase B in living healthy human subjects. *Neurobiol. Aging* 18(4), 431–435 (1997).

[31] Karolewicz B, Klimek V, Zhu H *et al.* Effects of depression, cigarette smoking, and age on monoamine oxidase B in amygdaloid nuclei. *Brain Res.* 1043(1–2), 57–64 (2005).

[32] Finberg JP. Pharmacology of rasagiline, a new MAO-B inhibitor drug for the treatment of Parkinson's disease with neuroprotective potential. *Rambam Maimonides Med. J.* 1(1), e0003 (2010).

[33] Strydom B, Bergh JJ, Petzer JP. Inhibition of monoamine oxidase by phthalide analogues. *Bioorg. Med. Chem. Lett.* 23(5), 1269–1273 (2013).

[34] Kristal BS, Conway AD, Brown AM *et al.* Selective dopaminergic vulnerability: 3,4-dihydroxyphenylacetaldehyde targets mitochondria. *Free Radic. Biol. Med.* 30(8), 924–931 (2001).

[35] Burke WJ, Li SW, Chung HD *et al.* Neurotoxicity of MAO metabolites of catecholamine neurotransmitters: role in neurodegenerative diseases. *Neurotoxicology* 25(1–2), 101–115 (2004).

[36] Goedert M, Spillantini MG. A century of Alzheimer's disease. *Science* 314(5800), 777–781 (2006).

[37] Shih JC, Chen K, Ridd MJ. Monoamine oxidase: from genes to behavior. *Annu. Rev. Neurosci.*22, 197–217 (1999).

[38] Scarpini E, Scheltens P, Feldman H. Treatment of Alzheimer's disease: current status and new perspectives. *Lancet Neurol.* 2(9), 539–547 (2003).

[39] Inestrosa NC, Álvarez A, Pérez CA *et al.* Acetylcholinesterase accelerates assembly of amyloidbeta-peptides into Alzheimer's fibrils: possible role of the peripheral site of the enzyme. *Neuron* 16(4), 881–891 (1996).

[40] Giacobini E. Cholinergic function and Alzheimer's disease. *Int. J. Geriatr. Psychiatry* 18(Suppl. 1), S1–S5 (2003).

[41] Li B, Stribley J, Ticu A *et al.* Abundant tissue butyrylcholinesterase and its possible function in the acetylcholinesterase knockout mouse. *J. Neurochem.* 75(3), 1320–1331 (2000).

[42] Darvesh S, Hopkins D, Geula C. Neurobiology of butyrylcholinesterase. *Nat. Rev. Neurosci.* 4(2), 131–138 (2003).

[43] Silver A. *The Biology of Cholinesterases (Frontiers of Biology, Volume 36).* Elsevier, North Holland, Amsterdam, 426–447 (1974).

[44] Giacobini E, Spiegel R, Enz A, Veroff A, Cutler NR. Inhibition of acetyl- and butyryl-cholinesterase in the cerebrospinal fluid of patients with Alzheimer's disease by rivastigmine: correlation with cognitive benefit. *J. Neural Trans.* 109(7–8), 1053–1065 (2002).

[45] Morphy JR. Historical strategies for lead generation. In: *Designing Multi-Target Drugs.* Morphy JR, Harris CJ (Eds). The Royal Society of Chemistry, Cambridge, UK, 114–115 (2012).

[46] Pérez V, Marco JL, Fernández-Alvarez E, Unzeta M. Relevance of benzyloxy group in 2-indolyl methylamines in the selective MAO-B inhibition. *Br. J. Pharmacol.* 127(4), 869–876 (1999).

[47] Youdim MB, Weinstock M. Molecular basis of neuroprotective activities of rasagiline and the anti- Alzheimer drug TV3326 [(N-propargyl-(3R)aminoindan-5-YL)-ethyl methyl carbamate]. *Cell Mol. Neurobiol.* 21(6), 555–73 (2001).

[48] Weinstock M, Bejar C, Wang RH *et al.* TV3326, a novel neuroprotective drug with cholinesterase and monoamine oxidase inhibitory activities for the treatment of Alzheimer's disease. *J. Neural Transm. Suppl.* 2000(60), 157–169 (2000).

[49] Weinreb O, Mandel S, Bar-Am O. *et al.* Multifunctional Neuroprotective Derivatives of Rasagiline as Anti-Alzheimer's Disease Drugs. *Neurotherapeutics.* 6(1), 163-174 (2009).

[50] Weinstock M, Goren T, Youdim MB. Development of a novel neuroprotective drug (TV3326) for the treatment of Alzheimer's disease, with cholinesterase and monoamine oxidase inhibitory activities. *Drug Dev. Res.* 50, 216–222 (2000).

[51] Weinreb O, Amit T, Mandel S, Kupershmidt L, Youdim MB. Neuroprotective multifunctional iron chelators: from redox-sensitive process to novel therapeutic opportunities. *Antioxid. Redox Signal.* 13(6), 919–49 (2010).

[52] Weinreb O, Amit T, Bar-Am O, Youdim MB. Ladostigil: a novel multimodal neuroprotective drug with cholinesterase and brain-selective monoamine oxidase inhibitory activities for Alzheimer's disease treatment. *Curr. Drug Targets* 13(4), 483–94 (2012).

[53] Sagi Y, Weinstock M, Youdim MB. Attenuation of MPTP-induced dopaminergic neurotoxicity by TV3326, a cholinesterase-monoamine oxidase inhibitor. *J. Neurochem.* 86(2), 290–297 (2003).

[54] O'Carroll AM, Fowler CJ, Phillips JP, Tobbia I, Tipton KF. The deamination of dopamine by human brain monoamine oxidase. Specificity for the two enzyme forms in seven brain regions. *Naunyn Schmiedebergs Arch. Pharmacol.* 322(3), 198–202 (1983).

[55] Green AR, Mitchell BD, Tordoff AF, Youdim MB. Evidencefor dopamine deamination by both type A and type B monoamine oxidase in rat brain *in vivo* and for the degree of inhibition of enzyme necessary for increased functional activity of dopamine and 5-hydroxytryptamine. *Br. J. Pharmacol.* 60(3), 343–349 (1977).

[56] Youdim MBH, Edmondson D, Tipton KF. The therapeutic potential of monoamine oxidase inhibitors. *Nat. Rev. Neurosci.* 7(4), 295–309 (2006).

[57] Barner EL, Gray SL. Donepezil use in Alzheimer disease. *Ann. Pharmacother.* 32(1), 70–77 (1998).

[58] Samadi A, Chioua M, Bolea I *et al.* Synthesis, biological assessment and molecular modeling of new multipotent MAO and cholinesterase inhibitors as potential drugs for the treatment of Alzheimer's disease. *Eur. J. Med. Chem.* 46(9), 4665–4668 (2011).

[59] Cutillas B, Ambrosio S, Unzeta M. Neuroprotective effect of the monoamine oxidase inhibitor PF 9601N [N-(2-propynyl)-2-(5-benzyloxy-indolyl) methylamine] on rat nigral neurons after 6-hydroxydopamine-striatal lesion. *Neurosci. Lett.* 329(2), 165–168 (2002).

[60] Prat G, Pérez V, Rubí A, Casas M, Unzeta M. The novel type B MAO inhibitor PF9601N enhances the duration of L-DOPA-induced contralateral turning in 6-hydroxydopamine lesioned rats. *J. Neural. Transm.* 107(4), 409–417 (2000).

[61] Bolea I, Juárez-Jiménez J, de los Ríos C *et al.* Synthesis, biological evaluation, and molecular modeling of donepezil and N-[(5-(benzyloxy)-1-methyl-1H-indol-2-yl)methyl]- N-methylprop-2-yn-1-amine hybrids as new multipotent cholinesterase/monoamine oxidase inhibitors for the treatment of Alzheimer's disease. *J. Med. Chem.* 54(24), 8251–8270 (2011).

[62] Bautista-Aguilera OM, Esteban G, Chioua M *et al.* Multipotent cholinesterase/monoamine oxidase inhibitors for the treatment of Alzheimer's disease: design, synthesis, biochemical evaluation, ADMET, molecular modeling, and QSAR analysis of novel donepezil-pyridylhybrids. *Drug Des. Devel. Ther.* 8, 1893–1910 (2014).

[63] Ellman GL, Courtney KD, Andres BJ, Feather-stone RM. A new and rapid colorimetric determination of acetylcholinesterase activity. *Biochem. Pharmacol.* 7, 88–95 (1961).

[64] Bautista-Aguilera OM, Esteban G, Bolea I *et al.* Design, synthesis, pharmacological evaluation, QSAR analysis, molecular modeling and ADMET of novel donepezileindolyl hybrids as multipotent cholinesterase/monoamine oxidase inhibitors for the potential treatment of Alzheimer's disease. *Eur. J. Med. Chem.* 75, 82–95 (2014).

[65] Zhou M, Panchuk-Voloshina N. A one-step fluorometric method for the continuous measurement of monoamine oxidase activity. *Anal. Biochem.* 253(2), 169–174 (1997).

[66] Trott O, Olson AJ. AutoDock Vina: improving the speed and accuracy of docking with a new scoring function, efficient optimization, and multithreading. *J. Comput. Chem.* 31(2), 455–461 (2010).

[67] Thomas T. Monoamine oxidase B inhibitors in the treatment of Alzheimer's disease. *Neurobiol. Aging* 21(2), 343–348 (2000).

[68] Riederer P, Danyelczyk W, Grunblat E. Monoamine oxidase inhibition in Alzheimer's disease. *Neurotoxicology* 25(1–2), 271–277 (2004).

[69] Youdim MB, Amit T, Bar-Am O, Weinreb O, Yogev-Falach M. Implications of co-morbidity for etiology and treatment of neurodegenerative diseases with multifunctional neuroprotective-neurorescue drugs: ladostigil. *Neurotoxic Res.* 10(3–4), 181–192 (2006).

[70] Tsunekawa H, Noda Y, Mouri A, Yoneda F, Nameshiba T. Synergistic effects of selegiline and donepezil on cognitive impaitment induced by amyloid beta (25–35). *Behav. Brain Res.* 190(2), 224–232 (2008).

[71] Camps P, Duque MD, Vázquez S *et al.* Synthesis and pharmacological evaluation of several ring-contracted amantadine analogs. *Bioorg. Med. Chem.* 16(23), 9925–9936 (2008).

[72] Stone TW, Addae JI. The pharmacological manipulation of glutamate receptors and neuroprotection. *Eur. J. Pharmacol.* 447(2–3), 285–296 (2002).

[73] Sobrado M, López MG, Carceller F, García AG, Roda JM. Combined nimodipine and citicoline reduce infarct size, attenuate apoptosis and increase bcl-2 expression after focal cerebral ischemia. *Neuroscience* 118(1), 107–113 (2003).

[74] Lipton SA. Paradigm shift in neuroprotection by NMDA receptor blockade: memantine and beyond. *Nat. Rev. Drug Discov.* 5(2), 160–170 (2006).

[75] Greenamyre JT, O'Brien CF. N-methyl-d-aspartate antagonists in the treatment of Parkinson's disease. *Arch. Neurol.* 48(9), 977–981 (1991).

[76] Geldenhuys WJ, Malan SF, Murugesan T, van der Schyf CJ, Bloomquist JR. Synthesis and biological evaluation of pentacyclo[5.4.0.02,6.03,10.05,9]undecane derivatives as potential therapeutic agents in Parkinson's disease. *Bioorg. Med. Chem.* 12(7), 1799–1806 (2004).

[77] Duque MD, Camps P, Torres E *et al.* New oxapolycyclic cage amines with NMDA receptor antagonist and trypanocidal activities. *Bioorg. Med. Chem.* 18(1), 46–57 (2010).

[78] Torres E, Duque MD, López-Querol M *et al.* Synthesis of benzopolycyclic cage amines: NMDA receptor antagonist, trypanocidal and antiviral activities. *Bioorg. Med. Chem.* 20(2), 942–948 (2012).

[79] Zindo FT, Barber QR, Joubert J, Bergh JJ, Petzer JP, Malan SF. Polycyclic propargylamine and acetylene derivatives as multifunctional neuroprotective agents. *Eur. J. Med. Chem.* 80, 122–134 (2014).

[80] Mdzinarishvili A, Geldenhuys WJ, Abbruscato TJ, Bickel U, Klein J, van der Schyf CJ. NGP1-01, a lipophilic polycyclic cage amine, is neuroprotective in focal ischemia. *Neurosci. Lett.* 383(1–2), 49–53 (2005).

[81] Geldenhuys WJ, Malan SF, Bloomquist JR, Marchand AP, van der Schyf CJ. Pharmacology and structure-activity relationships of bioactive polycyclic cage compounds: a focus on pentacycloundecane derivatives. *Med. Res. Rev.* 25(1), 21–48 (2005).

[82] Kiewert C, Hartmann J, Stoll J, Thekkumkara TJ, Geldenhuys WJ, Klein J. NGP1-01 is a brain permeable dual blocker of neuronal voltage-and ligand-operated calcium channels. *Neurochem. Res.* 31(3), 395–399 (2006).

[83] Hao J, Mdzinarishvili A, Abbruscato TJ *et al.* Neuroprotection in mice by NGP1-01 after transient focal brain ischemia. *Brain Res.* 1196, 113–120 (2008).

[84] Du Preez JL, Lotter AP, Guillory JK. Kinetics and mechanism of degradation of the heterocyclic cage compound NGP1-01 in aqueoussolution. *Pharmazie* 51, 223 (1996).

[85] Du Preez JL, Lotter AP. LC-MS identification of the degradates of NGP1-01 and subsequent development of a routine stability-indicating method of analysis. *Drug Dev. Ind. Pharm.* 22, 1249 (1996).

[86] Hollingsworth EB, McNeal ET, Burton JL, Williams RJ, Daly JW, Creveling CR. Biochemical characterization of a filtered synaptoneurosome preparation from guinea pig cerebral cortex: cyclic adenosine 3':5'-monophosphategenerating systems, receptors, and enzymes. *J. Neurosci.* 5(8), 2240–2253 (1985).

[87] Molecular Operating Environment (MOE), Version 2011.10. www.chemcomp.com

[88] Joubert J, Geldenhuys WJ, Van der Schyf CJ *et al.* Polycyclic cage structures as lipophilic scaffolds for neuroactive drugs. *ChemMedChem* 7(3), 375–84 (2012).

[89] Zah J, Terre'Blanche G, Erasmus E, Malan SF. Physicochemical prediction of a brain-blood distribution profile in polycyclic amines. *Bioorg. Med. Chem.* 11(17), 3569–3578 (2003).

[90] Brookes KB, Hickmott PW, Jutle KK, Schreyer CA. Introduction of pharmacophoric groups into polycyclic systems 4. aziridine, oxiran, and tertiary betahydroxyethylamine derivatives of adamantine. *S. Afr. J. Chem.* 45, 8–11 (1992).

[91] Huang X, Cuanjungco MP, Atwood CS *et al.* Cu(II) potentiation of alzheimer abeta neurotoxicity. Correlation with cell-free hydrogen peroxide production and metal reduction. *J. Biol. Chem.* 274(52), 37111–37116 (1999).

[92] Rausch WD, Hirata Y, Nagatsu T, Riederer P, Jellinger K. Tyrosine hydroxylase activity in caudate nucleus from Parkinson's disease: effects of iron and phosphorylating agents. *J. Neurochem.* 50(1), 202–208 (1988).

[93]Mounsey RB, Teismann P. Chelators in the treatment of iron accumulation in parkinson's disease. *Int. J. Cell Biol.* 9832, 45 (2012).

[94] Dexter DT, Wells FR, Agid F, Lees AJ, Jenner P, Marsden CD. Increased nigral iron content in postmortem parkinsonian brain. *Lancet* 2(8569), 1219–1220 (1987).

[95] Sofic E, Riederer P, Heinsen H *et al.* Increased iron (III) and total iron content in post mortem substantia nigra of Parkinsonian brain. *J. Neural Transm.* 74(3), 199–205 (1988).

[96] Jenner P, Olanow CW. Understanding cell death in Parkinson's disease. *Ann. Neurol.* 44(3 Suppl. 1), S72–S84 (1998).

[97] Youdim MB, Stephenson G, Ben Shachar D. Ironing iron out in Parkinson's disease and other neurodegenerative diseases with iron chelators: a lesson from 6-hydroxydopamine and iron chelators, desferal and VK-28. *Ann. NY Acad. Sci.* 1012, 306–325 (2004).

[98] Shachar DB, Kahana N, Kampel V, Warshawsky A, Youdim MB. Neuroprotection by a novel brain permeable iron chelator, VK-28, against 6-hydroxydopamine lesion in rats. *Neuropharmacology* 46(2), 254–263 (2004).

[99] Gal S, Zheng H, Fridkin M, Youdim MB. Novel multifunctional neuroprotective iron chelator-monoamine oxidase inhibitor drugs for neurodegenerative diseases. *In vivo* selective brain monoamine oxidase inhibition and prevention of MPTP-induced striatal dopamine depletion. *J. Neurochem.* 95(1), 79–88 (2005).

[100] Zheng H, Gal S, Weiner LM *et al.* Novel multifunctional neuroprotective iron chelator-monoamine oxidase inhibitor drugs for neurodegenerative diseases: *in vitro* studies on antioxidant activity, prevention of lipid peroxide formation and monoamine oxidase inhibition. *J. Neurochem.* 95(1), 68–78 (2005).

[101] Kupershmidt L, Weinreb O, Amit T, Mandel S, Bar-Am O, Youdim MB. Novel molecular targets of the neuroprotective/neurorescue multimodal iron chelating drug M30 in the mouse brain. *Neuroscience* 189, 345–358 (2011).

[102] Kupershmidt L, Amit T, Bar-Am O, Youdim MB, Weinreb O. The novel multitarget iron chelating-radical scavenging compound M30 possesses beneficial effects on major hallmarks of Alzheimer's disease. *Antioxid. Redox Signal.* 17(6), 860–77 (2012).

[103] Kupershmidt L, Amit T, Bar-Am O, Weinreb O, Youdim MB. Multi-target, neuroprotective and neurorestorative M30 improves cognitive impairment and reduces Alzheimer's-like neuropathology and age-related alterations in mice. *Mol. Neurobiol.* 46(1), 217–220 (2012).

[104] Youdim MB, Kupershmidt L, Amit T, Weinreb O. Promises of novel multi-target neuroprotective and neurorestorative drugs for Parkinson's disease. *Parkinsonism Relat. Disord.* 20(Suppl. 1), S132–S136 (2014).

[105] Wang L, Esteban G, Ojima M *et al*. Donepezil + propargylamine + 8-hydroxyquinoline hybrids as new multifunctional metal-chelators, ChE and MAO inhibitors for the potential treatment of Alzheimer's disease. *Eur. J. Med. Chem.* 80, 543–561 (2014).

[106] Zheng H, Weiner LM, Bar-Am O *et al*. Design, synthesis, and evaluation of novel bifunctional iron-chelators as potential agents for neuroprotection in Alzheimer's, Parkinson's, and other neurodegenerative diseases. *Bioorg. Med. Chem.* 13(3), 773–83 (2005).

[107] Zhu W, Xie W, Pan T *et al.* Prevention and restoration of lactacystin-induced nigrostriatal dopamine neuron degeneration by novel brain-permeable iron chelators. *FASEB J.* 21(14), 3835–3844 (2007).

[108] Fowler CJ, Tipton KF. Concentration dependence of the oxidation of tyramine by the two forms of rat liver mitochondrial monoamine oxidase. *Biochem. Pharmacol.* 30(24), 3329–3332 (1981).

[109] Avramovich-Tirosh Y, Amit T, Bar-Am O, Zheng H, Fridkin M, Youdim MB. Therapeutic targets and potential of the novel brain- permeable multifunctional iron chelatormonoamine oxidase inhibitor drug, M-30, for the treatment of Alzheimer's disease. *J. Neurochem.* 100(2), 490–502 (2007).

[110] Ozaita A, Olmos G, Boronat MA, Lizcano JM, Unzeta M, García-Sevilla JA. Inhibition of monoamine oxidase A and B activities by imidazol(ine)/guanidine drugs, nature of the

interaction and distinction from I2-imidazoline receptors in rat liver. *Br. J. Pharmacol.* 121(5), 901–912 (1997).

[111] Pérez V, Marco JL, Fernández-A lvarez E, Unzeta M. Relevance of benzyloxy group in 2-indolyl methylamines in the selective MAO-B inhibition. *Br. J. Pharmacol.* 127(4), 869–876 (1999).

[112] Huang CY. Determination of binding stoichiometry by the continuous variation method: the job plot. *Methods Enzymol.* 87, 509–525 (1982).

[113] Yee S. *In vitro* permeability across Caco-2 cells (colonic) can predict *in vivo* (small intestinal) absorption in man - fact or myth. *Pharm. Res.* 14(6), 763–766 (1997).

[114] Kirkinezos IG, Moraes CT. Reactive oxygen species and mitochondrial diseases. *Semin. Cell Dev. Biol.* 12(6), 449–457 (2001).

[115] Schulz JB, Matthews RT, Muqit MM, Browne SE, Beal MF. Inhibition of neuronal nitric oxide synthase by 7-nitroindazole protects against MPTP-induced neurotoxicity in mice. *J. Neurochem.* 64(2), 936–939 (1995).

[116] Hantraye P, Brouillet E, Ferrante R *et al.* Inhibition of neuronal nitric oxide synthase prevents MPTP-induced parkinsonism in baboons. *Nat. Med.* 2(9), 1017–1102 (1996).

[117] Beckman JS, Beckman TW, Chen J, Marshall PA, Freeman BA. Apparent hydroxyl radical production by peroxynitrite: implications for endothelial injury from nitric oxide and superoxide. *Proc. Natl Acad. Sci. USA* 87(4), 1620–1624 (1990).

[118] Avila M, Balsa MD, Fernandez-Alvarez E, Tipton KF, Unzeta M. The effect of side-chain substitution at positions 2 and 3 of the heterocyclic ring of N-acetylenic analogues of tryptamine as monoamine oxidase inhibitors. *Biochem. Pharmacol.* 45(11), 2231–2237 (1993).

[119] Unzeta M, Sanz E, NovelMAO-B inhibitors: potential therapeutic use of the selective MAO-B inhibitor PF9601N in Parkinson's disease. *Int. Rev. Neurobiol* 100, 217–236 (2011).

[120] Perez V, Unzeta M. PF 9601N [N-(2-propynyl)-2-(5-benzyloxy-indolyl) methylamine], a new MAO-B inhibitor, attenuates MPTP-induced depletion of striatal dopamine levels in C57/BL6 mice. *Neurochem. Int.* 42(3), 221–229 (2003).

[121] Cutillas B, Ambrosio S, Unzeta M. Neuroprotective effect of the monoamine oxidase inhibitor PF9601N [N-(2-propynyl)-2-(5-benzyloxy- indolyl) methylamine] on rat nigral neurons after 6-OH-DA striatal lesion. *Neuroscience Lett.* 329(2), 165–168 (2002).

[122] Sanz E, Romera M, Bellik L, Marco JI, Unzeta M. Indolalkylamines derivatives as antioxidant and neuroprotective agents in an experimental model of Parkinson's disease. *Med. Sci. Monit.* 10(12), BR477–BR484 (2004).

[123] Bellik L, Dragoni S, Pessina F, Sanz E, Unzeta M, Valoti M. Antioxidant properties of PF9601N, a novel MAO-B inhibitor: assessment of its ability to interact with reactive nitrogen species. *Acta Biochim. Pol.* 57(2), 235–239 (2010).

[124] Sanz E, Quintana A, Battaglia V *et al.* Anti-apoptotic effect of Mao-B inhibitor PF9601N [N-(2-propynyl)-2-(5-benzyloxyindolyl) methylamine] is mediated by p53 pathway inhibition in MPP+-treated SH-SY5Y human dopaminergic cells. *J. Neurochem.* 105(6), 2404–2417 (2008).

[125] Marini S, Nannelli A, Sodini D *et al.* Expression, microsomal and mitochondrial activities of cytochrome P450 enzymes in brain regions from control and phenobarbital-treated rabbits.0020*Life Sci.* 80(10), 910–917 (2007).

[126] Mihara T, Iwashita A, Matsuoka N. A novel adenosine A(1) and A(2A) receptor antagonist ASP5854 ameliorates motor impairment in MPTP-treated marmosets: comparison with existing anti-Parkinson's disease drugs. *Behav. Brain Res.* 194(2), 152–161 (2008).

- **Study on the novel adenosine A(1) and A(2A) receptor dual antagonist 5-[5 amino-3-(4-fluorophenyl)pyrazin-2-yl]-1-isopropylpyridine-2(1H)-one (ASP5854) showed it to be effective in various rodents models of PD and cognition.**

[127] Shook BC, Rassnick S, Osborne MC *et al. In vivo* characterization of a dual adenosine A2A/A1 receptor antagonist in animal models of Parkinson's disease. *J. Med. Chem.* 53(22), 8104–8115 (2010).

[128] Mihara T, Mihara K, Yarimizu J *et al.* Pharmacological characterization of a novel, potent adenosine A1 and A2A receptor dual antagonist, 5-[5-amino-3-(4-fluorophenyl) pyrazin-2-yl]-1-isopropylpyridine-2(1H)-one (ASP5854), in models of Parkinson's disease and cognition. *J. Pharmacol. Exp. Ther.* 323(2), 708–719 (2007).

[129] Dungo R, Deeks ED. Istradefylline: first global approval. *Drugs* 73(8), 875–882 (2013).

- **Summarizes the milestones in the development of istradefylline leading to its first approval for the treatment of patients with PD.**

[130] Muller CE, Ferré S. Blocking striatal adenosine A2A receptors: a new strategy for basal ganglia disorders. *Recent Pat. CNS Drug Discov.* 2(1), 1–21 (2007).

[131] Petzer JP, Castagnoli N Jr, Schwarzschild MA, Chen JF, Van der Schyf CJ. Dual-target-directed drugs that block monoamine oxidase B and adenosine A(2A) receptors for Parkinson's disease. *Neurotherapeutics* 6(1), 141 (2009).

[132] Pinna A, Simola N, Frau L, Morelli M. Symptomatic and neuroprotective effects of a2a receptor antagonists in Parkinson's disease. In: *Adenosine: A Key Link Between Metabolism and Brain Activity*. Masino S, Boison D (Eds). Springer, NY, USA, 361–384 (2013).

[133] Yu L, Shen HY, Coelho JE *et al.* Adenosine A2A receptor antagonists exert motor and neuroprotective effects by distinct cellular mechanisms. *Ann. Neurol.* 63(3), 338–346 (2008).

[134] Al-Nuaimi SK, Mackenzie EM, Baker GB. Monoamine oxidase inhibitors and neuroprotection: a review. *Am. J. Ther.* 19(6), 436–448 (2012).

- **Overview of the neuroprotective/neurorescue properties of multifaceted drugs phenelzine, (-)-deprenyl, rasagiline, ladostigil, tranylcypromine, moclobemide, and clorgyline and their possible neuroprotective mechanisms.**

[135] Hickey P, Stacy M. Adenosine A2A antagonists in Parkinson's disease: what's next? *Curr. Neurol. Neurosci. Rep.* 12(4), 376–385 (2012).

[136] Koch P, Akkari R, Brunschweiger A *et al.* 1,3-Dialkylsubstituted tetrahydropyrimido[1,2-f]purine-2,4-diones as multiple target drugs for the potential treatment of neurodegenerative diseases. *Bioorg. Med. Chem.* 21(23), 7435–7452 (2013).

[137] Drabczyńska A, Müller CE, Lacher SK *et al.* Synthesis and biological activity of tricyclic aryloimidazo-, pyrimido-, and diazepinopurinediones. *Bioorg. Med. Chem.* 14(21), 7258–7281 (2006).

[138] Samadi A, Valderas C, de los Ríos C *et al.* Cholinergic and neuroprotective drugs for the treatment of Alzheimer and neuronal vascular diseases. II. Synthesis, biological assessment, and molecular modelling of new tacrine analogues from highly substituted 2-aminopyridine-3-carbonitriles. *Bioorg. Med. Chem.* 19(1), 122–133 (2011).

[139] Dodd S, Dean O, Copolov DL, Malhi GS, Berk M. N-acetylcysteine for antioxidant therapy: pharmacology and clinical utility. *Expert Opin. Biol. Ther.* 8(12), 1955–1962 (2008).

[140] Rucins M, Kaldre D, Pajuste K *et al.* Synthesis and studies of calcium channel blocking and antioxidant activities of novel 4-pyridinium and/or N-propargyl substituted 1,4-dihydropyridine derivatives. *C. R. Chimie* 17, 69–80 (2014).

[141] Liu Z, Zhang H, Ye N *et al.* Synthesis of dihydrofuroaporphine derivatives: identification of a potent and selective serotonin 5-HT 1A receptor agonist. *J. Med. Chem.* 53(3), 1319–1328 (2010).

[142] Bossert F, Vater W. 1,4-Dihydropyridines - a basis for developing new drugs. *Med. Res. Rev.* 9(3), 291–324 (1989).

[143] Triggle DJ. Calcium channel antagonists: clinical uses - past, present and future. *Biochem. Pharmacol.* 74(1), 1–9 (2007).

[144] Duburs G, Vigante B, Plotniece A *et al.* Dihydropyridine derivatives as bioprotectors. *Chim. Oggi.* 26, 68–70 (2008).

[145] Joyce JN. Dopamine D3 receptor as a therapeutic target for antipsychotic and antiparkinsonian drugs. *Pharmacol. Ther.* 90(2–3), 231–259 (2001).

- **The cloning of the gene for the D3 receptor, the subsequent identification of its distribution in brain and the possibility that it might be a target for drugs used to treat schizophrenia and PD.**

[146] Pilla M, Perachon S, Sautel F *et al.* Selective inhibition of cocaine-seeking behaviour by a partial dopamine D3 receptor agonist. *Nature* 400(6742), 371–375 (1999).

[147] Koob GF, Caine SB. Cocaine addiction therapy - are we partially there? *Nat. Med.* 5(9), 993–995 (1999).

[148] Montplaisir J, Nicolas A, Denesle R, Gomez-Mancilla B. Restless legs syndrome improved by pramipexole: a doubleblind randomized trial. *Neurology* 52(5), 938–943 (1999).

[149] Levant B. The D3 dopamine receptor: neurobiology and potential clinical relevance. *Pharmacol. Rev.* 49(3), 231–252 (1997).

[150] Newman AH, Grundt P, Nader MA. Dopamine D3 receptor partial agonists and antagonists as potential drug abuse therapeutic agents. *J. Med. Chem.* 48(11), 3663–3679 (2005).

[151] Collins GT, Newman AH, Grundt P *et al.* Yawning and hypothermia in rats: effects of dopamine D3 and D2 agonists and antagonists. *Psychopharmacology (Berl.)* 193(2), 159–170 (2007).

[152] Alessandri B, Tsuchida E, Bullock RM. The neuroprotective effect of a new serotonin receptor agonist, BAY X3702, upon focal ischemic brain damage caused by acute subdural hematoma in the rat. *Brain Res.* 845(2), 232–235 (1999).

[153] Kamei K, Maeda N, Ogino R *et al.* New 5-HT1A receptor agonists possessing 1,4-benzoxazepine scaffold exhibit highly potent anti-ischemic effects. *Bioorg. Med. Chem. Lett.* 11(4), 595–598 (2001).

[154] Bibbiani F, Oh JD, Chase TN. Serotonin 5-HT1A agonist improves motor complications in rodent and primate parkinsonian models. *Neurology* 57(10), 1829 (2001).

- **Pharmaceuticals acting to stimulate 5-HT1A receptors could prove useful in the treatment of the motor response complications in parkinsonian patients.**

[155] Melamed E, Zoldan J, Friedberg G, Ziv I, Weizmann A. Involvement of serotonin in clinical features of Parkinson's disease and complications of L-DOPA therapy. *Adv. Neurol.* 69, 545–550 (1996).

[156] Lucas G, Bonhomme N, De Deurwaerdere P, Le Moal M, Spampinato U. 8-OH-DPAT, a 5-HT1A agonist and ritanserin, a 5-HT2A/C antagonist, reverse haloperidolinduced catalepsy in rats independently of striatal dopamine release. *Psychopharmacology (Berl.)* 131(1), 57–63 (1997).

[157] Nicholson SL, Brotchie JM. 5-hydroxytryptamine (5-HT, serotonin) and Parkinson's disease - opportunities for novel therapeutics to reduce the problems of levodopa therapy. *Eur. J. Neurol.* 9(Suppl. 3), 1–6 (2002).

[158] Avraham Pharmaceuticals Announces Successful Interim Results in Phase 2b Study of Ladostigil for the Treatment of MCI. www.businesswire.com

Chapter 3

Research Article 1: Polycyclic propargylamine and acetylene derivatives as multifunctional neuroprotective agents

Article published online on 13 April 2014

Eur. J. Med. Chem. 2014; 80:122-134. doi: 10.1016/j.ejmech.2014.04.039.

Polycyclic propargylamine and acetylene derivatives as multifunctional neuroprotective agents

Frank T. Zindo[a], Quinton R. Baber[b], Jacques Joubert[a], Jacobus J. Bergh[b], Jacobus P. Petzer[b] and Sarel F. Malan[a,b,*]

[a]*Pharmaceutical Chemistry, School of Pharmacy, University of the Western Cape, Bellville, South Africa, Private Bag X17, Bellville 7535, South Africa.*

[b]*Pharmaceutical Chemistry, North-West University, Private Bag X6001, Potchefstroom, 2520, South Africa.*

*Corresponding author at present address: School of Pharmacy, University of the Western Cape, Private Bag X17, Bellville 7535, South Africa. Tel: +27 21959 3190; fax: +27 21959 1588; e-mail: sfmalan@uwc.ac.za

Graphical Abstract

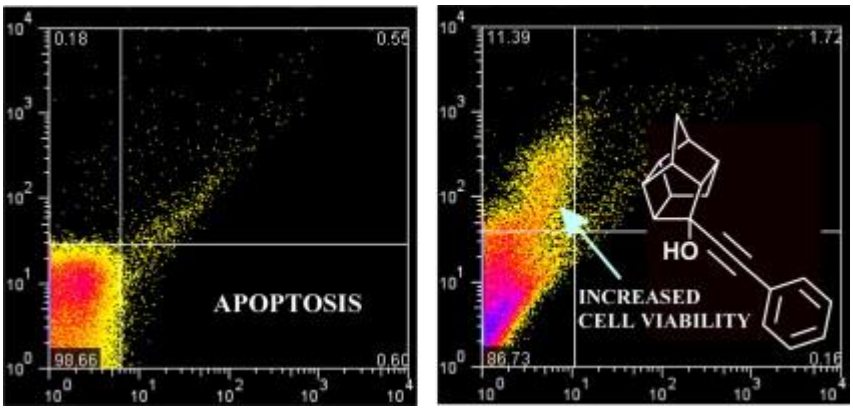

Abstract

The aim of this study was to design drug-like molecules with multiple neuroprotective mechanisms which would ultimately inhibit *N*-methyl-D-aspartate (NMDA) receptors, block *L*-type voltage gated calcium channels (VGCC) and inhibit apoptotic processes as well as the monoamine oxidase-B (MAO-B) enzyme in the central nervous system. These types of compounds may act as neuroprotective and symptomatic drugs for disorders such as Alzheimer's and Parkinson's disease. In designing the compounds we focused on the structures of rasagiline and selegiline, two well known MAO-B inhibitors and proposed neuroprotective agents. Based on this consideration, the compounds synthesized all contain the propargylamine functional group of rasagiline and selegiline or a derivative thereof, conjugated to various polycyclic cage moieties. Being non-polar, these polycyclic moieties have been shown to aid in the transport of conjugated compounds across the blood-brain barrier, as well as cell membranes and have secondary positive neuroprotective effects. All novel synthesized polycyclic derivatives proved to have significant anti-apoptotic activity ($p < 0.05$) which was comparable to the positive control, selegiline. Four compounds (**12**, **15** and **16)** showed promising VGCC and NMDA receptor channel inhibitory activity ranging from 18 % to 59 % in micromolar concentrations and compared favourably to the reference compounds. In the MAO-B assay, 8-phenyl-ethynyl-8-hydroxypentacycloundecane (**10**), exhibited MAO-B inhibition of 73.32 % at 300 μM. This compound also reduced the percentage of apoptotic cells by as much as 40 % when compared to the control experiments.

Keywords:

Polycyclic, Propargylamine, Neuroprotection, Apoptosis.

3.1. Introduction

The pathology of neurodegenerative disorders, such as Parkinson's disease (PD) and Alzheimer's disease (AD), is caused by the abnormal loss of neuronal cells in certain areas of the brain.[1] It consequently causes an imbalance of certain neurotransmitter levels in the brain, giving rise to the characteristic signs and symptoms of these disorders.[2,3] Ultimately, it compromises the normal functionality and well-being of the individual suffering from the disease,[3] thus making it an absolute necessity to create drugs which would halt this neuronal breakdown process and aid in treating the signs and symptoms of neurodegenerative disorders. The abnormal death of neurons in the central nervous system of individuals suffering from neurodegenerative diseases takes place by an intrinsic cell suicide program

known as apoptosis.[4-7] This process is triggered by several stimuli, and consists of numerous pathways and cascades, each one having an influence on the other, ultimately leading to cell death.[4-7] One such pathway is the excitotoxic process which leads to apoptosis. Excitotoxicity is a result of activation of postsynaptic receptors; including NMDA receptors, 2-amino-3-(3-hydroxy-5-methylisoxazol-4-yl) proprionate (AMPA), and kainate receptors. Upon their activation, these receptors open their associated ion channel to allow the influx of Ca^{2+} and Na^{+} ions. The excessive influx of calcium together with any calcium release from intracellular compartments can overwhelm Ca^{2+}-regulatory mechanisms and lead to cell death.[8] This mechanism of cell death suggests that the receptors and their associated calcium channels serve as drug target sites for curbing neurodegeneration. Several compounds, including polycyclic amines such as amantadine (**2**), NGP1-01 (**3**), MK-801 (**4**), and phencyclidine (PCP, **5**) have been reported to show inhibitory activities on NMDA receptors and calcium channels (Figure 1).[10]

The oxidative deamination reaction catalysed by monoamine oxidase B (MAO-B) is one of the major catabolic pathways of dopamine in the brain. Inhibition of this enzyme leads to enhanced dopaminergic neurotransmission and is currently used in the symptomatic treatment of PD.[11-14] Furthermore, MAO-B inhibitors may also exert a neuroprotective effect by reducing the concentrations of potentially hazardous by-products produced by MAO-B-catalysed dopamine oxidation.[15] In PD and AD it has been shown that there are age-related elevated levels of MAO-B, which not only act indirectly as a trigger to the apoptotic process, but also give rise to some of the signs and symptoms associated with these disorders.[16–18]

In the current study, the approach was to develop multifunctional drugs which would halt the apoptotic neuronal breakdown process and eliminate some of the signs and symptoms of diseases such as AD and PD by: (a) Inhibiting NMDA receptors and blocking *L*-type voltage gated calcium channels (VGCC) thus regulating the Ca^{2+} influx mediated excitotoxic process; (b) Inhibiting the MAO-B enzyme thus allowing increase in dopamine levels in the CNS and reducing the levels of the highly oxidative products produced by the activity of this enzyme; (c) Possess anti-apoptotic activity to halt the natural neuronal cell death process. With this in mind, we focused on the structures of pentacycloundecane (**1**), amantadine (**2**), rasagiline (**6**) and selegiline (**7**, Figure 1).

Rasagiline and selegiline are second generation propargylamine derivatives that irreversibly inhibit brain MAO-B, and have promising neuroprotective activities.[19] After several years of study and research, it has been established that the neuroprotective effects of rasagiline and selegiline can be attributed to its propargyl moiety.[16-18] This observation was made on the grounds that propargylamine (**8**), itself exerts the same neuroprotective effects as offered by

rasagiline. It has also been established that the MAO-B inhibiting activity is not a prerequisite for the neuroprotection provided by rasagiline, selegiline and propargylamine as these compounds have been shown to inhibit apoptosis through other anti-apoptotic mechanisms that may contribute to their possible disease-modifying activities.[20,21] Since MAO-B activity is increased in both AD and PD, MAO-B inhibitors may be of further therapeutic benefit.[22]

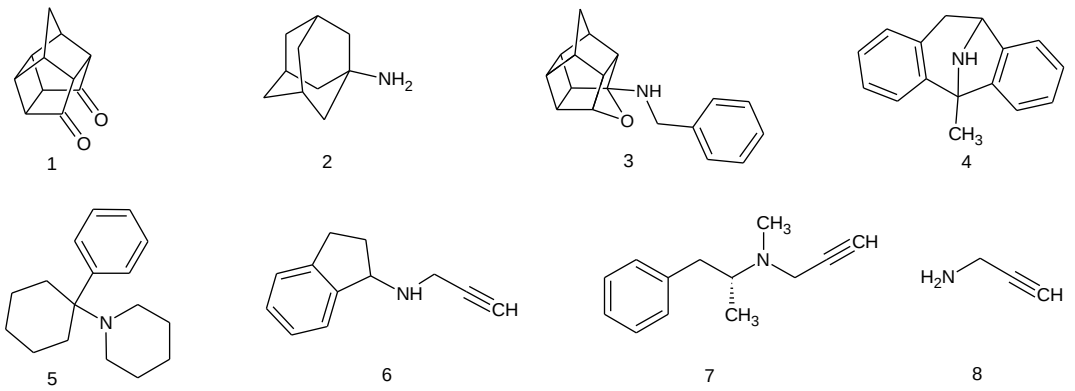

***Figure 1*:** Representative polycyclic cage compounds (**1** - **3**), NMDA receptor and calcium channel modulators - NGP1-01 (**3**), MK-801 (**4**) and phencyclidine (PCP, **5**), the neuroprotective MAO-B inhibitors - rasagiline (**6**) and selegiline (**7**), and propargylamine (**8**).

Polycyclic cage compounds, such as pentacycloundecane (PCU, **1**), amantadine (**2**) and NGP1-01 (**3**) have various biological applications, with special interest in the symptomatic and proposed curative treatment of neurodegenerative diseases.[23] These compounds can be used to modify and improve the pharmacokinetic and pharmacodynamic properties of drugs and it is apparent from literature that the polycyclic cage is useful as both a scaffold for side-chain attachment as well as for improving a drug's lipophilicity.[23] This lipophilicity enhances a drug's transport across cellular membranes, including the selectively permeable blood-brain barrier, and increases its affinity for lipophilic regions in target proteins.[23,24] In addition, these polycyclic moieties afford metabolic stability, thereby prolonging the pharmacological effect of a drug, leading to a reduction of dosing frequency and improving patient compliance thereof.[25] The known NMDA receptor channel antagonism of these cage compounds, combined with their *L*-type calcium channel blocking activity, suggest that these polycyclic cage moieties may potentially serve as therapeutic agents for neurodegenerative disorders.[10,23,26-28]

With the focus being on the development of multifunctional drugs, it was thus a rational decision to incorporate polycyclic cage moieties and propargylamine functional groups or derivatives thereof into the structures of the novel compounds to be synthesized, thus giving

rise to a series of compounds with the inherent therapeutic profiles of the contributing moieties (i.e. NMDA receptor channel antagonism, *L*-type calcium channel blocking activity, MAO-B inhibitory activity and anti-apoptotic activity). A single compound exhibiting such an array of multifunctional neuroprotective activities may curb the neurodegenerative process more effectively than a compound which functions on only one of the many drug target sites available.

3.2. Results and discussion

3.2.1. Synthesis

In synthesising the novel polycyclic compounds (**9** – **16**, Figure 2), propargylamine, propargylbromide or ethynyl magnesium bromide was reacted with the PCU (**1**, Cookson's diketone) or amantadine (**2**) scaffold to give the final compounds (Figure 2). Each compound was synthesized to evaluate the activity and benefit of the presence of a certain group of atoms in the molecule. These groups included the following: a terminal acetylene group (**9**), an acetylene group between two non-polar groups (**10**), a secondary propargylamine connected to an oxa-PCU structure (**11**, **12**), a tertiary propargylamine conjugated to an aza-PCU structure (**13**, **14**) and an adamantane structure (**15**, **16**).

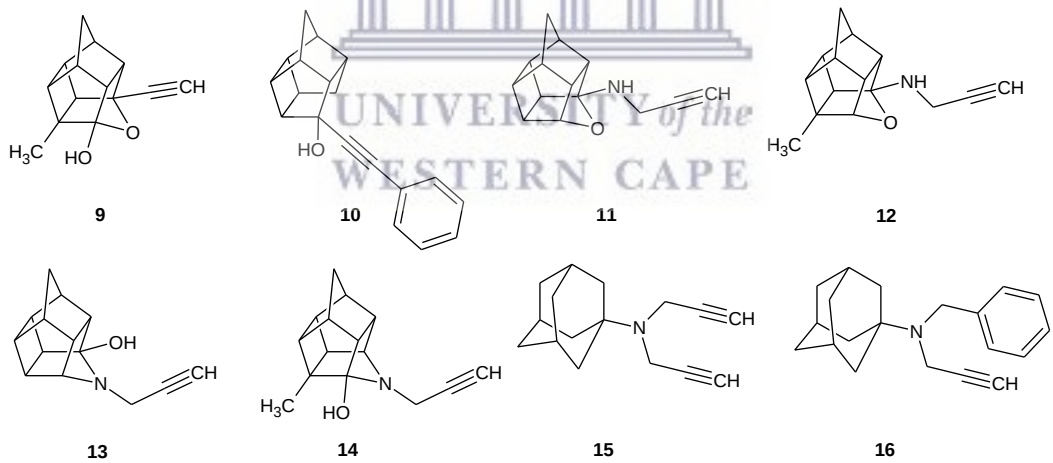

***Figure 2*:** Synthesized acetylene (**9** and **10**) and propagylamine (**11** – **16**) polycyclic compounds evaluated for anti-apoptotic activity, calcium modulating effects and MAO-B inhibition.

Starting from the PCU diketone (**1**) or the methyl-diketone (**a**, Scheme 1), depending on the compound to be synthesized, the reaction proceeded by conjugation of propargylamine through reductive amination with sodium borohydride, following steps i-iv to give the oxa-derivatives, **11** and **12**. The aza derivatives, **13** and **14**, were synthesized utilising sodium cyanoborohydride as reducing agent. Compound **9** was synthesized *via* the Grignard reaction

through conjugation of ethynyl magnesium bromide with the methyl-diketone producing the title compound **9** (Scheme 1).

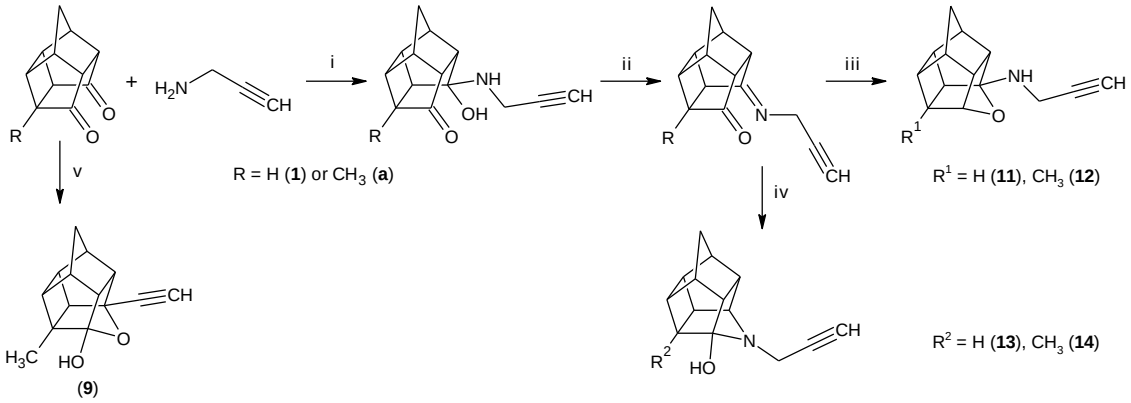

***Scheme 1*:** Reagents and conditions: (i) THF, -10°C, 45 min; ii) benzene, Dean-Stark, reflux, 1 h; (iii) THF/MeOH, $NaBH_4$, rt, 24 h; **11**, 10 %; **12**, 27% (iv) THF/MeOH, $NaCNBH_4$, rt, 24 h; **13**, 16 %; **14**, 4 %; (v) THF, ethynyl magnesium bromide, rt, 21 h, **9**, 16 %.

The synthesis of compound **10** commenced with the Cookson's diketone (Scheme 2), which was mono-protected as the corresponding ethylene acetal. The remaining ketone was reduced with lithium aluminium hydride and subsequent hydrolysis furnished the hydroxyl-ketone. Wolff-Kisher reduction of the hydroxyl-ketone under Huang-Minlon conditions gave the mono-alcohol, followed by oxidation with chromium trioxide to yield the mono-ketone (**b**). The mono-ketone (**b**) was conjugated to phenylacetelene in the presence of a potassium fluoride and alumina solution to yield the title compound **10** (Scheme 2).

The synthesis of compound **15** commenced through the conjugation of the primary amine of amantadine (**2**) and benzaldehyde with subsequent reduction, utilising LiAlH to give *N*-benzyl-adamantan-1-amine (**c**, Scheme 3). Propargylbromide was conjugated to (**c**), via a nucleophilic S_N2 substitution reaction, to produce compound **15**. Compound **16** was synthesized by means of microwave irradiation in the presence of an excess amount of propargylbromide (Scheme 3). The PCU structures, compounds (**9**-**14**), were obtained and evaluated as racemic mixtures and the structure and geometry of representative compounds were recently confirmed using single Xray crystallography and standard spectroscopy techniques.[29]

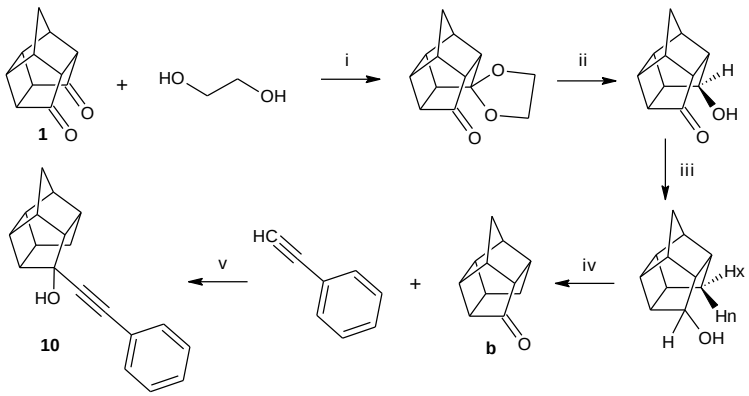

***Scheme 2*:** Reagents and conditions: (i) *p*-TsOH (cat), benzene, Dean-Stark, reflux, 3.5 h, 95 % (ii) $LiAlH_4$, Et_2O, reflux, 2 h then 6 % aq HCl, rt, 2 h, 61 %; (iii) $NH_2.NH_2.H_2O$, diethylene glycol, 120°C, 1.5 h, then KOH, 190°C, 3 h, 33 %; (iv) CrO_3, H_2O, 94 % aq CH_3COOH, 90°C, 4 h, **b**, 84 %; (v) KF/alumina, 60°C, 12 h, **10**, 73 %.

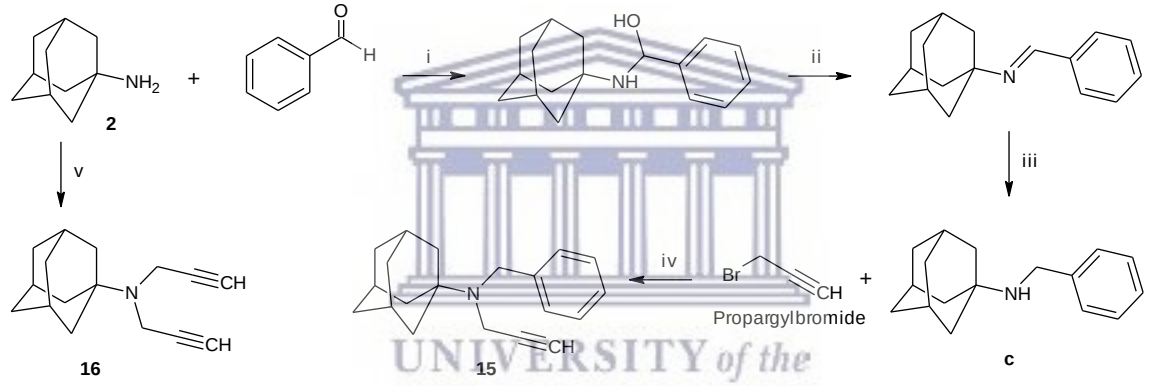

***Scheme 3*:** Reagents and conditions: (i) EtOH, rt, 4 days, 59 %; (ii) $-H_2O$; (iii) $NaBH_4$, reflux, 12 h, **c**, 59 %; (iv) DMF, rt, 24 h; **15**, 25 %; (v) Excess propargylbromide, aq NaOH, microwave (25 min, 80 °C – 100 °C, 250 W); **16**, 91 %.

3.2.2. Anti-apoptotic activity

The compounds' anti-apoptotic activity were evaluated *in vitro* using the DePsipher^{TM} kit, which marks changes in the mitochondrial membrane potential that takes place during apoptosis.[30] The quantitative and qualitative detection of apoptosis were done by means of flow cytometry, which made it possible to determine the percentage of cells that were still viable in the samples after treatment with the synthesized compounds. For this purpose SK-NBE(2) neuroblastoma cells were used, and apoptosis was induced using a serum-deprivation model. Control experiment 1 was included to evaluate the viability status of the cells, in the absence of test compound, with 1.25 % dimethyl sulphoxide (DMSO, Figure 3). The viability

data was used to compare the data generated with the test compounds in order to determine if the test compounds attenuated the progression of the apoptotic process. With this control experiment the effect of 1.25 % DMSO was also evaluated. Control experiment 2 was used to evaluate the viability of the cells and the progression of the apoptotic process in the absence of DMSO. When comparing the values of control experiments 1 and 2, it is clear that even though the final DMSO concentration in the samples was only 1.25 %, it had a negative effect on the viability of the cells. In control experiment 2, which did not contain any DMSO, cell viability increased with 7.19 %. It can thus be argued that the serum deprivation was not the only factor inducing apoptosis, but also the DMSO, which served as co-solvent for the test compounds. Control experiment 3 was used to evaluate the influence of re-introduction of serum rich medium, which significantly attenuated the apoptotic process. This control experiment was used to estimate the potencies of the test compounds as anti-apoptotic agents. Control experiment 4 was included to analyse and determine the viability status of the cells, when no apoptosis had been induced, and conditions had been favourable to the end of the experiment. It was also included to ensure that the cells analysed were indeed healthy before inducing apoptosis (see section 4.3.1. for a complete explanation of the experimental procedure).

The novel compounds were all tested in triplicate at three different concentrations (1 mM, 100 μM and 10 μM). The positive control, selegiline, was evaluated in triplicate at two concentrations (100 μM and 10 μM, Figure 3). Included in the assay was the prototype polycyclic cage moiety, 8-benzylamino-8,11-oxapentacyclo[5.4.0^{2,6}.0^{3,10}.0^{5,9}]undecane (NGP1-01),[31] which was also evaluated in triplicate at the highest concentration (1 mM). NGP1-01 is a well-known NMDA receptor channel inhibitor and calcium channel antagonist, and was evaluated for anti-apoptotic activity, as an abnormal increase in calcium levels can act as a trigger for apoptosis.[10] The positive control, selegiline, had 12-19 % more cells that were healthy and wherein apoptosis had either not been induced or reached the level of mitochondrial depolarisation, compared to control experiment 1 (Figure 3). When compared to control experiment 1, compounds **9** – **16** and NGP1-01 (**3**) all had significant anti-apoptotic activity improving cell health between 9 % and 41 %. The anti-apoptotic activity of **9** - **15** were the most significant ($p < 0.001$; Figure 3). The compound with the highest anti-apoptotic activity was **9**, where all cultures treated exhibited only 0.5 % apoptotic cells in the analysed samples. Compound **10** was slightly less active than compound **9**, with only 2.8 % of the cells showing apoptosis (Figure 3). Studying the results of these experiments, it is clear that the anti-apoptotic activity of propargylamine can most probably be attributed to the acetylene group, as compounds **9** and **10** have equivalent or even higher activity than

compounds **11** - **16**. For activity, this acetylene group can either be terminal (**9**) or between two non-polar groups (**10**), with the terminal acetylene group having slightly higher activity. It was also confirmed that when linked to a polycyclic cage structure, propargylamine and acetylene derivatives displayed increased anti-apoptotic activity. Further investigation must be conducted to ascertain whether this reported activity is solely due to the acetylene group, the cage moiety, or the acetylene group in conjunction with a nearby electronegative atom/group.

Comparing the activity of compounds **11** and **13**, it seems that the tertiary propargylamine had slightly higher activity than the secondary propargylamine, but the oxa- and aza-compounds in general had comparable activity activities. In the case of the oxa-compounds (**11**, **12**), the methylated cage showed increased activity. With the aza compounds (**13**, **14**), this was not observed. The adamantane compounds (**15**, **16**) had significantly lower activities than that of the pentacycloundecane compounds **9** – **13**. Solubility problems were also experienced with compounds **15** and **16** at higher concentrations, which may contribute to the observed lower anti-apoptotic action. It could also be attributed to the possibility that the pentacycloundecanes may have an increased ability to cross cell membranes due to their high degree of lipophilicity,[23] which would result in increased intracellular concentrations of the compounds. Comparing the percentage healthy cells of the samples treated with test compounds **9**, **10**, **12** and **13**, with that of the control experiment 4, which is representative of healthy cells in a favourable environment, it is interesting to note that these samples had more healthy cells than that of control experiment 4. This may be attributed to the compounds inhibiting even baseline apoptotic processes.

Although NGP1-01 exhibited significant anti-apoptotic activity, the activities of the synthesized compounds (**9** - **16**) were shown to be higher in comparison. This might be due to NGP1-01 only inhibiting one of the triggers of apoptosis, namely excitotoxicity due to calcium flux into the neuronal cells, whereas the newly synthesized compounds possibly inhibit the apoptotic cascade, directly or indirectly, at more than one point. However, further evaluations of these compounds are necessary to ascertain this.

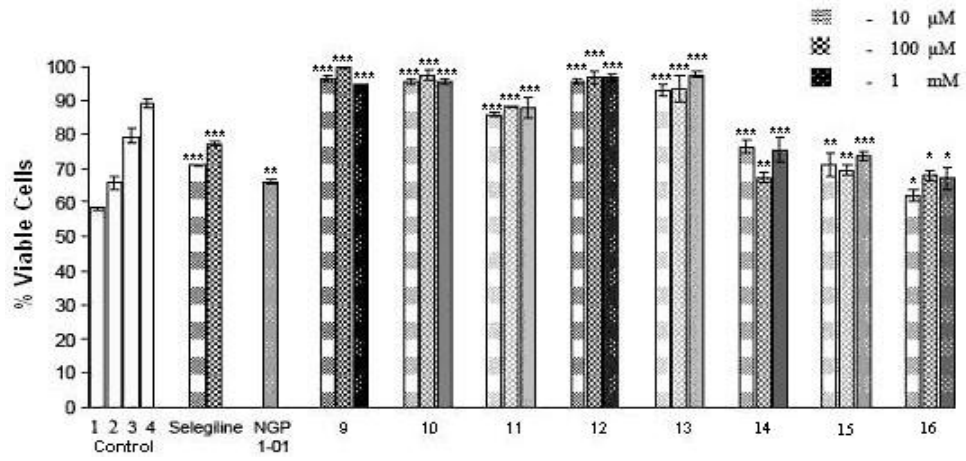

***Figure 3*:** Anti-apoptotic activity of the test compounds (*p < 0.05; **p < 0.01; ***p < 0.001)

3.2.3. VGCC and NMDA receptor channel activity

All polycyclic propargylamine and acetylene derivatives (**9**-**16**) were screened at 100 µM for their potential inhibitory activity on VGCC and/or NMDA receptor (NMDAR) channel. They were assessed using the fluorescent ratiometric indicator, Mag-Fura-2/AM, and a fluorescent plate reader. KCl mediated calcium influx in murine synaptoneurosomes was used to evaluate the influence of the test compounds on the calcium influx *via* VGCC. NMDA/Glycine mediated calcium influx was used to evaluate the influence of the test compounds on calcium influx *via* the NMDA receptor channel. Both assays were carried out with reference to standard controls. Results are shown in Table 1.

Fresh synaptoneurosomes were prepared[32] from rat brain homogenate and incubated with the ratiometric fluorescent calcium indicator, Fura-2/AM. The synthesized compounds were incubated for 30 minutes and a 140 mM KCl or a 100 µM NMDA/Glycine solution, in the VGCC and NMDA assay respectively, was added to depolarize the cell membranes or to stimulate calcium flux through the respective channels. Calcium influx was then monitored based on the fluorescence intensity relative to that of a negative control (without inhibiting compound) over a 5 min period. Two positive controls were included in the VGCC assay; nimodipine, a commercially available dihydropyridine *L*-type calcium channel blocker and the prototype pentacycloundecane compound NGP1-01. Two positive controls were also included in the NMDAR assay; MK-801, a commercially available potent high affinity NMDAR channel blocker and NGP1-01.

The results obtained showed variable activities from the compound series (Table 1). Compound **16**, an adamantane derivative, showed the best VGCC inhibitory activity within this series (45 %). This adamantine derived propargylamine compound showed activity

higher compared to that of NGP1-01 (**7**, 27 %). Although structurally similar to **16**, the substitution of the aromatic moiety of **16** with a propargyl moiety to give the di-substituted propargylamine adamantane compound (**15**), led to a significant decrease in VGCC activity (18 %). This observation indicates the importance of including the benzylamine moiety within these structures for optimal VGCC activity. The exact mechanism in which these compounds interact with the VGCC for activity is thus far unexplored. The presence of the polycyclic cage moieties in the series of compounds and similarities to NGP1-01 and other polycyclic cage benzylamines, supports a mechanism earlier described for NGP1-01 as being frequency- and voltage- dependent open calcium channel blockers.[33]

These compounds also exhibited of the highest NMDAR channel inhibitory activities within this test series (52 % and 59 % for **15** and **16** respectively). This high activity might be attributed to the inclusion of the adamantane moiety, which has known NMDAR inhibitory activity. Within the pentacycloundecane (PCU) test series, compounds **10** (19 %), **12** (26 %) and **13** (18 %) showed moderate VGCC blocking effects when compared to that of NGP1-01 (27 %). The remaining PCU derivatives showed low (**9** and **14**) to no VGCC activity (**11**). It is interesting that the inclusion of a methyl group to the structure of the inactive oxa-PCU compound **11** to give compound **12** improved the VGCC activity by 26 %. However, this trend was not observed for the aza-PCU compounds **13** (11 %) and **14** (18 %). NMDAR channel inhibition was observed for PCU compounds **10** (23 %) and **12** (38 %), which showed improved inhibitory activity when compared to NGP1-01 (18%). Compound **12** showed dual action on both VGCC (26 %) and NMDAR (38 %). This finding suggests that the inclusion of the methyl substituent contributes towards binding and activity on both these drug targets as the compound exhibited activity comparable to, and better than NGP1-01 on both the VGCC and NMDAR. Comparing the activities obtained with compound **12** to that of compound **14** (VGCC – 11 %, NMDAR – 11 %), suggests that the oxa compounds have better VGCC and NMDAR inhibitory activity compared to aza compounds. Removal of the methyl substituent from **14** to give compound **13** increased VGCC inhibitory activity to 18 % but decreased NMDAR inhibitory action to only 4 %. Compound **10**, which resembles NGP1-01 in the aromatic moiety, also showed dual action on the VGCC (19 %) and NMDAR (23%) as seen with NGP1-01, a known VGCC and NMDAR antagonist. It is suggested that these compounds (**9-16**) exhibit a blockade of the NMDA channel which is consistent with uncompetitive antagonism, similar to that reported for memantine. Memantine shares the phencyclidine (PCP)/tenocyclidine (TCP)/MK-801/ketamine binding site inside the NMDA channel pore. Radio-ligand binding studies with [3H]MK-801 and

[3H]TCP, however, showed little or no displacement of PCU compounds, including NGP1-01, from this binding site. The functional block of calcium observed for the PCU structures needs to be further explored to elucidate the exact mechanism of action. We hypothesize that the series described in this paper will exhibit a similar mechanism of action and act as direct NMDA channel blockers.[10]

3.2.4. MAO-B inhibitory activity

The synthesized compounds were also evaluated in vitro at various concentrations as inhibitors of MAO-B, using a spectrophotometric assay that utilised MMTP, an analogue of the neurotoxin MPTP as substrate, with baboon liver mitochondria serving as enzyme source. The potency of MAO-B inhibition was expressed as percentage inhibition of the MAO-B enzyme (Table 1). Only compound **10** showed significant MAO-B inhibition activity when compared to that of selegiline (93.22%), inhibiting the MAO-B enzyme by 73.32% at 300 µM. The rest of the compounds in the series either had no activity (**9**, **11**) or exhibited very limited inhibition, ranging from 5.83 to 20.13% (**12-16**). Comparing the MAO-B inhibition potencies of **11** with **12** and **13** with **14** reveals that in both cases the methyl group on the polycyclic cage, appeared to slightly increase MAO-B inhibition activity of the compounds. This may be ascribed to the enhanced interaction obtained with the non-polar entrance regions of the MAO-B enzyme. For comparison, NGP1-01 was also evaluated as a MAO-B inhibitor, but no significant activity was observed. The compounds containing a phenyl side chain (**10**, **15** and selegiline), were consistently better inhibitors than the rest of the series and it can be speculated that these compounds were able to block the entrance cavity of the MAO-B enzyme active site (see Fig. 4). This may possibly be attributed to the planar character of the phenyl ring and possibly to the extended planar character of compound **10**.

It has also been reported in literature that planar compounds frequently act as potent inhibitors of MAO-B.[34,35] Compound **10** contains both a hydroxyl and an extended planar phenyl moiety, which might further explain the significantly higher activity of **10** compared to that of the other synthesized compounds.

3.2.5. MAO-B molecular modelling

Computer-assisted simulated docking of compounds **9-16**, using Molecular Operating Environment (MOE), was carried out in an attempt to clarify the MAO-B inhibition activity – or lack thereof – for these structures[36]. The best-ranked docking solutions of the test compounds examined, showed that the proposed inhibitors occupy only the entrance cavity and barely access the substrate cavity of the MAO-B enzyme (PDB ID: 2V5Z, Fig. 4)[37]. In general, the amino acid residues between 120 and 220 are important in conferring substrate selectivity of MAO-B[38], most importantly residues Ile-199 (situated in the entrance cavity) and Gln-205 (situated in the substrate cavity). Interaction with these amino acid residues may confer a compound MAO-B inhibitory activity as shown by safinamide (Fig. 4), a known MAO-B inhibitor.

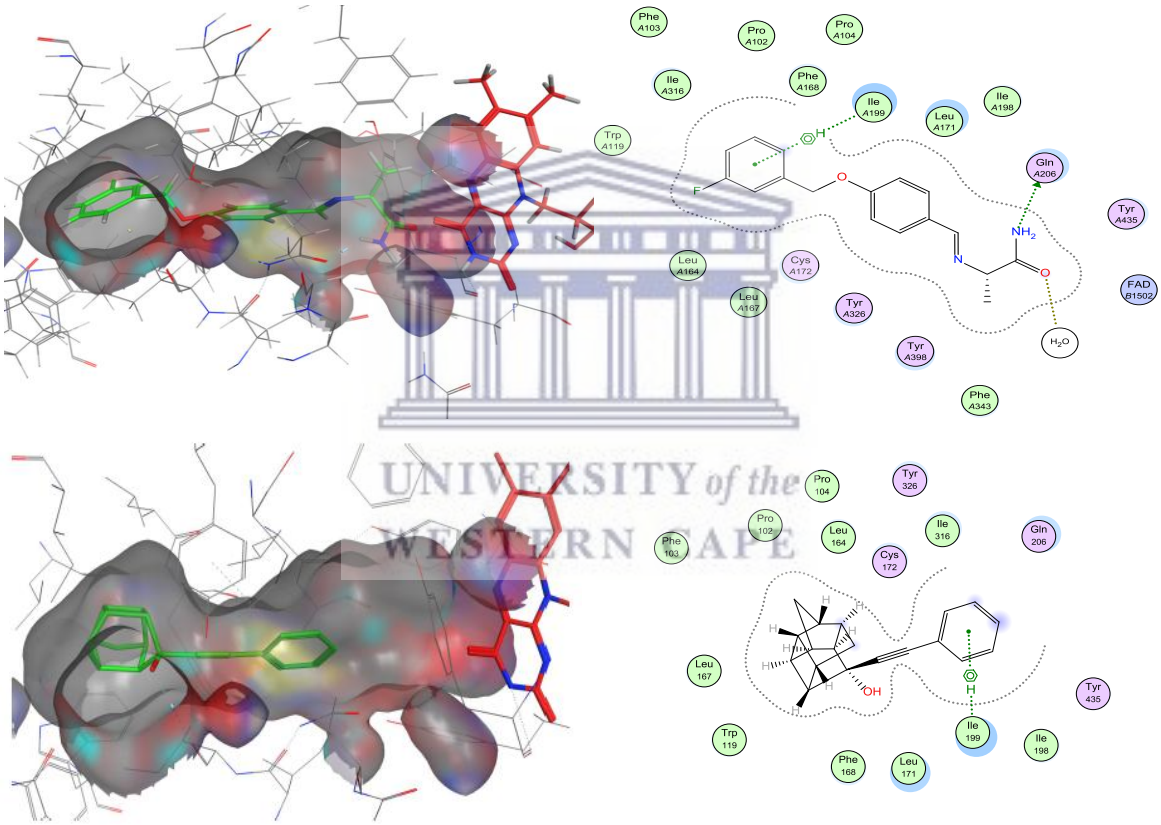

Figure 4: Comparison between the putative binding modes of safinamide and compound **10** to the human MAO-B enzyme active site. The compounds and FAD cofactor in bold lines (online indicated in green and red respectively) with their respective binding interactions with the amino acid residues (sticks) shown on the right of each enzyme cavity representation. Safinamide and compound **10** show productive interactions with amino acid residues Ile-199 and Gln 205, and Ile-199, respectively.

For compound **10** it was shown that the polycyclic moiety is stabilized within the entrance cavity with the extended planar phenyl moiety able to traverse deeper into the enzyme cavity and form the necessary interactions with Ile-199 (Fig. 4). This productive interaction between the phenyl function and the active site residue Ile-199 of the substrate cavity and/or the

stabilisation of the polycyclic moiety to actively block the entrance cavity, might explain the MAO-B inhibitory activity observed for **10**. All the polycyclic moieties are stabilised within the hydrophobic entrance cavity and were unable to traverse deeper into the substrate cavity, to from the necessary binding interactions with the flavin adenine dinucleotide (FAD) cofactor, which would have resulted in binding interactions and an increase the activity of these compounds (Fig. 4)[39,40].

Based on the molecular modelling results we are currently in process of developing a series of optimized PCUpropargylamine hybrid molecules with binding interactions and molecular orientations which might lead to enhanced MAO-B activity for these compounds. This series will enable the propargyl moiety to penetrate deeper into the cavity within close proximity of the FAD co-factor, similar to selegiline and rasagiline (data not shown)[19]. We also envision that the multifunctional activities shown for the current propargylamine derivatives will be retained in the new series.

3.3. Conclusion

This study aimed to develop compounds that would ultimately inhibit NMDA receptors, block VGCC and inhibit apoptotic processes as well as the MAO-B enzyme. Based on the results it can be concluded that compounds **10**, **12**, **15** and **16** showed the best range of activities. These compounds however showed little to no activity on the MAO-B enzyme except for 8-phenyl-ethynyl-8-hydroxypentacycloundecane (**10**) which inhibited the MAO-B enzyme by 73.32% at 300 µM. The compounds in the series all had significant anti-apoptotic activity comparable (**14-16**) to and better (**9-13**) than selegiline. Although the findings suggest compounds **9** and **11** to have little or no activity on the VGCC, NMDA receptors and MAO-B enzyme, the ability of these compounds to significantly inhibit apoptosis suggests that the compounds exhibit their neuroprotective action through some other mechanism(s) unexplored in this study. Having significant anti-apoptotic activity, this series of compounds might present interesting lead compounds in the design and development of more potent inhibitors. Further *in vitro* and *in vivo* studies into the anti-apoptotic cascade, dopamine transmission and blood-brain barrier permeability of these novel compounds are in process. Findings from these studies will elaborate on their potential as neuroprotective agents and might identify the point(s) at which these compounds inhibit the apoptotic process. The polycyclic propargylamines and acetylene derivatives thus have potential as novel multifunctional neuroprotective agents and further investigation is necessary to determine their maximum benefit in the treatment of neurodegenerative disorders.

3.4. Experimental

3.4.1. General procedures

Unless otherwise specified, materials were obtained from commercial suppliers and used without further purification. All reactions were monitored by thin-layer chromatography on 0.20 mm thick aluminium silica gel sheets (Alugram® SIL G/UV_{254}, Kieselgel 60, Macherey-Nagel, Düren, Germany). Visualisation was achieved using UV light (254 nm and 366 nm), an ethanol solution of ninhydrin or iodine vapours, with mobile phases prepared on a volume-to-volume basis. Chromatographic purifications were performed on silica gel (0.063–0.2 mm, Merck) except when otherwise stated. The mass spectra (MS) were recorded on an analytical VG 70-70E mass spectrometer using electron ionisation (EI) at 70 eV. Infra-red (IR) spectra were recorded on a Shimadzo IR prestige – 21 Fourier transform infrared spectrophotometer using KBr. Melting points were determined using a Gallenkamp and Stuart SMP-300 melting point apparatus and capillary tubes. All the melting points determined were recorded uncorrected. High resolution electron spray ionisation (HREI) mass spectra for all compounds were recorded on a Waters API Q-Tof Ultima mass spectrometer at 70 eV and 100 °C. All HREI samples were introduced by a heated probe and perfluorokerosene was used as reference standard. ^{1}H and ^{13}C NMR spectra were acquired on a Bruker Avance III 600 MHz spectrometer, with the ^{1}H spectra recorded at a frequency of 600.170 MHz and the ^{13}C spectra at 150.913 MHz. Tetramethylsilane (TMS) was used as internal standard, with $CDCl_3$ as solvent. All chemical shifts are reported in parts per million (ppm), relative to the internal standard. The following abbreviations are used to indicate the multiplicities of the respective signals: s - singlet; br s - broad singlet; d - doublet; dd - doublet of doublets; t - triplet; m - multiplet; and AB-q - AB quartet. The multiplicity of the identified carbons was confirmed with DEPT-spectra. Microwave synthesis was performed using a CEM Discover™ microwave synthesis system.

3.4.2. Synthesis of compounds

*3.4.2.1. Pentacyclo[5.4.1.$0^{2,6}$.$0^{3,10}$.$0^{5,9}$]undecane-8-11-dione (**1**)*

As described by Cookson *et al*. (1958, 1964).[41]

*3.4.2.2. 1-Methyl-pentacyclo[5.4.1.$0^{2,6}$.$0^{3,10}$.$0^{5,9}$]undecane-8-11-dione (**a**)*

As described by Marchand *et al*. (1984).[42]

*3.4.2.3. Pentacyclo[5.4.1.0^{2,6}.0^{3,10}.0^{5,9}]undecane-8-one (**b**)*

As described by Dekker and Oliver (1979).[43]

*3.4.2.4. 8-Benzylamino-8,11-oxapentacyclo[5.4.0^{2,6}.0^{3,10}.0^{5,9}]undecane (NGP1-01, **3**)*

As described by Van der Schyf *et al*. (1986).[31]

*3.4.2.5. 1-Methyl-8-ethynyl-11-hydroxy-8,11-oxapentacyclo[5.4.0^{2,6}.0^{3,10}.0^{5,9}]undecane (**9**)*

A solution of 1-methyl-pentacyclo[5.4.1.0^{2,6}.0^{3,10}.0^{5,9}]undecane-8-11-dione (**a**) (1.88 g; 10 mmol) in dry tetrahydrofuran (10 mL) was added to an excess of ethynyl magnesium bromide (1.0 M solution in tetrahydrofuran) (2.838 mL; 22 mmol) under argon, whilst stirring. The resulting mixture was stirred at ambient temperature for 21 hours. The reaction mixture was poured over saturated aqueous ammonium chloride (NH_4Cl) solution (100 mL), and the resulting suspension was extracted with diethyl ether (3 x 25 mL). The combined organic extracts were washed sequentially with water (25 mL) and brine (25 mL). The solvent was dried (Na_2SO_4) and filtered, and the filtrate was concentrated under reduced pressure. The residue, pale yellow oil, was successfully purified by precipitation from a mixture of ethyl acetate/petroleum ether (1:3), over a period of 24 hours at ambient temperature. This yielded the pure product as a light brown powder (yield: 0.762 g; 3.170 mmol; 15.87 %).

$C_{14}H_{14}O_2$; **MW,** 214.3 g/mol; **mp.** 126 °C; **IR (KBr)** *vmax*: 3260, 2125, 1211, 1031 cm^{-1}; **MS** (EI, 70 eV) m/z: 214 (M+), 186, 169, 158, 116, 91, 77, 39; **HR-ESI [M+H]$^+$**: calc. 215.1067, exp. 215.1069. **^{1}H NMR** (600 MHz, $CDCl_3$) δH: 3.72 (s, OH), 3.12 - 2.37 (m, 7H, H- 2,3,5,6,7,9,10), 2.31 (s, 1H, H-13), 1.88:1.54 (AB-q, 2H, J = 10.4 Hz, H-4a,4b), 1.10 (s, 3H, CH3); **^{13}C NMR** (150 MHz, $CDCl_3$) δc: 116.87 (1C, C-11), 81.18 (1C, C-8), 75.30 (1C, C-12), 61.84 (1C, C-13), 57.24 (1C, C-9), 56.91 (1C, C-7), 50.75 (1C), 47.46 (1C), 45.22 (1C), 43.49 (1C, C-4), 41.56 (1C), 39.19 (1C, C-1), 15.29 (1C, C-14).

*3.4.2.6. 8-Phenylethynyl-8-hydroxy-pentacyclo[5.4.0^{2,6}.0^{3,10}.0^{5,9}]undecane (**10**)*

Neutral alumina (60–80 mesh, 30 g) in water (150 mL) was added to a stirred solution of potassium fluoride (20 g) in water (150 mL). After 30 minutes the water was evaporated in a rotary evaporator at 80 °C. When most of the water had been removed, the remaining mixture was heated to, and maintained at 140–150 °C under vacuum (5 mm Hg) overnight to afford 50 g of KF/alumina reagent. Phenylacetylene (255.350 mg; 2.500 mmol),

pentacyclo[5.4.0^{2,6}.0^{3,10}.0^{5,9}]undecane-8-one (**b**, 480.650 mg; 3 mmol), and KF/alumina (2.500 g) were mixed in a 25 mL flask at 60 °C . The progress of the reaction was monitored by TLC. After 12 hours the reaction mixture was washed with petroleum ether, filtered, and the solvent was evaporated under vacuum, affording a clear yellow oil. The residue was purified by means of column chromatography, by using a versa flash silica-gel column with petroleum ether/ethyl acetate (10:2) as eluent, to afford the product as a light yellow wax (yield: 480 mg; 1.830 mmol; 73.18 %).

$C_{19}H_{18}O$; MW, 262.4 g/mol; **mp.** 90 °C; **IR (KBr)** *vmax*: 3069, 2225, 1599, 1491, 1125, 752 cm^{-1}; **MS** (EI, 70 eV) m/z: 262 (M+), 196, 183, 165, 129, 115, 91, 77; **HR-ESI [M+H]$^+$**: calc. 263.1430 exp. 263.1439; **^{1}H NMR** (600 MHz, $CDCl_3$) δH 7.36 – 7.13 (m, 5H, H 15,16,17,18,19), 2.77 – 2.28 (m, 8H, H-1,2,3,5,6,7,9,10), 1.93:1.60 (AB-q, 2H, H-11a,11b), 1.72:1.18 (AB-q, 2H, J = 10.4 Hz, H-4a,4b); **^{13}C NMR** (150 MHz, $CDCl_3$) δc: 131.51 (1C, C-14), 128.23 (2C, C-15,19), 128.10 (2C, C-16,18), 123.02 (1C, C-17), 94.15 (1C, C-8), 83.21 (1C, C-13), 75.91 (1C, C-12), 51.50 (1C), 47.27 (1C), 45.20 (1C), 44.95 (1C), 42.73 (1C, C-4), 41.50 (1C), 40.61 (1C), 36.62 (1C), 34.73 (1C), 28.98 (1C, C-11).

*3.4.2.7. 8-(N)-Propargylamino-8,11-oxapentacyclo[5.4.0^{2,6}.0^{3,10}.0^{5,9}]undecane **(11)***

Pentacyclo-[5.4.0^{2,6}.0^{3,10}.0^{5,9}]undecane-8-11-dione (**1**, 5 g; 0,029 mol) was dissolved in tetrahydrofuran (50 mL) and cooled to ± -10 °C, while stirring on an external bath, containing an acetone/NaCl/ice mixture. Propargylamine (1.600 g; 0.029 mol) was added drop-wise, with continued stirring of the reaction mixture at lowered temperature. The carbinolamine started precipitating after approximately 15 minutes, but the reaction was allowed to stir for an additional 30 minutes to reach completion. The carbinolamine was isolated by filtration and washed with ice cold THF. Water was removed azeotropically by refluxing the material in dry benzene (60 mL), under Dean–Stark dehydrating conditions for 1 hour, or until no more water was collected in the trap. The benzene was removed under reduced pressure, which yielded the Schiff base as yellow oil. The Schiff base (imine) was then dissolved in a mixture of anhydrous methanol (30 mL) and anhydrous tetrahydrofuran (THF) (150 mL). Reduction was carried out by adding sodium borohydride ($NaBH_4$) (1.500 g; 0.040 mol) in excess, and stirring the mixture for 24 hours at room temperature. The solvents were removed under reduced pressure, the residue suspended in water (100 mL) and extracted with methylene chloride (4 x 50 mL). The combined organic fractions were washed with water (2 x 100 mL), dried over anhydrous $MgSO_4$ and evaporated under reduced pressure to yield a milky yellowish oil. Purification of the product mixture was accomplished using column

chromatography on silica gel, with ethyl acetate/methylene chloride/petroleum ether (1:1:1) as eluent. This yielded the desired amine as a light yellow precipitate. Recrystallisation from absolute ethanol rendered the final product as a colourless microcrystalline solid (yield: 600 mg; 2.827 mmol; 9.75 %).

$C_{14}H_{15}O_1N_1$; MW, 213.28 g/mol; **mp.** 113 °C**; IR (KBr)** *vmax*: 3306, 3238, 2124, 1485, 1153, 1000 cm^{-1}; **MS** (EI, 70 eV) m/z: 213 (M+), 184, 134, 118, 91, 77, 39; **HR-ESI $[M+H]^+$**: calc. 214.1226, exp. 214.1225. **^{1}H NMR** (600 MHz, $CDCl_3$) δH: 4.63 (t, 1H, J = 5 Hz, H-11), 3.57:3.56 (dd, 2H, J = 2.5 Hz, H-12a,12b), 2.80 – 2.39 (m, 8H, H-1,2,3,5,6,7,9,10), 2.26 (br s, NH), 2.21 (s, 1H, H-14), 1.88:1.52 (AB-q, 2H, J = 10.4 Hz, H-4a,4b); **^{13}C NMR** (150 MHz, $CDCl_3$) δc: 108.98 (1C, C-8), 82.81 (1C, C-11), 82.76 (1C, C-13), 70.92 (1C, C-14), 55.46 (1C, C-7/9), 54.76 (1C, C-7/9), 44.84 (1C), 44.65 (1C), 44.54 (1C), 43.3 (1C), 43.07 (1C, C-12), 42.04 (1C), 41.54 (1C), 33.07 (1C).

*3.4.2.8. 1-Methyl-8-(N)-propargylamino-8,11-oxapentacyclo[5.4.$0^{2,6}$.$0^{3,10}$.$0^{5,9}$]undecane (**12**)*

1-Methyl-penta-cyclo[5.4.$0^{2,6}$.$0^{3,10}$.$0^{5,9}$]undecane-8-11-dione (**a**, 5.460 g; 0.029 mol) was dissolved in tetrahydrofuran (50 mL) and cooled to ± -10 °C, while stirring on an external bath containing an acetone/NaCl/ice mixture. Propargylamine (1.600 g; 0.029 mol) was slowly added with continued stirring of the reaction mixture at lowered temperature. The reaction mixture was stirred for an additional 1½ hours to reach completion. The THF was removed under reduced pressure, affording the carbinolamine as a red/brown oil. Water was removed azeotropically by refluxing this material in dry benzene (60 mL), under Dean–Stark dehydrating conditions for 1 hour, or until no more water was collected in the trap. The benzene was removed under reduced pressure, which yielded the Schiff base as a brown oil. The Schiff base (imine) was dissolved in a mixture of anhydrous methanol (30 mL) and anhydrous tetrahydrofuran (150 mL). Reduction was carried out by adding sodium borohydride (1.500 g; 0.040 mol) in excess and stirring the mixture for 24 hours at room temperature. The solvents were removed under reduced pressure, the residue suspended in water (100 mL) and extracted with methylene chloride (4 x 50 mL). The combined organic fractions were washed with water (2 x 100 mL), dried over anhydrous $MgSO_4$ and evaporated under reduced pressure to yield a dark brown oil. Purification of the product mixture was accomplished using column chromatography, with ethyl acetate/methylene chloride/petroleum ether (1:1:1) as eluent, yielding the desired amine as a dark brown oil (Yield: 1.753 g; 7.746 mmol; 26.71 %).

$C_{15}H_{17}O_1N_1$; MW, 227.3 g/mol; **IR (KBr)** *vmax*: 3310, 3250, 2100, 1452, 1153, 1007cm^{-1}; **MS** (EI, 70 eV) m/z: 227 (M+), 212, 198, 184, 158, 145, 131, 91, 77, 39; **HR-ESI $[M+H]^+$**: calc. 228.1383, exp. 228.1395. **^{1}H NMR** (600 MHz, $CDCl_3$) δH: 4.08 (d, 1H, J = 4.4 Hz, H-11), 3.57 (m, 2H, H-12a,12b), 2.73 – 2.20 (m, 7H, H- 2,3,5,6,7,9,10), 2.14 (br s, NH), 2.06 (d, 1H, J = 5.28 Hz, H-14), 1.86:1.51 (AB-q, 2H, J = 10.4 Hz, H-4a,4b), 1.15 (s, 3H, CH3); **^{13}C NMR** (150 MHz, $CDCl_3$) δc: 109.73 (1C, C-8), 87.15 (1C, C-11), 82.65 (1C, C-13), 70.95 (1C, C-14), 54.97 (1C, C-9), 54.66 (1C, C-7), 50.74 (1C), 46.99 (1C), 43.58 (1C), 43.18 (1C), 38.91 (1C, C-1), 33.07 (1C, C-12), 19.85 (1C, C-15).

*3.4.2.9. 8-Hydroxy-(N)-propargyl-8,11-azapentacyclo[5.4.$0^{2,6}$.$0^{3,10}$.$0^{5,9}$]undecane (**13**)*

Pentacyclo-[5.4.$0^{2,6}$.$0^{3,10}$.$0^{5,9}$]undecane-8-11-dione (**1**, 5 g; 0.029 mol) was dissolved in tetrahydrofuran (50 mL) and cooled to ± -10 °C, while stirring on an external bath, containing an acetone/NaCl/ice mixture. Propargylamine (1.600 g; 0.029 mol) was added slowly with continued stirring of the reaction mixture at lowered temperature. The carbinolamine started precipitating after approximately 60 minutes, but the reaction was stirred for an additional 45 minutes to reach completion. This carbinolamine was isolated by filtration. Water was removed azeotropically by refluxing this material in dry benzene (60 mL), under Dean–Stark dehydrating conditions for 1 hour, or until no more water was collected in the trap. The benzene was removed under reduced pressure and the Schiff base was used without further purification. It was dissolved in a solution of acetic acid (15 mL) and dry methanol (250 mL). To the resulting solution was added sodium cyanoborohydride ($NaBH_3CN$) (2.510 g; 40 mmol) portion wise, with stirring at room temperature over a period of 5 minutes. The resulting mixture was stirred at room temperature for 2 hours. The reaction mixture was then concentrated under reduced pressure, and water (100 mL) was added to the residue. The resulting suspension was stirred and solid sodium bicarbonate was added portion wise until evolution of carbon dioxide ceased. Excess solid sodium bicarbonate (2.000 g) was added, and the aqueous suspension was extracted with methylene chloride (4 x 50 mL). The combined extracts were washed with water (2 x 100 mL), dried with anhydrous magnesium sulphate and filtered. The filtrate was concentrated under reduced pressure. A yellow solid was thereby obtained. Purification of the product mixture was accomplished using column chromatography on silica, with ethyl acetate/methylene chloride/ethanol (10:5:1) as eluent. The desired amine was obtained as an off-white powder. Recrystallisation from cyclohexane rendered the final product as an off white microcrystalline solid (Yield: 960 mg; 4.501 mmol; 15.52 %).

$C_{14}H_{15}O_1N_1$; MW, 213.3 g/mol; **mp.** 140 °C**; IR (KBr)** *vmax*: 3225, 3100, 2114, 1120, 1070, cm^{-1}; **MS** (EI, 70 eV) m/z: 213 (M+), 196, 174, 147, 134, 118, 91, 77, 39; **HR-ESI $[M+H]^+$**: calc. 214.1226, exp. 214.1222; **^{1}H NMR** (600 MHz, $CDCl_3$) δH: 3.71 (s, 1H, H-12), 3.35 (d, 1H, J = 16.5 Hz, H-11), 3.00 – 2.43 (m, 8H, H-1,2,3,5,6,7,9,10), 2.25 (s, 1H, H-14), 1.82:1.49 (AB-q, 2H, J = 10.4 Hz, H-4a,4b); **^{13}C NMR** (150 MHz, $CDCl_3$) δc: 125.53 (1C, C-8), 81.23 (1C, C-13), 71.37 (1C, C-14), 65.52 (1C, C-11), 45.62 (1C, C-7/9), 43.12 (1C, C-7/9), 41.74 (1C, C-4), 41.60 (1C), 36.79 (1C), 30.33 (1C, C-12

*3.4.2.10. 1-Methyl-8-hydroxy-(N)-propargyl-8,11-azapentacyclo[5.4.0^{2,6}.0^{3,10}.0^{5,9}]undecane (**14**)*

1-Methyl-pentacyclo[5.4.0^{2,6}.0^{3,10}.0^{5,9}]undecane-8-11-dione (**b**, 10.658 g; 56.620 mmol) was dissolved in tetrahydrofuran (50 mL) and cooled to ± -10 °C, while stirring on an external bath containing an acetone/NaCl/ice mixture. Propargylamine (3.119 g; 56.620 mmol) was added drop wise with continued stirring of the reaction mixture at lowered temperature. The reaction mixture was stirred for 5½ hours to reach completion. The THF was removed under reduced pressure, affording a red/brown oil, the carbinolamine. Water was removed azeotropically by refluxing this material in dry benzene (60 mL), under Dean–Stark dehydrating conditions for 1 hour, or until no more water was collected in the trap. The benzene was removed under reduced pressure, which yielded the Schiff base as a dark brown oil. The Schiff base was used without further purification. It was dissolved in a solution of acetic acid (30 mL) in dry methanol (500 mL). To the resulting solution, sodium cyanoborohydride (3.970 g; 63 mmol) was added portion wise, with stirring at room temperature over a period of 5 minutes. The resulting mixture was stirred at room temperature for 14 hours. The reaction mixture was then concentrated under reduced pressure, and water (150 mL) was added to the residue. The resulting suspension was stirred, and solid sodium bicarbonate was added portion wise until evolution of carbon dioxide ceased. Excess solid sodium bicarbonate (3.000 g) was added, and the aqueous suspension was extracted with methylene chloride (4 x 50 mL). The combined extracts were washed with water (2 x 100 mL), dried with anhydrous magnesium sulphate, and filtered. The filtrate was concentrated under reduced pressure, leaving a deep orange oil as residue. Purification of the product mixture was accomplished using column chromatography on silica, with ethyl acetate/tetrahydrofuran (5:1) as eluent. This yielded the desired amine as a light yellow oil, which precipitated when ethanol was added. Recrystallisation from ethanol rendered the final product as a light yellow microcrystalline solid (Yield: 555 mg; 2.442 mmol; 4.31 %).

$C_{15}H_{17}O_1N_1$; MW, 227.3 g/mol; **mp.** 125 °C; **IR (KBr)** *vmax*: 3225, 3078, 2124, 1119, 1070 cm^{-1}; **MS** (EI, 70 eV) m/z: 227 (M+), 188, 134, 118, 91, 77, 39; **HR-ESI $[M+H]^+$**: calc. 228.1388, exp. 228.1392; **^{1}H NMR** (600 MHz, $CDCl_3$) δH: 3.46 - 3.34 (m, 1H, H-11), 3.22:3.09 (d, 2H, J = 17.3 Hz, H-12a,12b), 2.57 – 2.09 (m, 8H, H-2,3,5,6,7,9,10,14), 1.60:1.06 (AB-q, 2H, J = 10.4 Hz, H-4a,4b), 1.19 (s, 3H, CH3); **^{13}C NMR** (150 MHz, $CDCl_3$) δc: 125.53 (1C, C-8), 80.31 (1C, C-13), 72.68 (1C, C-14), 57.40 (1C, C-11), 46.62 (1C, C-9), 46.10 (1C, C-7), 45.09 (1C), 41.54 (1C, C-4), 37.63 (1C), 36.33 (1C), 34.52 (1C), 30.32 (1C, C-12), 21.98 (1C, C-15).

*3.4.2.11. N,N-Dipropargyl-adamantan-1-amine (**15**)*

Excess propargylbromide (0.595 mL; 6.677 mmol), amantadine (**2**, 302.49 mg; 2 mmol) and aqueous sodium hydroxide (NaOH) solution (180 mg in 6 mL water; 4.5 mmol) were placed in a round-bottom glass flask equipped with a condenser and a magnetic stirrer. The flask was placed in a CEM discover focused microwave synthesis system, and subjected to microwave irradiation at 80–100 °C (power 250 Watt) for 25 minutes. After completion of the reaction, the product was extracted into ethyl acetate. The solvent was then removed under reduced pressure. The unreacted amantadine was removed from the residue by adding acetone to the residue and collecting the amantadine by filtration. The acetone was then removed under reduced pressure from the filtrate, affording orange crystals which were recrystallised out of ethyl acetate to afford the pure product as light yellow crystals (412 mg; 1.812 mmol; 90.61 %).

$C_{16}H_{21}N_1$; MW, 227.35 g/mol; **mp.** 76 °C; **IR (KBr)** *vmax*: 3237, 2099, 1119 cm^{-1}; **MS** (EI, 70 eV) m/z: 227 (M+), 184, 144, 132, 91, 79, 53, 39; **HR-ESI $[M+H]^+$**: calc. 228.1752, exp. 228.1755; **^{1}H NMR** (600 MHz, $CDCl_3$) δH: 3.65 (s, 4H, H 11a,11b,14a,14b), 2.17 (s, 2H, H-13,16), 2.06 (s, 3H, H-3,5,8), 1.80 (s, 6H, H-2a,2b,6a,6b,7a,7b), 1.63 – 1.46 (m, 6H, H-4a,4b,9a,9b,10a,10b);**^{13}C NMR** (150 MHz, $CDCl_3$) δc: 82.12 (2C, C-12,15), 72.08 (2C, C-13,16), 55.45 (1C, C-1), 39.96 (3C, C-3,5,8), 36.54 (3C, C-2,6,7), 35.03 (2C, C- 11,14), 29.70 (3C, C-4,9,10).

*3.4.2.12. N-Propargyl-N-benzyl-adamantan-1-amine (**16**)*

A solution of amantadine (**2**, 5 g; 33.056 mmol) and benzaldehyde (3.51 g; 33.073 mmol) in ethanol (60 mL) was stirred for 4 days at ambient temperature under nitrogen atmosphere. The solvents were removed *in vacuo*. The resulting oil was dissolved in 80 ml benzene and

refluxed under Dean-Stark conditions for 6 hours, where after the benzene was removed *in vacou*. The resulting reaction mixture was dissolved in 60 ml ethanol and solid sodium borohydride ($NaBH_4$) (2.5 g; 66.085 mmol) was then added slowly in small portions over 30 minutes, and stirring of the resulting suspension was continued at room temperature for 30 minutes under nitrogen atmosphere. The reaction mixture was refluxed for 12 hours. After cooling to ambient temperature, the mixture was diluted with ethanol (60 mL), and the excess sodium borohydride was destroyed by adding aqueous hydrochloric acid (HCl) (10 mL, 5 M) drop wise. The reaction mixture was then made alkaline, to pH 12, by adding aqueous sodium hydroxide (NaOH) solution. Finally, the desired product was extracted to methylene chloride (4 x 10 mL) and dried over anhydrous magnesium sulphate ($MgSO_4$). The solvent was evaporated under reduced pressure to afford the intermediate product, *N*-benzyl-adamantan-1-amine (**c**), as white crystals (yield: 4.757 g; 19.6 mmol; 59.29 %). This intermediate product was subsequently used in the following steps without any further purification. A solution was made of *N*-benzyl-adamantan-1-amine (**c**, 4.757 g; 19.6 mmol) and excess propargylbromide (2.3 ml; 25.81 mmol) in dry dimethylformamide (30 mL), and left for 24 hours to react at ambient temperature. After this period of time the mixture was diluted with water (50 mL), and an extraction was done using methylene chloride (DCM) (3 x 50 mL) and dried over anhydrous sodium sulphate (Na_2SO_4). The solvent was removed under reduced pressure to afford a thick dark orange residue. The desired product was precipitated out of the residue by the addition of chloroform (30 mL), which allowed the collection of the final product by filtration as an off-white powder (yield: 1.352 g; 4.82 mmol; 24.59 %).

$C_{20}H_{25}N_1$; MW, 279.3 g/mol; **mp.** 81 °C; **IR (KBr)** *vmax*: 3210, 3062, 2091, 1495, 1130, 748cm^{-1}; **MS** (EI, 70 eV) m/z: 279 (M+), 236, 222, 185, 135, 91; **HR-ESI $[M+H]^+$**: calc. 280.2065, exp. 280.2063; **^{1}H NMR** (600 MHz, $CDCl_3$) δH: 7.35-7.20 (m, 5H, H-16,17,18,19,20), 3.84 (s, 2H, H-14a,14b), 3.32 (s, 2H, H-11a,11b), 2.15 (s, 3H, H-3,5,8), 2.09 (s, 1H, H-13), 1.90 (s, 6H, H-2a,2b,6a,6b,7a,7b), 1.65 (s, 6H, H-4a,4b,9a,9b,10a,10b); **^{13}C NMR** (150 MHz, $CDCl_3$) δc: 141.11 (1C, C-15), 128.65 (2C, C-16,20), 128.18 (2C, C-17,19), 126.66 (1C, C-18), 83.22 (1C, C 12), 72.08 (1C, C-13), 55.05 (1C, C-1), 48.98 (1C, C-14), 40.53 (3C, C-3,5,8), 36.77 (3C, C-2,6,7), 34.79 (1C, C-11), 29.86 (3C, C-4,9,10).

3.4.3. Biological evaluations

3.4.3.1. Apoptosis detection - DePsipher™ assay

DePsipher™ utilises a lipophilic cation (5,5′,6,6′-tetrachloro-1,1′,3,3′-tetraethylbenzimidazolyl carbocyaniniodide), which can be used as a mitochondrial activity marker to evaluate the viability of a cell population, detecting early apoptosis, and evaluating the effect of drugs on the cell population.[30] The cation aggregates upon membrane polarisation, forming an orange-red fluorescent compound. If the potential is disturbed, the dye cannot access the transmembrane space and remains orange-red or reverts to its green monomeric form. Thus, healthy cells present both the polymeric (orange-red) and monomeric (green) form of the cation, with the monomeric form residing in the cytoplasm and the aggregated form in the transmembrane space. It can be concluded that in comparison with healthy cells, wherein apoptosis has not been induced, the ratio of orange-red fluorescence to green fluorescence of apoptotic cells will be lower. The fluorescence can be observed and measured by flow cytometry with the red aggregates having absorption/emission maxima of 585/590 nm, and the green monomers absorption/emission maxima of 510/527 nm.

3.4.3.1.1. Biological material

3.4.3.1.1.1. Cell cultivation

In the current study the SK-N-BE(2) neuroblastoma cells were used to evaluate the anti-apoptotic activity of the synthesized compounds. The cells were cultivated in serum-rich growing medium, consisting of F12 nutrient (F12) supplemented with 10 % foetal bovine serum (FBS), 1 % penicillin/streptomycin (Pen/Strep) (10 000 units/100 mL stock) and 0.1 % fungizone (FZ) (2.5 µg/mL units stock). They were incubated at 37 °C in a 5 % CO_2 and 95 % O_2 humidified atmosphere. The cells duplicated every 30-48 hours and when a confluency of 80 % was reached, the adherent cells were detached from the flask bottom by means of trypsination. To ensure complete detachment of the cells, they were incubated with trypsine for approximately 10 minutes. After trypsination, the cells were seeded in new flasks at a density of no less than 1/6 confluency.

3.4.3.1.1.2. Induction of apoptosis

In the current study, trophic factor deprivation/serum starvation was used to induce apoptosis in cells. With growth factors being essential to the normal development and survival of neuronal cells, a shortage thereof would cause neurons to compete with one another for

neurotrophic factors, with the unsuccessful ones dying. With no serum (neurotrophic factors) available, all the cells will die in a given time. The serum deprived medium consisted of F12, Pen/Strep and FZ in the same ratio as mentioned in section 3.4.3.2.2.

3.4.3.1.1.3. Cells used to evaluate anti-apoptotic activity of compounds

After the cells reached 80 % confluency, the serum rich medium was replaced with serum deprived medium. The cells were then incubated under normal conditions (see section 4.3.2.2) for a period of 24 hours, which was sufficient time for apoptosis to be induced. Examining the cells under the microscope after this period of time, it was clear that their morphology had changed. The cells were no longer attached to the bottom of the flask, and their shape had also changed from the sprouting appearance to a spherical shape, being indicative of unhealthy cells. After being incubated in the serum deprived medium for the indicated time, the medium was removed, using centrifugation. The cells were then seeded in 24-well plates, with each well containing a concentration of 1 x 106 cells per 2 mL of serum deprived medium containing the test compounds, which were dissolved in dimethyl sulphoxide. Final concentrations of samples to be analysed contained 1.25 % (v/v) DMSO. The cells were then incubated under normal conditions for a period of 36 hours before being analysed. The test compounds (**6** - **13**) were all tested in triplicate at three different concentrations (1 mM, 100 μM and 10 μM). The positive control, selegiline, was tested in triplicate at two concentrations (100 μM and 10 μM). Included into the research was NGP1-01 which was also tested in triplicate at the highest concentration (1 mM).

3.4.3.1.1.4. Cells used for control experiments

In this study four control experiments were included.

3.4.3.1.1.4.1. Control experiment 1

After the cells reached 80 % confluency, the serum rich medium was replaced with *serum deprived medium*. The cells were then incubated under normal conditions for a period of 24 hours. After being incubated in the *serum deprived medium*, the medium was removed by centrifugation. The cells were subsequently seeded in 24-well plates, with each well containing a concentration of 1 x 106 cells per 2 mL of *serum deprived medium* and DMSO (1.25 % (v/v)). After this, the cells were incubated under normal conditions (37 °C in a 5 % CO_2 and 95 % O_2 humidified atmosphere) for a period of 36 hours before being analysed. Control experiment 1 was included to evaluate the viability status of the cells in the absence

of test compound. The viability data will be compared to the data generated with the test compounds in order to determine if the test compounds attenuated the progression of the apoptotic process. With this control experiment, the effect of DMSO was also evaluated.

3.4.3.1.1.4.2. Control experiment 2

After the cells reached 80 % confluency, the serum rich medium was replaced with *serum deprived medium*. The cells were then incubated under normal conditions for a period of 24 hours. After being incubated in the *serum deprived medium*, the medium was removed by centrifugation. The cells were subsequently seeded in 24-well plates, with each well containing a concentration of 1 x 10^6 cells per 2 mL of *serum deprived medium* with no DMSO content. The cells were incubated under normal conditions for a period of 36 hours before being analysed. Control experiment 2 was used to evaluate the effect of DMSO on the viability of the cells and on the progression of the apoptotic process.

3.4.3.1.1.4.3. Control experiment 3

After the cells reached 80 % confluency, the serum rich medium was replaced with *serum deprived medium*. The cells were subsequently incubated under normal conditions for a period of 24 hours. After being incubated in the *serum deprived medium*, the medium was removed by centrifugation. The cells were then seeded in 24-well plates, with each well containing a concentration of 1 x 106 cells per 2 mL of fresh *serum rich medium* with no DMSO present. After this the cells were incubated under normal conditions for a period of 36 hours before being analysed. Since the re-introduction of serum rich medium is expected to significantly attenuate the apoptotic process, this control experiment will be used to estimate the potencies of the test compounds as anti-apoptotic agents.

3.4.3.1.1.4.4. Control experiment 4

After the cells reached 80 % confluency, the serum rich medium was replaced with *fresh serum rich medium*. The cells were then incubated under normal conditions for a period of 24 hours. After being incubated in the *serum rich medium*, the medium was removed by centrifugation. The cells were subsequently seeded in 24-well plates, with each well containing a concentration of 1 x 106 cells per 2 mL of *serum rich medium* with no DMSO present. The cells were incubated under normal conditions for a period of 36 hours before being analysed. Control experiment 4 was included to analyse and determine the viability

status of the cells, when no apoptosis had been induced, and conditions had been favourable to the end. It was also included to ensure that the cells analysed were indeed healthy before inducing apoptosis.

3.4.3.1.2. Assay procedure

The cells of each sample were harvested consecutively as follows: After incubating the cells for 36 hours, the medium was removed from the cells using centrifugation. The cells that had adhered to the bottom of the flasks were removed by trypsination. The trypsine/cell mixture was added to the cells from which the medium had been removed. The trypsine was removed from the cells by centrifugation at 500 x g for five minutes at room temperature. The cells of each sample were then resuspended in 1 mL of diluted DePsipher solution, consisting of 1 µL DePsipher dye and 1 mL of pre-warmed F12 medium. The cells were incubated for 20 minutes at 37 °C and 5 % CO_2. The samples were washed twice in PBS, and centrifuged at 500 x g between each wash. The cells were subsequently resuspended in 1 mL PBS and immediately taken to be analysed on the flow cytometer. The samples were kept shielded from light until analysis, since the DePsipher™ agent is light sensitive.

3.4.3.1.3. Data analysis

Analysis of the samples were performed on a BD FacsCalibur® flow cytometer [Becton Dickinson, San Jose (USA)], equipped with a 15 mV 488 nm, air-cooled argon-ion laser. Cells were gated in a forward scatter/side scatter plot to exclude debris. Green and red fluorescence were detected in the corresponding FL-1 and FL-2 photomultipliers through 530 nm (FITC) or 585 nm (PE/PI) bandpass filters respectively. In generating the data, the flow cytometer was set to analyse 50 000 events/cells. Figures 1-3 (supplementary material) contains representative pseudo-colour graphs of every sample, which was generated using FlowJo®, based on the data of the flow cytometry. On the x-axis the FL-1 (green) fluorescence intensity is plotted, and on the y-axis the FL-2 (red) fluorescence intensity is plotted. Both intensities are measured in MFI (mean fluorescence intensity). Each spot is representative of a single cell analysed with the flow cytometer. The graphs are divided into four separate quadrants, each containing a population of cells, which exhibit the same characteristics. In the upper left quadrant (Q1) lies all the cells which emit only red fluorescence, whereas the cells which emit only green fluorescence can be found in the lower right quadrant (Q4). The cells which emit both wavelengths of fluorescence can be found in

the upper right quadrant (Q2), and the cells emitting neither of the two in the lower left quadrant (Q3). The following can be concluded by taking note of the explanations of the different quadrants as well as the characteristics of cells in each of these quadrants: As healthy cells contain both the monomeric and polymeric form of the cation dye, and would thus have intensity in both the FL1 and FL2 channels used to analyse the samples, the MFI values of these cells will lie in Q2 (see control experiment 4). The cells with MFI values in Q1 have only red fluorescence, which might be due to low concentrations of the dye inside the cell, indicating that all the monomers were polymerised. All these cells can thus also be said to be healthy, together with these found in Q2. Cells wherein apoptosis have been induced only contain the monomeric form of the dye, will not colour red at all, and will thus have MFI values in Q4. The cells lying in Q3 have not been dyed successfully or intensively enough, and have thus not coloured either red or green. From the pseudo-colour graphs it is clear that there was a difference in the number of apoptotic/healthy cells present in the different samples. Control experiment 1 had the least MFI values in Q1+Q2, and control experiment 4 the most. The MFI values of the other samples were either between the values of control experiments 1 and 4, or just above that of control experiment 4 (All pseudo-colour graphs are supplied in the supplementary material).

The data generated by these flow cytometry experiments were used to determine if the test compounds have anti-apoptotic properties on cultured cells. The values utilised to quantify cell viability were determined by the flow cytometer. Equation 1 was used to calculate the percentage of cells which were still viable in the samples analysed. In determining this value, the amount of cells in quadrant 1 (Q1), quadrant 2 (Q2) and quadrant 3 (Q3) and the total amount of events analysed (Qtotal) were utilised.

% Viable cells = [(Q1 + Q2)/(Qtotal - Q3)] x 100 - **Equation 1**

The results confirmed that a significant percentage of the cells had indeed coloured successfully with the dye. The percentage of the coloured cells that had fluorescence intensity in the FL2 channel, gave a quantitative indication of the number of healthy cells present in each sample, wherein apoptosis had not progressed or been induced. In control experiment 1, 41.62 % of the cells were apoptotic, with only 58.38 % remaining healthy. This indicates that the method of apoptosis induction had indeed been successful. Comparing the values of control experiments 1 and 2, it is clear that even though the final DMSO content in the samples was only 1.25 %, it had a negative effect on the health of the cells. In control experiment 2, which did not contain any DMSO, there were 7.19 % more cells that were

healthy. It can thus be said that the serum deprivation was not the only factor inducing apoptosis, but also the DMSO which served as solvent for the test compounds.

3.4.3.2. NMDA and VGCC

3.4.3.2.1. Animals

The study protocol was approved by the Ethics Committee for Research on Experimental Animals of the University of the Western Cape (SRIRC 2012/06/13). Adult Winstar rats were sacrificed by decapitation and the brain tissue was removed and kept on ice for homogenation. After homogenation, the alliquoted brain homogenate was immediately used in the subsequent assay.

3.4.3.2.2. Methods

The fluorescent ratiometric indicator, Mag-Fura-2/AM, and a Bio-Tek® fluorescence plate reader were used to evaluate the influence of the test compounds on calcium homeostasis *via* the VGCC and NMDA receptor channels utilizing murine synaptoneurosomes. Preparation of synaptoneurosomes, solutions and experimental techniques were similar to those of published studies.[26,44] All data analysis, calculation and graphs were done using Prism 6.0® (GraphPad, La Jolla, CA). Data analysis was carried out using the Student Newman Keuls multiple range test and the level of significance was accepted at $p < 0.05$.

3.4.3.2.3. Preparation of synaptoneuromes

Adult Winstar rats were used. Rats were sacrificed by decapitation, and the whole brains were removed. Whole-brain synaptoneurosomes were prepared by the techniques of Hollingsworth *et al*.[45], modified slightly. The brain from one rat was homogenized (8 strokes by hand using a glass homogenizer) in 30 ml of ice–cold incubation buffer (NaCl, 118 mM; KCl, 4.7 mM; MgCl, 1.18 mM; $CaCl_2$ 0.1 mM; HEPES, 20 mM and glucose, 30.9 mM. pH 7.4). From this step forward the homogenate was kept ice–cold at all times to minimize proteolysis throughout the isolation procedure. The tissue suspension was placed in a 50 ml polycarbonate tube and then centrifuged for 5 min at 1000 g and 0 ºC using a Labofuge 20® centrifuge. After centrifugation, the supernatant was decanted into a 50 ml polycarbonate tube and placed on ice. The supernatant was then divided into 2 ml eppendorf vials whose weight had been previously recorded. This was followed by a second centrifugation at 15000

g for 20 min at 0 ºC. The supernatant was discarded and the mass of the resulting pellet was calculated. Sufficient calcium-free buffer (NaCl, 118 mM; KCl, 4.7 mM; MgCl, 1.18 mM; HEPES, 20 mM and glucose, 30.9 mM. pH 7.4) was added to obtain a 3 mg/ml protein concentration (protein yield is approximately 10 mg/g of tissue).[45]

3.4.3.2.4. General procedure for loading FURA-2 AM and incubating test compounds

Experiments were carried out at 37 ºC and fluorescence was measured with a flourescent plate reader (Bio-Tek®). 1990 µl of synaptoneurosome suspension prepared above was allowed to reach room temperature, thereafter 10 µl of Fura-2 AM (1 mM in DMSO) was added to produce a final concentration of 5 µM. Synaptoneurosomes were then incubated at 37 ºC for 30 min after which the suspension was centrifuged on a desktop centrifuge at 7000 g for 5 min and the supernatant decanted to remove all extracellular Fura-2 AM. The resulting pellet was resuspended in 2 mM $CaCl_2$ containing buffer to obtain a final protein concentration of 0.6 mg/ml.

3.4.3.2.5. Measurement of intracellular calcium

For the screening test 10 mM stock solutions of the compounds in DMSO were prepared, with the control containing 1% DMSO and no test compound. 2 µl of the individual stock solutions were added to a 96 well plate in triplicate followed by the addition of 200 µl of synaptoneurosomal-Fura-2 AM solution prepared above. This gave rise to a final concentration of 100 µM of the compounds. The 96 well plate was shaken and incubated for 30 min at 37 ºC and used immediately after incubation. The measurement was then performed at 37 ºC in a 96 well plate using dual wavelength excitation at 340 nm and 380 nm. The resting fluorescence was measured at 510 nm after which the changes in fluorescence intensity following the addition of 10 µl depolarizing solution using auto-injectors was recorded over a period of 5 min. The changes in fluorescence indicated the effect of the test compound on calcium flux.

3.4.3.2.6. KCl mediated calcium stimulation

The wavelengths selected were 340 nm and 380 nm for excitation and 510 nm for emission, with a runtime of 5 min with 5 ms intervals. The test compound was incubated for 30 min at 37 ºC and used immediately after incubation. The procedure was initiated and kept at 37 ºC.

At 10 s into the recording 10 µl of KCl (140 mM) depolarization solution (5.4 mM NaCl, 140 mM KCl, 10 mM $NaHCO_3$, 1.4 mM $CaCl_2$, 0.9 mM $MgSO_4$, 5.5 mM Glucose monohydrate, 0.6 mM KH_2PO_4, 0.6 mM Na_2HPO_4, and 20 mM HEPES. pH adjusted to 7.4 with NaOH) was added to the membrane preparation to depolarize the synaptoneurosomes and activate the calcium flux (addition was done using auto-injectors). Experiments were repeated three times on different tissue preparations with three determinations in each replicate

3.4.3.2.7. NMDA/Glycine mediated calcium stimulation

The wavelengths selected were 340 nm and 380 nm (excitation) and 510 nm (emission) with a runtime of 5 min with 5 ms intervals. The test compound was incubated for 30 min at 37 ºC and used immediately after incubation. The procedure was initiated and kept at 37 ºC. At 10 s into the recording 10 µl of NMDA/Glycine (0.1 mM) depolarization solution (0.1 mM $CaCl_2.2H_2O$, 0.1 mM NMDA, 0.1 mM Glycine, 118 mM NaCl, 4.7 mM KCl, 30.9 mM Glucose monohydrate and 20 mM HEPES. pH adjusted to 7.4 with NaOH) was added to the membrane preparation to depolarize the synaptoneurosomes and activate the calcium flux (Addition was done using auto-injectors). The addition of NMDA (0.1 mM) and Gly (0.1 mM) resulted in activation of NMDAR mediated calcium flux. Experiments were repeated three times on different tissue preparations with three determinations in each replicate.

3.4.3.2.8. Percentage inhibition calculations

The data obtained from the fluorescent readings of each well were expressed in the form of a ratio (340 nm reading / 380 nm reading). This ratio indicated the net movement of Ca^{2+} ions across the membrane as it represents the ratio between unbound-Ca^{2+} and Ca^{2+}-bound to Fura-2 AM. The average ratio over a 10 s interval after 1 min of stimulation was then subtracted from the average ratio of over the last 10 s interval to give the net change in Ca^{2+} movement (Nc) across the membrane over the 5 min period. This calculation was performed for each individual well and the averages of wells containing the same test compound were calculated (Nc_{Ave}). These averages were used to calculate the percentage inhibition of the test compounds relative to the control by use of the following equation:

% inhibition = [Nc_{Ave} (Control) – Nc_{Ave} (Test compound)] / Nc_{Ave} (Control) x 100 % - **Equation 2**

3.4.3.3. MAO-B inhibition

The mitochondrial fraction of baboon liver tissue, as source of the MAO-B enzyme, was isolated as described previously by Salach & Wyler, 1987,[46] and stored at -70 ºC. Following addition of an equal volume of sodium phosphate buffer (100 mM, pH 7.4) containing glycerol (50 %, w/v) to the mitochondrial isolate, the protein concentration was determined by the method of Bradford using bovine serum albumin as reference standard.[47] In the current study, MMTP (K_m = 68.3 ± 1.60 μM for baboon liver MAO-B) served as substrate for the inhibition studies.

The enzymatic reactions were conducted in sodium phosphate buffer (100 mM, pH 7.4) and contained MMTP (50 μM), the mitochondrial isolate (0.15 mg protein/mL) and various concentrations of the test compounds, spanning at least three orders of magnitude (0.3 – 300 μM). The concentration of the test compounds used in this study were 0.3 μM, 1 μM, 3 μM, 10 μM, 30 μM, 100 μM and 300 μM. The final volume of the incubations was 500 μL. The stock solutions of the inhibitors were prepared in DMSO and were added to the incubation mixtures to yield a final DMSO concentration of 4 % (v/v) as concentrations higher than 4 % are reported to inhibit MAO-B.[48] The reactions were incubated at 37 ºC for 10 minutes and then terminated by the addition of 10 μL perchloric acid (70 %). The samples were centrifuged at 16,000 g for 10 minutes, and the concentrations of the MAO-B generated product, $MMDP^+$,[49] were measured spectrophotometrically at 420 nm (ε = 25,000 M^{-1}) in the supernatant fractions.

The enzyme inhibition activities of the test compounds were determined using equation 2 to calculate the inhibition potencies of the compounds. These potencies are expressed as percentage inhibition (% inh) of the enzyme. In determining these values, the concentration of $MMDP^+$ produced in the absence of a test compound (C_0) and the concentration of $MMDP^+$ produced by MAO-B in the presence of a maximal concentration of the test compound (C_{300}) were utilised. All determinations were conducted in duplicate, yielding the percentage inhibition as an average of the two sets of data.

$$\% \text{ inhibition} = 100 - [(C_{300} \times 100)/C_0] \quad \text{- Equation 3}$$

3.4.4. Molecular modeling

Computer-assisted docking were carried out using the CHARMm force field and the human MAO-B crystal structure (PDB ID: 2V5Z)[37], which were recovered from the Brookhaven Protein Database (www.rcsb.org/pdb). Docking simulations were performed on the

synthesized compounds (**9-16**) using Molecular Operating Environment (MOE)[36] with the following protocol. (1) Enzyme structures were checked for missing atoms, bonds and contacts. (2) Hydrogen atoms were added to the enzyme structure. Bound ligands were manually deleted and the ordered water molecules including 58W and 47W retained (important for the formation of a triad [Lys-H_2O-flavin N(5)] and the hydrophilic section required for recognition and directionality of the substrate amine functionality)[50] as seen with safinamide (Fig. 4). (3) The ligand molecules were constructed using the builder module and were energy minimized. (4) The active sitewas generated using the MOE-Alpha Site Finder. (5) Ligands were docked within the MAO-B active site using MOEDock with simulated annealing utilised as the search protocol and CHARMm molecular mechanics force field. (6) The lowest energy conformation of the docked ligand complex was selected and subjected to a further energy minimization using CHARMm force field with all possible bond rotations and chiralities explored. To determine the accuracy of this docking protocol, the co-crystallised ligand, safinamide (PDB ID: 2V5Z), was re-docked into the MAO-B active site. This procedure was repeated three times and the best ranked solutions of safinamide exhibited an RMSD value of 1.34 Å from the position of the co-crystallised ligand. In general, RMSD values smaller than 2.0 Å generally indicate that the docking protocol is capable of accurately predicting the binding orientation of the co-crystallised ligand[50,51]. This protocol was thus deemed to be suitable for the docking of inhibitors into the active site model of MAO-B.

Acknowledgements

We are grateful to the North-West University, University of the Western Cape, Medical Research Council of South Africa and the National Research Foundation of South Africa for financial support.

Author Contributions

F.T.Z., J.J. and S.F.M. conceived of the presented idea. F.T.Z. designed and performed the calcium modulation assays and computer modelling studies, processed the experimental data, performed the analysis and drafted the manuscript. Q.R.B. synthesized and characterized the compounds. J.J.B., J.P.P., S.F.M. and J.J. supervised the findings of this work. All authors discussed the results and contributed to the final manuscript.

Supplementary data

Supplementary data related to this article can be found in the supplementary materials section of this thesis and at http://dx.doi.org/10.1016/j.ejmech.2014.04.039

References

[1] H.P. Rang, M.M. Dale, J.M. Ritter, Rang and Dale's Pharmacology, Elsevier, Philadelphia, 2007, p. 508 (Chapter 35).

[2] T. Araki, T. Kumagai, K. Tanaka, M. Matsubara, H. Kato, Y. Itoyama, Y. Imai, Brain: *A Journal of Neurology* 918 (2001) 176.

[3] (a) T. Alexi, C.V. Borlongan, R.L.M. Faull, C.E. Williams, R.G. Clark, P.D. Gluckman, P.D. Gluckman, P.E. Huges, *Progress in Neurobiology* 60 (2000) 409; (b) J.G. Greene, J.T. Greenamyre, *Progress in Neurobiology* 48 (1996) 613.

[4] J.U. Schweichel, H.J. Merker, *Teratology* 7 (1973) 253.

[5] M.P. Mattson, *Nature Reviews* 1 (2000) 120.

[6] N.J. Holbrook, G.R. Martin, R.A. Lockshin (Eds.), Cellular Aging and Cell Death, WileyeLiss, New York, 1996, p. 319.

[7] A.H. Wyllie, J.F.R. Kerr, A.R. Currie, *International Review of Cytology* 68 (1980) 251.

[8] M. Arundine, M. Tymianski, Molecular mechanisms of calcium-dependent neurodegeneration in excitotoxicity, *Cell Calcium* 34 (4-5) (2013) 325.

[9] M. Arundine, M. Tymianski, Cellular and Molecular Life Sciences: *CMLS* 61 (2004) 657.

[10] W.J. Geldenhuys, S.F. Malan, T. Murugensan, C.J. Van der Schyf, J.R. Bloomquist, *Bioorg. Med. Chem.* 12 (2004) 1799.

[11] M.B. Youdim, G.G. Collins, M. Sandler, A.B. Bevan Jones, C.M. Pare,W.J. Nicholson, *Nature* 236 (1972) 225.

[12] G.G. Collins, M. Sandler, E.D. Williams, M.B. Youdim, *Nature* 225 (1970) 817.

[13] D.A. Di Monte, L.E. DeLanney, I. Irwin, J.E. Royland, P. Chan, M.W. Jakowec, J.W. Langston, *Brain Research* 738 (1996) 53.

[14] J.P. Finberg, J. Wang, K. Bankiewich, J. Harvey-White, I.J. Kopin, D.S. Goldstein, *Journal of Neural Transmission* Supplement 52 (1998) 279.

[15] M.B.H. Youdim, Y.S. Bakhle, *British Journal of Pharmacology* 147 (2006) S287.

[16] A. Nicotra, F. Pierucci, H. Parvez, O. Senatori, *Neurotoxicology* 25 (2004) 155.

[17] J.S. Fowler, N.D. Volkow, G.J. Wang, J. Logan, N. Pappas, C. Shea, R. MacGregor, *Neurobiology of Aging* 18 (1997) 431.

[18] B. Karolewicz, V. Klimek, H. Zhu, K. Szebeni, E. Nail, C.A. Stockmeier, L. Johnson, G.A. Ordway, *Brain Research* 1043 (2005) 57.

[19] J.J. Chen, D.M. Swope, K. Dashtipour, *Clinical Therapeutics* 9 (2007) 1825.

[20] O. Bar-Am, O. Weinreb, T. Amit, M.B.H. Youdim, *FASEB* 19 (2005) 1899.

[21] P.H. Yu, B.A. Davis, A.A. Boulton, *Journal of Medicinal Chemistry* 35 (1992) 3705.

[22] S. Mandel, O. Weinreb, T. Amit, M.B.H. Youdim, *Brain. Research Reviews* 48 (2005) 379.

[23] J. Joubert, W.J. Geldenhuys, C.J. Van der Schyf, D.W. Oliver, H.G. Kruger, T. Govender, S.F. Malan, *Chemmedchem* 7 (2012) 375.

[24] J. Zah, G. Terre'blanche, E. Erasmus, S.F. Malan, *Bioorg. Med. Chem.* 11 (2003) 3569.

[25] K.B. Brookes, P.W. Hickmott, K.K. Jutle, C.A. Schreyer, *SAJC* 45 (1992) 8.

[26] J. Joubert, S. Van Dyk, I.R. Green, S.F. Malan, *Bioorg. Med. Chem.* 19 (2011) 3935.

[27] J. Joubert, S. Van Dyk, I.R. Green, S.F. Malan, *European Journal of Medicinal Chemistry* 46 (2011) 5010.

[28] H.J.R. Lemmer, J. Joubert, S. van Dyk, F.H. van der Westhuizen, S.F. Malan, *Medicinal Chemistry*. [Medicinal Chemistry (Shariqah (United Arab Emirates))] 8 (2012) 361.

[29] J. Joubert, H. Samsodien, Q.R. Baber, D.L. Cruickshank, M.R. Caira, S.F. Malan, *Journal of Chemical Crystallography* 44 (2014) 194.

[30] Mitochondrial Membrane Potential Disruption Assay. DePsipher_ assay kit. http://www.rndsystems.com/product_detail_objectname_mitochondrial_membrane_disruption .aspx (accessed 31.03.14.).

[31] C.J. Van der Schyf, G.J. Squier, W.A. Coetzee, *Pharmacological Research Communications* 18 (1986) 407.

[32] E.B. Hollingsworth, E.T. McNeal, J.L. Burton, R.J. Williams, J.W. Daly, C.R. Creveling, The Journal of Neuroscience: *The Official Journal of the Society for Neuroscience* 5 (1985) 2240.

[33] J.J. Van der Walt, C.J. Van der Schyf, J.M. Van Rooyen, J. De Jager, M.N. Van Aarde, *South African Journal of Science* 84 (1988) 448e450.

[34] A.E. Medvedev, A.S. Ivanov, N.S. Kamyshanskaya, A.Z. Kirkel, T.A. Moskvitina, V.Z. Gorkin, N.Y. Li, V.Y. Marshakov, *Journal of. Biochemistry and Molecular Biology* 36 (1995) 113.

[35] J.P. Petzer, N.C. Castagnoli, M.A. Schwarzschild, J. Chen, C. Van der Schyf, *Journal of Neurotherapy* 6 (2009) 141.

[36] Molecular Operating Environment (MOE), Version 2011.10. http//www. chemcomp.com.

[37] C. Binda, J. Wang, L. Pisani, C. Caccia, A. Carotti, P. Salvati, D.E. Edmondson, A. Mattevi, *Journal of Medicinal Chemistry* 50 (2007) 5848.

[38] Y. Tsugeno, I. Hirashiki, F. Ogata, A. Ito, *Journal of Biochemistry* 118 (1995) 974-980.

[39] A.L. Maycock, R.H. Abeles, J.I. Salach, T.P. Singer, *Biochemistry* 15 (1976) 114.

[40] D.J. Mitchell, D. Nikolic, E. Rivera, S.O. Sablin, S. Choi, R.B. van Breemen, T.P. Singer, R.B. Silverman, *Biochemistry* 40 (2001) 5447.

[41] R.C. Cookson, E. Crundwell, R.R. Hill, J. Hudec, *Chemistry and Industry* (1958) 1003.

[42] A.P. Marchand, S.C. Suri, A.D. Earlywine, D.R. Powell, D. Van der Helm, *The Journal of Organic Chemistry* 49 (1984) 670.

[43] T.G. Dekker, D.W. Oliver, *SAJC* 32 (1979) 45.

[44] (a) S.J. Benavide, Y. Claustre, B. Scatton, *The Journal of Neuroscience: the Official Journal of the Society for Neuroscience* 8 (1988) 3607; (b) W.J. Geldenhuys, S.F. Malan, J.R. Bloomquist, C.J. Van der Schyf, *Bioorg. Med. Chem.* 15 (2007) 1525; (c) K. Resch, W. Imm, E. Ferber, D.F.H. Wallach, H. Fischer, *Die Naturwissenschaften* 58 (1971) 220; (d) A.K. Stout, I. Reynolds, *The Journal of Neuroscience: the Official Journal of the Society for Neuroscience* 89 (1999) 91.

[45] E.B. Hollingsworth, E.T. McNeal, J.L. Burton, R.J. Williams, J.W. Daly, C.R. Creveling, *The Journal of Neuroscience: the Official Journal of the Society for Neuroscience* 5 (1985) 2240.

[46] J.I. Salach, W. Weyler, *Methods in Enzymology* 142 (1987) 627.

[47] M.M. Bradford, *Analytical Biochemistry* 72 (1976) 248.

[48] C. Gnerre, M. Catto, F. Leonetti, P. Weber, P.A. Carrupt, C. Altomare, A. Carotti, B.J. Testa, *Journal of Medicinal Chemistry* 43 (2000) 4747.

[49] H. Inoue, K. Castagnoli, C.J. Van der Schyf, S. Mabic, K. Igarashi, N. Castagnoli, *Journal of Pharmacology and Experimental Therapeutics* 291 (1999) 856.

[50] C. Binda, M. Li, F. Hubalek, N. Restelli, D.E. Edmondson, A. Mattevi, *PNAS* 100 (2003) 9753.

[51] J. Boström, J.R. Greenwood, J. Gottfries, *Journal of Molecular Graphics & Modelling* 21 (2003) 449.

Chapter 4

Research Article 2: Design, synthesis and evaluation of pentacycloundecane and hexacycloundecane propargylamine derivatives as multifunctional neuroprotective agents

Article submitted for publication on 9 November 2018

Eur. J. Med. Chem.

Design, synthesis and evaluation of pentacycloundecane and hexacycloundecane propargylamine derivatives as multifunctional neuroprotective agents

Frank T. Zindo[a], Sarel F. Malan[a], Sylvester I. Omoruyi[b], Adaze B. Enogieru[b], Okobi E. Ekpo[b], Jacques Joubert[a]*

[a]*Pharmaceutical Chemistry, School of Pharmacy, University of The Western Cape, Private Bag X17, Bellville 7535, South Africa*

[b]*Department of Medical Biosciences, University of the Western Cape, Private Bag X17, Cape Town, Bellville 7535, South Africa.*

*Corresponding author at present address: School of Pharmacy, University of the Western Cape, Private Bag X17, Bellville 7535, South Africa. Tel: +27 21 959 2195; e-mail: jjoubert@uwc.ac.za

Graphical Abstract

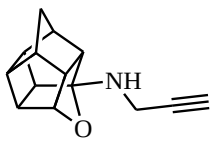

P1

Neuroprotective

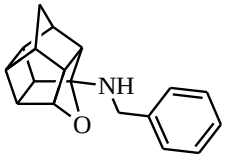

NGP1-01

Neuroprotective

VGCC blocker

NMDAr antagonist

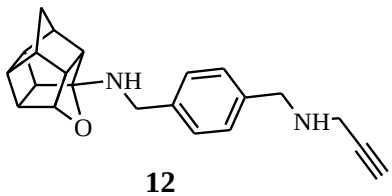

12

Neuroprotective

VGCC blocker

NMDAr antagonist

MAO-B inhibitor

Abstract

The multifactorial pathophysiology of neurodegenerative disorders remains one of the main challenges in the design of a single molecule that may ultimately prevent the progression of these disorders in affected patients. In this article, we report on twelve novel polycyclic amine cage derivatives, synthesized with or without a propargylamine function, designed to possess inherent multifunctional neuroprotective activity. The MTT cytotoxicity assay results showed the SH-SY5Y human neuroblastoma cells to be viable with the twelve compounds, particularly at concentrations less than 10 μM. The compounds also showed significant neuroprotective activity, ranging from 31% to 66% at 1 μM, when assayed on SH-SY5Y human neuroblastoma cells in which neurodegeneration was induced by MPP^+. Calcium regulation assays conducted on the same cell line showed the compounds to be significant VGCC blockers with activity ranging from 26.6% to 51.3% at 10 μM; as well as significant NMDAr antagonists, with compound **5** showing the best activity of 88.3% at 10 μM. When assayed on human MAO isoenzymes, most of the compounds showed significant inhibitory activity, with compound **5** showing the best activity (MAO-B: IC_{50} = 1.70 μM). Generally, the compounds were about 3 – 52 times more selective to the MAO-B isoenzyme than the MAO-A isoenzyme. Based on the time-dependency studies conducted, the compounds can be defined as reversible MAO inhibitors. Several structure activity relationships were derived from the various assays conducted, and the compounds' possible putative binding modes within the MAO-B enzyme cavity were assessed *in silico*.

Keywords: Neurodegeneration, apoptosis, neuroprotection, multifunctional, polycyclic amine, propargylamine, excitotoxicity, monoamine oxidase.

4.1. Introduction

Neurodegenerative disorders (NDs) refers to a cluster of neuronal diseases that are characterised by transient and irreversible loss of neuronal cells in the brain due to apoptosis [1]. Examples of these diseases include Alzheimer's Disease (AD), Huntington's Disease (HD) and Parkinson's Disease (PD). Though the pathogenesis is yet to be fully understood, it is known that several factors are involved in the etiology of these disorders. Some of the established theories of disease causation include, but are not limited to, disturbances in neurotransmitter systems such as the monoaminergic system [2,3], as well as excitotoxicity resulting from excessive calcium influx into neuronal cells [4,5].

Patients with PD and AD have been shown to have age-related elevated levels of the B-type monoamine oxidase isoenzyme (MAO-B) in the brain [6]. This enzyme does not only act indirectly as a trigger to the apoptotic process in neuronal cells, but together with the A-type isoenzyme (MAO-A), they form the major catabolic pathways of dopamine [7] and give rise to some of the signs and symptoms associated with these disorders [8]. Both these isoenzymes are therefore promising drug target sites for the treatment of NDs and as such, monoamine oxidase enzyme inhibitors (MAOI's) have been the mainstay therapy for the management of NDs. By inhibiting the activity of the MAO isoenzymes, MAOI's may exert neuroprotective effects by inhibiting the formation of toxic by-products of MAO-catalyzed oxidation of neurotransmitters [9]. Further to this, MAOI's enhance dopaminergic neurotransmission in the nigro-striatal pathway, thereby providing symptomatic relief in patients with PD [10].

The first generation of MAOI's such as tranylcypromine are nonspecific and irreversible inhibitors of both isoforms of MAO. While these dual inhibiting compounds produce a significant rise in dopamine levels and behavioural changes after administration [11], they present a drawback of causing clinically significant potentiation of the 'pressor response', a common adverse effect associated with ingesting tyramine containing foods together with nonspecific MAOI's. Potentiation of this adverse effect is mainly influenced by the irreversibility of the inhibitor and the degree of MAO-A inhibition [12]. This has been shown to be due to MAO-A being the major form of MAO in the liver and stomach. Reversible inhibitors of MAO-A are therefore preferred to their irreversible counterparts as they show a reduced hypertensive response [13].

A more widely explored strategy entails selectively inhibiting the MAO-B isoenzyme by inhibitors such as rasagiline and selegiline (Figure 1). This approach is based on the fact that the extrapyramidal region of the human brain has approximately 4-times more MAO-B isoenzyme than the MAO-A isoenzyme [14]. Rasagiline and selegiline are second generation propargylamine derivatives that irreversibly inhibit brain MAO-B, and have promising neuroprotective activities [15]. Their activity can be attributed to the propargyl moiety [8], that after oxidation, reacts with the flavin prosthetic group in the active site of the MAO-B enzyme, forming a covalent adduct at the *N*5 position of the flavin adenine dinucleotide (FAD) [16]. The propargyl moiety is also now known to play an important role in providing neuronal and mitochondrial protective properties [17] as well as anti-apoptotic properties [18]. This moiety has been particularly useful for incorporation into multi-target compounds with inherent MAO-B inhibitory capacity [19].

While inhibiting the oxidative deamination reaction catalysed by the MAO isoenzymes is a useful strategy in managing NDs, targeting a single enzymatic system or receptor has proved to be insufficient for the treatment of these multifactorial diseases [20]. A more effective therapy would result from the use of multi-target directed ligands (MTDLs) able to intervene in the different pathological events implicated in the etiology of neuronal disorders [21].

Calcium homeostasis in neuronal cells has also been implicated in the pathogenesis of NDs. Given the crucial and widespread role calcium signalling has in excitable cells, it is not surprising that alterations in calcium homeostasis is linked to several NDs [22,23]. Maintenance of intracellular calcium homeostasis is essential for the functioning and survival of neurons and is a fundamental component of synaptic transmission for both pre- and postsynaptic mechanisms [24]. Excessive influx of calcium can therefore overwhelm Ca^{2+}-regulatory mechanisms and lead to excitotoxicity and neuronal cell death [25]. The activation of the postsynaptic *N*-methyl-D-aspartate receptors (NMDAr), 2-amino-3-(3-hydroxy-5-methylisoxazol-4-yl)proprionate receptors and kainate receptors allows for opening of their associated ion channels to allow the influx of Ca^{2+} and Na^{+} ions into the neuronal cells. Calcium entry may also occur through *L*-type voltage gated calcium channels (VGCC) and result in both calcium overload and mitochondrial disruption [25]. This mechanism of cell death suggests these receptors and their associated calcium channels to be supplementary drug target sites for the treatment of NDs.

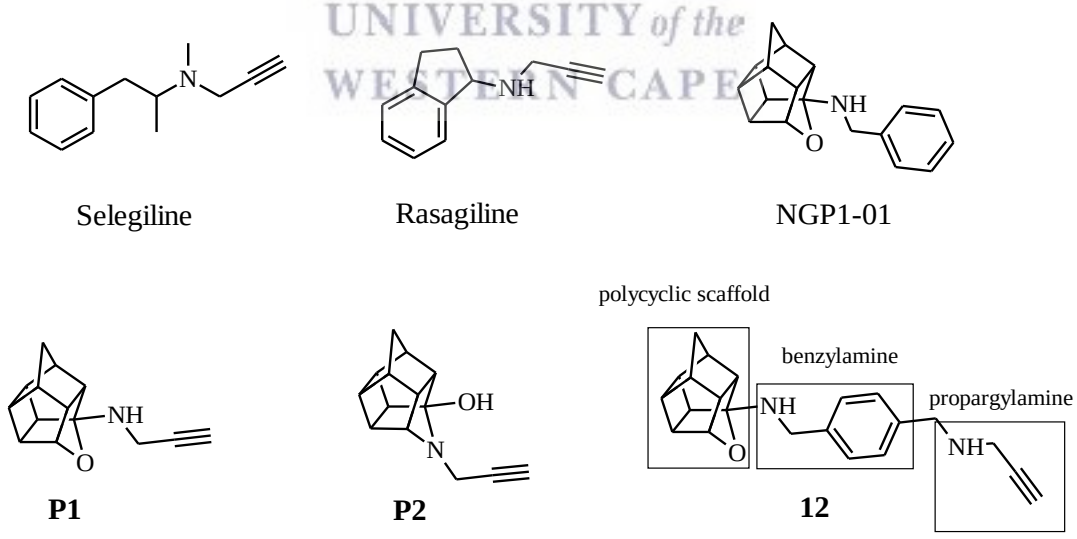

Figure 1. The molecular structures of the selective MAO-B inhibitors selegiline and rasagiline, the VGCC blocker and NMDAr antagonist NGP1-01, compounds from a previous study **P1** and **P2**, and the new series represented by compound **12**, with the polycyclic scaffold, benzylamine and propargylamine moieties highlighted.

In our previous work [26], we designed and synthesized polycyclic propargylamines, represented by **P1** and **P2** (Figure 1), to serve as multifunctional drug ligands by inhibiting MAO-B enzyme activity, and as regulators of cytosolic calcium entry predominantly mediated by NMDAr and VGCC. While these compounds showed good *in vitro* anti-apoptotic activity, they showed little to no MAO-B inhibitory activity and were inactive as NMDAr antagonist and VGCC blockers. These findings suggested that **P1** and **P2** exhibit their neuroprotective effect through some other mechanism(s) implicated in the complex etiology of neurodegeneration unexplored in the study. We further postulated that the lack of calcium regulatory activity in **P1** and **P2** was due to the absence of a benzylamine moiety within their structures. This moiety, which is present in structure of NGP1-01, a molecule known to have neuroprotective properties through VGCC blockade and NMDAr antagonistic activity [27], seems to be vital for calcium modulatory activity in such polycyclic analogues. It is for this reason that we incorporated a benzylamine moiety in the design of a new series of compounds reported in this current study (represented by compound **12**, Figure 1).

Further investigation to clarify the lack of MAO-B inhibitory activity in these compounds was carried out by performing computer-assisted simulated docking in the MAO-B enzyme (PDB ID: 2V5Z) [28], utilizing Molecular Operating Environment (MOE) as previously described [29]. The best-ranked docking solutions showed that compound **P1** and **P2** occupy only the entrance cavity of the MAO-B enzyme and barely access the substrate cavity to form the necessary binding interactions with the FAD cofactor, which could have resulted in increased activity of these compounds (Figure 2). With the inclusion of a benzylamine moiety in the structures of the new series of compounds, as seen in compound **12** (Figure 1 and Figure 2), we envisaged better MAO-B inhibitory activity as this moiety significantly elongates the compound allowing the adjacent propargylamine moiety to come in close proximity to the FAD cofactor of the enzyme.

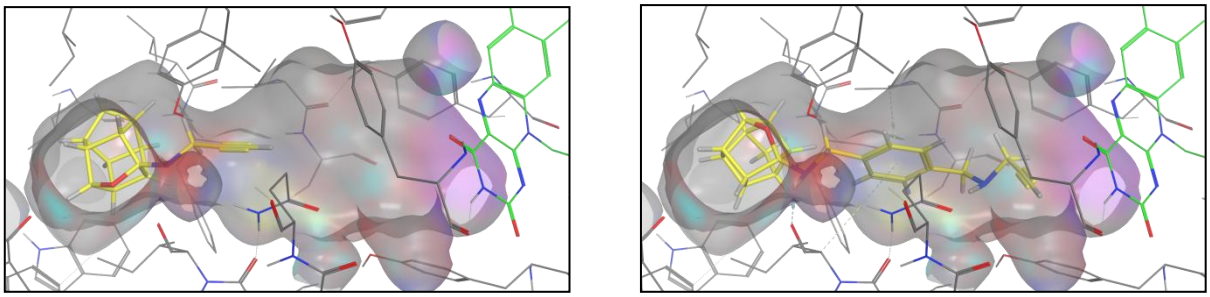

Figure 2. Schematics showing inactive compound **P1** (left) and a representative of the new polycyclic propargylamine derived series compound **12** (Right) in a computer simulated MAO-B enzyme cavity. The compounds are shown in yellow and the FAD co-factor in green. Note that compound **P1** merely occupies the entrance cavity of the enzyme pocket and remains distant from the FAD co-factor rendering it inactive, while the new series traverses deeper into the enzyme cavity to come in close proximity with the FAD co-factor allowing for potential binding interactions which may result in improved MAO-B activity.

The findings from our previous work have thus inspired the design, synthesis and evaluation of a new series of twelve pentacycloundecane and hexacycloundecane derivatives, synthesized with or without a propargylamine function. The compounds in this series, represented by compound **12** (Figure 1 and Figure 2), carry some or all of the following features; (a) a polycyclic cage scaffold - for side-chain attachment as well as for improving the drug's lipophilicity [30] and enhance drug transport across cellular membranes, including the selectively permeable blood–brain barrier, and also to increase drug affinity for lipophilic regions in target proteins [30,31]; (b) a benzylamine moiety - as present in the structure of NGP1-01, for improved VGCC blockade and NMDAr antagonism [27]; (c) a propargylamine moiety - for inherent MAO inhibitory capacity and to provide neuronal and mitochondrial protective properties [17], as well as anti-apoptotic properties [18]; (d) an elongated orientation – resulting from the inclusion of a benzylamine moiety, to promote molecular interaction between the propargylamine function and the FAD cofactor of the MAO enzyme. Compounds that show such multi-mechanistic activity may have promising potential to curtail the multifactorial etiology of neurodegenerative disorders.

The novel compounds were therefore synthesized and screened for cytotoxicity, neuroprotection, NMDAr antagonism and VGCC blockade by performing *in vitro* assays on human neuroblastoma SH-SY5Y cells. Further to this, *in vitro* assays on the human MAO–A and MAO–B enzymes were performed in order to determine their inhibitory potential on the respective isoenzymes.

4.2. Results and discussion

4.2.1. Chemistry

Each compound was synthesised to evaluate the activity and benefit of the presence of certain functional groups in the molecule. These groups included the following; a terminal propargylamine (**5**, **6**, **9** and **12**), a terminal secondary amine (**1**, **2**, **4** and **10**), as well as the ketal (**1** - **6**), aza (**7** - **9**) and oxa (**10** - **12**) variations of the polycyclic cage scaffold. The common starting Cookson's diketone (**a**), was prepared according to the method of Cookson *et al*. [32] From the Cookson's diketone, the monoprotected ketal polycyclic cage (**b**) was prepared according to the method of Dekker *et al*. [33] NGP1-01 was synthesized according to an adaptation of the microwave assisted method (MWAM) described by Joubert *et al*. [34**]** To synthesize the mono amine cage (**c**), debenzylation of NGP1-01 was carried out under high-pressure catalytic hydrogenation as reported by Marchand *et al*. [35] (Scheme 1).

Compounds **1** – **12**, were subsequently synthesized by direct conjugation of various analogues to the three polycyclic cage scaffolds (**a** – **c**) using microwave irradiation. MWAMs present several advantages which include; remarkable reduction of reaction time, improved yields, cleaner reactions and reduction or elimination of hazardous solvents compared to reactions performed under conventional thermal heating conditions [36,37]. As such, MWAMs have since been adopted by several researchers as the preferred strategy for the synthesis of these cage-derived organic compounds [34,38].

The synthesis of compounds **1**, **2** and **3** was performed by conjugating their respective primary diamines to the mono ketal polycyclic cage (**b**) through a direct amination reaction using microwave irradiation (Scheme 2). An excess amount of *p*-xylylenediamine (5.0 equiv) was used for the synthesis of compound **2** in order to promote the formation of a mono-substituted amine, however, a significant percentage of the di-substituted derivative **3** formed during the reaction and was successfully isolated giving respective yields of 32% and 13%. The serendipitously synthesized compound **3** was also included in the series of compounds for screening of potential activity. Propargyl chloride was conjugated to compound **2** using MWAMs through an S_N2 nucleophilic substitution reaction, in the presence of K_2CO_3, to produce compound **5**. To synthesize compounds **4** and **6**, reductive amination of the imines **2** and **5** was carried out using $NaBH_4$. A comparison of the biological activities of these four compounds provides insight on the influence of the imine bond on their activity. The reduction of the imines **1** and **2** with $NaBH_4$, followed by acid hydrolysed transanular cyclization using HCl, gave the desired aza-bridged compounds **7** and **8** respectively.

Propargyl chloride was conjugated to compound **8** through a nucleophilic S_N2 substitution reaction using MWAMs to yield compound **9** (Scheme 2).

Compound **10**, which is an oxa analogue and structural isomer of **7**, was synthesized by conjugating 4-amino benzylamine to the Cookson's diketone (**a**), followed by reduction with $NaBH_4$ (Scheme 3). A microwave assisted nucleophilic S_N2 substitution reaction was employed to conjugate the mono amine cage (**c**) to *p*-xylylene dichloride to yield compound **11** and to conjugate propargyl chloride to **11** and yield final compound **12** (Scheme 3). Compounds **1**, **7** and **10** were synthesized to serve as intermediates to potential subsequent propargyl derivatives. However, due to the low reactivity of the aniline amine, reactions with halopropargyls in the form of propargyl chloride and propargyl bromide could not yield the desired derivatives. All compounds (**1** – **12**) were protected from light after synthesis and were appropriately stored at -84 °C to prevent degradation.

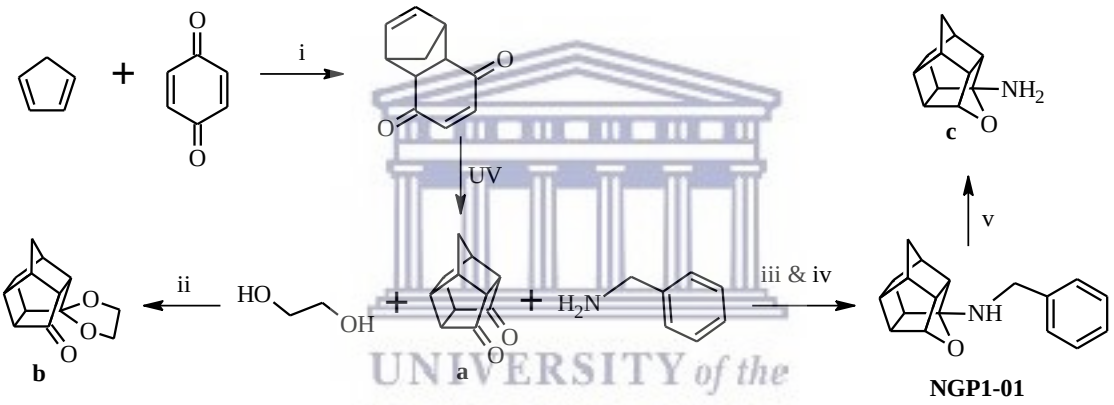

Scheme 1: Reagents and conditions for the synthesis of diketone (**a**), ketal (**b**) and monoamine (**c**) polycyclic scaffolds: (i) benzene, 0 °C, 1 h, 74%; (ii) benzene, *p*-TsOH (cat), Dean–Stark reflux, 5 h, 72%; (iii) ethanol, MW, 80 °C, 100 W, 100 psi, 2 h, quantitative yield; (iv) ethanol, $NaBH_4$, rt, 8 h, 62%; (v) ethanol, 10% Pd/C, H_2, 206 kPa, 50 °C, 14 h, 32%.

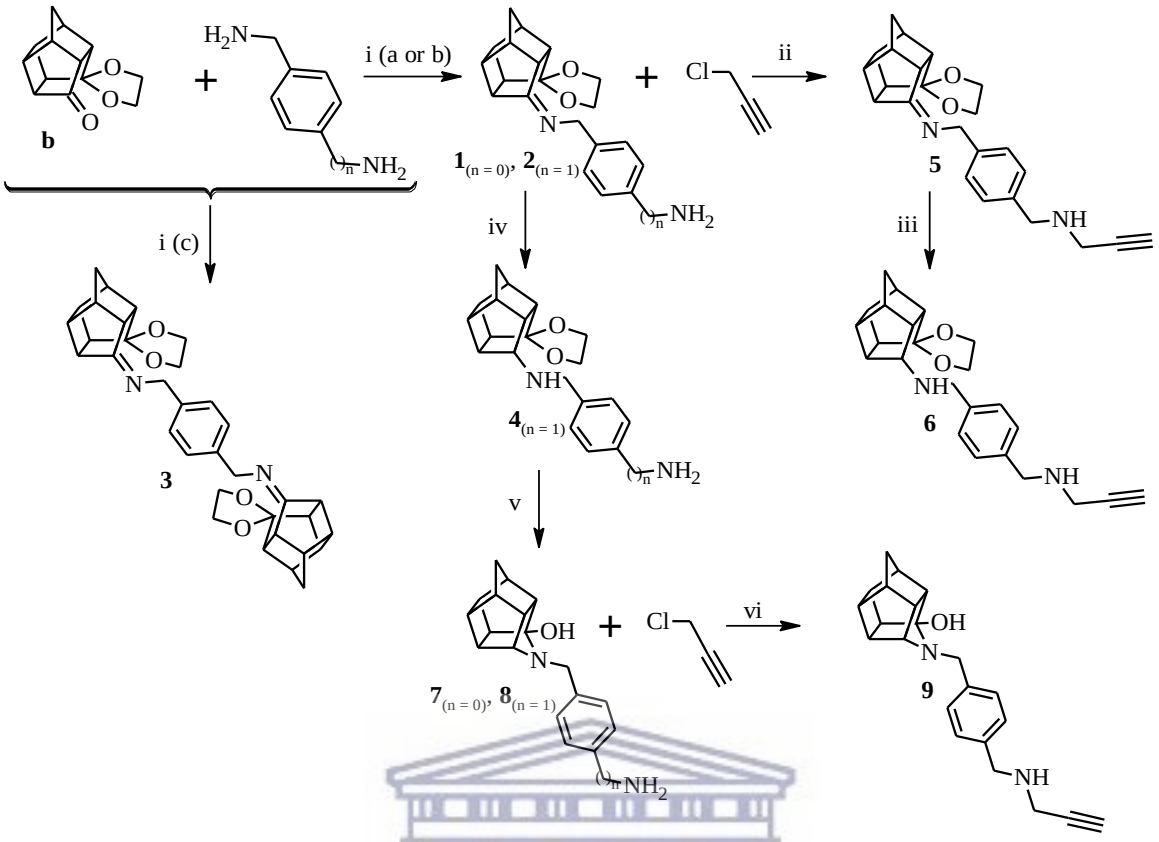

Scheme 2: Reagents and conditions for the synthesis of ketal- and aza-polycyclic derivatives (compounds **1** – **9)**: (i, a: n = 0) ethanol, MW, 80W, 150 psi, 100 °C, 30 min, 65%; (i, b: n = 1) ethanol, rt 1 h, then MW, 60 W, 80 psi, 100 °C, 3 h, 32%; (i, c) ethanol, rt 1 h, then MW, 60 W, 80 psi, 100 °C, 3 h, 13%; (ii) acetonitrile, K_2CO_3, 60 °C, 4 h, 21%; (iii) ethanol, $NaBH_4$, rt, 8 h, 72%; (iv) ethanol, $NaBH_4$, rt, 8 h, 69%; (v) acetone, 4 M HCl, rt, 12 h, 42% and 78%; (vi) acetonitrile, K_2CO_3, MW, 60 W, 60 °C, 2.5 h, 18%.

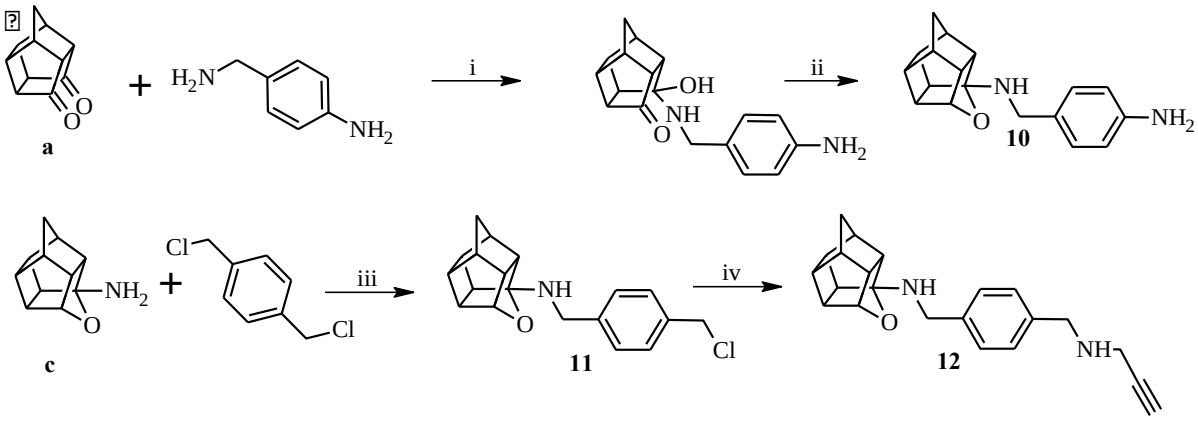

Scheme 3: Reagents and conditions for the synthesis of oxa-polycyclic derivatives (compounds **10** – **12)**: (i) ethanol, MW, 100 W, 100 psi, 80 °C, 2 h; (ii) ethanol, $NaBH_4$, rt, 8 h, 32%; (iii) acetonitrile, K_2CO_3, MW, 150 W, 20 psi, 70 °C, 1 h, 19%; (iv) acetonitrile, K_2CO_3, MW, 150 W, 20 psi, 70 °C, 1 h, 21%.

Characterization of all the compounds was carried out by means of ^{1}H-, ^{13}C-NMR, IR and HREI-mass spectra. A common structural feature in all the synthesized compounds was the polycyclic cage moiety. This structural moiety showed characteristic signal peaks on the ^{1}H-NMR spectra which included a characteristic AB quartet signal, due to the two unsymmetrical protons on the bridgehead. This signal appeared at a chemical shift in the range of δ 1.10–1.91 ppm, with a coupling constant in the range of 10.6–10.8 Hz. The rest of the protons making up the polycyclic cage appeared as multiplets or groups of multiplets, apparent quartets, and apparent triplets in the range of δ 2.30–3.00 ppm. These signals confirmed the presence of the polycyclic scaffold in the compound structures [38].

All ketal derivatives (**1** – **6**) showed a characteristic multiplet signal in the range of δ 3.70–3.95 ppm, owing to the four protons on the ketal carbons. In compounds were the polycyclic cage scaffold was linked to the rest of the molecule *via* a rigid imine bond (**1**, **2**, **3** and **5)**, the ketal moiety seemed to influence the signal of the two protons of the -N-CH_2- linker by virtue of long-range coupling. Due to this coupling, the two protons appeared on the ^{1}H-NMR spectra as apparent doublet of doublets at about δ 4.30–4.60 ppm, with a coupling constant of 3.2 Hz. When the imine bond was reduced to a rotatable amine bond, in the case of **4** and **6**, this coupling effect was lost and the signal appeared as a multiplet at an upfield shift of about δ 3.95 ppm.

A typical signal for the presence of the aza-cage moiety (**7** – **9**), was a triplet at a chemical shift in the range of δ 3.21–3.95 ppm, with coupling constants in the range of 4.8–5.2 MHz. This triplet corresponded to the single proton at the -CH-N- position, and its multiplicity is attributed to the presence of two protons at the adjacent carbons atoms within the polycyclic cage [38]. In the case of the oxa-cage moiety (**10** – **12**), this triplet signal was at a range of about δ 4.65–4.73 ppm with a coupling constant in the range of 4.8–5.0 Hz. The downfield shift of this methine hydrogen resulted from the deshielding effect of the adjacent oxygen atom. This downfield shift, compared with that of its aza analogues, is attributed to the electronegativity difference between nitrogen and oxygen, and thus, an increased deshielding effect compared to the aza derivatives.

The presence of a propargyl moiety in the structures of compounds **5**, **6**, **9** and **12** was confirmed by a characteristic ^{1}H-NMR triplet at a chemical shift in the range of δ 2.20–2.30 ppm, with a coupling constant of about 2.4 Hz. This triplet corresponds to the terminal acetylene proton and its multiplicity is attributed to the neighbouring methylene protons which influence it *via* long-range coupling. The terminal acetylene proton equally influenced

the two symmetrical methylene protons, which form part of the propargyl moiety, to appear as a doublet in the range of δ 3.40–3.50 ppm, with a coupling constant of about 2.4 Hz.

Further characterization of these compounds was carried out by means of ^{13}C-NMR, IR and HREI-mass spectra, which all supplemented the ^{1}H-NMR spectra findings, further confirming the structures of the compounds.

4.2.2. Cytotoxicity

Compounds **1-12** were assayed for cell viability on SH-SY5Y human neuroblatoma cells using a standard 3-[4,5-dimethylthiazol-2-yl]-2,5-diphenyl tetrazolium bromide (MTT) assay method [39]. The results are depicted in Figure 3 and Table 1. This assay, which measures cell metabolic activity, was used to determine the cytotoxicity of the test compounds at 10 µM, 50 µM and 100 µM concentrations. The cells were exposed to test compounds for 48 hours, after which cell viability was determined spectrophotometrically. Vehicle control cells were treated with dimethyl sulfoxide (DMSO, solvent for dissolving test compounds) and served as a reference for 100% cell viability. NGP1-01, known to have neuroprotective properties [27], was also used as a reference control for relative comparison.

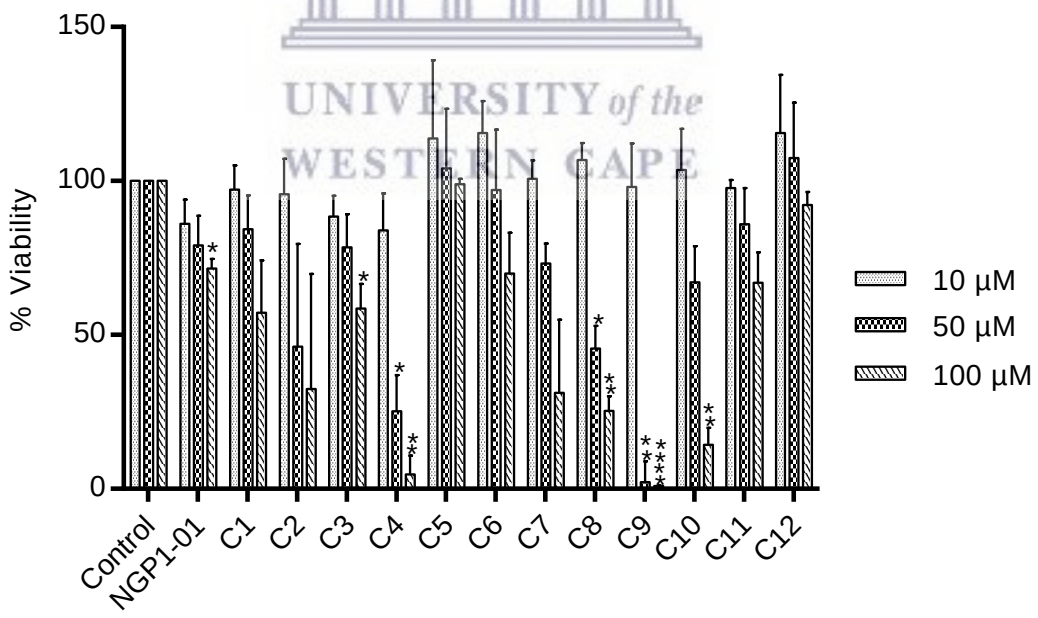

Figure 3. Percentage cell viability of compounds **1-12** assessed by means of measuring the metabolic activity of SH-SY5Y neuroblatoma cells, after 48 h exposure to test compound, relatcive to a control of untreated viable cells. Data are mean ± SEM (n = 3, four fields per repeat). Data were subjected to an ANOVA statistical analysis and significance was defined as [(*) $p < 0.05$, (**) $p < 0.001$, (***) $p < 0.0001$].

The results from this assay suggested the SH-SY5Y human neuroblastoma cells to be viable with the test compounds, particularly at 10 μM, as none of the compounds showed statistically significant cytotoxicity on the cell line at this concentration (Figure 3). Percentage cell viability at this concentration ranged from 84% to 116% relative to the untreated control. This was comparable to NGP1-01, which was found to be 86% viable at the same concentration. The influence of the propargyl moiety was evident at higher concentrations of test compound as seen when comparing the propargyl containing compound **5**, which was 99% viable at 100 μM, with its precursor devoid of this moiety, compound **2**, which was only 32% viable at the same concentration. This observation suggests compound **2** to be 3-times more toxic than its propargyl containing derivative. The same observation was made when comparing compound **6**, which was 70% viable at 100 μM, to its precursor compound **4**, which was only 5% viable at the same concentration, suggesting the inclusion of a propargyl moiety to be responsible for a 14-fold decrease in cytotoxicity.

4.2.3. Neuroprotection

The SH-SY5Y cytotoxicity assay results were used to determine the test concentration of compounds **1-12** which would insignificantly affect the viability of the SH-SY5Y cells. Based on the SH-SY5Y cytotoxicity analysis, it was decided to conduct the neuroprotection studies at test concentrations between 1 μM and 10 μM, in order to maintain cell viability.

In this study, we employed a widely used cellular model in which neurotoxicity was induced by 1-methyl-4-phenyl pyridinium (MPP^+) in SH-SY5Y neuroblastoma cells [40,41]. MPP^+ is highly toxic to neurons and has been widely used to induce neurodegeneration in various *in vitro* and *in vivo* models [40,41]. Several signaling pathways have been suggested to be responsible for MPP^+-mediated neurotoxicity in SH-SY5Y cells, for instance, trigger of oxidative stress [42], induction of apoptosis [43], and inactivation of pro-survival phosphoinositide 3-kinase (PI3-K)/Akt cascade [44,45]. This assay was deemed appropriate to test for initial neuroprotective ability of the compounds because of the multitude of pathways involved in MPP^+ mediated neurotoxicity and the potential multifunctional inhibitory abilities of the test compounds.

Briefly, the assay entailed treating the SH-SY5Y cell line with different concentrations (1 μM, 5 μM, 10 μM) of test compounds two hours prior to MPP^+ treatment. After 48 hours of incubation, the neuroprotective effect of the compounds was assessed by means of the MTT mitochondrial function assay which measured cell viability. Vehicle control cells were

treated with DMSO (solvent for dissolving test compounds) and served as a reference for 100% cell viability. Percentage neuroprotection values were calculated as the difference between the final percentage cell viability of the test compound treated cell line and that of the MPP^+ only treated cell line. These values are presented in Figure 4 and Table 1. NGP1-01, known to have neuroprotective properties [27], was also used as a reference control for relative comparison.

As illustrated in Figure 4, after the exposure to 1000 µM MPP^+ for 48 hours, the cell viability declined significantly to around 45%. However, its cytotoxic effects were significantly ameliorated in the presence of the test compounds at 1 µM, 5 µM and 10 µM concentrations. All compounds in the series exhibited significant neuroprotective effects at a 1 µM concentration as they managed to improve cell viability to values between 86% and 110%. This was expected from these compounds as they all share molecular similarities with NGP1-01 which is known to have neuroprotective properties as confirmed in this assay [27]. At 5 µM and 10 µM a slight decrease in cytoprotection was observed for most of the compounds. This may indicate that the neurotoxin challenged state of the SH-SY5Y cells may be more sensitive to the cytotoxic effect of the test compounds at higher concentrations.

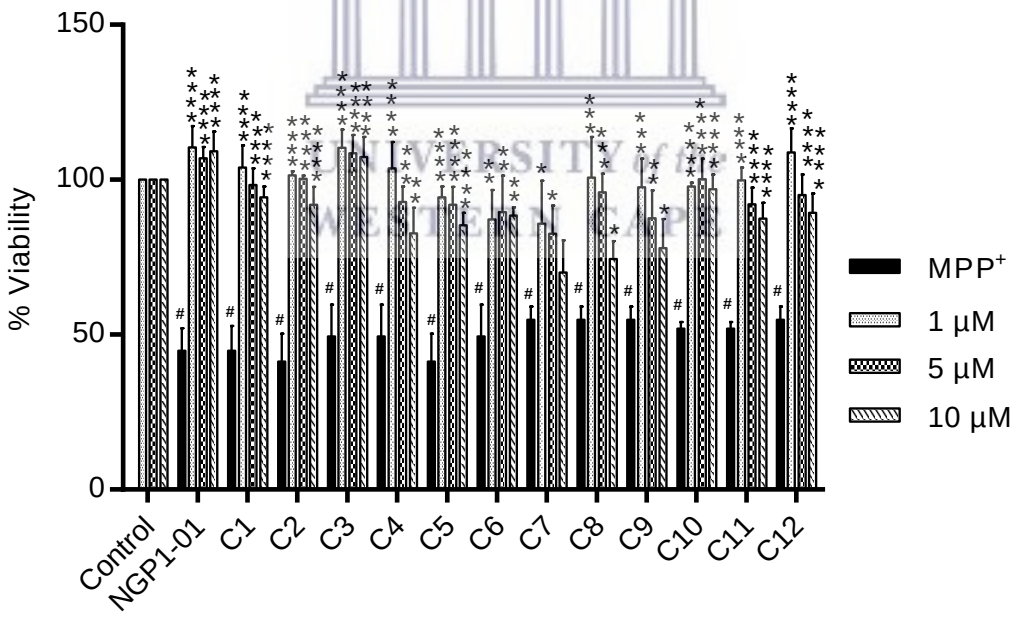

Figure 4. The effects of compounds **1-12** on MPP^+-induced (1000 µM) cytotoxicity in SH-SY5Y cells. The viability of the untreated control was defined as 100%. MPP^+ without test compound showed a significant decrease in cell viability relative to the control (#, $p < 0.05$). Data are mean ± SEM (n = 3, four fields per repeat). The level of statistical significance for the test compounds is set at * $p < 0.05$ compared to the MPP^+ only treated control. Tukey's multiple comparisons statistical analysis was performed on all raw data and significant neuroprotective effect was defined as [(*) $p < 0.05$, (**) $p < 0.01$, (***) $p < 0.001$, (****) $p < 0.0001$].

4.2.4. VGCC assay

To investigate the test compounds' potential VGCC blocking effect, we developed an assay based on the methods described by Young *et al*. [46] and León *et al*. [47] Briefly, SH-SY5Y human neuroblastoma cells loaded with the ratiometric fluorescent calcium indicator, Mag-Fura-2/AM, were incubated at 37 ºC in the presence of the test compounds at a 10 µM concentration for 30 mins, then stimulated with a concentrated solution of KCl to allow opening of the calcium channels. The assay was performed at a 10 µM concentration as determined by the cytotoxicity assay performed on the same cell line. Changes in fluorescence as a consequence of an increase in cytosolic calcium elicited by high K^+ concentrations were measured in a Biotek® fluorescent microplate reader. Two positive controls were included in the VGCC assay; nimodipine, a commercially available dihydropyridine *L*-type calcium channel blocker [48], and the prototype polycyclic amine cage compound, NGP1-01 [49]. The percentage VGCC blockade of each compound was calculated relative to the activity of nimodipine and the data is presented in Table 1.

Based on the assay results, all compounds, except **3**, **6** and **10**, showed significant VGCC inhibitory activity; ranging from 26.6% to 51.3%, relative to a 10 µM solution of nimodipine. This activity is comparable to that of NGP1-01, which inhibited calcium influx by 25.7% at the same concentration. This general improvement in activity, compared to **P1** and **P2** which were inactive as VGCC blockers at 100 µM [26], emphasizes the need to include a benzylamine moiety in the structure of polycyclic amine cage derived compounds designed for VGCC blockade as we previously postulated [26].

It seems that a primary terminal amine imparts the molecules with increased VGCC inhibition. This was seen in compounds **1**, **2**, **4**, **7** and **8**, which showed activities of 40%, 35%, 43%, 36% and 51% respectively, a significant improvement to the activity noted for NGP1-01. When this primary amine terminal was converted to a secondary amine, by conjugating a propargyl moiety, in the case of compounds **5**, **6** and **9**, the VGCC inhibitory activity notably decreased to 26%, 22.9% and 39% respectively, when compared to their primary amine carrying precursors (**2**, 35%; **4**, 43% and **8**, 51%). A terminal primary amine could be necessary for the formation of productive binding interactions between the respective compounds and the binding site of the VGCC resulting in their blockade.

4.2.5. NMDA assay

To assess the compounds' ability to block Ca^{2+} influx *via* the NMDAr channels, a similar method as in the VGCC assay was used. However, a concentrated NMDA/Glycine solution, instead of KCl, was used to stimulate calcium flux through the NMDAr. Two positive controls were included in this assay; MK-801, a commercially available non-competitive antagonist of the NMDAr [50], and NGP1-01 [49]. All compounds were assayed at 10 µM and the percentage NMDAr inhibition of each compound was calculated relative to the activity of MK-801. The calculated percentage inhibition values are presented in Table 1.

Several compounds showed great NMDAr antagonism, with compound **5** showing the highest activity of 88.3%. Compounds **1**, **3** and **6** also showed good activity with percentage inhibition values of 63.1%, 70.5% and 63.9% respectively. These four compounds, as well as compound **2**, which showed significant activity of 49.5%, showed NMDAr antagonism comparable to NGP1-01, which exhibited 32.5% inhibition at the same concentration. A common structural feature of these five compounds is a ketal moiety which seemed to be important for increased NMDAr antagonism. This observation was more compelling when considering that compounds **9** and **10**, which were devoid of this functional moiety, were both inactive; as well as compounds **7** and **11**, which also lacked the ketal moiety, showed statistically insignificant activity of 11.9% and 26.1% respectively. The ketal moiety could be providing necessary bulk and charge which could allow for productive ligand-NMDAr binding interactions. Further mechanistic studies could provide further insight on the putative binding mode of these compounds.

The inclusion of a propargyl moiety in the compound structures seemed to contribute to improved NMDAr antagonism. This was evident when comparing the propargyl carrying compounds **5** and **6**, which were 88.3% and 63.9% active respectively, to their precursor compounds **2** and **4**, devoid of this moiety, which were 49.5% active and inactive respectively. An imine bond between the polycyclic cage and the benzylamine moiety, as seen in compounds **2** and **5**, seemed to be ideal for NMDAr inhibitory activity compared to the simple amine bond contained in the structures of compounds **4** and **6**. When the imine bond in compound **2** is reduced to a simple amine bond in compound **4**, the NMDAr antagonistic activity was completely lost. Similarly, there was about 25% decrease in activity when the imine bond in compound **5** was reduced to afford compound **6**. The rigid imine bond seemed to be ideal for NMDAr inhibition. A probable explanation for this could be that the rigid ligand confirmation allows the compounds to adequately traverse the ligand-

recognition region of the NMDAr subunit which is defined by two polypeptide segments, S1 and S2 [51].

Generally, these compounds seem to possess calcium regulatory potential comparable to the prototype NGP1-01 by acting on both VGCC and NMDAr. However, the compounds appeared to be more active as NMDAr antagonists than they are VGCC blockers.

4.2.6. MAO-A and MAO-B inhibition studies

The target compounds were investigated for their inhibitory activity against human MAO (hMAO) by measuring the extent to which the test compounds reduce the oxidative catalysis of kynuramine, a mixed MAO-A/B substrate, by the respective MAO enzymes [52]. The fluorescence of the MAO generated 4-hydroxyquinoline in the supernatant fractions were measured using a Biotek® fluorescent microplate reader at an excitation wavelength of 310 nm and an emission wavelength of 400 nm. IC_{50} values were calculated as the compound concentration that produces 50% enzyme activity inhibition. The inhibition potencies of the test compounds and reference compounds, selegiline and clorgyline, are presented in Table 1.

Based on the results, most of the active compounds displayed higher inhibitory potencies against the MAO-B compared to the MAO-A isoenzyme as suggested by the selectivity index (SI) values. The only exception was compound **10,** which showed selectivity to the MAO-A isoenzyme. The ketal moiety seemed to be influential in conferring the molecules MAO-B selectivity as observed from the high SI values of compounds **1**, **2**, **5** and **6**, which all carry this moiety. These compounds were about 3 to 52 times more selective to the MAO-B compared to the MAO-A isoenzyme. Conversely, compounds **9** and **12**, though devoid of the ketal moiety, also showed selectivity to MAO-B with SI values of 14.8 and 3.6 respectively.

Several structure activity relationships could be derived from comparing the MAO IC_{50} values of the various compounds in the series. Interesting to note, was that the propargylamine carrying compounds **5**, **6**, **9** and **12** showed MAO-B inhibition values which ranged between 1.7 µM and 36.31 µM (IC_{50}). This was a significant improvement from the activities shown by the previously reported compounds **P1** and **P2**, which were inactive as MAO-B inhibitors [26]. This improved activity can be attributed to the increased molecular length of these compounds as a result of the incorporation of a benzylamine moiety into their structures.

The data from this study suggests the juxtapositioned benzylamine and propargyl moieties are imperative in rendering the compounds better MAO-B inhibitory activity. This

observation was noted by comparing the activity of compounds **4** and **8**, which both lacked the propargyl moiety but carried the benzylamine moiety, to the activity of compounds **6** and **9**, with both moieties. Compounds **4** and **8** showed IC_{50} values of more than 100 µM, while compounds **6** and **9** showed values of 36.31 µM and 3.89 µM respectively. It is important to note that when the benzylamine moiety is absent in the molecular structure of these compounds, as in the case of **P1** and **P2**, the propargylamine moiety alone fails to render significant activity on the MAO-B enzyme, thus further supporting the need for both moieties in the structures of these type of compounds for activity.

Table 1: The biological activity profiles of compounds **1-12** and related reference compounds.

Compound	Cell Viability %	Neuro-protection %[a]	VGCC %	NMDA %	MAO- A	MAO-B	SI MAO-B[b]
	10 µM	1 µM	10 µM	10 µM	IC_{50} µM	IC_{50} µM	
Selegiline	-	-	-	-	-	<10 nM	-
Clorgyline	-	-	-	-	<10 nM	-	-
MK-801	-	-	Inactive	100.0	-	-	-
Nimodipine	-	-	100.0	Inactive	-	-	-
NGP1-01	86 ± 7.8	66 ± 6.9****	25.7 ± 9.2*	32.5 ± 9.9*	>100	>100	-
P1[26]	-	-	Inactive	Inactive	-	Inactive	-
P2[26]	-	-	18	4	-	6%	-
1	97 ± 7.9	59 ± 7.2****	40.1 ± 3.1***	63.1 ± 11.3****	>100	1.91**	>52.4
2	96 ± 11.4	60 ± 1.3****	35.0 ± 10.2**	49.5 ± 6.0**	>100	13.80*	>7.2
3	88 ± 6.8	61 ± 5.9****	24.3 ± 15.7	70.5 ± 4.2***	>100	100	-
4	84 ± 12.0	54 ± 8.5****	43.2 ± 3.9***	Inactive	>100	>100	-
5	114 ± 25.3	53 ± 3.5****	26.6 ± 3.9*	88.3 ± 7.9****	>100	1.70*	>58.8
6	116 ± 10.4	38 ± 9.4**	22.9 ± 5.5	63.9 ± 13.4**	>100	36.31*	>2.8
7	101 ± 6.0	31 ± 13.0*	36.5 ± 8.2***	11.9 ± 7.8	>100	>100	-
8	107 ± 5.5	46 ± 13.2***	51.3 ± 10.4****	59.0 ± 4.7****	>100	>100	-
9	98 ± 14.2	43 ± 9.2***	39.4 ± 8.0***	0.6 ± 8.1	56.23	3.80*	14.8
10	104 ± 13.4	46 ± 1.2****	7.6 ± 1.3	Inactive	2.37**	100	0.02
11	98 ± 2.7	48 ± 4.1****	31.6 ± 1.7**	26.1 ± 2.0	>100	14.13**	7.08
12	116 ± 18.8	54 ± 7.8****	29.1 ± 5.8**	31.4 ± 6.8*	>100	28.18**	3.55

By comparing derivatives **5** and **6**, whose IC_{50} values were 1.70 µM and 36.31 µM respectively, the influence of the imine bond between the polycyclic scaffold and the benzylamine moiety could be appreciated. This bond seemed to confer compound **5** a 16-fold increase in activity when compared to compound **6**, in which the imine bond was reduced to a secondary amine. The same was true for the precursors of compounds **5** and **6**, compounds **2** (imine) and **4** (amine), whose IC_{50}'s were 13.8 µM and >100 µM respectively. Perhaps this is because the imine bond, present in compounds **2** and **5**, is more rigid than the rotatable amine bond present in compounds **4** and **6**, thus allowing compounds **2** and **5** to be confined to a fixed region of the MAO-B enzyme active site allowing for more productive binding interactions.

When compound **2** is di-substituted with the ketal-polycyclic moiety to give compound **3**, MAO-B inhibitory activity is lost. The di-substituted molecule appears to be bulky and probably fails to make access into the enzyme active pocket, rendering it inactive. The absence of a propargyl function within the structure of compound **3** further explains the lack of MAO inhibition observed from this compound.

NGP1-01 showed little activity on both MAO-A and MAO-B enzymes, IC_{50} >100 µM on both isoenzymes, but when para-substituted with a primary amine to give compound **10**, MAO-A inhibition improved (IC_{50} = 2.37 µM)**.** This improved activity may be due to the involvement of the amine group in the formation of binding interactions with amino acid residues found in the substrate cavity of the MAO-A enzyme. Contrary to this, compound **4**, which was also para-substituted with a secondary amine, showed little activity on the MAO-A isoenzyme. This could be due to the presence of the bulk ketal moiety attached to the polycyclic cage scaffold, which may be hindering the entrance of the molecule into the enzyme substrate cavity. It is important to note that all ketal derivatives **1** – **6** showed little activity on the MAO-A isoenzyme of IC_{50} > 100 µM.

In general, compounds **1**, **2**, 5, **6, 9** and **12** showed the best overall MAO inhibitory activity and appear to be selective for the MAO-B isoenzyme. Although the MAO-B inhibitory activity herewith reported was a significant improvement in comparison to the previously reported compounds **P1** and **P2**, it is important to note that this activity was still about 1000-fold weaker than selegiline. Further structural modifications of these compounds may therefore be necessary to afford molecules which may potentially show improved MAO-B inhibition.

4.2.7. MAO reversibility studies

To determine the binding mode of the studied compounds on MAO-A and/or -B, a time dependency of enzyme inhibition was measured. If the compounds form a covalent adduct with the enzyme, a time-dependent reduction of enzyme activity would be expected. In this regard, the time dependent inhibition of MAO-A and-B by the active compounds **1, 5, 6, 9** and **12**, were evaluated (Figure 5). Briefly, recombinant human MAO-A and MAO-B was preincubated with the test compounds for periods of 0, 15, 30 and 60 min prior to starting the enzyme reaction and the residual rates of the MAO-A and -B catalysed oxidation of kynuramine were measured. For this purpose, the concentrations of the test compounds chosen were approximately twofold the measured IC_{50} values for the inhibition of the

respective enzymes. Clorgyline, with known irreversible inhibition for MAO-A [53], and selegiline, with known irreversible inhibition for the MAO-B [54], were used as a reference compounds.

As shown in Figure 5, only compound **9** showed a significant reduction in enzymatic activity with increased preincubation time when assayed on the MAO-A isoenzyme, suggesting compound **9** to be an irreversible inhibitor of MAO-A. MAO-B enzyme activity was not reduced by compounds **1, 5, 6, 9** and **12** with increased preincubation time. This indicates that the selected compounds were reversible inhibitors of MAO-B. Preliminary MAO-A molecular modelling studies performed on compound **9** (data not shown) showed potential involvement of the free hydroxyl group attached to the polycyclic moiety in forming covalent binding interactions with amino acid residue Gln215 of the MAO-A substrate cavity. This interaction could be the explanation for the observed irreversible MAO-A inhibition exhibited by compound **9**. No covalent interactions were observed between compound **9** and the MAO-B isoenzyme (see Figure 7), perhaps explaining the reversible MAO-B inhibition observed for compound **9**. It also was interesting to note that compounds **1** and **5** showed a notable increase in enzymatic activity over time. This might be due to test compound degradation in the aqueous medium as both compounds possess a ketal moiety as well as an imine bond. The imine function is known to undergo hydrolysis in aqueous medium [55], however, further degradation studies on these compounds are necessary to validate this notion.

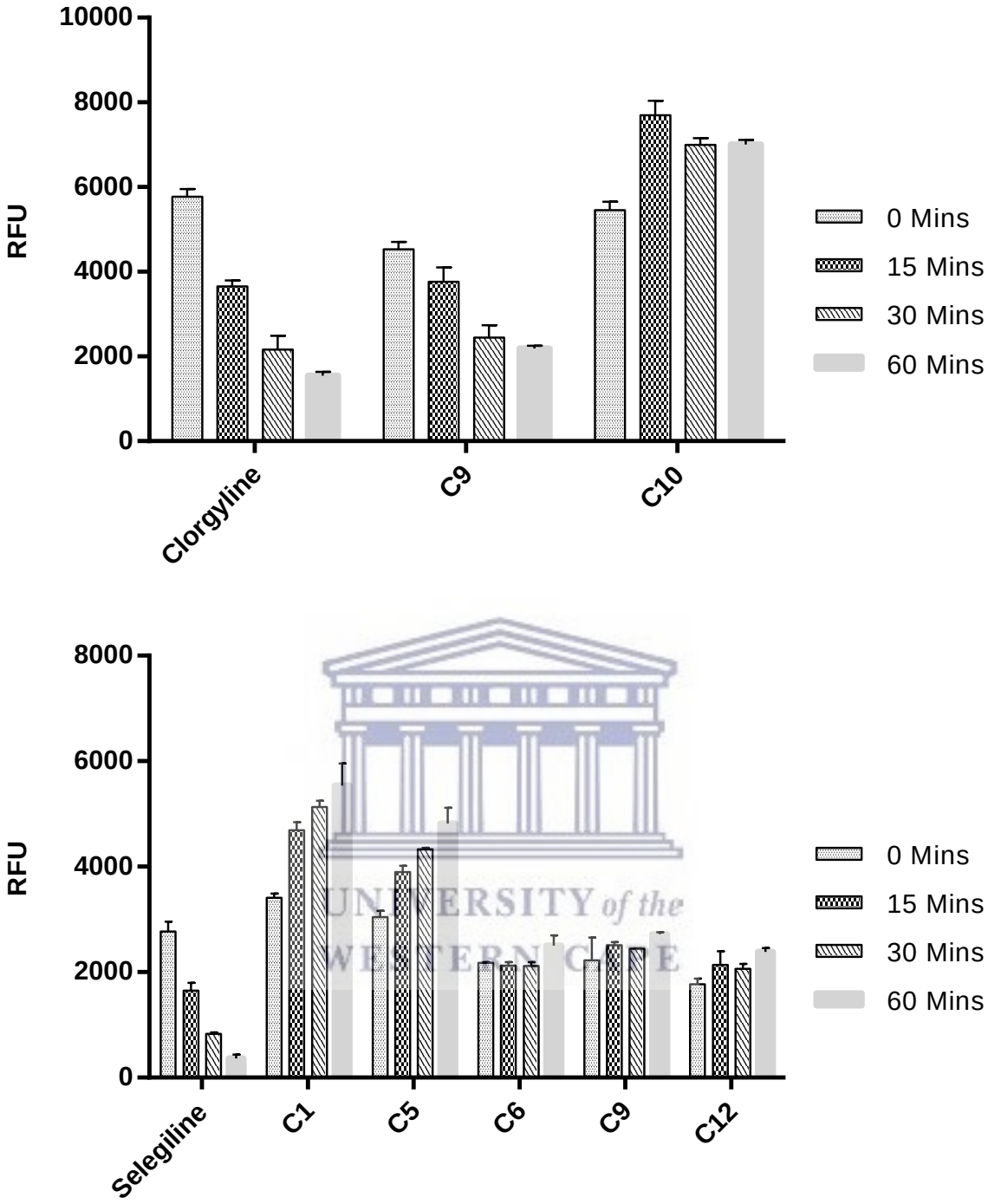

Figure 5. Time-dependent inhibition of the recombinant human MAO-A (top) and MAO-B (bottom) catalysed oxidation of kynuramine by the selected active compounds. The enzymes were preincubated for various periods of time (0–60 min, x-axis) Data are expressed as the mean RFU (relative fluorescent units) ± SEM of three independent experiments.

4.2.8. MAO-B molecular modelling studies

With most compounds showing selectivity for the MAO-B isoenzymes, the binding modes of all twelve compounds in the MAO-B substrate cavity were examined *in silico*. Docking simulations were performed on the human MAO-B crystal structure (PDB ID: 2V5Z) [28], using the Molecular Operating Environment (MOE) software [29]. In general, the amino acid residues between 120 and 220, as well as the FAD cofactor, are important in conferring substrate selectivity of MAO-B [56], most importantly residues Ile-199, situated in the entrance cavity, and Gln-206, situated in the substrate cavity. Interaction with these amino acid residues may confer a compound MAO-B inhibitory activity as shown by safinamide (Figure 6), a known MAO-B inhibitor.

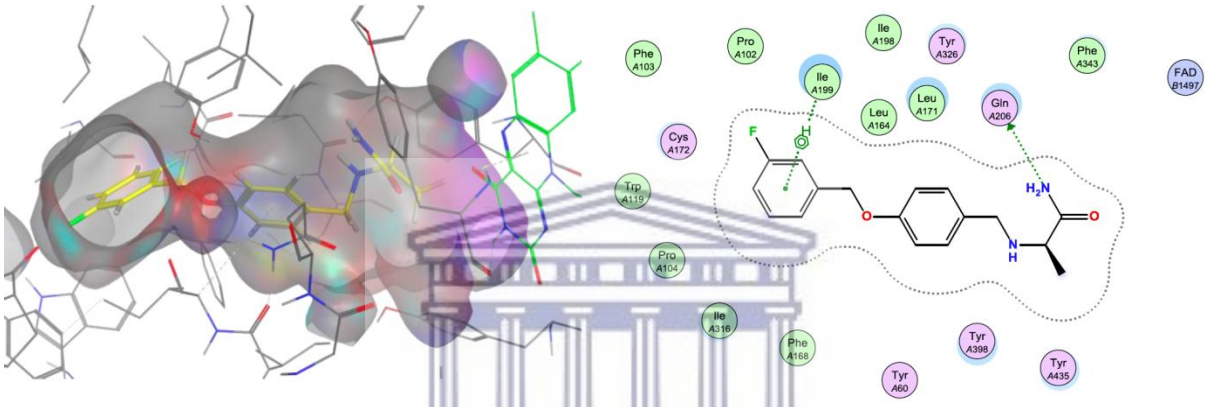

Figure 6. The putative binding modes of safinamide within the human MAO-B enzyme active site. Safinamide and the FAD cofactor are shown in the docking simulation on the left as bold lines (indicated in yellow and green respectively), and the binding interactions with the amino acid residues shown on the right. Safinamide shows productive interactions with amino acid residues Ile-199 and Gln-206.

The docking simulation results generally showed that the lipophilic polycyclic cage unit, carried by all the test compounds, stabilized within the hydrophobic environment of the enzymes entrance cavity, while the rest of the molecular structure traversed deep into the substrate cavity (see Figure 7). Further analysis of the best-ranked docking solutions showed all active compounds to be forming productive binding interactions with the MAO-B substrate cavity. Interestingly, most of the active compounds, particularly compounds **1**, **2**, **5**, **9**, **11** and **12**, seemed to be forming binding interactions specifically with Ile-199, an observation which could explain their noted *in vitro* activity. The electron-rich π system, presented by the aromatic ring within these compounds' structures, appeared to be vital for the formation of 'arene-hydrogen' interactions with the amino acid Ile-199.

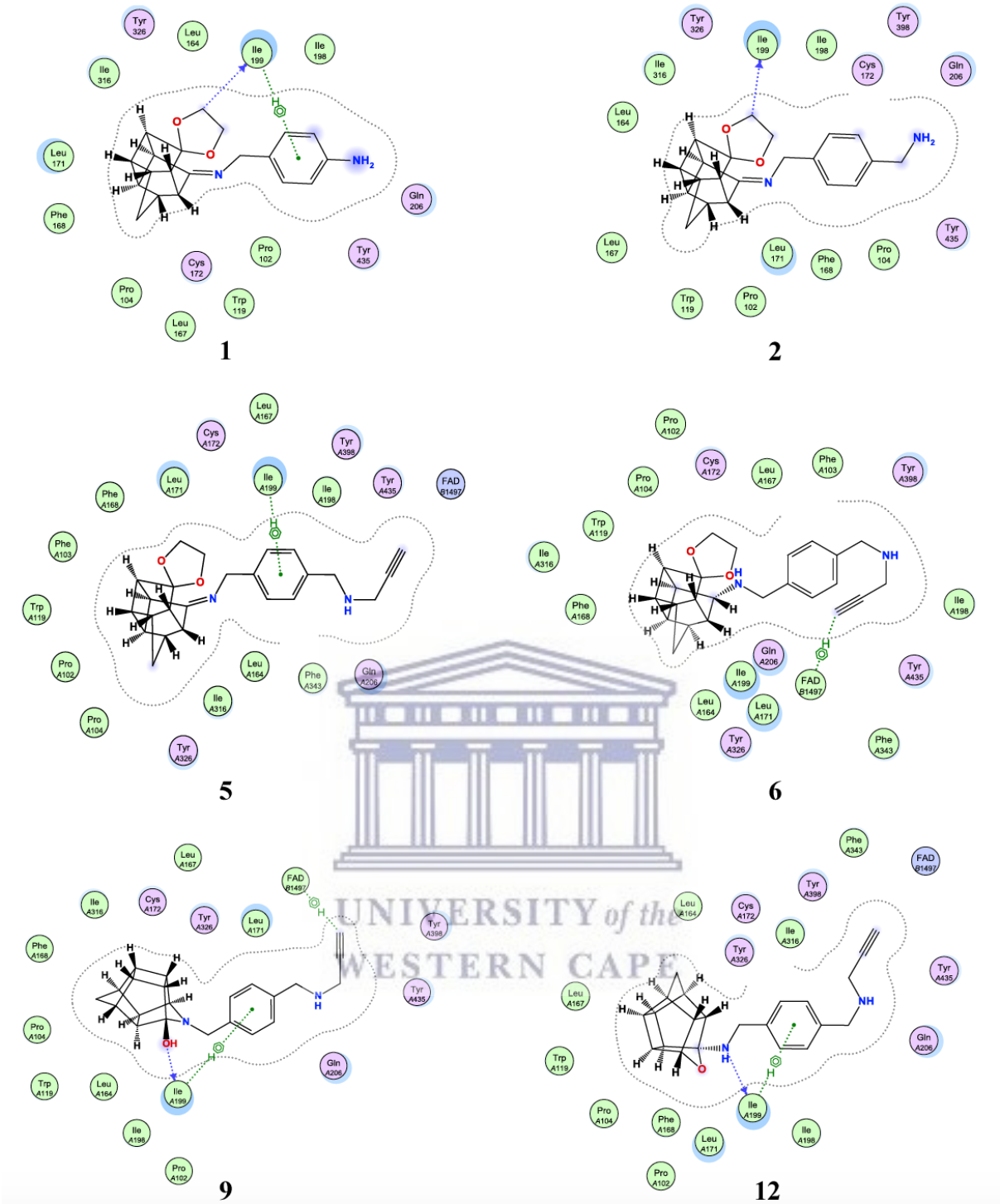

Figure 7: MOE generated binding interactions of compounds **1**, **2**, **5**, **6**, **9** and **12** with the respective amino acid residues within the human MAO-B enzyme active site.

In the case of compounds **1** and **2**, the ketal moiety also seemed to be involved in the formation of binding interactions with Ile-199. This interaction may be due to the electronegative oxygen atom which creates a slightly positive environment on the adjacent -CH_2 group causing it to serve as a proton donor to the amino acid residue. While the aromatic system and ketal moiety seemed to be important for the formation of productive interactions with the enzyme cavity, it appeared as though these interactions were dependent on the

presence of an imine bond between the polycyclic cage and the benzylamine moiety. This was evident when comparing binding interactions observed for compounds **1**, **2** and **5**, which all carried this bond and showed interactions with Ile-199, to the binding interactions observed for compounds **4** and **6**, which lacked this bond and hence failed to interact with Ile-199. This observation suggests the imine bond to be important for stabilizing the molecules' benzylamine moiety within the MAO-B enzyme cavity, thus allowing for the formation of productive binding interactions. The observation correlates with the observed *in vitro* activity of compounds **1**, **2** and **5**, which all showed significant MAO-B inhibition of IC_{50}: 1.91 µM, 13.80 µM and 1.70 µM, respectively. While compound **6,** shows no interaction with Ile-199 due to the absence of an imine linkage, the compound remains active due to the presence of a propargylamine group which forms interactions with the FAD cofactor.

The inactive compounds **7**, **8** and **10**, the oxa- and aza-type derivatives with a terminal primary amine group, showed no interaction with any amino acid residues within the MAO-B active site. This observation may be the explanation to these compounds' lack of activity. Interesting to note was that when the secondary amine group was conjugated to a propargyl function, as seen in compound **9**, the resultant compound showed interactions with Ile-199 and the FAD cofactor. The role of the propargyl moiety seems to be particularly important for MAO-B inhibitory activity as suggested by the *in vitro* activities of compounds **5**, **6**, **9** and **12** (IC_{50}: 1.70 µM, 36.31 µM, 3.80 µM and 28.18 µM, respectively). Molecular modelling findings showed the propargyl moieties of these four compounds to either be in close proximity to the FAD cofactor, in the case of compounds **5** and **12**, or to be forming binding interactions with the FAD cofactor, in the case of compounds **6** and **9**.

4.3. Conclusion

We have successfully designed and synthesized twelve novel pentacycloundecane and hexacycloundecane derived compounds which showed promising neuroprotective potential. Regarding cytotoxicity, the SH-SY5Y human neuroblastoma cells seemed to be viable with all the test compounds, particularly at 10 µM, as none of the compounds showed statistically significant cytotoxicity at this concentration. At a 1 µM concentration, the compounds significantly improved the viability of SH-SY5Y neuroblastoma cells, previously exposed to the neurotoxin MPP^+, from about 45% to values between 86% and 110%.

Most of the compounds, except **3**, **6** and **10**, showed statistically significant VGCC inhibitory activity ranging from 26.6% to 51.3%, relative to a 10 µM solution of nimodipine. This was

comparable to that of NGP1-01, which inhibited calcium influx by 25.7% at the same concentration. Compounds **1**, **2**, **3**, **5**, **6**, **8** and **12**, showed significant NMDAr inhibitory activity ranging between 31.4% and 88.3%, relative to a 10 µM solution of MK-801.

When assayed for MAO inhibition, most of the active compounds (**1**, **2**, **5**, **6**, **9**, **11** and **12**) displayed selectivity to the MAO-B isoenzyme with IC_{50} values ranging from 1.70 µM to 36.31 µM, with the only exception being compound **10**, which showed selectivity to the MAO-A isoenzyme. The most active MAO-A inhibitor, compound **10**, as well as the MAO-B inhibitors, compounds **1**, **5**, **6**, **9** and **12**, all appeared to be reversible MAO inhibitors as defined by the time-dependency studies conducted. Compound **9** however, seemed to be an irreversible inhibitor of the MAO-A isoenzyme, an undesirable type of inhibition which has been shown to cause the unwanted hypertensive response in patients [13]. Further structural modifications to compound **9** are therefore necessary in order to afford a resultant molecule with the desired reversible MAO-A inhibitory potential.

Molecular modelling studies gave some insight on the compounds' potential binding interactions with the MAO-B isoenzyme. Based on the *in silico* studies, the benzylamine moiety seemed to be a very important structural component in affording this series MAO-B inhibitory activity. Not only was it important for elongating the molecules to allow for the propargylamine moiety to interact with the isoenzyme's FAD cofactor, but it also seemed to be involved in most of the binding interactions observed *in silico* with the MAO-B substrate cavity, particularly with Ile-199.

Various other structure-activity relationships were derived from the series of compounds, and these include the influence of; (a) the propargyl moiety, in reduced cytotoxicity, improved NMDAr antagonism and improved MAO-B inhibition, (b) a terminal primary amine, which improved VGCC blockade (c) a benzylamine moiety for improved VGCC blockade as well as MAO-B inhibition, (d) an imine bond between the polycyclic cage and the benzylamine moiety, which was ideal for NMDAr antagonism and MAO-B inhibition, (e) a ketal moiety, which seemed to be important for increased NMDAr antagonism and conferring the compounds MAO-B selectivity.

When considering multifunctionality, compounds **1**, **2**, **5** and **12** showed the best overall activity as viable neuroprotective agents with inherent calcium regulatory potential, by blocking VGCC and NMDAr, and MAO-B inhibitory capacity. More importantly, due to the inclusion of a propargyl moiety within their structures, compounds **5** and **12** are promising leads to multi-mechanistic compounds the may be useful as drug agents for the treatment of neurodegenerative disorders. Further *in vitro* and *in vivo* studies, which may include

mechanistic studies as well as elucidation of the actual binding mode of these compounds, would provide better insight on their drugability. Also, these analogues may be screened for potential neuroprotective activity on various other drug targets implicated in neurodegeneration.

4.4. Experimental

4.4.1. Chemistry

General procedures

Unless otherwise specified, materials were obtained from commercial suppliers and used without further purification. Microwave synthesis was performed using a CEM Discover_SP® microwave synthesis system. All reactions were monitored by thin-layer chromatography on 0.20 mm thick aluminium silica gel sheets (Alugram® SIL G/UV254, Kieselgel 60, Macherey-Nagel, Düren, Germany). Visualisation was achieved using a variable wavelength UV-detector, iodine vapours or an ethanol solution of ninhydrin, with mobile phases prepared on a volume-to-volume basis. Chromatographic purifications were performed on silica gel (0.063–0.2 mm, Sigma Aldrich) or versa flash silica gel apparatus (20 – 45 μm, VersaPak™, Sigma Aldrich). High resolution electron spray ionisation (HREI) mass spectra for all compounds were recorded on a Waters API Q-Tof Ultima mass spectrometer at 70 eV and 100 °C. The IR spectra were recorded on a Perkin Elmer Spectrum 400 spectrometer, fitted with a diamond attenuated total reflectance (ATR) attachment. Melting points were determined using a Stuart SMP-10 melting point apparatus and capillary tubes. All the melting points determined were recorded uncorrected. ^{1}H and ^{13}C NMR spectra were determined using a Bruker Avance III HD spectrometer at a frequency of 400 MHz and 100 MHz, respectively. Both ^{1}H NMR and ^{13}C NMR spectra were referenced internally on $CDCl_3$ (δ: ^{1}H 7.26, ^{13}C 77.20). All chemical shifts are reported in parts per million (ppm), relative to the internal standards. The following abbreviations are used to indicate the multiplicities of the respective signals: s – singlet; br s – broad singlet; d – doublet; dd – doublet of doublets; t – triplet and m – multiplet; and AB-q – AB quartet.

Synthesis of pentacyclo[5.4.0.0^{2,6}.0^{3,10}.0^{5,9}]undecane-8,11-dione (a)

A stiochiometric volume of freshly monomerised cyclopentadiene (15.26 ml; 92.5mmol) was slowly added drop-wise (1 g every 10 mins) to a solution of *p*-benzoquinone (10 g; 92.5

mmol) in dry benzene (400 ml). The reaction was maintained on an ice bath at a temperature below ± 5 °C, to prevent the formation of the undesired Diels Alder di-adduct. The reaction was protected from light and left to stir for 1 hour to reach completion. The reaction was complete when the p-benzoquinone spot was no longer visible on TLC analysis. This was followed by the addition of 3 spatula scoops of activated charcoal (± 0.50g) and the mixture was stirred for a further 30-60 minutes. After filtration through Celite® to remove the activated charcoal, the solvent was evaporated *in vacuo* and the residue, a yellow syrupy oil, was left overnight in a dark fume hood. This allowed full evaporation of the benzene, affording the Diels Alder adduct as yellow crystals. The Diels Alder adduct was dissolved in ethyl acetate (± 4 g/100 ml) and irradiated for ± 6 hours in a photochemical reactor (1000 W medium pressure UV lamp, Phillips HPA 1000/20). Decolouration of the solution confirmed complete cyclization of the adduct. The solvent was subsequently removed *in vacuo* to afford the impure pentacyclo-dione as a beige/yellow residue. This residue was purified in 2 cycles of Soxhlett extractions in cyclohexane to produce the pure diketone as a waxy, off-white precipitate (**a**; yield = 12.040 g, 74.72%, m.p.: 242 ºC). The data from the physical characterisation of the obtained compound correlates with that of the pentacyclo[5.4.0.0^{2,6}.0^{3,10}.0^{5,9}]undecane-8,11-dione as described by Cookson *et al*. (1958).[74]

Synthesis of spiro[1,3-dioxolane-2,8'-pentacyclo[5.4.0.0^{2,6}.0^{3,10}.0^{5,9}]undecan]-11'-one (b)

A mixture of pentacyclo[5.4.0.0^{2,6}.0^{3,10}.0^{5,9}]undecane-8,11-dione (**a**: 2.0 g 11.48 mmol), ethylene glycol (0.642 ml 11.48 mmol, 1.0 equiv.) and *p*-toluenesulfonic acid monohydrate (21.87 mg, 0.1148 mmol, 0.01 equiv.) was prepared in 35 ml of benzene and refluxed under Dean-Stark conditions for 5 hours with stirring. The reaction mixture was cooled and slowly poured into an ice cold saturated aqueous sodium carbonate (Na_2CO_3) solution (10 ml) for neutralisation. This was followed by extraction with DCM (3 x 25 ml). The organic phase was dried over anhydrous magnesium sulphate ($MgSO_4$) then filtered and concentrated *in vacuo*. The crude material was crystallised from hexane to afford colourless oxo-acetal white crystals (**b**; yield = 1.820 g, 72.02%, m.p.: 71 ºC). The data from the physical characterisation of the obtained compound correlates with that of the spiro[1,3-dioxolane-2,8'-pentacyclo[5.4.0.0^{2,6}.0^{3,10}.0^{5,9}]undecan]-11'-one described by Dekker *et al*. (1979).[75]

Synthesis of *N*-benzyl-5-oxahexacyclo[5.4.1.$0^{2,6}$.$0^{3,10}$.$0^{4,8}$.$0^{9,12}$]dodecan-4-amine (NGP1-01)

Pentacyclo[5.4.0.$0^{2,6}$.$0^{3,10}$.$0^{5,9}$]undecane-8,11-dione (**a**, 2.012 g, 11.55 mmol) and benzylamine (1.238 g, 11.55 mmol) were dissolved in EtOH (20 ml) and transferred to a sealed microwave vessel (35 ml capacity). The mixture was placed in a CEM Discover_SP microwave reactor and irradiated for 2 h at 100 W, 80 °C and 100 psi. The mixture was removed from the microwave reactor and $NaBH_4$ (0.870 g, 23.10 mmol) was added portionwise in excess. This mixture was stirred at room temperature for 8 h, after which the solvents were removed *in vacuo*. The residue was suspended in water (20 ml) and extracted with DCM (3 x 20 ml). The combined organic fractions were washed with water (2 x 20 mL), dried (anhydrous $MgSO_4$), filtered and evaporated *in vacuo* to yield a light-yellow oil. Crystallisation from ethyl acetate rendered the final product as a colourless microcrystalline solid (NGP1-01; yield = 1.908 g, 62.26%, m.p.: 86 ºC). The physical characteristics of this compound were the same as those described in the literature.[50,51]

Synthesis of 5-oxahexacyclo[5.4.1.$0^{2,6}$.$0^{3,10}$.$0^{4,8}$.$0^{9,12}$]dodecan-4-amine (c)

A solution of NGP1-01 (3.501 g, 13.19 mmol) in ethanol (50 ml) was prepared in a pressure tube along with a stirring bar. To this solution, 10% Pd/C (0.659 g; calculated as 50 mg per mmol of compound) was added. Special care was taken to make sure that Pd/C is added in small amounts while opening the pressure reactor for as little time as possible considering the pyrophoric nature of dry Pd/C. After the addition of Pd/C the pressure tube was sealed properly and attached to the hydrogen supply. Hydrogen was flushed through the sealed pressure reactor six times before filling it with hydrogen gas at 206 kPa pressure. The pressure tube was stirred for 14 h maintaining the internal temperature of the reaction mixture at 50 °C. Upon reaction completion, the mixture was filtered under vacuum through a sintered glass funnel. Residual Pd/C waste was transferred to a labelled container which contained water. The filtrate was concentrated *in vacuo* and 20 ml of saturated $NaHCO_3$ was added. Resulting reaction mixture was extracted with DCM (3 x 15 ml), dried (anhydrous $MgSO_4$) and filtered to get a clear organic layer. The DCM was evaporated *in vacuo* to get a white solid. Pure mono amine cage product (**c**; yield = 0.739 g, 31.99%, m.p.: 166 – 168 ºC**)** was obtained by crystallisation using DCM/hexane (1:1). The physical characteristics of this compound were the same as those described in the literature.[51]

Synthesis of 4-[({spiro[1,3-dioxolane-2,8'-pentacyclo[5.4.0.0^{2,6}.0^{3,10}.0^{5,9}]undecan]-11'-ylidene}amino)methyl]aniline (1)

A mixture of **b** (1.0 g; 4.58 mmol), 4-amino benzylamine (0.559 g; 4.58 mmol; 1.0 equiv.) was prepared in ethanol (30 ml). The mixture was reacted under microwave conditions of 80 W and 150 psi at 100 °C for 30 minutes. The reaction mixture was concentrated *in vacuo* and 30 ml of water was added followed by extraction with DCM (3 x 15 ml). The organic extracts were washed sequentially with water (25 mL) and brine (25 mL). The organic fraction was dried over anhydrous $MgSO_4$, filtered and concentrated *in vacuo*. The resultant crude mixture was purified using a versa flash silica-gel column with ethanol/ethyl acetate (1:1) as eluent, to give a brown wax (**1**; yield = 0.969 g, 65.59%).

$C_{20}H_{22}N_2O_2$; MW, 322.40 g/mol; **mp:** wax; **IR (ATR)** V_{max}: 3351, 2969, 2864, 1604, 1516, 1336, 1088, 823 cm^{-1}; **HR-ESI [M+H]$^+$**: calc. 323.1760, exp. 323.1765; **^{1}H NMR** (400 MHz, $CDCl_3$) δ_H: 7.26 - 7.08 (m, 2H), 6.65 - 6.62 (m, 2H), 4.46 - 4.34 (m, 2H), 3.93 - 3.73 (m, 4H), 2.81 – 2.39 (m, 8H), 1.82:1.51 (AB-q, 2H, J = 10.4 Hz); **^{13}C NMR** (100 MHz, $CDCl_3$) δ_C: 129.1, 115.1, 65.5, 63.8, 56.6, 53.1, 51.9, 50.5, 45.4, 43.8, 42.7, 41.5, 39.4, 38.7, 38.0, 37.4, 36.3, 32.1.

Synthesis of 1-[4-(aminomethyl)phenyl]-N-{spiro[1,3-dioxolane-2,8'-pentacyclo[5.4.0.0^{2,6}.0^{3,10}.0^{5,9}]undecan]-11'-ylidene}methanamine (2) and *N*-{spiro[1,3-dioxolane-2,8'-pentacyclo[5.4.0.0^{2,6}.0^{3,10}.0^{5,9}]undecan]-11'-ylidene}-1-{4-[({spiro[1,3-dioxolane-2,8'-pentacyclo[5.4.0.0^{2,6}.0^{3,10}.0^{5,9}]undecan]-11'-ylidene}amino)methyl]phenyl}methanamine (3)

A 10 ml ethanol solution of **b** (2.001 g; 9.17 mmol) was added drop-wise to a 20 ml ethanol solution of *p*-xylylenediamine (6.240 g; 45.81 mmol; 5.0 equiv.) on ice. After complete addition of **b**, the mixture was stirred at room temperature for 1 hour then reacted under microwave conditions of 60 W and 80 psi at 100 °C for 3 hours. Upon completion, the reaction mixture was concentrated *in vacuo* and 30 ml of water was added, followed by extraction with DCM (3 x 15 ml). The organic extracts were washed sequentially with water (25 mL) and brine (25 mL). The organic fraction was dried over anhydrous $MgSO_4$ then filtered and concentrated *in vacuo*. The resultant crude mixture was purified by gradient column chromatography using ethanol and ammonia solution/methanol/DCM (1:9:90) as eluents, respectively to give a light-yellow wax (**2**; yield = 0.998 g, 32.42%) and a yellow clear wax (**3**; yield = 0.148 g, 12.91%).

Compound **2**: **$C_{21}H_{24}N_2O_2$; MW,** 336.43 g/mol; **mp:** wax; **IR (ATR)** V_{max}: 3356, 2970, 2864, 1683, 1336, 1105, 811 cm^{-1}; **HR-ESI [M+H]$^+$**: calc. 336.1600, exp. 336.1601; **^{1}H NMR** (400 MHz, $CDCl_3$) δ_H: 7.32 - 7.24 (m, 4H), 4.54 - 4.42 (m, 2H), 3.90 - 3.83 (m, 6H), 2.92 - 2.42 (m, 8H), 1.83:1.53 (AB-q, 2H, *J* = 10.4 Hz); **^{13}C NMR** (100 MHz, $CDCl_3$) δ_C: 128.3, 127.0, 65.5, 63.7, 56.8, 51.2, 50.5, 46.2, 45.3, 45.0, 43.7, 42.7, 41.9, 40.7, 40.6, 39.4, 38.0, 37.3, 32.1.

Compound **3**: **$C_{34}H_{36}N_2O_4$; MW,** 536.66 g/mol; **mp:** wax; **IR (ATR)** V_{max}: 2971, 2864, 1683, 1337, 1104, 730 cm^{-1}; **HR-ESI [M+H]$^+$**: calc. 537.2753, exp. 537.2756; **^{1}H NMR** (400 MHz, $CDCl_3$) δ_H: 7.27 - 7.24 (m, 4H), 4.56 - 4.43 (m, 4H), 3.95 - 3.83 (m, 8H), 2.92 - 2.40 (m, 16H), 1.83:1.53 (AB-q, 4H, *J* = 10.4 Hz); **^{13}C NMR** (100 MHz, $CDCl_3$) δ_C: 138.3, 127.9, 65.5, 63.7, 56.9, 51.2, 50.7, 45.3, 45.0, 43.7, 42.7, 41.9, 40.8, 39.4, 38.7, 37.7, 32.1.

Synthesis of *N*-{[4-(aminomethyl)phenyl]methyl}spiro[1,3-dioxolane-2,8'-pentacyclo[5.4.0.0^{2,6}.0^{3,10}.0^{5,9}]undecan]-11'-amine (4)

To a 15 ml ethanol solution of compound **2** (0.050 g; 0.149 mmol), $NaBH_4$ (0.0112 g; 0.298 mmol 2.0 equiv.) was added. The reaction mixture was stirred at room temperature for 8 hours. Upon reaction completion, the crude mixture was concentrated *in vacuo* and 30 ml of water was added, followed by extraction with DCM (3 x 15 ml). The collected organic extract was washed sequentially with water (25 ml) and brine (25 ml). The organic fraction was dried over anhydrous $MgSO_4$ then filtered and concentrated *in vacuo* without further purification, to yield a yellow wax (**4**; yield = 0.035 g, 69.40%).

$C_{21}H_{26}N_2O_2$; MW, 338.44 g/mol; **mp:** wax; **IR (ATR)** V_{max}: 3353, 2956, 2862, 1473, 1344, 1097, 816 cm^{-1}; **HR-ESI [M+H]$^+$**: calc. 339.2073, exp. 339.2074; **^{1}H NMR** (400 MHz, $CDCl_3$) δ_H: 7.31 (d, 2H, *J* = 8.0 Hz), 7.24 (d, 2H, *J* = 8.0 Hz), 3.95 - 3.92 (m, 2H), 3.87 - 3.78 (m, 4H), 3.76 (d, 2H, *J* = 3.2 Hz), 2.70 (t, 1H, *J* = 2.8 Hz,), 2.56 - 2.14 (m, 8H), 1.62:1.14 (AB-q, 2H, *J* = 10.4 Hz); **^{13}C NMR** (100 MHz, $CDCl_3$) δ_C: 141.8, 138.8, 128.4, 127.1, 115.6, 65.7, 62.5, 59.9, 52.2, 46.6, 46.2, 45.4, 44.9, 44.3, 39.8, 36.6, 34.53, 30.9, 22.8.

Synthesis of 1-(4-{[(prop-2-yn-1-yl)amino]methyl}phenyl)-*N*-{spiro[1,3-dioxolane-2,8'-pentacyclo[5.4.0.0^{2,6}.0^{3,10}.0^{5,9}]undecan]-11'-ylidene}methanamine (5)

Propargyl chloride (0.179 g; 2.399 mmol) was dissolved in 5 ml acetonitrile and added drop-wise to a 15 ml acetonitrile mixture of compound **2** (0.807 g; 2.399 mmol; 1.0 equiv.) and potassium carbonate (0.398 g; 2.878 mmol; 1.2 equiv.). The mixture was refluxed at 60 °C

for 4 hours. Upon reaction completion, the crude mixture was concentrated *in vacuo* to remove acetonitrile and 30 ml of water was added, followed by extraction with DCM (3 x 15 ml). The collected organic fraction was washed sequentially with water (25 ml) and brine (25 ml). The organic fraction was dried over anhydrous $MgSO_4$ then filtered and concentrated *in vacuo*. The resultant crude mixture was purified by gradient column chromatography with DCM/ethyl acetate/petroleum ether (1:1:1) and ammonia solution/methanol/DCM (1:9:90) as eluents respectively, yielding a brown oil (**5**; yield – 0.192 g; 21.37%).

$C_{24}H_{26}N_2O_2$; MW, 374.48 g/mol; **mp:** oil; **IR (ATR)** V_{max}: 3274, 2973, 1743, 1681, 1337, 1105, 934 cm^{-1}; **HR-ESI [M+H]$^+$**: calc. 375.2073, exp. 375.2074; **^{1}H NMR** (400 MHz, $CDCl_3$): 7.27 - 7.24 (m, 4H), 4.54 - 4.38 (m, 2H), 3.87 - 3.77 (m, 6H), 3.38 (d, 2H, *J* = 2.4 Hz), 2.79 - 2.35 (m, 8H), 2.22 (t, 1H, *J* = 6 Hz) 1.84:1.47 (AB-q, 2H, *J* = 10.4 Hz); **^{13}C NMR** (100 MHz, $CDCl_3$) δ_C: 139.2, 137.4, 128.4, 128.2, 114.9, 113.9, 82.0, 71.5, 65.7, 64.5, 63.82, 56.9, 53.0, 50.7, 45.8, 42.9, 42.3, 41.5, 39.4, 38.7, 36.3, 32.1.

Synthesis of *N*-[(4-{[(prop-2-yn-1-yl)amino]methyl}phenyl)methyl]spiro[1,3-dioxolane-2,8'-pentacyclo[5.4.0.0^{2,6}.0^{3,10}.0^{5,9}]undecan]-11'-amine (6)

To a 10 ml ethanol solution of compound **5** (0.065 g; 0.174 mmol), $NaBH_4$ (0.0131 g; 0.348 mmol 2.0 equiv.) was added. The reaction mixture was stirred at room temperature for 8 hours. Upon complete reduction, the crude mixture was concentrated *in vacuo* and 20 ml of water was added, followed by extraction with DCM (3 x 15 ml). The collected organic extract was washed sequentially with water (20 ml) and brine (20 ml). The organic fraction was dried over anhydrous $MgSO_4$ then filtered and concentrated *in vacuo* to yield a light-yellow oil (**6**; yield = 0.047 g, 72.35%).

$C_{24}H_{28}N_2O_2$; MW, 376.49 g/mol; **mp:** oil; **IR (ATR)** V_{max}: 3288, 2960, 2888, 2360, 1454, 1345, 1098, 802 cm^{-1}; **HR-ESI [M+H]$^+$**: calc. 377.2229, exp. 377.2227; **^{1}H NMR** (400 MHz, $CDCl_3$) δ_H: 7.34 - 7.31 (m, 4H), 3.96 - 3.78 (m, 6H), 3.66 (m, 2H), 3.39 (d, 2H, *J* = 2.4 Hz), 2.92 (t, 1H, *J* = 3.6 Hz), 2.67 - 2.25 (m, 8H), 2.15 (t, 1H, *J* = 6.0 Hz), 1.66:1.18 (AB-q, 2H, *J* = 10.4 Hz); **^{13}C NMR** (100 MHz, $CDCl_3$) δ_C: 136.9, 129.4, 128.7, 127.2, 115.5, 78.7, 73.2, 72.3, 65.7, 62.74, 59.2, 56.7, 51.7, 46.5, 45.3, 44.8, 43.9, 41.7, 39.8, 36.1, 34.5, 29.6.

Synthesis of 5-[(4-aminophenyl)methyl]-5-azahexacyclo[5.4.1.$0^{2,6}$.$0^{3,10}$.$0^{4,8}$.$0^{9,12}$]dodecan-4-ol (7)

Compound **1** (0.450 g; 1.396 mmol) was dissolved in ethanol (20 ml) and a spatula point (± 0.15 g) of sodium borohydride was added to the solution. The mixture was allowed to stir at room temperature for 8 hours. The reaction was concentrated *in vacuo,* distilled water (20 ml) was added, followed by extraction with DCM (3 x 15 ml). The combined organic layers were washed with brine (30 ml) then dried (anhydrous $MgSO_4$) and filtered. The collected filtrate was concentrated *in vacuo*. To the crude residue, acetone (10 ml) and aqueous 4M HCl (10 ml) was added. This reaction mixture was stirred at room temperature for 12 h. Water (150 ml) was added to the reaction solution and basified to pH 14 with 1 M NaOH. This was followed by extraction with DCM (3 x 25 ml) and the combined organic layers were dried (anhydrous $MgSO_4$) and filtered. The filtrate was concentrated *in vacuo* to give the crude residue. The resultant crude residue was purified by column chromatography, using EtOAc/DCM (7:3) as eluent, to yield a yellow amorphous powder (**7**; yield = 0.167 g, 42.75%).

$C_{18}H_{20}N_2O$; MW, 280.36 g/mol; **mp:** 120 °C; **IR (ATR)** V_{max}: 3368, 2955, 2861, 2827, 1615, 1518, 1325, 1107, 809 cm^{-1}; **HR-ESI $[M+H]^+$**: calc. 281.1654, exp. 281.1655; **^{1}H NMR** (400 MHz, $CDCl_3$) δ_H: 7.18 (d, 2H, *J* = 8.4 Hz), 6.66 (d, 2H, *J* = 8.4 Hz), 3.85 (d, 2H, *J* = 13.2 Hz), 3.37 (t, 1H, *J* = 5.2 Hz), 2.78 - 2.60 (m, 8H), 1.86:1.53 (AB-q, 2H, *J* = 10.4 Hz); **^{13}C NMR** (100 MHz, $CDCl_3$) δ_C: 145.8, 129.4, 128.5, 115.1, 72.1, 58.3, 52.3, 45.9, 45.1, 44.4, 43.0, 40.8, 39.9, 37.4, 35.2, 34.2.

Synthesis of 5-{[4-(aminomethyl)phenyl]methyl}-5-azahexacyclo[5.4.1.$0^{2,6}$.$0^{3,10}$.$0^{4,8}$.$0^{9,12}$]dodecan-4-ol (8)

Compound **4** (0.15 g; 0.443 mmol) was dissolved in acetone (15 ml) and aqueous 4M HCl (15 ml) was added. This reaction mixture was stirred at room temperature for 12 h. Water (20 ml) was added to the reaction solution and basified to pH 14 with 1 M NaOH. This was followed by extraction with DCM (3 x 25 ml) and the combined organic layers were dried (anhydrous $MgSO_4$) and filtered. The filtrate was concentrated *in vacuo* to give the crude residue. The resultant crude residue was purified by column chromatography, using ammonia solution/methanol/DCM (1:9:90) as eluent, yielding an off-white amorphous powder (**8**; yield = 0.102 g; 78.26%).

$C_{19}H_{22}N_2O$; MW, 294.39 g/mol; **mp:** 145 °C; **IR (ATR)** V_{max}: 3308, 2961, 2863, 2783, 1327, 1109, 767 cm^{-1}; **HR-ESI $[M+H]^+$**: calc. 295.1810, exp. 295.1812; **^{1}H NMR** (400 MHz, $CDCl_3$) δ_H: 7.29 - 7.25 (m, 4H), 3.84 (m, 3H), 3.43 (d, 1H), 3.29 (t, 1H, *J* = 5.2 Hz), 2.84 - 2.57 (m, 8H), 1.83:1.50 (AB-q, 2H, *J* = 10.4 Hz); **^{13}C NMR** (100 MHz, $CDCl_3$) δ_C: 142.0, 140.4, 137.6, 128.9, 128.2, 127.1, 106.4, 64.2, 51.4, 51.0, 46.2, 45.6, 44.3, 42.8, 42.1, 41.8, 41.0.

Synthesis of 5-[(4-{[(prop-2-yn-1-yl)amino]methyl}phenyl)methyl]-5-azahexacyclo[5.4.1.0^{2,6}.0^{3,10}.0^{4,8}.0^{9,12}]dodecan-4-ol (9)

Propargyl chloride (0.070 g; 0.942 mmol) was dissolved in 5 ml acetonitrile and added drop-wise to a 15 ml acetonitrile mixture of compound **8** (0.277 g; 0.942 mmol; 1.0 equiv.) and potassium carbonate (0.156 g; 1.131 mmol; 1.2 equiv.). The mixture was reacted under microwave conditions of 60 W, in a closed vessel at 60 °C for 2.5 hours. Upon reaction completion, the crude mixture was concentrated *in vacuo* to remove acetonitrile and 30 ml of water was added, followed by extraction with DCM (3 x 15 ml). The collected organic fraction was washed sequentially with water (25 ml) and brine (25 ml). The organic fraction was dried over anhydrous $MgSO_4$ then filtered and concentrated *in vacuo*. The resultant crude mixture was purified by column chromatography with ammonia solution/methanol/DCM (1:9:90) as eluent, yielding a yellow-orange wax (**9**; yield = 0.057 g, 18.07%).

$C_{22}H_{24}N_2O$; MW, 332.43 g/mol; **mp:** wax; **IR (ATR)** V_{max}: 3298, 2963, 2863, 2829, 1727, 1323, 1107, 732 cm^{-1}; **HR-ESI $[M+H]^+$**: calc. 333.1967, exp. 333.1967; **^{1}H NMR** (400 MHz, $CDCl_3$) δ_H: 7.32 (m, 4H), 3.86 (m, 3H), 3.65 (s, 1H), 3.41 (t, 1H, *J* = 5.2 Hz), 3.31 (m, 2H), 2.63 - 2.38 (m, 8H), 1.80:1.48 (AB-q, 2H, *J* = 10.4 Hz); **^{13}C NMR** (100 MHz, $CDCl_3$) δ_C: 137.9, 136.6, 129.2, 128.7, 128.4, 127.1, 82.0, 71.5, 62.4, 51.9, 51.3, 50.8, 49.8, 46.2, 45.5, 42.9, 41.6, 41.3, 40.7, 37.2.

Synthesis of *N*-[(4-aminophenyl)methyl]-5-oxahexacyclo[5.4.1.0^{2,6}.0^{3,10}.0^{4,8}.0^{9,12}]dodecan-4-amine (10)

The diketone cage (**a**: 1.0 g; 5.74 mmol) was dissolved in ethanol (25 ml) and cooled down to 0 °C while stirring on an external ice bath. 4-amino benzylamine (0.7 g; 5.74 mmol) dissolved in 5 ml ethanol was added drop-wise with continuous stirring. The reaction mixture was stirred for 30 mins on an ice bath after which it was reacted under microwave conditions

of 100 W, 100 psi, at 80 °C for 2 hours. $NaBH_4$ (± 0.30g) was added to the reaction and stirred at room temperature for 8 hours. The reaction mixture was concentrated in vacuo to remove the ethanol. The resulting residue was dissolved in DCM (25 ml) then washed with brine (50 ml). The collected DCM fraction was dried using anhydrous $MgSO_4$, filtered and concentrated *in vacuo*. The resultant crude mixture was purified using column chromatography with ethanol/ethyl acetate (1:1) as eluent, yielding a light yellow amorphous powder (**10**; yield = 0.518 g, 32.21%).

$C_{18}H_{20}N_2O$; MW, 280.36 g/mol; **mp:** 116 °C; **IR (ATR)** V_{max}: 3251, 2969, 2859, 1615, 1513, 1357, 1015, 825 cm^{-1}; **HR-ESI [M+H]$^+$**: calc. 281.1654, exp. 281.1653; **^{1}H NMR** (400 MHz, $CDCl_3$) δ_H: 7.12 (d, 2H, *J* = 8.4 Hz), 6.83 (d, 2H, *J* = 8.4 Hz), 4.72 (t, 1H, *J* = 5.2 Hz), 3.74 (s, 2H), 2.85-2.50 (m, 8H), 1.90:1.58 (AB-q, 2H, *J* = 10.4 Hz); **^{13}C NMR** (100 MHz, $CDCl_3$) δ_C: 143.3, 134.2, 127.7, 116.7, 105.6, 82.7, 55.9, 54.5, 46.1, 44.9, 44.5, 44.4, 43.3, 42.9, 41.6, 41.5.

Synthesis of *N*-{[4-(chloromethyl)phenyl]methyl}-5-oxahexacyclo[5.4.1.$0^{2,6}$.$0^{3,10}$.$0^{4,8}$.$0^{9,12}$]dodecan-4-amine (11)

A 20 ml acetonitrile solution of **c** (0.50 g; 2.85 mmol) was added drop-wise to a 60 ml acetonitrile solution of *p*-xylylene dichloride (2.498 g; 14.27 mmol; 5.0 equiv.) and potassium carbonate (0.473 g; 3.42 mmol; 1.2 equiv.) on ice. After complete addition of **c**, the mixture was stirred at room temperature for 1 hour then reacted under microwave conditions of 150 W and 20 psi at 70 °C for 1 hour. Upon completion, the reaction mixture was concentrated *in vacuo* and 40 ml of water was added, followed by extraction with DCM (3 x 25 ml). The organic extracts were washed sequentially with water (25 mL) and brine (25 mL). The organic fraction was dried over anhydrous $MgSO_4$ then filtered and concentrated *in vacuo*. The resultant crude mixture was purified using a flash silica-gel column with petroleum ether/ethyl acetate/DCM (1:1:1) as eluent, to give a yellowish oil (**11**; yield = 0.172 g, 19.19%).

$C_{19}H_{20}ClNO$; MW, 313.82 g/mol; **mp:** oil; **IR (ATR)** V_{max}: 3321, 3208, 2960, 2860, 1513, 1444, 1265,1012, 821 cm^{-1}; **HR-ESI [M+H]$^+$**: calc. 314.1312, exp. 314.1315; **^{1}H NMR** (400 MHz, $CDCl_3$) δ_H: 7.35 - 7.32 (m, 4H), 4.65 (t, 1H, *J* = 5.2 Hz), 4.67 (s, 2H), 4.02 (s, 2H), 2.86 - 2.54 (m, 8H), 1.91:1.56 (AB-q, 2H, *J* = 10.4 Hz); **^{13}C NMR** (100 MHz, $CDCl_3$) δ_C: 137.6, 128.9, 128.7, 128.3, 127.9, 127.8, 55.0, 46.1, 46.0, 45.7, 45.6, 44.7, 43.4, 43.0, 41.5, 41.2, 29.6.

Synthesis of *N*-[(4-{[(prop-2-yn-1-yl)amino]methyl}phenyl)methyl]-5-oxahexacyclo[5.4.1.$0^{2,6}$.$0^{3,10}$.$0^{4,8}$.$0^{9,12}$]dodecan-4-amine (12)

A mixture of compound **11** (0.123 g; 0.392 mmol), propargylamine (0.022 g; 0.392 mmol; 1.0 equiv.) and potassium carbonate (0.065 g; 0.47 mmol; 1.2 equiv.) was prepared in 30 ml acetonitrile. The mixture was stirred at room temperature for 1 hour then reacted under microwave conditions of 150 W and 20 psi at 70 °C for 1 hour. Upon completion, the reaction mixture was concentrated *in vacuo* and 40 ml of water was added, followed by extraction with DCM (3 x 25 ml). The organic extracts were washed sequentially with water (25 mL) and brine (25 mL). The organic fraction was dried over anhydrous $MgSO_4$ then filtered and concentrated *in vacuo*. The resultant crude mixture was purified using gradient column chromatography with DCM/ethyl acetate/petroleum ether (1:1:1) and ethyl acetate as eluents respectively, yielding a yellow oil (**12**; yield = 0.028 g; 21.57%).

$C_{22}H_{24}N_2O$; MW, 332.44 g/mol; **mp:** oil; **IR (ATR)** V_{max}: 3299, 2959, 2925, 2857, 1734, 1353, 1014, 858 cm^{-1}; **HR-ESI [M+H]$^+$**: calc. 333.1967, exp. 333.1972; **^{1}H NMR** (400 MHz, $CDCl_3$) δ_H: 7.33 - 7.27 (m, 4H), 4.66 (t, 1H, *J* = 5.2 Hz), 3.98 (d, 2H, *J* = 4.8 Hz), 3.86 (s, 2H), 3.41 (d, 2H, *J* = 2.4 Hz), 2.84 - 2.54 (m, 8H), 2.25 (t, 1H, *J* = 2.4 Hz), 1.91:1.55 (AB-q, 2H, *J* = 10.4 Hz); **^{13}C NMR** (100 MHz, $CDCl_3$) δ_C: 139.7, 137.9, 128.5, 128.0, 109.6, 82.5, 82.0, 71.5, 55.2, 54.8, 51.9, 47.5, 44.8, 44.5, 43.7, 42.0, 41.56, 38.7, 37.2, 29.6.

4.4.2. Biological evaluation

Cell line and culture conditions

The human neuroblastoma cell line SH-SY5Y was generously donated by our collaborator at the Division of Molecular Biology and Human Biology, Stellenbosch University, Tygerberg, Cape Town. Cells were cultured in monolayer using Dulbeco Modified Eagles Medium (DMEM, Gibco, Life Technologies Ltd) supplemented with 10% foetal bovine serum (FBS, Gibco, Life Technologies Ltd.) and 1% 100 U/mL penicillin and 100 µg/mL streptomycin (Lonza Group Ltd., Base Switzerland). Cells were grown at 37 °C, in a humidified atmosphere consisting of 5% CO_2 and 95% air. Media was replaced every two to three days and cells were sub-cultured by splitting with trypsin (Lonza Group Ltd., Base Switzerland).

SH-SY5Y cytotoxicity assay

The 3-[4,5-dimethylthiazol-2-yl]-2,5-diphenyl tetrazolium bromide (MTT) is a yellow tetrazolium salt that is reduced to purple formazan in the presence of living cells. This assay which measures cell metabolic activity was used to determine cytotoxicity as described by Mosmann, (1983).[55] Briefly, SH-SY5Y cells were plated in flat bottom 96 well plates in growth medium as stated above at a density of 7,500 cells/well. Cells were allowed to adhere to the plate surface for 24 hours and used media were replenished with fresh media containing test compounds at 10 µM, 50 µM and 100 µM. Vehicle control cells were treated with dimethyl sulfoxide (DMSO, solvent for dissolving test compounds) at a concentration similar to that contained in the highest concentration of test compounds. After 48 hours, 10 µL of MTT solution (5 mg/mL) was added to each well and incubated for 4 hours and the purple formazan formed was solubilized with 100 µL DMSO and plates were read spectrophotometrically to determine absorbance at 570 nm using a BMG Labtech Omega® POLARStar multimodal plate reader. Percentage cell viability was calculated relative to control using the formula below:

$$\% \text{ Cell Viability} = \frac{\text{Absorbance of treated well}}{\text{Absorbance of Untreated well}} \text{ X } 100$$

SH-SY5Y neuroprotection assay

1-Methyl-4-phenyl pyridinium (MPP^+), the active metabolite of 1-methyl-4-phenyl-1,2,6-tetrahydropyridine (MPTP), is highly toxic to dopaminergic neurons and has been widely used to induce Parkinson-like syndromes in various *in vitro* and *in vivo* models associated with PD.[56,57] The ability of the novel compounds to restore cell viability to MPP^+ stressed SH-SY5Y cells was thus evaluated. In this assay, SH-SY5Y cells were seeded onto a 96-well plate at a density of 7,500 cells/well and treated with 1000 µM MPP^+ for approximately 48 hours to induce cytotoxicity. Different concentrations (1 µM, 5 µM, 10 µM) of test compounds were administrated two hours prior to MPP^+ treatment. Afterwards, cell viability was measured by MTT colorimetric assay and performed as stated in the cytotoxicity assay.

To determine the data's statistical significance, a Turkey's multiple comparison test was conducted on all experimental replicates using GraphPad Prism®.

VGCC and NMDAr modulation assays

For these experiments, SH-SY5Y human neuroblastoma cells were sub-cultured at a seeding density of 1×10^5 cells per well in 96-well black plates and incubated at 37 °C for 24 hours to allow for cell adherence. On the day of the experiment, the DMEM solution was replaced with a 5 µM Fura-2/AM-DMEM solution and incubated for 1 h at 37 °C. The Fura-2/AM loaded DMEM was removed from each well and the extracellular Fura-2/AM was washed twice with Ca^{2+}-free Krebs–Hepes solution. 98 µL of calcium containing buffer was added to each well and kept at 37 °C for 30 min before beginning the experiment, to allow for complete dye de-esterification. 2 µL of test compound, dissolved in DMSO, was added to each well (10 µM final concentration). Two positive controls were included in the VGCC assay; nimodipine, a commercially available dihydropyridine *L*-type calcium channel blocker and the prototype polycyclic amine compound NGP1- 01. Two positive controls were also included in the NMDAr assay; MK-801, a commercially available potent high affinity NMDAr channel blocker and NGP1-01. The 96 well plate was allowed to incubate at 37 °C in a Biotek® fluorescent microplate reader for 10 mins with shaking every minute. A 10 µL solution of a 770 mM KCl buffer or 0.55 mM NMDA/Glycine solution, in the VGCC and NMDA assay respectively, was used to stimulate the opening of the respective calcium channels and allow for calcium entry. Calcium influx was monitored over a 35 s period, at wavelengths of excitation and emission of 340 and 380 nm, respectively and the resting fluorescence measured at 510 nm. Percentage inhibition values were calculated relative to the positive controls nimodipine and MK-801 for the VGCC and NMDAr assays, respectively.

To determine the data's statistical significance, a One-way ANOVA; multiple comparison test was conducted on all experimental replicates using GraphPad Prism®.

MAO-A and MAO-B assays

The MAO assays were conducted using a similar procedure as previously described.[69] Recombinant human MAO-A and -B (5 mg/mL) were obtained from Sigma–Aldrich and were pre-aliquoted and stored at -80 °C. All enzymatic reactions were carried out to a final volume of 250 µL in potassium phosphate buffer (100 mM, pH 7.4, made isotonic with NaCl) and contained kynuramine as substrate, MAO-A or MAO-B (0.0075 mg/mL) and various concentrations of the test inhibitor (0.01 – 100 µM). The final concentration of kynuramine in the reactions was 45 µM and 30 µM for MAO-A and -B, respectively. Stock solutions of the test inhibitors were prepared in DMSO and added to the reactions to yield a final concentration of 2% (v/v) DMSO. The reactions were incubated for 20 min at 37 °C and

were terminated with the addition of 200 µL NaOH (2 N). Finally, 100 µL from each eppendorf vial was added to individual black plate wells. The fluorescence of the MAO generated 4-hydroxyquinoline in the supernatant fractions were measured using a Biotek® fluorescent microplate reader at an excitation wavelength of 310 nm and an emission wavelength of 400 nm. IC_{50} values were calculated as concentration of the compound that produced 50% enzyme activity inhibition, using the Graph Pad Prism 6 software (San Diego, CA, USA).

Time-dependent inhibition studies

To investigate the reversibility of the observed MAO enzyme inhibition, time-dependent inhibition studies were carried out on the active inhibitors. Briefly, recombinant human MAO-A or human MAO-B (0.0075 mg/mL) enzymes were preincubated with inhibitor for periods of 0, 15, 30, 60 min at 37 °C. The concentration of inhibitor in these incubations was approximately twofold the measured IC_{50} values for the inhibition of the respective MAO enzymes. Potassium phosphate buffer (100 mM, pH 7.4, made isotonic with NaCl) was used as the incubation medium. A final concentration of 45 µM kynuramine for MAO-A and 30 µM kynuramine for MAO-B were then added to the preincubated enzyme preparations and the resulting 250 µL reactions were incubated at 37 °C for 15 min. The reactions were terminated with the addition of 200 µL NaOH (2 N) and a volume of 600 µL distilled water was added to each reaction. The fluorescence of the MAO generated 4-hydroxyquinoline in the supernatant fractions were measured using a Biotek fluorescent microplate reader at an excitation wavelength of 310 nm and an emission wavelength of 400 nm. Time dependent graphs were plotted against the relative fluorescent unit readings (RFU).

4.4.3. Molecular modelling

Computer-assisted docking were carried out using the CHARMm force field and the human MAO-B crystal structure (PDB ID: 2V5Z),[44] which were recovered from the Brookhaven Protein Database (www.rcsb.org/pdb). Docking simulation was performed on the test compounds using Molecular Operating Environment (MOE)[45] with the following protocol. (1) Enzyme structures were checked for missing atoms, bonds and contacts. (2) Hydrogen atoms were added to the enzyme structure. Bound ligands were manually deleted and the ordered water molecules were retained (3) The ligand molecules were constructed using the builder module and were energy minimized. (4) The active site was generated using the

MOE-Alpha Site Finder. (5) Ligands were docked within the MAO-B active sites using MOEDock with simulated annealing utilised as the search protocol and CHARMm molecular mechanics force field. (6) The lowest energy conformation of the docked ligand complex was selected and subjected to a further energy minimization using CHARMm force field with all possible bond rotations and chiralities explored. To determine the accuracy of this docking protocol, the co-crystallised ligand, safinamide (PDB ID: 2V5Z), was re-docked into the MAO-B active site. This procedure was repeated three times and the best ranked solutions of safinamide exhibited RMSD values of 1.34 Å from the position of the co-crystallised ligand. In general, RMSD values smaller than 2.0 Å indicate that the docking protocol is capable of accurately predicting the binding orientation of the co-crystallised ligand.[76,77] These protocols were thus deemed to be suitable for the docking of inhibitors into the active site model of MAO-B.

Acknowledgements

We are grateful to the University of the Western Cape and the National Research Foundation of South Africa for financial support. Prof E. Antunes at the NMR facility of the University of the Western Cape is also acknowledged.

Author Contributions

F.T.Z. and J.J. conceived of the presented idea. F.T.Z. designed, synthesized and characterized the compounds, performed all biological and in silico evaluations, processed the experimental data, performed the analysis and drafted the manuscript. F.T.Z., S.I.O., A.B.E. and O.E.E. performed cytotoxicity and neuroprotection assays. S.F.M. and J.J. supervised the findings of this work. All authors discussed the results and contributed to the final manuscript.

Supplementary material

Supplementary data to this article including additional molecular modelling data and NMR spectra can be found in the supplementary data section of this thesis.

References

[1] Dauer, W.; Przedborski, S. Parkinson's disease: mechanisms and models. *Neuron.* 39(6), 889-909 (2003).

[2] Baker, G.B.; Reynolds, G.P.; Biogenic amines and their metabolites in Alzheimer's disease: noradrenaline, 5-hydroxytryptamine and 5-hydroxyindole-3-acetic acid are depleted in the hippocampus but not in substantia innominata. *Neurosci. Lett.* 100(1–3), 335–339 (1989).

[3] Cross, A.J. Serotonin in Alzheimer type dementia and other dementing illnesses. *Ann. NY Acad. Sci.* 600, 405–415 (1990).

[4] Arundine, M.; Tymianski, M. Molecular mechanisms of calcium-dependent neurodegeneration in excitotoxicity. *Cell Calcium.* 34(4-5), 325-37 (2013).

[5] Arundine, M.; Tymianski, M. Molecular mechanisms of glutamate-dependent neurodegeneration in ischemia and traumatic brain injury. *Cell Mol Life Sci.* 61(6), 657-68 (2004).

[6] Nicotra, A.; Pierucci, F., Parvez, H.; Senatori, O. Monoamine oxidase expression during development and aging. *Neurotoxicology*. 25(1–2), 155–165 (2004).

[7] Youdim, M.B.H.; Edmondson, D.; Tipton, K.F. The therapeutic potential of monoamine oxidase inhibitors. *Nat. Rev. Neurosci.* 7(4), 295–309 (2006).

[8] Nicotra, A.; Pierucci, F.; Parvez, H.; Senatori, O. Monoamine oxidase expression during development and aging. *Neurotoxicology*. 25(1-2), 155-65 (2004).

[9] Strydom, B.; Bergh, J.J.; Petzer, J.P. Inhibition of monoamine oxidase by phthalide analogues. *Bioorg Med. Chem. Lett.* 23(5), 1269–1273 (2013).

[10] Youdim, M.B.; Collins, G.G.; Sandler, M.; Bevan Jones, A.B.; Pare, C.M.; Nicholson, W.J. Human brain monoamine oxidase: multiple forms and selective inhibitors. *Nature.* 236(5344), 225-8 (1972).

[11] Green, A.R.; Mitchell, B.D.; Tordoff, A.F.; Youdim, M.B. Evidence for dopamine deamination by both type A and type B monoamine oxidase in rat brain *in vivo* and for the degree of inhibition of enzyme necessary for increased functional activity of dopamine and 5-hydroxytryptamine. *Br. J. Pharmacol.* 60(3), 343–349 (1977).

[12] Zimmer, R. Relationship between tyramine potentiation and monoamine oxidase (MAO) inhibition: comparison between moclobemide and other MAO inhibitors. *Acta Psychiatr Scand Suppl.* 360, 81-3 (1990).

[13] Tipton, K.F. Monoamine oxidase inhibitors and pressor response to dietary amines. *Vopr Med Khim.* 43(6), 494-503 (1997).

[14] O'Carroll, A.M.; Fowler, C.J.; Phillips, J.P.; Tobbia, I.; Tipton, K.F. The deamination of dopamine by human brain monoamine oxidase. Specificity for the two enzyme forms in seven brain regions. *Naunyn Schmiedebergs Arch. Pharmacol.* 322(3), 198–202 (1983).

[15] Chen, J.J.; Swope, D.M.; Dashtipour, K. Comprehensive review of rasagiline, a second-generation monoamine oxidase inhibitor, for the treatment of Parkinson's disease. *Clin. Ther.* 9, 1825-49 (2007).

[16] Edmondson, D.E.; Binda, C.; Mattevi, A. Structural insights into the mechanism of amine oxidation by monoamine oxidases A and B. *Arch. Biochem. Biophys.* 464(2), 269-76 (2007).

[17] Maruyama, W.; Akao, Y.; Carrillo, M.C.; Kitani, K.; Youdium, M.B.H.; Naoi, M. Neuroprotection by propargylamines in Parkinson's disease: suppression of apoptosis and induction of prosurvival genes. *Neurotoxicol. Teratol.* 24(5), 675–682 (2002).

[18] Youdim, M.B.; Weinstock, M. Molecular basis of neuroprotective activities of rasagiline and the anti-Alzheimer drug TV3326 [(N-propargyl-(3R)aminoindan-5-YL)-ethyl methyl carbamate]. *Cell. Mol. Neurobiol.* 21(6), 555–573 (2002).

[19] Zindo, F.T.; Joubert, J.; Malan, S.F. Propargylamine as functional moiety in the design of multifunctional drugs for neurodegenerative disorders: MAO inhibition and beyond. *Future Med. Chem.* 7(5), 609–629 (2015).

[20] Youdim, M.H.B.; Buccafusco, J.J. CNS Targets for multifunctional drugs in the treatment of Alzheimer's and Parkinson's diseases. *J. Neural. Transm.* 112(4), 519-537 (2005).

[21] Bolea, I.; Gella, A.; Unzeta, M. Propargylamine-derived multitarget-directed ligands: fighting Alzheimer's disease with monoamine oxidase inhibitors. *J. Neural. Transm.* 120(6), 893-902 (2013).

[22] Mattson, M.P. Calcium and neurodegeneration. *Aging Cell*. 6(3), 337-50 (2007).

[23] Bezprozvanny, I. Calcium signaling and neurodegenerative diseases. *Trends Mol Med.* 15(3), 89-100 (2009).

[24] Berridge, M.J.; Lipp, P.; Bootman, M.D. The versatility and universality of calcium signaling. *Mol Cell Biol*. 1(1), 11–21 (2000).

[25] Camps, P.; Duque, M.D.; Vázquez, S. *et al.* Synthesis and pharmacological evaluation of several ring-contracted amantadine analogs. *Bioorg. Med. Chem.* 16(23), 9925-9936 (2008).

[26] Zindo, F.T.; Barber, Q.R.; Joubert, J.; Bergh, J.J.; Petzer, J.P.; Malan, S.F. Polycyclic propargylamine and acetylene derivatives as multifunctional neuroprotective agents. *Eur. J. Med. Chem.* 80, 122-134 (2014).

[27] Geldenhuys, W.J.; Malan, S.F.; Murugesan, T.; van der Schyf, C.J.; Bloomquist, J.R. Synthesis and biological evaluation of pentacyclo[5.4.0.02,6.03,10.05,9]undecane derivatives as potential therapeutic agents in Parkinson's disease. *Bioorg. Med. Chem.* 12(7), 1799-1806 (2004).

[28] Binda, C.; Wang, J.; Pisani, L.; Caccia, C.; Carotti, A.; Salvati, P.; Edmondson, D.E.; Mattevi, A. Structures of human monoamine oxidase B complexes with selective noncovalent inhibitors: safinamide and coumarin analogs. *J Med Chem.* 50(23), 5848-52 (2007).

[29] Molecular Operating Environment (MOE), Version 2018.01. http//www. chemcomp.com.

[30] Joubert, J.; Geldenhuys, W.J.; Van der Schyf, C.J. *et al.* Polycyclic cage structures as lipophilic scaffolds for neuroactive drugs. *ChemMedChem* 7(3), 375-84 (2012).

[31] Zah, J.; Terre'Blanche, G.; Erasmus, E.; Malan, S.F. Physicochemical prediction of a brain-blood distribution profile in polycyclic amines. *Bioorg. Med. Chem.* 11(17), 3569-78 (2003).

[32] Cookson, R.C.; Grundwell, E.; Hudec, J. Synthesis of cage-like molecules by irradiation of Diels-Alder adducts. *Chem. Ind. (London)* 1003-1004 (1958).

[33] Dekker, T.G.; Oliver, D.W. Synthesis of (D_3) trishomocuban-4-ol via carbenium ion rearrangement of pentacyclo[5.4.0.0^{2,6}.0^{3,1}0.0^{5,9}]undecan-8-ol. *S. Afr. J. Chem.* 32, 45-48 (1979).

[34] Joubert, J.; Sharma, R.; Onani, M.; Malan, S.F. Microwave-assisted methods for the synthesis of pentacyclo[5.4.0.0^{2,6}.0^{3,1}0.0^{5,9}]undecylamines. *Tetrahedron Lett.* 54, 6923-6927 (2013).

[35] Marchand, A. P.; Arney, B. E.; Dave, P. R.; Satyanarayana, N.; Watson, W. H.; Nagl, A. Transannular cyclizations in the pentacyclo [5.4. 0.0$^{2,\ 6}$.0$^{3,\ 1}$0.0$^{5,\ 9}$] undecane-8, 11-dione system. A reinvestigation. *J. Org. Chem.* 53, 2644-2647 (1988).

[36] Kappe, C.O.; Stadler, A. Microwaves in Organic and Medicinal Chemistry. *Wiley-VCH*. Weinheim, 2005.

[37] Wathey, B.; Tierney, J.; Lidstrom, P.; Westman, J. The impact of microwave-assisted organic chemistry on drug discovery. *Drug Discov. Today.* 7(6), 373-80 (2002).

[38] Sharma, R.; Joubert, J.; Malan, S.F. Synthesis and Biological Evaluations of NO-Donating Oxa- and Aza-Pentacycloundecane Derivatives as Potential Neuroprotective Candidates. *Molecules.* 23(2), 308 (2018).

[39] Mosmann, T. Rapid colorimetric assay for cellular growth and survival: application to proliferation and cytotoxicity assays. *J. Immunol. Methods.* 65(1-2), 55-63 (1983).

[40] Cui, W.; Zhang, Z.; Li, W.; Hu, S.; Mak, S.; Zhang, H.; Han, R.; Yuan, S.; Li, S.; Sa, F.; Xu, D.; Lin, Z.; Zuo, Z.; Rong, J.; Ma, E. D. L.; Choi, T. C.; Lee, S. M. Y.; Han, Y. The anti-cancer agent SU4312 unexpectedly protects against MPP(+)-induced neurotoxicity via selective and direct inhibition of neuronal NOS. *Br. J. Pharmacol.* 168(5), 1201-1214 (2013).

[41] Jantas, D.; Greda, A.; Golda, S.; Korostynski, M.; Grygier, B.; Roman, A.; Pilc, A.; Lason, W. Neuroprotective effects of metabotropic glutamate receptor group II and III activators against MPP(+)-induced cell death in human neuroblastoma SH-SY5Y cells: the impact of cell differentiation state. *Neuropharmacology.* 83, 36-53 (2014).

[42] Pyszko, J.; Strosznajder, J.B. Sphingosine kinase 1 and sphingosine-1-phosphate in oxidative stress evoked by 1-methyl-4-phenylpyridinium (MPP+) in human dopaminergic neuronal cells. *Mol. Neurobiol.* 50(1), 38-48 (2014).

[43] Wang, Y.; Gao, J.; Miao, Y.; Cui, Q. *et al.* Pinocembrin Protects SH-SY5Y Cells Against MPP+-Induced Neurotoxicity Through the Mitochondrial Apoptotic Pathway. *J. Mol. Neurosci.* 53(4), 537-545 (2014).

[44] Tasaki, Y.; Omura, T.; Yamada, T.; Ohkubo, T. *et al.* Meloxicam protects cell damage from 1-methyl-4-phenyl pyridinium toxicity via the phosphatidylinositol 3-kinase/Akt pathway in human dopaminergic neuroblastoma SH-SY5Y cells. *Brain Res.* 1344, 25-33 (2010).

[45] Zhu, G.; Wang, X.; Wu, S.; Li, Q. Involvement of activation of PI3K/Akt pathway in the protective effects of puerarin against MPP+-induced human neuroblastoma SH-SY5Y cell death. *Neurochem. Int.* 60(4), 400-408 (2012).

[46] Young, L.M.; Geldenhuys, W.J.; Domingo, O.C.; Malan, S.F.; Van der Schyf, C.J. Synthesis and Biological Evaluation of Pentacycloundecylamines and Triquinylamines as Voltage-Gated Calcium Channel Blockers. *Arch Pharm (Weinheim).* 349(4), 252-67 (2016).

[47] León, R.; de los Ríos, C.; Marco-Contelles, J. *et al.* New tacrine-dihydropyridine hybrids that inhibit acetylcholinesterase, calcium entry, and exhibit neuroprotection properties. *Bioorg. Med. Chem.* 16(16), 7759-69 (2008).

[48] Cohen, C.J.; McCarthy, R.T. Nimodipine block of calcium channels in rat anterior pituitary cells. *J Physiol.* 387, 195-225 (1987).

[49] Van der Schyf, C.J.; Squier, G.J.; Coetzee, W.A. Characterization of NGP 1-01, an aromatic polycyclic amine, as a calcium antagonist. *Pharmacol. Res.* 18(5), 407-17 (1986).

[50] Wong, E.H.; Kemp, J.A.; Priestley, T.; Knight, A.R.; Woodruff, G.N.; Iversen, L.L. The anticonvulsant MK-801 is a potent N-methyl-D-aspartate antagonist. *Proc Natl Acad Sci U S A.* 83(18), 7104-7108 (1986).

[51] Stern-Bach, Y.; Bettler, B.; Hartley, M.; Sheppard, P.O.; O'Hara, P.J.; Heinemann, S.F. Agonist selectivity of glutamate receptors is specified by two domains structurally related to bacterial amino acid-binding proteins. *Neuron.* 13(6), 1345-57 (1994).

[52] Novaroli, L.; Reist, M.; Favre, E.; Carotti, A.; Catto, M.; Carrupt, P. Human recombinant monoamine oxidase B as reliable and efficient enzyme source for inhibitor screening. *Bioorganic Med. Chem.* 13(22), 6212- 6217 (2005).

[53] Gleiter, C.H; Mühlbauer, B.; Schulz, R.M.; Nilsson, E.; Antonin, K.H.; Bieck, P.R. Monoamine oxidase inhibition by the MAO-A inhibitors brofaromine and clorgyline in healthy volunteers. *J. Neural Transm.* 95(3), 241-245 (1994).

[54] Knoll, J. Pharmacological basis of the therapeutic effect of (-)deprenyl in age-related neurological diseases. *Med. Res. Rev.* 12(5), 505-524 (1992).

[55] Layer, R.W. The Chemistry of Imines. *Chem. Rev.* 63(5), 489–510 (1963).

[56] Tsugeno, Y.; Hirashiki, I.; Ogata, F.; Ito, A. Regions of the Molecule Responsible for Substrate Specificity of Monoamine Oxidase A and B: A Chimeric Enzyme Analysis. *J. Biochem.* 118(5), 974-980 (1995).

Chapter 5

Research Article 3: Adamantane amine derivatives as dual acting NMDA receptor and voltagegated calcium channel inhibitors for neuroprotection

Article published online on 1 November 2014

Med. Chem. Commun., 2014, 5: 1678–1684. DOI: 10.1039/c4md00244j

Adamantane amine derivatives as dual acting NMDA receptor and voltagegated calcium channel inhibitors for neuroprotection

Yakub E. Kadernani[a], Frank T. Zindo[a], Erika Kapp[a], Sarel F. Malan[a], Jacques Joubert[a]*

[a]*Pharmaceutical Chemistry, School of Pharmacy, University of the Western Cape, Bellville, South Africa, Private Bag X17, Bellville 7535, South Africa.*

*Corresponding author at present address: School of Pharmacy, University of the Western Cape, Private Bag X17, Bellville 7535, South Africa. Tel: +27 21 959 2195; e-mail: jjoubert@uwc.ac.za

Graphical Abstract

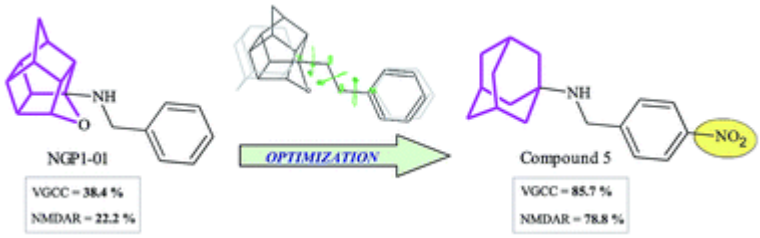

Abstract

The pathology of neurodegenerative disorders involves multiple steps, and it is probably for this reason that targeting one particular step in a multi-step process has only yielded limited results. In the CNS, the *N*-methyl-D-aspartate receptor (NMDAR) channel in its active state allows the influx of calcium ions for normal neuronal functioning. Over activation of the NMDAR channel leads to excitotoxicity, this can ultimately contribute to neuronal cell death. Calcium entry through voltage-gated calcium channels (VGCC) may also contribute to this process. In previous studies, the pentacycloundecylamine, NGP1-01 and a number of its derivatives showed promising dual acting NMDAR and VGCC inhibition. This paper describes the synthesis of a series of adamantane-derived compounds, structurally similar to NGP1-01, to act as dual channel inhibitors. By conjugating benzyl and phenylethyl moieties with different functional groups (-H, $-NO_2$, $-NH_2$, $-OCH_3$) to the structure of amantadine, we were able to synthesize compounds that display both VGCC and NMDAR channel inhibition. Compounds **1**, **2**, **5** and **10** displayed good inhibitory activity against both NMDAR channel (66.7 - 89.5 % at 100 µM) and VGCC (39.6 – 85.7 % at 100 µM). The results obtained indicate that these compounds hold potential as neuroprotective drug candidates.

Keywords: Amantadine, Neurodegeneration, NMDA receptors, voltage gated calcium channels.

5.1. Introduction

An important drug target for the treatment of neurodegenerative disorders is the ionotropic glutamate *N*-methyl-$_D$-aspartate receptor (NMDAR) which is thought to play a role in multiple neurodegenerative disorders including Parkinson's disease (PD) and Alzheimer's disease (AD).[1] The NMDAR is unique in that it requires the binding of two agonists, namely glutamate and glycine, for activation. In its active state the channel allows the influx of sodium and calcium ions. Although calcium ions are important for cell growth, survival and physiological functioning, an excess is responsible for excitotoxicity, ultimately leading to neurodegeneration.[2] Blockers of NMDAR have been shown to have neuroprotective activity[3] and it is therefore a prime drug target for neurodegenerative diseases where excitotoxicity is involved.[4] Unfortunately, NMDAR antagonists are associated with adverse central nervous system (CNS) side effects which include hallucinations.[4] These effects are especially seen with highaffinity NMDAR channel blockers such as phencyclidine (PCP) and dizocilpine

(MK-801). MK-801 and PCP bind in a use-dependant manner to the MK-801/PCP binding site located in the inner pore of the NMDAR channel when it is activated and in its open state.[1] The amino-adamantane derivatives amantadine and memantine are low affinity uncompetitive NMDAR antagonists which also bind to the MK-801/PCP binding site and display a better side effect profile compared to MK-801 and PCP.[1,5–7] Both amantadine and memantine are FDA approved for PD and AD respectively and are safe and effective treatment options. Amantadine expresses additional neurotherapeutic ability through the increment of extracellular dopamine levels via dopamine re-uptake inhibition and increased dopamine release,[8] which may be additionally useful in treatment of the motor symptoms of PD.[9] In addition to calcium overload associated with NMDAR, excessive calcium influx through voltagegated calcium channels (VGCC) may also contribute to excitotoxicity and mitochondrial dysfunction.[10,11] Studies have shown that calcium channel blockers such as nimodipine have a synergistic effect when combined with NMDAR inhibitors in neuroprotective studies.[12,13] A compound with multimodal activity, including NMDAR antagonism, calcium channel blocking activity and the ability to increase dopamine levels, could be a valuable treatment option for neurodegenerative disorders.[14] NGP1-01 is a multifunctional agent which blocks both the NMDAR as well as VGCC and also inhibits dopamine reuptake, with resulting neuroprotective activity shown *in vivo*.[15–18] Several (2-oxaadamant-1-yl)amines, structurally similar to NGP1-01 have also shown improved NMDAR activity when compared to amantadine.[19]

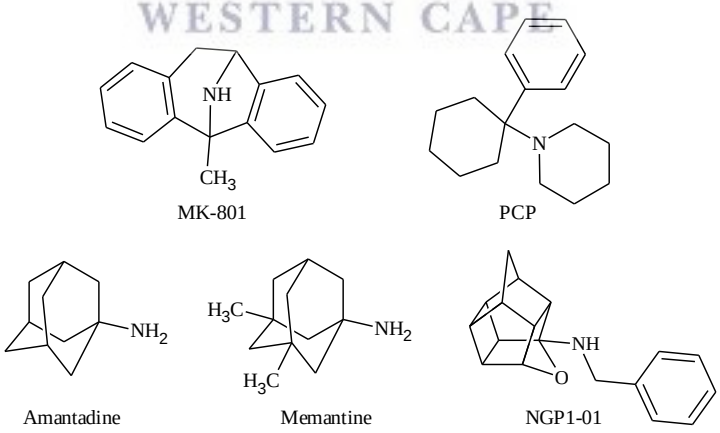

Fig. 1 Structures of the high affinity NMDAR blockers MK-801 and PCP, and amantadine, memantine and NGP1-01.

Therefore the aim of this study was to synthesize compounds containing different aromatic moieties attached via the amine to the adamantine scaffold of amantadine. It was postulated that these compounds would display improved multifunctional neuroprotective effects

compared to NGP1-01, especially NMDAR antagonism, because of the adamantane scaffold (Fig. 1).

5.2. Results and discussion

The target adamantane amine derivatives (**1**,[20] **3**–**8**, **10**) were synthesized by reacting amantadine with the respective benzylbromide moieties by means of S_N2 nucleophilic addition (Scheme 1). Compound **2** (ref. 21) was synthesized using 2-bromoethylbenzene to provide the ethyl linkage between the adamantane amine and the phenyl moiety as opposed to compound **1**, which was synthesized using benzylbromide. Both these compounds were synthesized utilizing microwave irradiation, (MW, 100 ºC, 100 W, 1 atm, 1 hour) in yields of 48% and 47%, respectively. In both these cases the reaction time was reduced from 12 hours to 1 hour and the yields significantly improved when compared to the traditional method where only thermal heating was applied. The general synthetic route followed for the synthesis of compounds **3**–**5** (ref. 22) was initiated through the conjugation of a nitrobenzyl bromide to amantadine, followed by reduction of the nitro groups to the respective amines (**6**–**8**)[23] with tin powder over 10% HCl in ethanol. The synthesis of compounds 9 (ref. 24) and 10 (ref. 25) and the corresponding *ortho*-methoxy derivative were attempted utilizing both conventional thermal heating as described for **3**,**4**,**5** and through MW irradiation. The conventional method was found to be ineffective as no or only trace amounts of the compounds formed after 24 hours of reflux (as per TLC). This might be because the methoxybenzyl bromide derivatives were not as reactive as the other corresponding benzylbromide moieties. Utilizing MW irradiation with conditions set at 100 ºC, 100 W, 1 atm (open vessel) for 1 hour only compound **9** was synthesized in sufficient yield (18%). Both the synthesis of compounds **10** and the corresponding *ortho*-methoxy derivative were attempted in the same manner as **9**, however, both reactions did not proceed successfully. The MW irradiation conditions were increased up to 150 ºC, 250 W, 240 psi (closed vessel) for 24 hours with still no compound formed in sufficient yield. A different strategy was employed where 1-bromo-adamantane and the *ortho*- or *para*-methoxybenzyl amine were used as starting reagents and conjugated via S_N2 nucleophilic substitution with MW irradiation (150 ºC, 250 W, 240 psi). Utilizing this method we were able to synthesize compound **10** in an 25% yield. The synthesis of the *ortho*-methoxy derivative using this method was unsuccessful. This could have resulted because of a chemical hindrance or deactivation of the reagent due to the methoxy substituent being in the *ortho* position of the benzyl moiety. All final compounds were confirmed by NMR, MS and IR.[20–25]

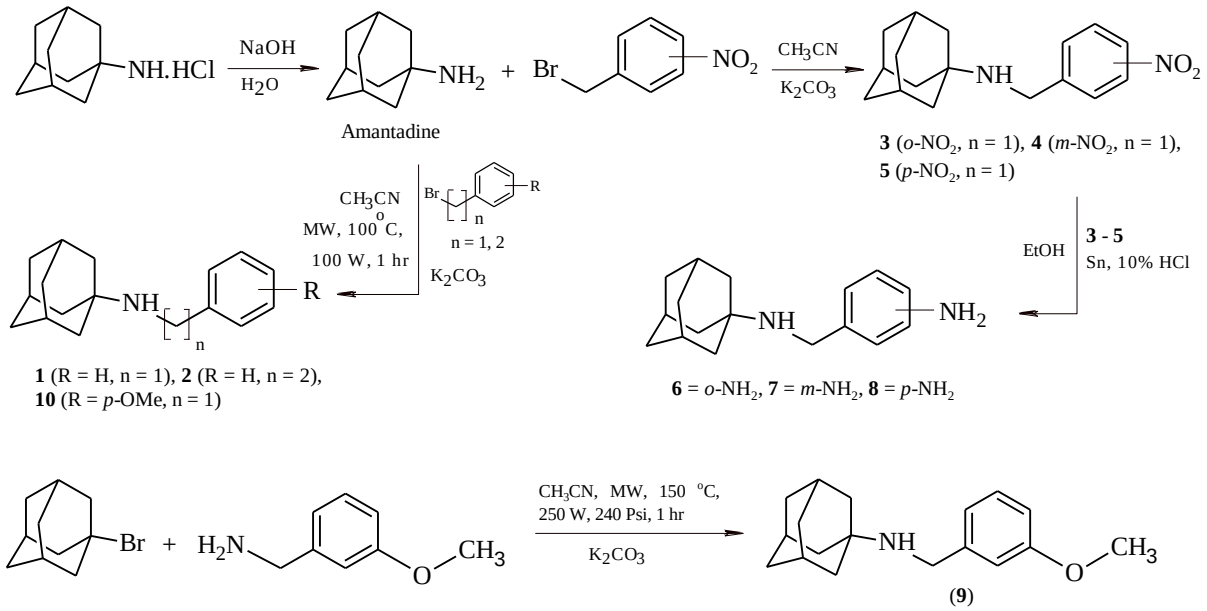

Scheme 1 General reaction schemes for the synthesis of compounds 1–10.

All synthesized amantadine derivatives (**1**–**10**) were screened at 100 µM for their potential inhibitory activity on the VGCC and NMDAR channel exactly as previously described,[26] using the fluorescent ratiometric indicator, Fura-2 AM. Fresh synaptoneurosomes were prepared from rat brain homogenate[27] and incubated with Fura-2 AM. Thereafter the synthesized compounds were incubated for 30 minutes and a 140 mM KCl or a 100 mM NMDA/glycine solution, in the VGCC and NMDAR assay respectively, was added to depolarize the cell membranes or to stimulate calcium influx through the NMDAR channels. Calcium influux was then monitored based on the fluorescence intensity relative to that of a blank control (without inhibiting compound) over a 5 minute period. Two positive controls were included in the VGCC assay; nimodipine, a commercially available dihydropyridine calcium channel blocker and the prototype pentacycloundecane compound NGP1-01. Four positive controls, MK-801, NGP1-01, amantadine and memantine, were included in the NMDAR assay. Results are shown in Table 1 and Fig. 2.

Table 1: Summary of effects the adamantane derivatives and related compounds on inhibition of NMDA/glycine induced calcium influx (at 100 μM) and KCl induced calcium influx inhibition (at 100 μM).

Test compound	Structure	[a]%NMDA activity	[a]%VGCC activity
NGP1-01	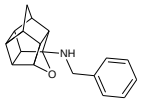	22.2**	38.4**
(**1**)	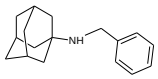	66.7***	39.6***
(**2**)	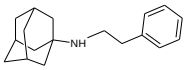	89.5***	42.0***
(**3**)	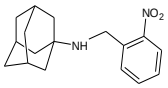	60.6***	49.2***
(**4**)	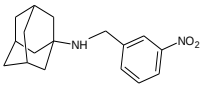	36.6***	14.3*
(**5**)	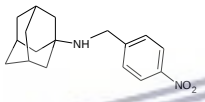	74.8***	85.7***
(**6**)	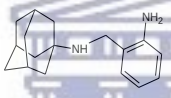	31.3***	37.1***
(**7**)	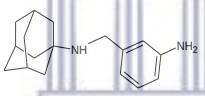	48.3***	30.0***
(**8**)	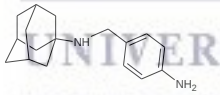	50.4***	49.5***
(**9**)	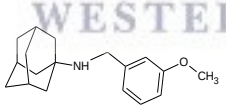	70.2***	44.7***
(**10**)	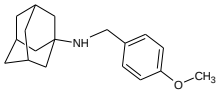	79.2***	71.2***
Nimodipine	-	inactive	100***
MK-801	-	100***	inactive
Amantadine	-	84.6***	2.76
Memantine	-	92.5***	5.20

[a]Control was taken as 0 % inhibition. Asterisks signifying statistical significance, (*) $p < 0.05$, (**) $p < 0.01$ and (***) $p < 0.001$.

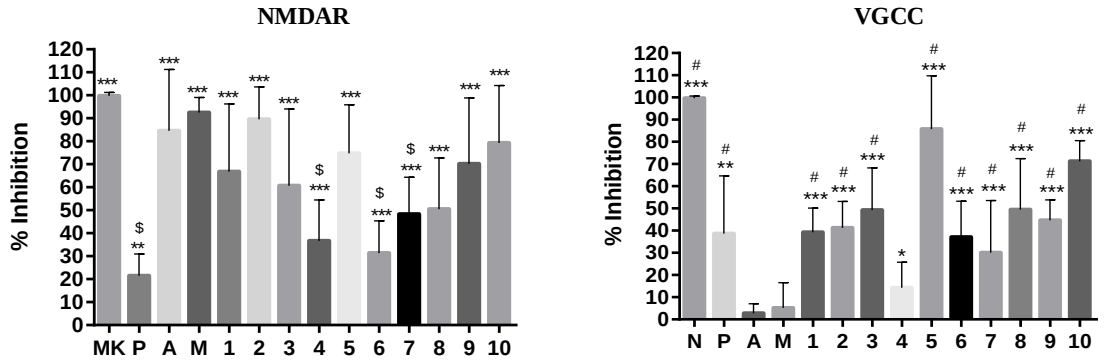

Fig. 2 Screening of test compounds (100 mM, n ¼ 9) for inhibition of NMDAR-mediated (left) and VGCC-mediated (right) calcium influx into murine synaptoneurosomes. Each bar represents mean percentage inhibition _ SEM. Abbreviations are: MK-801 (MK), NGP1-01 (P), amantadine (A), memantine (M) and nimodipine (N). Statistical analysis was performed on raw data (t-test, Prism 4.03) with asterisks signifying significant inhibitory effect [(*) $p < 0.05$, (**) $p < 0.01$, (***) $p < 0.001$] Compounds showing significant decrease in activity compared to amantadine are indicated by ($) $p < 0.05$, and compounds showing significant increase in inhibitory activity compared to amantadine are indicated by (#) $p < 0.05$.

In the NMDAR experiments, synaptoneurosomes incubated with test compounds **1** (66.7%), **2** (89.5%), **3** (60.6%), **5** (74.8%), **9** (70.2%) and **10** (79.2%) showed promising inhibitory activity of NMDA/glycine-mediated calcium influx (Table 1 and Fig. 2). Compounds **4** (47.2%), **6** (31.3%), **7** (48.3%) and **8** (50.4%) showed weaker inhibitory activity, although better than the reference compound NGP1-01 (22.2%). Of the controls, MK-801 (100%) was the most potent inhibitor followed by memantine (92.5%) and amantadine (84.6%). This was in agreement with previous studies.[9,14,15] MK-801 showed a complete blockage of NMDAR-mediated calcium entry. Compound **2** showed the highest percentage NMDAR inhibition (89.5%) of all synthesized compounds. An increase in chain length between the amantadine moiety and the aromatic group thus led to a significant increase ($p < 0.05$) in NMDAR inhibitory activity as can be seen when the activities of **1** (66.7%) and **2** (89.5%) are compared. Although both compounds are thought to fit into the channel in such a way as to allow free movement of the polycyclic adamantane structure to a certain degree, the ethyl linker is thought to enable the compound to penetrate deeper into the channel lumen thereby enabling more favourable interactions with the PCP-binding site. Geldenhuys and colleagues (2004, 2007) observed similar results in their work on NGP1-01 and its phenethyl derivative.[15,18] Further research will be conducted using radio-ligand and/or fluorescent ligand binding studies using techniques and compounds as described in one of our previous papers to confirm these observations.[28]

Of the three nitro containing compounds, **4** showed the weakest, albeit still moderate, activity with 36.6% inhibition. Compound **5** showed the highest activity with 74.8% inhibition and the rank order that is followed for these compounds is *para* > *ortho* > *meta*. The good inhibitory activity of the nitro compounds may be as a result of the nitro group contributing to the *S*-nitrosylation of cysteine residues in the NMDAR channels, thus increasing NMDAR activity compared to **1** and NGP1- 01.[29,30] The weaker activity of **3** (60.1%) and **4** (36.6%) compared to **5** (74.8%) may be attributed to steric or conformational effects of the aromatic ring due to the nitro group being in the *ortho* or *meta* position. The nitro group in the *para* position in **5** may thus enable the compound to fit better at the site of interaction. The amine compounds (**6**–**8**) show weaker activity (31–51%) than their respective nitro counterparts (**3**,**4**,**5**), as well as the methoxy compounds (**9** and **10**). This could indicate that the nitro group was involved in favourable binding interactions with NMDAR channels, and the reduction to the amines led to a decrease in activity. The methoxy derivatives **9** and **10** both showed good and improved inhibitory activity (70.2% and 79.2%, respectively) compared to **1** and NGP1-01. All the tested compounds showed better activity than NGP1-01 and none of them showed better NMDAR inhibitory activity than memantine. All the inhibitors and controls displayed statistically significant activity ($p < 0.05$), but very little or no improvement on the base structure, amantadine. Significant decreased activity, compared to amantadine (Fig. 2), was observed for compounds **4**, **6** and **7**.

For the VGCC assay, the controls that were tested included nimodipine (100%), NGP1-01 (38.40%), amantadine (2.76%) and memantine (5.20%). Of the polycyclic structures, NGP1-01 was the only control compound that displayed statistically significant ($p < 0.05$) inhibition of calcium influx via VGCC. Both amantadine and memantine showed little or no activity. In murine synaptoneurosomes incubated with the test compounds, **5** (85.7%) and **10** (71.2%) displayed promising inhibitory activity (Table 1) of calcium influx through VGCC. Both these compounds showed significantly better activity than NGP1-01. Compounds **1**–**3**, **6**–**8** and **9** showed moderate VGCC inhibitory ability within the same range as NGP1-01. All the test compounds, except **4**, showed a significant improvement on VGCC blocking activity when compared to amantadine (Fig. 2).

The *para*-nitro compound (**5**, 85.7%) displayed the best inhibition of calcium influx through VGCCs. The other nitro-derivatives compounds **3** (49.2%) and especially **4** (14.3%) showed significantly weaker inhibitory activity ($p < 0.05$) than **5**. This may also be attributed to steric or conformational effects on the aromatic ring due to the nitro group being in the *ortho* or *meta* position. The good inhibitory activity of **5** may be as a result of the nitro group being in

the *para* position, which enables the compound to fit better in the binding pocket at the site of interaction. Compound **2** (42.0%) showed slightly, though not significantly, better activity than **1** (39.6%) and the length of the linker does not exert the same effect as observed with the NMDAR assay. The amine compounds (**6** and **8**) show weaker activity (30–49.5%) than their respective nitro counterparts (**3** and **5**). However, **7** (30.0%) displayed better inhibitory activity than **4** (14.3%) indicating that the smaller NH_2 moiety had a reduced effect on the possible binding conformation of these structures. The rank order for the amines is the same as that of the nitro compounds, *para* > *ortho* > *meta*. The *para*-methoxy derivative **10** (71.2%) showed better inhibitory activity than the *meta*-methoxy compound (**9**, 44.7%).

Test compounds **1**, **2**, **5** and **10** showed promising dual NMDAR and VGCC inhibitory activity. NGP1-01 also had significant inhibition on both NMDAR and VGCC calcium influx. Compounds **1** and **2** showed VGCC inhibition in the same range as NGP1-01, however their NMDAR channel inhibitory activity was significantly improved. This could largely be attributed to the incorporation of the amantadine moiety in **1** and **2**. The activity of **2** shows that a two carbon spacer provides improved dual channel blocking activity and future studies will include investigation of optimal chain length of the adamantine derivatives described in this study. Both compounds **1** and **2** may be better therapeutic options than NGP1-01 and amantadine or memantine because of this improved dual acting ability. The incorporation of the *para*-nitro and *para*-methoxy moieties on the benzyl function of **5** and **9** respectively, further improved this dual activity (Table 1). This is in agreement with previous studies done on similar pentacycloundecane derivatives.[18,31] Amantadine and memantine are known NMDAR channel inhibitors, but have no VGCC activity. Therefore, the dual acting adamantane derivatives may enhance the neuroprotective effects known for amantadine and memantine by inhibiting two excitotoxic pathways simultaneously. Amantadine is also known to increase dopamine release and decrease dopamine reuptake in the CNS[8] and we expect that the new compounds could show similar activity. This needs to be confirmed in future studies.

5.3. Conclusion

We described the synthesis and biological evaluation of **10** adamantane amine compounds as potential dual VGCC blockers and NMDAR antagonists. Compounds **1**, **2**, **5** and **10** displayed significant inhibitory activity against both NMDAR and VGCC calcium influx. These adamantane derived compounds are potentially better neurotherapeutic options than amantadine and memantine as they inhibit both NMDAR and VGCC-mediated calcium influx, whereas the base adamantine structures only inhibit NMDAR-mediated calcium influx. Additional assays on the influence of these compounds on dopamine transmission and apoptosis, and in *in vivo* models will elaborate on the potential neuroprotective value.

Acknowledgements

We are grateful to the University of the Western Cape and the National Research Foundation of South Africa for financial support. We would also like to acknowledge the contribution of the 2013 Pharmaceutical Chemistry Research Group at the University of the Western Cape.

Author Contributions

Y.E.K., F.T.Z. and J.J. conceived of the presented idea. Y.E.K. and F.T.Z. designed, synthesized and characterized the compounds. F.T.Z. and Y.E.K. performed the calcium modulation assays, processed the experimental data and performed the analysis. S.F.M. and J.J. supervised the findings of this work. All authors discussed the results and contributed to the final manuscript.

Notes and references

1. R. Dingledine, K. Broges, D. Bowie and S. F. Traynelis, *Pharmacol. Rev.*, 1999, **51**, 7.

2. M. Arundine and M. Tymianski, *Cell Calcium*, 2013, **34**(4–5), 325.

3. W. Danysz and C. G. Parsons, *Int. J. Geriatr. Psychaitry*., 2003, **8**, S23.

4. W. Danysz and T. H. Lanthorn, *Amino Acids*, 2000, **19**, 131.

5. C. G. Parsons, W. Danysz and G. Quack, *Neuropharmacology*, 1999, **38**, 735.

6. J. Bornmann, *Eur. J. Pharmacol.*, 1989, **166**, 591.

7. J. Kornhuber, J. Bornmann, W. Retz, M. hubers and P. Riederer, *Eur. J. Pharmacol*., 1989, **166**, 589.

8. K. Mizoguci, H. Yokoo, M. Yoshida, T. Tanaka and M. Tanake, *Brain Res*., 1994, **662**, 255.

9. W. Danysz, C. G. Parsons, J. Kornhuber, W. J. Schmidt and G. Quack, *Neurosci. Biobehav. Rev*., 1997, **21**, 455.

10. M. P. Mattson, *Neuromol. Med.*, 2003, **3**, 65.

11. M. F. Cano-Abad, M. Villarroya, A. G. Garcia, N. H. Gabilan and M. G. Lopez, *J. Biol. Chem*., 2001, **276**, 39695.

12. A. Schurr, Curr. *Drug Targets*, 2004, **5**, 603.

13. B. T. Stuiver, B. R. Douma, R. Bakker, C. Nyakas and P. G. Luiten, *Neurodegeneration*, 1996, **5**, 153.

14. J. Joubert, S. Van Dyk, I. R. Green and S. F. Malan, *Bioorg. Med. Chem.*, 2011, **19**, 3935–3944.

15. W. J. Geldenhuys, S. F. Malan, J. R. Bloomquist and C. J. Van der Schyf, *Bioorg. Med. Chem*., 2007, **5**, 1525.

16. C. Kiewert, J. Hartmann, J. Stoll, T. J. Thekkumkara, C. J. Van der Schyf and J. Klein, *Neurochem. Res.*, 2006, **31**, 395.

17. A. Mdzinarishvili, W. J. Geldenhuys, T. J. Abbruscato, U. Bickel, J. Klein and C. J. Van der Schyf, Neurosci. Lett., 2005, **383**, 49.

18. W. J. Geldenhuys, S. F. Malan, T. Murugesan, C. J. Van der Schyf and J. R. Bloomquist, *Bioorg. Med. Chem*., 2004, **12**, 1799.

19. M. D. Duque, P. Camps, L. Pro・re, S. Montaner, S. V´azquez, F. X. Sureda, J. Mallol, M. L´opez-Querol, L. Naesens, E. De Clercq, S. R. Prathalingam and J. M. Kelly, *Bioorg. Med. Chem*., 2009, **17**, 3198.

20. *Synthesis of **1***: Amantadine (11.4 mmol) and benzyl bromide (10.3 mmol) were added to a mixture of acetonitrile (10 ml) and K_2CO_3 (15.5 mmol). The reaction vial was placed in a CEM Discover Labmate (model number 908010) microwave reactor and reacted at 100 ^oC and 100 W for 60 min. After irradiation, the mixture was filtered to remove the K_2CO_3 and unreacted amantadine free base. The filtrate was collected and the excess solvent evaporated *in vacuo*. The reaction mixture was then acidified using 30 ml water which was made acidic

with HCl until the pH was 3. This was followed by an extraction with DCM (3 x 30 ml). The combined aqueous layers were collected and made basic (pH = 12-14) using water saturated with NaOH and this was followed by a second extraction with DCM (3 x 30 ml). The combined organic layers were dried over anhydrous $MgSO_4$, filtered and the solvent evaporated *in vacuo* to yield *N*-benzyltricyclo[3.3.1.1^{3,7}]decan-1-amine (**1**) as a light yellow oil. $C_{17}H_{23}N$; Yield: 48%; mp: oil; ^{1}H NMR (200 MHz, $CDCl_3$) δ_H: 7.4-7.1 (m, 5H), 3.8-3.6 (s, 2H), 2.2-2.0 (m, 3H), 1.8-1.4 (m, 12H); ^{13}C NMR (50 MHz, $CDCl_3$) δ_C: 141.4, 128.3, 128.3, 126.7, 50.9, 45.1, 42.8, 36.7, 29.6; MS (ESI-MS) *m/z*: 242.12 (M^+), 134.97, 78.94; IR (ATR; cm^{-1}): 3025.9, 2900.9, 2845.9, 1603.7, 1451.3, 1146.4, 734.2, 694.6.

21. *Synthesis of **2***: Amantadine (3.3 mmol) and 2-bromoethylbenzene (3.3 mmol) were added to a mixture of acetonitrile (10 ml) and K_2CO_3 (4.5 mmol). The synthetic procedure from this point was the same as described for **1** which yielded *N*-(2-phenylethyl)tricyclo[3.3.1.1^{3,7}]decan-1-amine (**2**) as a white wax. *Physical data:* $C_{18}H_{25}N$; Yield: 47 %; mp: wax; ^{1}H NMR (200 MHz, $CDCl_3$) δ_H: 7.4-7.1 (m, 5H), 3.6-3.5 (t, 2H), 3.1-3.0 (t, 2H), 1.9-1.5 (m, 3H), 1.4-1.1 (m, 12H); ^{13}C NMR (50 MHz, $CDCl_3$) δ_C: 138.9, 128.8, 128.6, 126.9, 50.00, 42.77, 41.63, 36.8, 35.4, 29.7; MS (ESI-MS) *m/z*: 256.15 (M^+), 134.96, 78.95; IR (ATR; cm^{-1}): 2912.2, 2891.9, 2802.6, 1603.4, 1455.2, 1362.8, 1075.0, 776.9, 695.8.

22. *Synthesis of **3-5***: Amantadine (11.4 mmol) and the appropriate nitrobenzyl bromide derivative (10.3 mmol) were added to a round-bottomed flask followed by acetonitrile (10 ml) and K_2CO_3 (15.5 mmol). This mixture was refluxed for 24 hours where after it was filtered. The filtrate was collected and the excess solvent evaporated *in vacuo*. The mixture was purified *via* flash chromatography to yield the title compounds (**3-5**) as yellow amorphous solids.

*N-(2-nitrobenzyl)tricyclo[3.3.1.1^{3,7}]decan-1-amine (**3**)*: $C_{17}H_{22}N_2O_2$; Yield: 32 %; mp: 94 ^{o}C; ^{1}H NMR (200 MHz, $CDCl_3$) δ_H: 7.9-7.8 (dd, J = 8.11 Hz, 1.37 Hz), 7.7-7.5 (m, 2H), 7.4-7.3 (m, 1H), 4.0-3.8 (s, 2H, CH_2), 2.2-1.9 (m, 3H), 1.8-1.4 (m, 12H); ^{13}C NMR (50 MHz, $CDCl_3$) δ_C: 149.6, 136.2, 133.3, 132.1, 127.8, 124.5, 51.1, 45.13, 42.4, 36.6, 29.5; MS (ESI-MS) *m/z*: 287.17 (M^+), 214.02, 135.00, 79.89; IR (ATR; cm^{-1}): 2900.3, 2848.6, 1524.1, 1463.3, 1355.3, 1133.8, 779.4, 739.6.

*N-(3-nitrobenzyl)tricyclo[3.3.1.1^{3,7}]decan-1-amine (**4**):* $C_{17}H_{22}N_2O_2$; Yield: 54 %; mp: 61 ^{o}C; ^{1}H NMR (200 MHz, $CDCl_3$) δ_H: 8.3-8.2 (s, 1H), 8.1-8.0 (m, 1H), 7.7-7.6 (dd, 1H, J = 7.83 Hz, 1.64 Hz), 7.5-7.4 (m, 1H), 3.9-3.8 (s, 2H, CH_2), 2.2-2.0 (m, 3H), 1.8-1.4 (m, 12H); ^{13}C NMR (50 MHz, $CDCl_3$) δ_C: 144.3, 134.3, 129.1, 123.0, 121.7, 51.0, 45.1, 42.9, 36.7, 29.6;

MS (ESI-MS) *m/z*: 287.17 (M^+), 214.04, 135.00, 79.98; IR (ATR; cm^{-1}): 2898.3, 2847.1, 1524.5, 1463.3, 1359.3, 1133.5, 778.8, 715.8.

*N-(4-nitrobenzyl)tricyclo[3.3.1.1^{3,7}]decan-1-amine (**5**):* $C_{17}H_{22}N_2O_2$; Yield: 57 %; mp: 94 ^oC; ^1H NMR (200 MHz, $CDCl_3$) δ_H: 8.1-8.0 (d, 2H, J = 8.9 Hz), 7.6-7.4 (d, 2H, J = 8.9 Hz), 4.0-3.8 (s, 2H, CH_2), 2.2-2.0 (m, 3H), 1.8-1.4 (m, 12H); ^{13}C NMR (50 MHz, $CDCl_3$) δ_C: 149.9, 146.1, 128.7, 123.5, 51.0, 44.5, 42.9, 36.6, 29.8; MS (ESI-MS) *m/z*: 287.14 (M^+), 214.00, 134.94, 78.95; IR (ATR; cm^{-1}): 2900.0, 2848.5, 1523.8, 1477.3, 1354.9, 1133.8, 779.5, 716.5.

23. *Synthesis of **6**-**8***: Previously prepared nitrobenzyltricyclo[3.3.1.1^{3,7}]decan-1-amines (**3**, **4** or **5**, 0.5 mmol) and tin powder (0.8 mmol) were added to a round-bottomed flask and set up under reflux conditions. This was followed by addition of 10 % hydrochloric acid (1.5 ml) down the condenser with continuous stirring, while elevating the temperature to reflux conditions. Ethanol (5 ml) was added as a solubilisation agent. Further HCl additions (2 x 2.3 ml) were made at 10 minute intervals. The reaction was refluxed overnight followed by an aqueous extraction with DCM (3 x 20 ml). The water phase was collected and alkalinised using a 40 % NaOH solution just past the turning point, and then extracted with DCM (3 x 20 ml). The combined organic fractions were washed with brine (2 x 15 ml), dried with anhydrous $MgSO_4$ and the solvent evaporated *in vacuo* to yield the products (**6**-**8**) as light brown amorphous solids.

*N-(2-aminobenzyl)tricyclo[3.3.1.1^{3,7}]decan-1-amine (**6**)*: $C_{17}H_{24}N_2$; Yield: 70 %; mp: 71 ^oC; ^1H NMR (200 MHz, $CDCl_3$) δ_H: 6.9-6.8 (m, 2H), 6.5-6.3 (m, 2H), 3.6-3.4 (s, 2H, CH_2), 2.1-1.8 (m, 3H), 1.8-1.4 (m, 12H); ^{13}C NMR (50 MHz, $CDCl_3$) δ_C: 146.9, 129.5, 128.0, 125.3, 117.7, 115.7, 50.5, 43.9, 42.7, 36.7, 29.5; MS (ESI-MS) *m/z*: 257.14 (M^+), 105.94, 78.95; IR (ATR; cm^{-1}): 3402.2, 3282.5, 2903.1, 2849.3, 1616.9, 1494.4, 1357.8, 1072.3, 785.1, 710.0.

*N-(3-aminobenzyl)tricyclo[3.3.1.1^{3,7}]decan-1-amine (**7**)*: $C_{17}H_{24}N_2$; Yield: 75 %; mp: 79 ^oC; ^1H NMR (200 MHz, $CDCl_3$) δ_H: 6.9-6.7 (m, 1H), 6.5-6.2 (m, 3H), 3.6-3.4 (s, 2H, CH_2), 2.1-1.8 (m, 3H), 1.8-1.4 (m, 12H); ^{13}C NMR (50 MHz, $CDCl_3$) δ_C: 146.4, 142.7, 129.2, 118.4, 115.0, 113.5, 50.7, 45.0, 42.7, 36.7, 29.5; MS (ESI-MS) *m/z*: 257.13 (M^+), 76.99; IR (ATR; cm^{-1}): 3399.9, 3174.3, 2897.4, 2845.9, 1603.7, 1493.6, 1356.6, 1343.0, 1067.8, 1038.0, 773.5, 708.4.

*N-(4-aminobenzyl)tricyclo[3.3.1.1^{3,7}]decan-1-amine (**8**)*: $C_{17}H_{24}N_2$; Yield: 90 %; mp: 91 ^oC; ^1H NMR (200 MHz, $CDCl_3$) δ_H: 6.9-6.8 (d, 2H, J = 8.8 Hz), 6.4-6.3 (d, 2H, J = 8.8 Hz), 3.6-3.4 (s, 2H, CH_2), 2.1-1.8 (m, 3H), 1.8-1.4 (m, 12H); ^{13}C NMR (50 MHz, $CDCl_3$) δ_C: 145.0, 129.3, 128.8, 115.1, 50.7, 44.5, 42.7, 36.7, 29.5; MS (ESI-MS) *m/z*: 257.15 (M^+), 105.93,

78.95; IR (ATR; cm^{-1}): 3429.1, 3315.8, 2898.2, 2847.5, 1610.1, 1518.8, 1357.2, 1069.7, 1038.9, 761.6, 708.4.

24. *Synthesis of* ***9***: Amantadine free base (3.3 mmol) were added to a round-bottomed flask containing acetonitrile (10 ml), K_2CO_3 (4.5 mmol) and 3-methoxybenzylchloride (3.3 mmol). The synthetic procedure from this point was the same as described for **1** which yielded *N*-(3-methoxybenzyl)tricyclo[3.3.1.$1^{3,7}$]decan-1-amine (**9**) as a white powder. *Physical data:* $C_{18}H_{25}NO$; Yield: 18 %; mp: 124 ^oC; ^1H NMR (200 MHz, $CDCl_3$) δ_H: 7.7-7.5 (m, 1H), 7.4-6.7 (m, 2H), 4.6-4.2 (bs, NH), 4.0-3.7 (2 x s, 5H), 2.1-1.8 (m, 3H), 1.8-1.4 (m, 12H); ^{13}C NMR (50 MHz, $CDCl_3$) δ_C: 162.5, 132.1, 129.7, 121.7, 110.6, 110.2, 55.2, 44.4, 42.5, 35.3, 29.2; MS (ESI-MS) *m/z*: 313.23, [M+ACN+H] 151.98, 78.91; IR (ATR; cm^{-1}): 2934.6, 2864.2, 1586.1, 1454,8, 1265.0, 1174.7, 1075.2, 852.2.

25. *Synthesis of* ***10***: 1-Bromoadamantane (2.3 mmol) were added to the reaction vessel containing acetonitrile (3 ml), K_2CO_3 (3.5 mmol) and 4-methoxybenzylamine (2.3 mmol). The mixture was placed in the microwave reactor (240 Psi, 300 W, 150 ^oC, 60 min). After irradiation, the mixture was filtered by vacuum filtration to remove the K_2CO_3. The filtrate was collected and the excess solvent evaporated *in vacuo* and purified *via* flash chromatography to yield *N*-(4-methoxybenzyl)tricyclo[3.3.1.$1^{3,7}$]decan-1-amine (**10**) as a white powder. *Physical data:* $C_{18}H_{25}NO$; Yield: 25 %; mp: 225 ^oC; ^1H NMR (200 MHz, $CDCl_3$) δ_H: 7.3-7.1 (dd, 2H J = 6.62 Hz, 2.16 Hz), 6.9-6.7 (dd, 2H, J = 6.62 Hz, 2.16 Hz), 5.2-4.6 (bs, NH), 4.0-3.7 (2 x s, 5H), 2.2-1.8 (m, 3H), 1.8-1.4 (m, 12H); ^{13}C NMR (50 MHz, $CDCl_3$) δ_C: 158.5, 129.7, 128.4, 114.4, 55.2, 51.6, 45.2, 42.4, 35.5, 29.2; MS (ESI-MS) *m/z*: 313.23, [M+ACN+H] 78.95; IR (ATR; cm^{-1}) : 2905.9, 2849.6, 1627.7, 1453.7, 1248.0, 1176.7, 1087.8, 813.0.

26. F. T. Zindo, Q. R. Barber, J. Joubert, J. J. Bergh, J. P. Petzer and S. F. Malan, *Eur. J. Med. Chem.*, 2014, **80**, 122.

27. E. B. Hollingsworth, E. T. McNeal, J. L. Burton, R. J. Williams, J. W. Daly and C. R. Creveling, *J. Neurosci.*, 1985, **5**, 2240.

28. J. Joubert, S. Van Dyk, I. R. Green and S. F. Malan, *Eur. J. Med. Chem.*, 2011, **46**, 5010–5020.

29. H. J. R. Lemmer, J. Joubert, S. van Dyk, F. H. van der Westhuizen and S. F. Malan, *Med. Chem.*, 2012, **8**, 361.

30. S. A. Lipton, *Nat. Res. Drug. Discovery*, 2006, **5**, 160.

31. W. Liebenberg, J. J. Van der Walt and C. J. Van der Schyf, *Pharmazie*, 2000, 833.

Chapter 6
Conclusion

The complex pathogenesis and aetiology of neurodegenerative diseases (NDs) make it clear that drugs targeting a single receptor or enzymatic system will not result in successful retardation and treatment of these multifactorial diseases. As highlighted in the review article presented in chapter 2 [1], the advent of the multitarget-directed ligand (MTDL) approach has over the last few decades seen the development of compounds that combine symptomatic treatment and neuroprotection in one molecule by acting simultaneously on different receptors and target sites implicated in NDs.

This study focused on the development of novel MTDL's using polycyclic structures as scaffolds with inherent activity and the ability to promote favourable pharmacokinetic and pharmacodynamic properties of the resultant MTDL's. The resultant compounds were designed to serve as neuroprotective agents by inhibiting NMDA receptors, blockade of VGCC's and by inhibiting the apoptotic process resulting from the activity of the MAO isoenzymes.

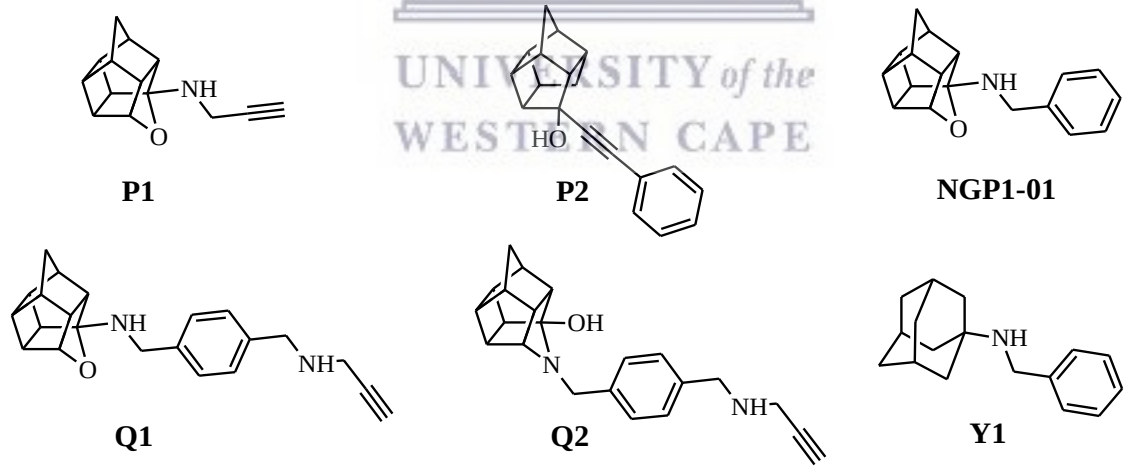

Figure 8.1: Representative structures of the various compounds designed and synthesised in this study and NGP1-01, a known neuroprotective agent.

As reported in research article 1 (Chapter 3) [2], a series of polycyclic propargylamine and acetylene derivatives, represented by **P1** and **P2** (Figure 8.1), showed significant anti-apoptotic activity comparable to selegiline at 10 µM. The results of the anti-apoptotic assay suggested the anti-apoptotic activity of the propargylamine moiety to be attributed to the

acetylene group. For activity, this acetylene group can either be terminal (**P1**) or between two non-polar groups (**P2**), with the terminal acetylene group having slightly higher activity. It was also confirmed that when linked to a polycyclic cage structure, propargylamine and acetylene derivatives displayed increased anti-apoptotic activity. Further investigation must however be conducted to ascertain whether this reported anti-apoptotic activity is solely due to the acetylene group, the cage moiety, or the acetylene group in conjunction with a nearby electronegative atom/group. When assayed for multifunctional activity, this series showed little to no activity on the VGCC, NMDA receptors and MAO-B enzyme even at concentrations above 100 µM. The ability of these compounds to significantly inhibit apoptosis suggests that these compounds exhibited their neuroprotective action through some other mechanism(s) unexplored in this study.

Follow up work on **P1** and **P2** successfully yielded a series of pentacycloundecane and hexacycloundecane propargylamine derivatives presented in research article 2 (Chapter 4) [3], represented by **Q1** and **Q2** (Figure 8.1), which showed promising neuroprotective potential. These compounds showed the ability to significantly improve the viability of SH-SY5Y neuroblastoma cells, previously exposed to the neurotoxin MPP^+, by 31% and 61% at a 1 µM concentration. The influence of the acetylene moiety in reducing the cytotoxicity of this series was evident at 100 µM. By comparing the cytotoxicity displayed by the propargyl containing compounds within this series with their respective precursors devoid of this moiety, it was observed that the propargyl moiety was responsible for a decrease in cytotoxicty by about 3-14 times at 100 µM. These compounds also showed dual calcium modulation activity by blocking VGCC's (26.6% to 51.3%, at 10 µM) and by blocking NMDAR (31.4% and 88.3%, at 10 µM). This activity was comparable to that of NGP1-01, a known dual acting calcium channel blocker [4]. This general improvement in activity, compared to **P1** which was inactive as a VGCC blocker at 100 µM, emphasizes the need to include a benzylamine moiety in the structure of polycyclic amine derived compounds designed to possess inherent VGCC blockade activity. The inclusion of a propargyl moiety in the compound structures seemed to contribute to improved NMDAR antagonism as compounds devoid of this moiety within the series generally showed lower NMDAR inhibitory potentials compared to the propargyl carrying compounds. When assayed for MAO inhibition, most of the active compounds displayed selectivity to the MAO-B isoenzyme with IC_{50} values ranging from 1.70 µM to 36.31 µM and appeared to be reversible MAO inhibitors as defined by the time-dependency studies conducted. This improved activity, compared to **P1** and **P2**, can be attributed to the increased molecular length of these

compounds as a result of the incorporation of a benzylamine moiety into their structures. The juxtapositioned benzylamine and propargyl moieties seemed to be imperative in rendering the compounds better MAO-B inhibitory activity and afforded them multi-mechanistic neuroprotective potential. Inhibiting the MAO-B enzyme is an important feature of these compounds as this enzyme has been reported to play a critical role in the pathogenesis of NDs. Although the MAO-B inhibitory activity of these compounds was a significant improvement in comparison to the previously reported compounds **P1** and **P2**, it remains about 1000-fold weaker than the activity of selegiline. Further structural modifications of these compounds may therefore be necessary to afford molecules which may potentially show improved MAO-B inhibition.

In research article 3 (Chapter 5) [5], several compounds represented by **Y1** (Figure 8.1) were designed to carry the adamantane amine moiety as a polycyclic scaffold rather than the pentacycloundecane moiety seen in **P1**, **P2**, **Q1**, **Q2** and NGP1-01. These compounds displayed good inhibitory activity against both NMDAR channel (66.7 - 89.5 % at 100 μM) and VGCC (39.6 – 85.7 % at 100 μM), and appeared to be superior calcium modulators to NGP1-01. These adamantane derived compounds are potentially better neurotherapeutic options than amantadine as they were shown to inhibit both NMDAR and VGCC-mediated calcium influx, whereas the base adamantine structures only inhibit NMDAR-mediated calcium influx. Various structure-activity relationships were drawn from this study. For example, an increase in chain length between the amantadine moiety and the aromatic group was shown to significantly increase the NMDAR inhibitory activity. An ethyl linker in particular, was thought to enable the compound to penetrate deeper into the channel lumen thereby enabling more favourable interactions with the PCP-binding site of the receptor. Of the nitro containing compounds of this series, the rank order of NMDAR antagonistic activity that was followed was *para* > *ortho* > *meta*. The weaker activity of the *ortho* or *meta* substituted nitro containing compounds may be attributed to steric or conformational effects of the *ortho* or *meta* substituted aromatic ring. The nitro group in the *para* position seemed to enable the compounds better fit at the site of interaction rendering them activity as NMDAR antagonists.

In conclusion, the compounds presented in this thesis are promising leads to multi-mechanistic compounds that may be useful as drug agents for the treatment of neurodegenerative disorders. Further *in vitro* and *in vivo* studies, which may include mechanistic studies as well as elucidation of the actual binding mode of these compounds, their direct involvement in the anti-apoptotic cascade, dopamine transmission and blood-

brain barrier permeability, would provide better insight on their drugability. Also, these analogues may be screened for potential neuroprotective activity on various other drug targets implicated in neurodegeneration.

References

[1] Zindo, F.T.; Joubert, J.; Malan, S.F. Propargylamine as functional moiety in the design of multifunctional drugs for neurodegenerative disorders: MAO inhibition and beyond. *Future Med. Chem.* 7(5), 609–629 (2015).

[2] Zindo FT, Barber QR, Joubert J, Bergh JJ, Petzer JP, Malan SF. Polycyclic propargylamine and acetylene derivatives as multifunctional neuroprotective agents. *Eur. J. Med. Chem.* 80, 122–134 (2014).

[3] Zindo F.T., Malan S.F., Omoruyi S.I., Enogieru A.B., Ekpo O.E., Joubert J. Design, synthesis and evaluation of pentacycloundecane and hexacycloundecane propargylamine derivatives as multifunctional neuroprotective agents. *Eur. J. Med. Chem.* [Submitted for publication 9 November 2018].

[4] Kiewert C., Hartmann J., Stoll J., Thekkumkara T.J., Van der Schyf C.J., Klein J. NGP1-01 is a brain-permeable dual blocker of neuronal voltage- and ligand-operated calcium channels. *Neurochem. Res.* 31(3), 395-9 (2006).

[5] Kadernani Y.E., Zindo F.T., Kapp E., Malan S.F., Joubert J. Adamantane amine derivatives as dual acting NMDA receptor and voltage-gated calcium channel inhibitors for neuroprotection. *Med. Chem. Commun.* 5(11), 1678-1684 (2014).

Chapter 7

Additional research outputs

7.1. Research Article 4: Design, synthesis and evaluation of indole derivatives as multifunctional agents against Alzheimer's disease

Article submitted for publication on 16 January 2018

Med. Chem. Commun. 2018; 2:1- 27. DOI: 10.1039/C7MD00569E.

Design, synthesis and evaluation of indole derivatives as multifunctional agents against Alzheimer's disease

Ireen Denya[1], Sarel F. Malan[1], Adaze B. Enogieru[2], Sylvester I. Omoruyi[2], Okobi E. Ekpo[2], Erika Kapp[1], Frank T. Zindo[1], Jacques Joubert[1]*

[1]*Pharmaceutical Chemistry, School of Pharmacy, University of The Western Cape, Private Bag X17, Bellville 7535, South Africa*

[2]*Department of Medical Biosciences, University of the Western Cape, Private Bag X17, Cape Town, Bellville 7535, South Africa.*

*Corresponding author at present address: School of Pharmacy, University of the Western Cape, Private Bag X17, Bellville 7535, South Africa. Tel: +27 21 959 2195; e-mail: jjoubert@uwc.ac.za

Graphical Abstract

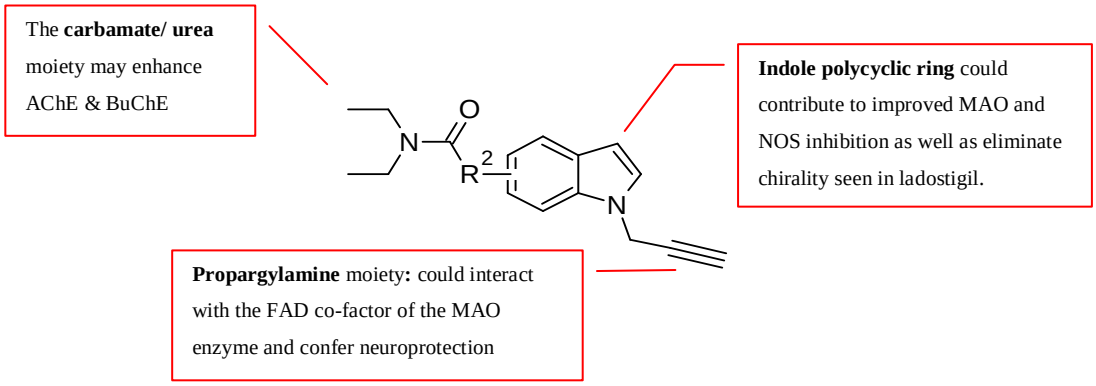

Abstract

A series of indole derivatives was designed and synthesized to improve on activity and circumvent pharmacokinetic limitations experienced with the structurally related compound, ladostigil. The compounds consisted of a propargylamine moiety (a known MAO inhibitor and neuroprotector) at the *N*1 position and a ChE inhibiting diethyl-carbamate/urea moiety at the 5 or 6 position of the indole ring. In order to prevent or slow down the *in vivo* hydrolysis and deactivation associated with the carbamate function of ladostigil, a urea moeity was incorporated into selected compounds to obtain more metabolically stable structures. The majority of the synthesized compounds showed improved MAO-A inhibitory activity compared to ladostigil. The compounds possessing the propargylamine moiety showed good MAO-B inhibitory activity with **6** and **8** portraying IC_{50} values between 14 – 20 fold better than ladostigil. The ChE assay results indicated that the compounds have non-selective inhibitory activities on eeAChE and eqBuChE regardless of the type or position of substitution (IC_{50}: 2-5 μM). MAO-A and MAO-B docking results showed that the propargylamine moiety was positioned in close proximity to the FAD cofactor suggesting that the good inhibitory activity may be attributed to the propargylamine moiety and irreversible inhibition as confirmed in the reversibility studies. Docking results also indicated that the compounds have interactions with important amino acids in the AChE and BuChE catalytic sites. Compound **6** was the most potent multifunctional agent showing better *in vitro* inhibitory activity than ladostigil on all enzymes tested (hMAO-A IC_{50} = 4.31 μM, hMAO-B IC_{50} = 2.62 μM, eeAChE IC_{50} = 3.70 μM, eqBuChE IC_{50} = 2.82 μM). Chemical stability tests confirmed the diethyl-urea containing compound **6** to be more stable than its diethyl-carbamate containing counterpart compound **8**. Compound **6** also exerted significant neuroprotection (52.62 % at 1 μM) against MPP+ insult to SH-SY5Y neural cells and have good *in silico* predicted ADMET properties. The favourable neuronal enzyme inhibitory activity, likely improved pharmacokinetic properties *in vivo* and the potent neuroprotective ability of compound **6** make it a promising compound for further development.

Keywords: Alzheimer's disease, Indole, Propargylamine, Monoamine oxidase, Cholinesterase, Ladostigil

7.1.1. Introduction

Alzheimer's disease (AD) is an age related neurodegenerative disorder characterised by progressive memory loss and cognitive impairment occurring as a result of a process of programmed cell death known as apoptosis.[1,2] Over the years several pathways have been indicated in the pathology of the disease. The cholinergic hypothesis states that there is an extensive loss of cholinergic neurons in the central nervous system that contributes to impairment in the cognitive and memory symptoms of the affected person.[3] Oxidative stress and amyloid β (Aβ) plaque formation have been shown to be involved in the pathophysiology of the disease.[4,5] Acetylcholinesterase (AChE) inhibitors in AD act by increasing the endogenous levels of acetylcholine (ACh) in the brain and thereby enhance cholinergic transmission and improve cognitive functions (Figure 1).[6,7] They however do not halt the process of apoptosis nor improve the depressive symptoms of the disease due to the multifactorial nature of AD. Butyrylcholinesterase (BuChE) also has the capacity to hydrolyse acetylcholine. Excess ACh levels in the brain cause saturation of AChE and in turn increase the activity of BuChE towards the neurotransmitter.[8] Even though AChE hydrolyses more ACh than BuChE, the latter contributes more to AD because of the decreased levels of the true cholinesterase, hence its inhibition is of value to AD.[9,10] Accordingly, a compound that inhibits this enzyme, in addition to AChE, would prove beneficial for treatment of AD.

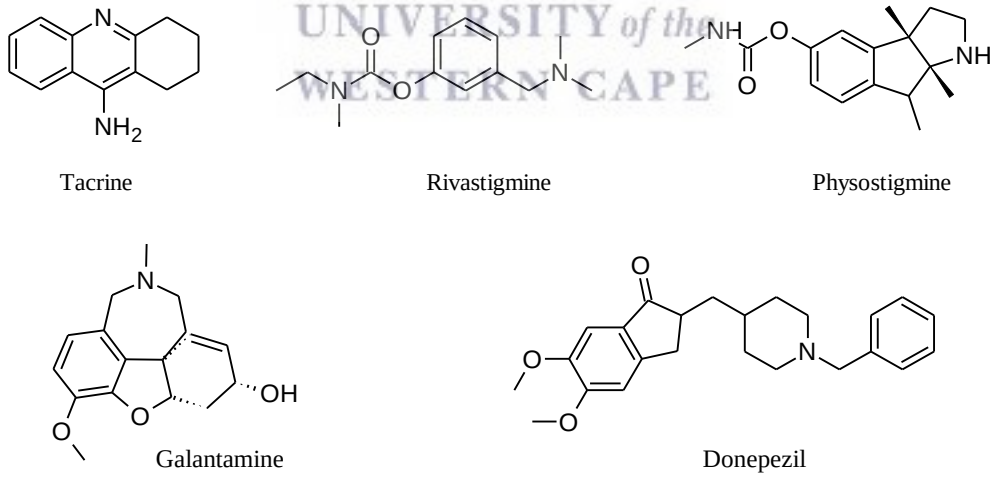

Tacrine | Rivastigmine | Physostigmine

Galantamine | Donepezil

Figure 1: Structures of previously described cholinesterase inhibitors.

The monoamine oxidase (MAO) enzymes natively metabolise amine neurotransmitters such as dopamine and 5-hydroxytryptamine[11] and have been identified as attractive targets for the treatment of neurological disorders.[12] The enzyme, occurring in two isoforms, MAO-A and MAO-B, produces peroxides that cause oxidative stress alongside the depletion of

neurotransmitters.[13] MAO-B constitutes about 80% of the total MAO activity in the human brain and is the predominant form of the enzyme in the striatum, while MAO-A is mainly distributed peripherally.[13,14] Inhibition of MAO-A and MAO-B permits accumulation of neurotransmitters and reduces the formation of oxidative free radicals to confer neuroprotection. Inhibitors of the enzymes are thus expected to protect from neurodegeneration due to their ability to reduce the formation of peroxides and radical species from amine catalysis.[15-18] Although MAO-B is present in higher concentrations than MAO-A in the human basal ganglia, MAO-A inhibitors have also been shown to enhance dopamine levels in this region.[19,20] In order to conserve dopamine in the basal ganglia, mixed MAO-A/B inhibitors may therefore be more efficacious than selective inhibitors and may be of value in the treatment of AD and other neurodegenerative disorders.[12] Propargylamine derived MAO inhibitors such as rasagiline and ladostigil (Figure 2) have also shown antiapoptotic activity unrelated to their MAO inhibitory activity.[21,22]

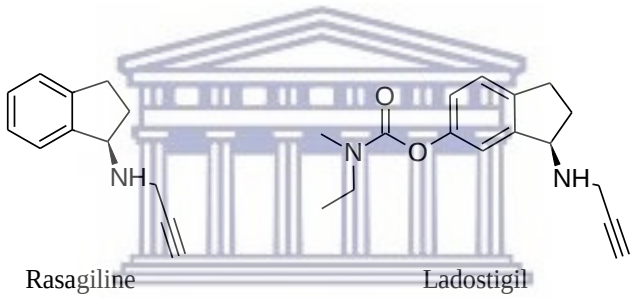

Rasagiline Ladostigil

Figure 2: Structure of the MAO inhibitor rasagiline and the MTDL ladostigil

All of the drugs presently approved for AD treatment offer transient symptomatic relief only. Current treatment options have moved towards including multiple therapies to address the varied pathological aspects of AD.[23] The multi-target-directed ligand (MTDL) approach is a promising strategy that yielded ladostigil.[24] Ladostigil or TV3326 is a neuroprotective bifunctional analogue with the aminoindan structure of rasagiline (Figure 2) and the carbamate cholinesterase inhibitory moiety of rivastigmine and physostigmine (Figure 1).[24,25] It was initially designed for AD in high doses but failed to meet its endpoint in a Phase 2b clinical trial in 2012. It is currently under investigation for mild cognitive impairment due to its neuroprotective, anti-oxidant and microglial activation abilities.[26] Various MTDL combinations featuring two or more of the following properties; MAO-, cholinesterase- and Aβ inhibition, anti-inflammatory activity, metal and iron homeostasis and anti-apoptotic activity have been described in the literature.[23,27] Recent observations have suggested that dual ChE and MAO inhibition, as is the case with ladostigil, is likely to be more effective against AD.[27] However only the *R*-enantiomer of ladostigil is active, raising issues with

synthesis and quality control. The carbamate on ladostigil is also open to acid hydrolysis and enzymatic metabolism, and once this metabolism takes place, it leaves a non-enzyme inhibiting neuroprotective molecule TV3279.[28,29] This loss of enzymatic ability may account for one of the reasons why ladostigil failed in Phase 2b AD clinical trials. In order to overcome these unfavourable properties of ladostigil, a series of compounds structurally similar to ladostigil, but based on an indole structure was designed (**1** – **8**, Figure 3 and 4). The propagylamine moiety has been shown to inhibit MAO as well as confer neuroprotection[22] and was incorporated at the *N*1 position of compounds **5** – **8** to eliminate the chirality associated with rasagiline and ladostigil. The ChE inhibiting carbamoyl moiety in the form of a diethylcarbamate/urea was conjugated at the 5 or 6 position with the aim of inhibiting ACh hydrolysis by AChE and BuChE.[30] The diethyl moeity was selected for conjugation over the methyl-ethyl moeity of ladostigil and rivastigmine. Preliminary molecular modelling studies utilising the ChE enzymes during the initial design phase of this study suggested that the diethyl moeity will show improved binding in the ChE active site pockets and stabilise the molecules leading to optimal activity. In order to prevent or slow down the *in vivo* hydrolysis associated with the carbamate function of ladostigil a urea moeity was incorporated into compounds **1**, **2**, **5** and **6**. It is expected that the urea containing compounds will be more metabolically stable than their carbamate counterparts (**3**, **4**, **7** and **8**) and lead to improved enzymatic inhibition *in vivo*. In the context of the discovery of neuroprotective agents an indole scaffold was selected because it possesses efficiency in scavenging free radicals and as an antioxidant.[31,32] The indole heterocycle has also been investigated in the design of AChE-induced Aβ aggregation and neuronal nitric oxide synthase (nNOS) inhibitors[32] and MAO-B inhibitors.[31,33]

The objective of this study was therefore to improve the inhibitory, neuroprotective and stability profile and eliminate the stereochemistry associated with rasagline and more recently, ladostigil. It is expected that these novel compounds will serve as dual AChE/BuChE and MAO-A and MAO-B inhibitors and possess similar activity with improved pharmacokinetic profiles compared to ladostigil and other related anti-AD/neuroprotective agents.

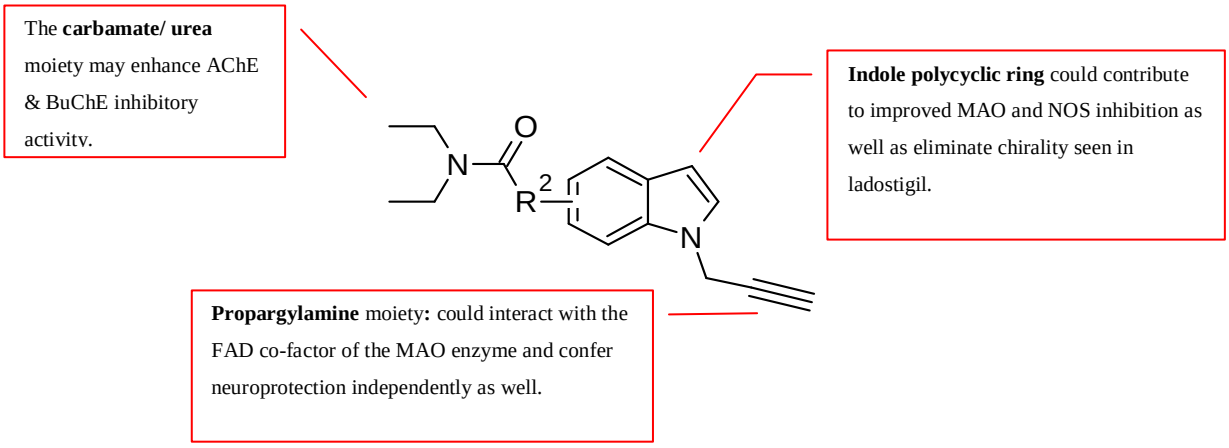

Figure 3: Design strategy for the novel indole derivatives incorporating the carbamoyl/urea and propargylamine moieties.[22, 30-32] R^2 = NH or O.

7.1.2. Results and discussion

7.1.2.1. Chemistry

The synthetic strategy developed to obtain the novel MTDLs provides several advantages, including the elimination of the chiral centre on the indane ring of rasagiline and ladostigil, easy accessibility of the final product by one step or two step processes using commercially available starting materials and simple scale-up from grams to larger quantities. The synthesis utilises the commercially available 5- or 6-hydroxy/amino indole (**1a** – **1d**) that was conjugated to a diethyl-carbamoyl chloride moiety at position 5 or 6 via a nucleophilic addition-elimination reaction using acetonitrile as solvent in the presence of potassium carbonate (**1** – **4**, Figure 4). These intermediates were then treated with sodium hydride in dimethylformamide and propargyl bromide and reacted under optimized microwave irradiation conditions (150 W, 95 °C, 2-4 hrs) to give the final compounds **5** - **8** in high yields (> 87 %).

In order to characterise the novel compounds, analytical instruments and techniques as described in the experimental section were used. Compounds with similar substitutions showed similar signal patterns on their NMR and IR spectra. The five aromatic protons of the indole were observed between 7.70 and 6.30 ppm on the ^{1}H NMR, with the carbamate/urea portion showing a triplet at around 1.25 ppm (CH_3) and a multiplet at around 3.40 ppm (CH_2). The presence of the propargyl moiety in compounds **5** - **8** was confirmed by a doublet and triplet peak at around 4.50 ppm (CH) and 2.50 ppm (CH_2) respectively. The ^{13}C NMR of the compounds showed the distinct peak of the carbonyl carbon of the carbomoyl or urea

moiety in the vicinity of 158 ppm. The molecular mass of each compound was confirmed using MS and HR-MS.

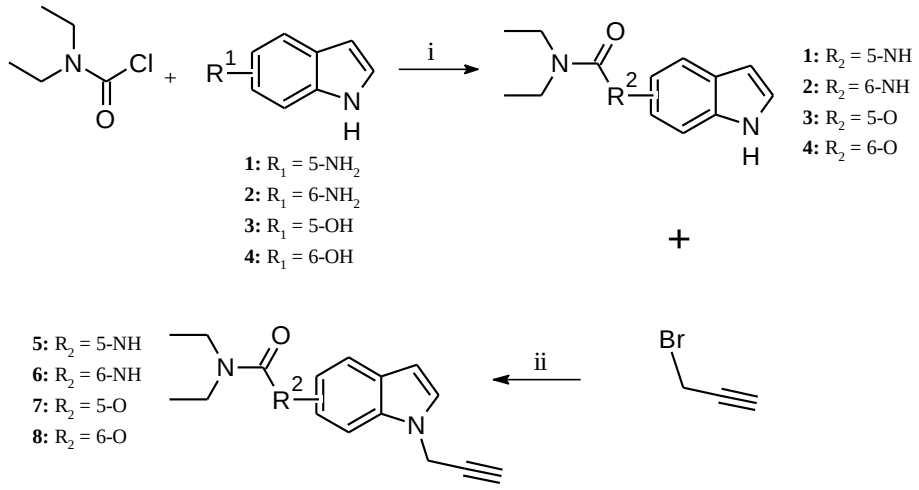

Figure 4: Synthetic pathway of the novel compounds **1** – **8.** Reagents and conditions: (i) CH_3CN, K_2CO_3, rt, 2 h; (ii) DMF, NaH, microwave (2-4 h, 95 ºC, 150 W)

7.1.2.2. Monoamine oxidase inhibition studies

The compounds were investigated for inhibition of human MAO-A and MAO-B using recombinant human enzymes. Enzyme inhibition tests of reference and test compounds were performed by a fluorescence based assay with the substrate kynuramine measuring the production of 4-hydroxyquinoline formed as a by-product of the enzymatic deamination reaction.[34] The selective inhibitors clorgiline (IC_{50} = 1.06 nM) and selegiline (IC_{50} = 20 nM) were used as the positive controls for the MAO-A and MAO-B assays respectively. IC_{50} values of the test compounds are presented in Table 1. The assay results showed that all the compounds, except **1**, had the ability to inhibit the MAO-A enzyme at concentrations below 100 µM. As observed from the IC_{50} values the compounds that did not possess the propargylamine moiety (**1** – **4**) had, in general, lower activity when compared to their propargylamine containing counterparts (**5** – **8**). Literature confirms that the propargylamine moiety is responsible for the MAO inhibitory properties of compounds containing this functional group.[29] The results obtained agree with this, as can be seen by the more potent IC_{50} values upon inclusion of this moiety. The presence of a urea moiety (compounds **5** and **6**) resulted in compounds that have comparably better inhibitory abilities than the carbamate compounds **7** and **8**. Compound **6** had the lowest IC_{50} within the series (IC_{50} = 4.31 µM) towards MAO-A. The comparable compound **8** with similar orientation, except for a

carbamate instead of the urea, is 12 times less potent (IC_{50} = 52.64 μM) towards the enzyme. This may indicate that the hydrogen donating ability of the secondary amine in the urea moieties may contribute to important interactions with amino acids in the active site of the enzyme. Overall the compounds were moderately good inhibitors of the MAO-A enzyme showing better activity compared to ladostigil *in vitro*.

Table 1: *In vitro* IC_{50} values (μM) of test compounds for hMAO-A, hMAO-B, eeAChE and eqBuChE

Compound	MAO-A	MAO-B	SI MAO-B[a]	AChE	BuChE	SI AChE[b]
1	>100	>100	n.d.	1.97	3.48	1.77
2	20.37	>100	< 0.20	2.28	4.55	2.0
3	13.15	>100	< 0.13	2.78	2.29	0.82
4	88.11	>100	< 0.88	3.72	3.18	0.86
5	33.42	28.84	1.16	2.77	3.96	1.43
6	4.31	2.62	1.65	3.70	2.82	0.76
7	99.08	16.52	6.00	2.57	3.01	1.17
8	51.64	1.84	28.06	2.41	5.01	2.08
Ladostigil[c]	>100	37.1	-	31.80	1.98	16.10

[a]hMAO-B selectivity index = IC_{50}(hMAO-A)/IC_{50}(hMAO-B); [b]AChE selectivity index = IC_{50} (eeBuChE)/IC_{50} (eqAChE); [c]IC_{50} values of ladostigil obtained from references 21 and 37; n.d. = not determined.

The results of the MAO-B assay indicated that compounds **1**-**4** had MAO-B IC_{50} values above 100 μM. These compounds did not possess the propargylamine substitution at position *N*1 and may lack vital interactions with the flavin adenine dinucleotide (FAD) co-factor as observed for the propargylamine containing compounds, rasagiline and selegiline.[29] The conjugation of the propargylamine moiety (**5**-**8**) led to a significant improvement in MAO-B inhibition. This is in line with literature that suggests that the propargylamine moiety is a good contributor towards MAO-B inhibitory capacity.[29] The compounds that contain a carbamate showed, in general, slightly better MAO-B activity (although not significantly, $p > 0.05$) compared to their urea counterparts. This is observed when compound **5** is compared with **7** and **6** with **8**. This observation may indicate that the electron accepting abilities of the oxygen molecule contributes to some interaction in the MAO-B active site. Compounds **6** and **8** had the lowest MAO-B IC_{50} values of 2.62 μM and 1.84 μM, respectively. These compounds had the carbamate/urea at the 6 position and the *N*1 propargylamine moiety similar to ladostigil. This orientation of the propargylamine to the carbamoyl/urea moiety seems to be favourable for good MAO inhibitory activity of these compounds.

7.1.2.3. MAO reversibility studies

Compound **6** was selected for MAO reversibility studies because it showed the most promising activities on both enzymes. This study aimed to investigate if the interaction between the propargyl moiety of **6** and the FAD co-factor is reversible or irreversible. For this purpose the time dependence of MAO-A and -B inhibition by compound **6** was evaluated. Recombinant human MAO-A and MAO-B was preincubated with the test compounds for periods of 0, 15, 30 and 60 min and the residual rates of the MAO-A and –B catalysed oxidation of kynuramine were measured. The concentration of compound **6** used was approximately twofold the measured IC_{50} value for the inhibition of the respective enzymes. Clorgyline and selegiline, known irreversible inhibitors of MAO-A and MAO-B respectively, were used as a reference compounds. As shown in Figure 5 and Figure 6, both clorgyline and selegiline showed a time-dependent reduction in the rates of MAO-A and –B catalysed oxidation of kynuramine, confirming irreversible inhibition. Compounds **6** also showed time-dependent reduction in the rates of MAO-A and –B catalysed oxidation of kynuramine. From these results it can be concluded that the inhibition of MAO-A and -B by compound **6** is irreversible, at least for the time period (60 min) and at the inhibitor concentrations (2 x IC_{50}) evaluated. This irreversible MAO inhibition of compound **6** indicates that the interaction between the propargyl moiety and the FAD cofactor of MAO-A and MAO-B is also present in these structures as is the case for the irreversible MAO inhibitor ladostigil.[24,25] This finding also shows that the propargylamine can be incorporated within the heterocycle and retain its irreversible MAO inhibition.

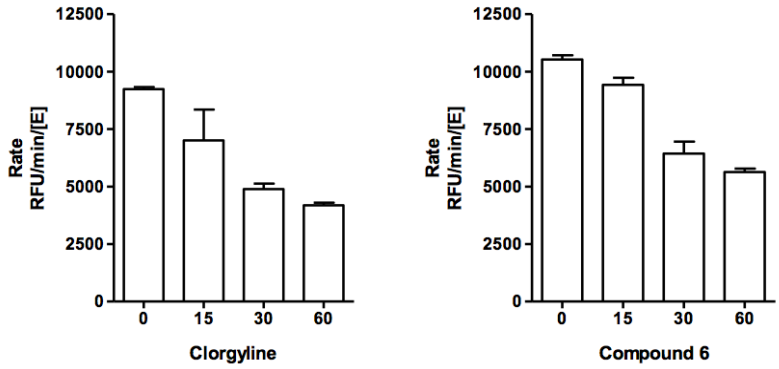

Figure 5: Time-dependent inhibition of the recombinant human MAO-A catalysed oxidation of kynuramine by clorgyline and **6**. The enzyme was preincubated for various periods of time (0–60 min, *x*-axis) with clorgyline and **6** at concentrations of 0.002 μM and 8.62 μM. The concentration of kynuramine used was 45 μM.

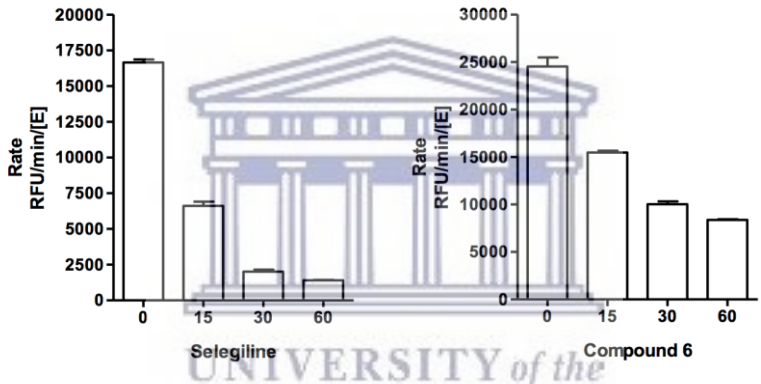

Figure 6: Time-dependent inhibition of the recombinant human MAO-B (Panel B) catalysed oxidation of kynuramine by selegiline and **6.** The enzymes were preincubated for various periods of time (0–60 min, *x*-axis) with selegiline and **6** at concentrations of 0.040 μM and 5.24 μM. The concentration of kynuramine used was 30 μM.

7.1.2.4. Cholinesterase inhibition studies

The compounds were also evaluated for inhibitory activity on eeAChE (*electric eel*) and eqBuChE (equine serum) according to Ellman's method,[36] with tacrine (AChE IC50 = 0.11 μM; BuChE IC50 = 0.017) as positive control. All the compounds were able to inhibit AChE with IC_{50} values between 1 μM and 4 μM (Table 1). This illustrates that both the carbamate and urea functional groups contributes to inhibition of the AChE enzyme. Also, the compounds exerted good activity regardless of the position of the carbamate or urea function. Addition of the propargylamine moiety did not affect the inhibitory capacity of the

compounds indicating that the carbamate and urea moieties are highly involved in activity. Comparing the IC_{50} values of the test compounds to that of ladostigil shows that the test compounds more active AChE inhibitors. The role that BuChE plays in the progression of AD is its ability to hydrolyse acetylcholine in the event of AChE saturation.[8] Accordingly, a compound that inhibits this enzyme, in addition to AChE, would prove beneficial for the treatment of AD. Carbamoyl containing compounds have also been shown to be BuChE enzyme substrates[37] and it is postulated that the diethylcarbamoyl moiety interacts with the enzyme to block its catalytic activity. The results showed that the synthesized compounds had good activity in inhibiting the BuChE enzyme with IC_{50} values between 2 and 5 μM comparable to that of ladostigil. When the different substitutions of the test compounds are compared, it is observed that the 5 substituted compounds yielded similar results compared to the 6 substituted compounds. Selectivity indices were close enough for the compounds to be classified as non-selective ChE inhibitors *in vitro* with a good balance between AChE and BuChE activities. Importantly, the compounds portray non-selective inhibitory activities compared to ladostigil, which is 16 times more selective towards BuChE over AChE *in vitro*.[21,35] Moreover, literature has reported that AChE promotes the assembly of Aβ into amyloid fibrils hence these compounds, with the improved AChE inhibitory activity compared to ladostigil, may also prove to reduce the conglomeration of amyloid fibrils into plaques in addition to reducing ACh hydrolysis.[38,39]

7.1.2.5. Molecular modelling

To provide insight, the binding mode of compounds **1-8** in hMAO-A, hMAO-B, eeAChE and eqBuChE were examined using molecular docking. The structures of human MAO-A cocrystallized with clorgiline (PDB entry: 2BXS),[40] human MAO-B co-crystallized with safinamide (PDB entry: 2V5Z)[41] and *ee*AChE co-crystallized with donepezil (PDB entry: 1EVE)[42] were retrieved from the Brookhaven Protein Data Bank (www.rcsb.org/pdb) and the docking was carried out with the Dock application of the Molecular Operating Environment (MOE) software.[43] In the absence of a X-ray structure of eqBuChE, a homology model was used to rationalize the experimental data. The modeling of the 3D structure was performed by an automated homology-modeling program (SWISS-MODEL).[44,45] The putative 3D structure of eqBuChE has been created based on the crystal structure of hBuChE (PDB: 2PM8) as these two enzymes exhibited 89% sequence identity. The docking of the compounds into this homology model of eqBuChE was carried out with Autodock Vina.[46] The docking results were analyzed with MOE.

7.1.2.5.1. MAO molecular modelling studies

Docking results showed that as expected compounds **1-4** lacked interactions with vital residues in the active site of MAO-A (Figure 7). The indole heterocyclic ring of **1-4** was best orientated towards the FAD cofactor in the substrate cavity with the diethylcabamoyl/urea moiety occupying the entrance cavity. In the compounds that contained the propargylamine moiety (**5-8**), this moiety is found within close proximity to the FAD cofactor with the rest of the molecule occupying the active site (Figure 7). This orientation has been reported to be essential for MAO inhibitory capacity.[47] The indole heterocyclic ring did not portray any significant interactions with the MAO-A active site, but the compounds were well accommodated within in the active site which may account for the good inhibitory activities observed for some of these compounds.

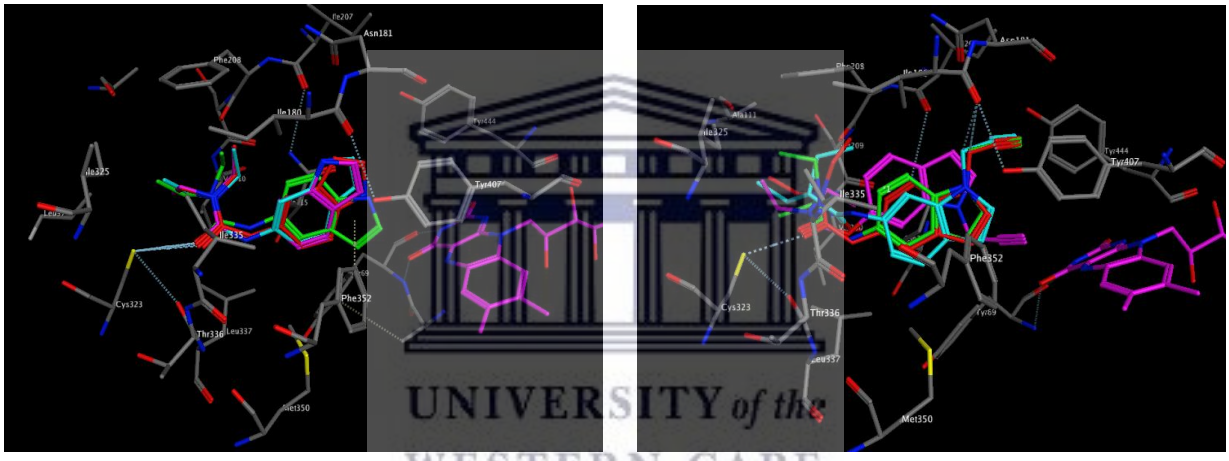

Figure 7: The MAO-A active site cavity displaying the binding and interactions of compounds **1-4** (left) and compounds **5-8** (right). Compound **1** and **5** are shown in green, compound **2** and **6** in light blue, compound **3** and **7** in red and compound **4** and **8** in magenta. The FAD co-factor is shown to the right, in magenta, in the outside of the binding pocket.

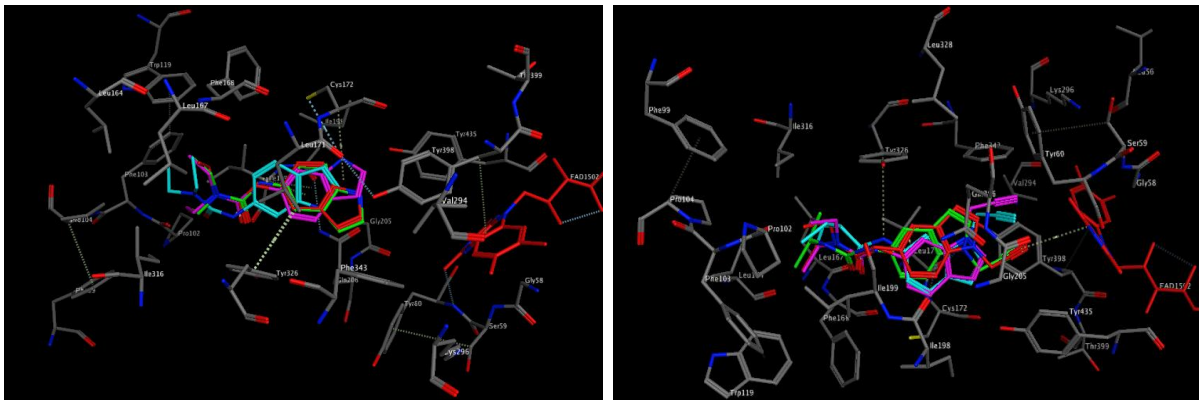

Figure 8: The MAO-B active site cavity displaying the binding and interactions of compounds **1-4** (left) and compounds **5-8** (right). Compound **1** and **5** are shown in green, compound **2** and **6** in light blue, compound **3** and **7** in red and compound **4** and **8** in magenta. The FAD co-factor is shown to the right, in red, in the outside of the binding pocket.

The MAO-B molecular docking experiments showed that compounds **1-4** were not able to reach the substrate cavity but rather maintained interactions in the entrance cavity (Figure 8). This inability of **1-4** to reach the substrate cavity may indicate the reason why these compounds did not show MAO-B activity. The propargylamine containing compounds (**5-8**) were able to reach the substrate cavity and compounds **6** and **8** showed π-H interactions between the propargylamine moiety and the FAD co-factor (Figure 8). Compounds **5** and **7** adopted an inverted orientation compared to **6** and **8**, and lacked the π-H interaction. This observation may account for the improved MAO-B inhibitory activity of the 6-substituted indole derivatives, **6** and **8** (Table 1).

7.1.2.5.2. ChE molecular modelling studies

The assay results indicated that all the compounds were able to inhibit ChE enzymes with IC_{50} values between 1 μM and 5 μM and molecular docking was employed to gain insight into the binding modes of all the compounds in the active site of AChE and BuChE. The docking results, Figure 8, showed that compounds **1-8** mainly interact within the CAS of AChE. The alkyl component of the diethyl-carbamate/urea of compounds **1-4** showed π-H interactions with Trp84 in the CAS. This interaction has been reported to be crucial for AChE inhibitory activity.[48] The indole heterocycle of **1-4** mainly sits in the active site gorge and does not occupy the PAS. The indole moiety of compounds **5-8** possesses π-π stacking interactions with Trp334 and Phe330 (a key residue involved in ligand binding in the active gorge).[49] The interaction with Trp84 was also observed for compounds **5-8**. This may explain why the good inhibitory activities were retained across the series. It is important to note that

the propargylamine moiety does not show any significant interactions with amino acids in the active site but occupied the gorge facing the PAS.

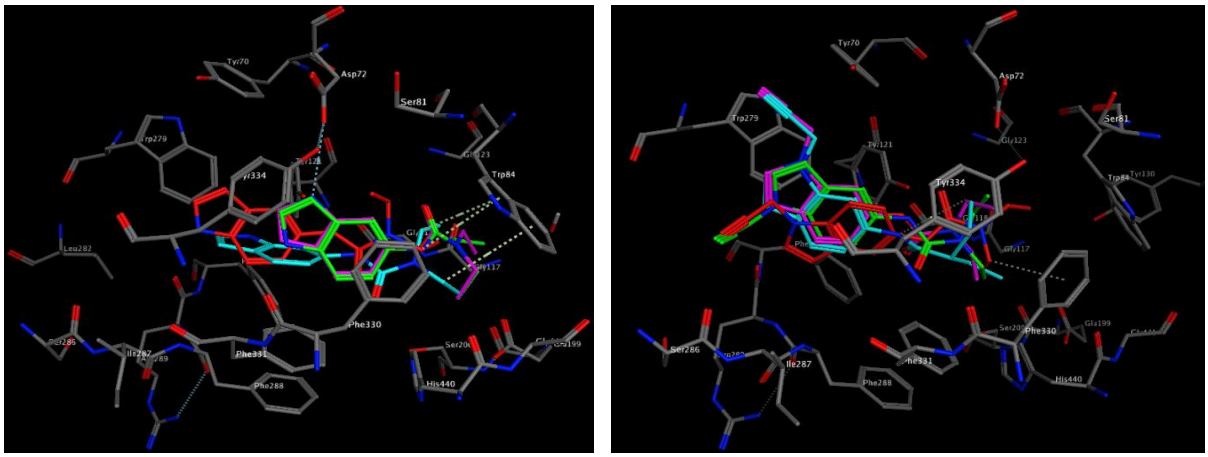

Figure 8: The AChE active site cavity displaying the binding and interactions of compounds **1**-**4** (left) and compounds **5**-**8** (right). Compound **1** and **5** are shown in green, compound **2** and **6** in light blue, compound **3** and **7** in red and compound **4** and **8** in magenta.

The binding mode of the non-propargyl containing compounds, **1**–**4**, at the active site of the eqBuChE homology model are illustrated in Figure 9. The docking results showed that the lowest energy binding orientation all four compounds adopted a similar conformation with the indole moiety forming π-π stacking interactions with Phe329 in the anionic site of the enzyme. The diethylcarbamate/urea moiety binds in the CAS region of the enzyme,[50] establishing π-π stacking interactions with Trp82 and a hydrogen bond interaction with His438 of the catalytic-triad. The propargylamine containing compounds, **5**-**8**, were all well accommodated inside the active site gorge showing similar orientations. The lowest energy binding orientations enabled the indole moiety to interact with Trp82 and His438 in the CAS through π-π stacking interactions. The diethyl-carbamate/urea moiety is orientated away from the CAS region and forms an interaction with Trp231. The *N*1-propargyl substitution caused these molecules to adopt an inverted orientation compared to their non-propargyl containing counterparts. However, even though the adopted orientation is significantly different important interactions were still retained and may account for the similar BuChE activity observed for compounds **5**-**8** compared to **1**-**4**.

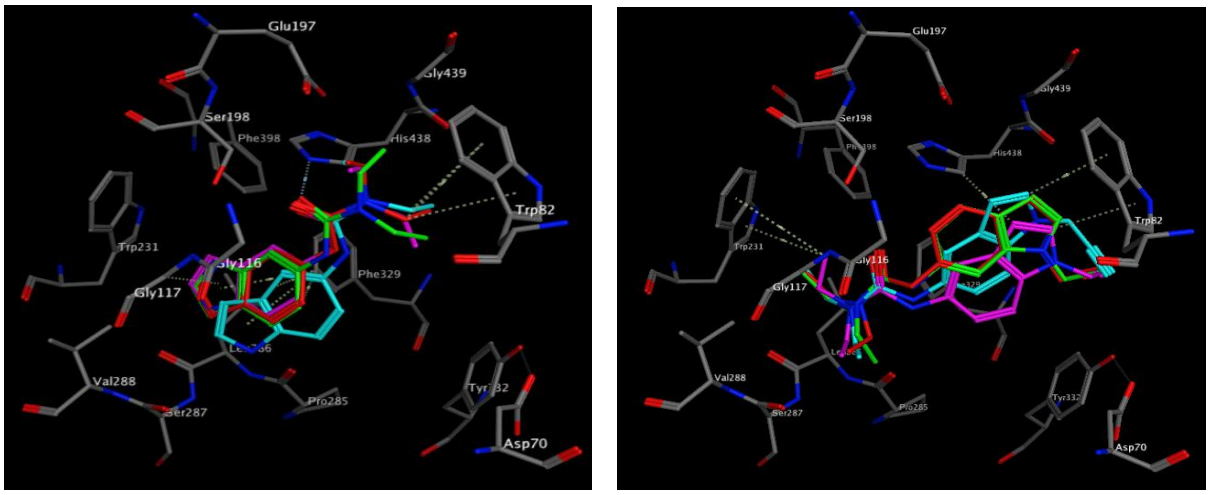

Figure 9: Overlays of compounds **1**-**4** (left) and compounds **5**-**8** (right) in complex with the eqBuChE homology model. Compound **1** and **5** is shown in green, compound **2** and **6** in light blue, compound **3** and **7** in red and compound **4** and **8** in magenta.

7.1.2.6. Chemical stability study

Chemical stability of pharmaceutical molecules is a matter of great importance as it ultimately affects the stability and efficacy of the final drug product. One of the drawbacks of the carbamate of ladostigil is its liability to rapid hydrolysis in acidic conditions. *In vivo* ladostigil undergoes rapid acid and enzyme hydrolysed metabolism into a non-enzyme inhibiting neuroprotective molecule TV3279.[27,28] Considering that compounds **1 - 8** contain a carbamate or urea that may affect stability and ultimately metabolism, it was decided to employ a forced chemical degradation test to study the stability of these moieties in both acidic and alkaline conditions. Compounds **6** and **8** were selected for stability testing because they contained both the carbamoyl/urea and propargylamine moiety and portrayed good activity as either a urea (**6**) or carbamate (**8**) derivative. The forced degradation study was done according to the slightly modified method of Blessy *et al*., 2014.[51] The test compound (1 mg /ml) were dissolved in aqueous 0.1 M HCl or 0.1 M NaOH with DMF (5 %) as co-solvent. The test solutions were kept at 37 ºC in an incubator for 7 days and sampled on days 0, 1, 3, 4 and 7. UV/vis absorbance of the sample was measured at maximal wavelengths of 232 nm for **6** and 234 nm for **8**. It is important to note that both the urea and carbamate functional groups undergo hydrolysis but at different rates.[52] Figure 10 shows the results of the compounds **6** and **8** after 7 days in 0.1 M HCl and 0.1 M NaOH. Compound **6** displayed an almost linear degradation rate compared to **8** that portrayed a more rapid decay. From these results, it is evident that the carbamate derivatives are less stable than their urea containing counterparts. Ladostigil is a carbamate compound and could act similarly to **8** in acidic conditions. Following this logic, urea (**6**) should prove to be more stable than the

carbamate derived ladostigil. This should minimise the metabolic effects that induce rapid hydrolysis to prevent limiting factors such as a short half-life and the rapid formation of non-inhibiting metabolites. The compounds behaved in a similar manner in alkaline conditions. At this stage we are not informed as to the activity of the metabolites of the compounds, but like rasagiline and ladostigil whose metabolites portray neuroprotective activity[21,27]; the compounds described in this paper may act in a similar manner.

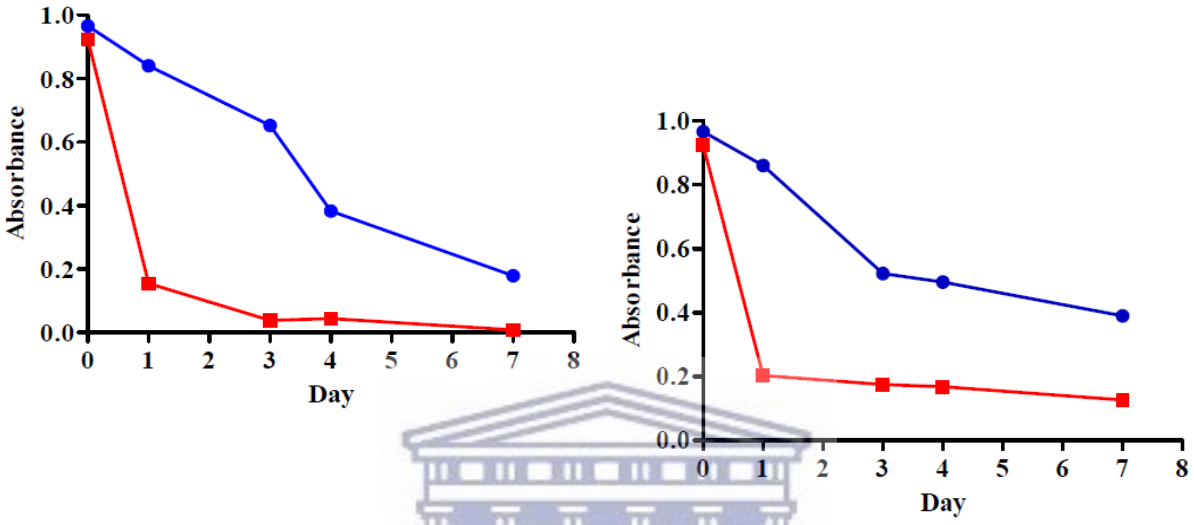

Figure 10: Forced degradation results of compounds **6** (blue) and **8** (red) in acidic (left) and alkaline (right) conditions.

7.1.2.7. SH-SY5Y cell viability studies

In order to investigate the influence of the test compounds on neuronal cell viability, SHSY5Y cells were treated with various concentrations (10 µM, 50 µM and 100 µM) of compounds **2** and **6** for 48 hours and evaluated using the 3-[4,5-dimethylthiazol-2-yl]-2,5-diphenyl tetrazolium bromide (MTT) assay.[53] Compound **6** was chosen for this assay as it showed the most promising inhibitory activity on all enzymes tested and contained both the more stable urea functional group and the *N*1-propargyl moiety. Compound **2** was included to explore the influence of the *N*1-propargyl moiety. Exposure of SH-SY5Y cells to compounds **2** and **6** lead to a reduction in cell viability in a concentration-dependent manner (Figure 11). At 10 µM the compounds did not show any significant ($p > 0.05$) effect on cell viability. In general, based on this preliminary data, compound **6** seems to be slightly less toxic than compound **2** at the three concentrations tested. Another finding from these studies is that the CC_{50} values of both compounds **2** and **6** on SH-SY5Y human neuroblastoma cells are more than 100 µM. This indicates that at the concentrations where especially compound **6** inhibit

ChE and MAO (IC_{50} values less that 5 μM, see table 1) it will have very limited toxicity towards human cells.

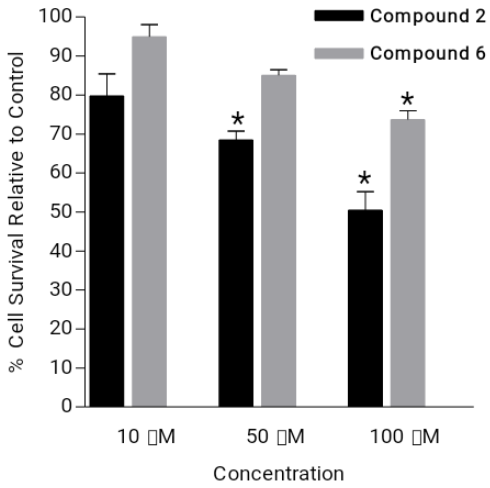

Figure 11: Cellular viability of SH-SY5Y cells treated with compounds **2** and **6** at 10 μM, 50 μM and 100 μM for 48 hours. Data is presented as mean ± SEM. Significance is set at a level of *p<0.05 compared to vehicle treated control cells (taken as 100 % cell viability).

Based on the SH-SY5Y cytotoxicity analysis it was decided that the MPP^+ neuroprotection studies would be done at compound concentrations between 1 μM and 10 μM in order not to significantly affect the viability of the cells. MPP^+ is highly toxic to neurons and has been widely used to induce neurodegeneration in various *in vitro* and *in vivo* models.[54,55] Several signaling pathways have been suggested to be responsible for MPP^+-mediated neurotoxicity in SH-SY5Y cells, for instance, trigger of oxidative stress,[56] induction of apoptosis,[57] and inactivation of pro-survival phosphoinositide 3-kinase (PI3-K)/Akt cascade.[58-60] This assay was deemed appropriate to test for initial neuroprotective ability of compounds **2** and **6** because of the multitude of pathways involved in MPP^+ mediated neurotoxicity and the multifunctional enzyme inhibitory abilities of the test compounds, especially **6**. SH-SY5Y cells were exposed to the neurotoxin MPP^+ with or without test compound, and cell viability was evaluated using the MTT mitochondrial function assay.[53] As illustrated in Figure 12, after the exposure to 1000 μM MPP^+ for 48 hours, the cell viability declined significantly to 52.78 ± 7.35 %. However, its cytotoxic effects were ameliorated in the presence of compounds **2** and **6** at 1 μM, 5 μM and 10 μM concentrations. The compounds, at a 1 μM concentration, restored cell survival to 84.32 ± 4.62 % and 107.40 ± 6.26 %, respectively. At 5 μM and 10 μM a slight decrease in cytoprotection, although still significant ($p < 0.05$), was observed for **2** and **6**. This may indicate that in the neurotoxin challenged state the SH-SY5Y

cells may be more sensitive to the cytotoxic effect of the test compounds. Therefore, **2** and **6** might have enhanced the toxicity of the neurotoxin which resulted in lower neuroprotection values observed at higher concentrations. Compound **6** containing the propargyl substitution at the *N*1 position showed significantly improved cytoprotection ($p < 0.05$) at all three concentrations tested compared to compound **2** which is devoid of the propargyl substitution. This observation confirms that the propargyl function improves the neuroprotective ability of these compounds in this assay. Thus, in general and especially at a 1 µM concentration, these compounds, and particularly **6**, exerted highly significant cytoprotection against MPP^+ insults to the SH-SY5Y neural cells.

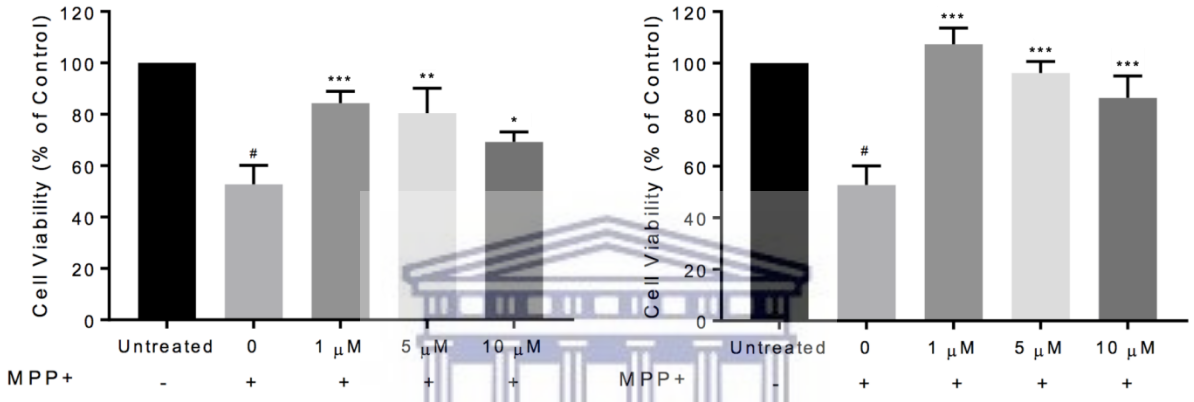

Figure 12: The effects of compounds **2** (left) and **6** (right) on MPP^+-induced (1000 µM) cytotoxicity in SH-SY5Y cells. The viability of untreated controls was defined as 100%. The level of significance for the test compounds is set at $^{\#}p<0.05$ compared to the MPP^+ only treated control (0). Statistical analysis (Tukey post hoc test) was performed on raw data, with asterisks signifying significant cytoprotection. *p<0.05; **p<0.001; ***P<0.0001. Data are expressed as means ± S.D. (n = 12).

7.1.2.8. *In silico* ADMET studies

Selected ADMET properties of compounds **6**, **8** and ladostigil were calculated using webbased applications. Compounds **6** and **8** were selected because they contained both the propargylamine- and urea/carbamate moiety similar to ladostigil and showed the most promising activities within the series. Blood–brain barrier (BBB) penetration, human intestinal absorption (HIA), Caco-2 cell permeability, logP and AMES test were calculated using https://preadmet.bmdrc.kr. The predicted ADMET data is summarized in Table 2. Based on the predicted values for BBB penetration, both compounds **6** and **8** should be able to penetrate into the central nervous system. It is interesting to note that compound **6**, the most active compound in the series, should show better BBB penetration than **8** and ladostigil based on the BBB penetration and logP values. The compounds were also predicted to be

well absorbed based on the human intestinal absorption and Caco-2 permeability predictions. Moreover, the compounds did not show mutagenic effect with respect to the AMES test data. This data has significance indicating that the new compounds should have good ADMET profiles thus encouraging further drug design and development endeavours. The improved stability of compound **6** combined with the best overall predicted ADMET properties provide further evidence that it is a promising compound for further development.

Table 2: Predicted ADMET properties of selected compounds.

Compound	BBB penetration	HIA[b] (%)	Caco-2 permeability[c]	LogP	AMES toxicity[d]
6	2.10	96.13	42.12	3.18	None
8	0.47	99.55	53.80	2.95	None
Ladostigil	0.99	95.47	33.81	2.40	None

[a]BBB penetration parameters; <0.1 = low penetration; 0.1 – 2 = medium penetration; >2 = high penetration. [b]Human intestinal absorption; values of > 70 % = high absorption. [c]Values between 4 and 70 indicates medium cell penetration. [d]Mutagenic potential of chemicals.

7.1.3. Conclusion

The main objective of this study was to design a series of compounds with improved pharmacokinetic properties compared to ladostigil able to inhibit hMAO-A, hMAO-B, eeAChE and eqBuChE and provide neuroprotection. The results obtained indicate that the compounds act as dual ChE and MAO inhibitors. Molecular modelling showed significant interactions with vital resides in the active sites of the enzymes. Compound **6** was identified as a potent MTDL (IC_{50}; MAO-A = 4.31 μM, MAO-B = 2.62 μM, AChE = 3.70 μM, BuChE = 2.82 μM) with AChE and MAO-B inhibitory activity 9 and 14 times that of ladostigil respectively (Table 1). Compound **6** also showed irreversible inhibition of MAO, similar to that reported for ladostigil. The results of the chemical stability tests showed that **6** is also more stable than the carbamate compound **8** by virtue of possessing the urea functional group. Compound **6** would thus probably prove more chemically and metabolically stable than ladostigil and lead to better enzymatic inhibition *in vivo* which may provide improved ability to treat AD. Elimination of the stereochemistry associated with ladostigil was also achieved while maintaining and even improving neuronal enzyme inhibitory activities. Compound **6** also exerted highly significant cytoprotection towards MPP^+ insults to the SHSY5Y neural cells and can thus be considered for optimisation and perhaps development

as a multipotent drug molecule against Alzheimer's- and/or other neurodegenerative disease(s).

Further investigations exploring the pharmacokinetics and *in vivo* activities as well as further mechanism of action studies are recommended for these compounds.

7.1.4. Experimental

7.1.4.1. Chemistry

Unless otherwise specified, materials were obtained from commercial suppliers and used without further purification. All reactions were monitored by thin-layer chromatography on 0.20 mm thick aluminium silica gel sheets (Alugram® SIL G/UV_{254}, Kieselgel 60, Macherey-Nagel, Düren, Germany). Visualisation was achieved using UV light (254 nm and 366 nm), an ethanol solution of ninhydrin or iodine vapours, with mobile phases prepared on a volume-to-volume basis. Chromatographic purifications were performed on silica gel (0.063–0.2 mm, Sigma Aldrich) except when otherwise stated. The MS spectra were recorded on a Perkin Elmer Flexar SQ 300 mass spectrometer by means of direct injection with a syringe pump. High resolution electron spray ionisation (HREI) mass spectra for all compounds were recorded on a Waters API Q-Tof Ultima mass spectrometer at 70 eV and 100 °C. The IR spectra were recorded on a Perkin Elmer Spectrum 400 spectrometer, fitted with a diamond attenuated total reflectance (ATR) attachment. Melting points were determined using a Stuart SMP-300 melting point apparatus and capillary tubes. All the melting points determined were recorded uncorrected. ^{1}H and ^{13}C NMR spectra were determined using a Bruker Avance III HD spectrometer at a frequency of 400 MHz and 100 MHz, respectively. Tetramethylsilane (TMS) was used as internal standard. All chemical shifts are reported in parts per million (ppm), relative to the internal standard. The following abbreviations are used to indicate the multiplicities of the respective signals: s - singlet; s - broad singlet; d - doublet; dd - doublet of doublets; t – triplet and m - multiplet.

General procedure for the synthesis of compounds 1-4

The appropriate amino- or hydroxylindole (1 mmol) was conjugated to carbomoyl chloride at position 5 or 6 in a 1:1 ratio, using acetonitrile (10 ml) and 1.2 mmol K_2CO_3. The mixture was stirred for 2 hours at room temperature. Once the reaction was complete the mixture was filtered to remove the K_2CO_3 and the solvent removed *in vacuo*. An extraction was carried

out using DCM (3 x 15 ml). The organic phase was further washed with brine and water. The DCM was removed *in vacuo* to render a blackish waxy product which was purified via column chromatography (1:2 hexane: ethyl acetate) rendering the products as pure amorphous solids.

***N,N*-Diethyl-*N*'-1H-indol-5-ylurea (1)**

Yield: 74 %; **mp**: 143 ºC; **Rf**: 0.68; **^{1}H NMR**: (400 MHz, $CDCl_3$) □H: 7.89 (s, 1 H, H – 4), 7.49 - 7.47 (d, 1 H, J = 8.4 Hz, H – 7), 7.11 – 7.10 (t, 1 H, J = 5.6; 2.8 Hz, H – 2), 6.77 – 6.75 (dd, 1 H, J = 4.8; 2.4 Hz, H – 6), 6.45 – 6.34 (m, 1 H, H – 3), 3.42 – 3.37 (m, 4 H, H – 14; 16), 1.26 – 1.24 (t, 6 H, J = 8.0; 4.0 Hz, H – 15, 17); **^{13}C NMR** (100 MHz, CD_3OD): 158.15, 137.74, 134.54, 126.26, 125.37, 120.74, 116.81, 106.73, 102.10, 42.43, 14.12; **IR** (FT – IR, cm^{-1}): 3247.42, 2978.13, 1220.22; **MS** (EI, 70 ev) m/z: 232.10 $(M+H)^+$; HR-ESI $[M+H]^+$: calcd. 232.1443, found. 232.1447.

***N,N*-Diethyl-*N*'-1H-indol-6-ylurea (2)**

Yield: 52 %; **mp**: 141 ºC; **Rf**: 0.71; **^{1}H NMR**: (400 MHz, $CDCl_3$) □H: 7.63 (s, 1 H, H – 7), 7.28 - 7.26 (d, 1 H, J = 8.0 Hz, H – 5), 7.16 – 7.15 (d, 1 H, H – 4), 6.47 – 6.46 (t, 1 H, J = 4.8; 2.4 Hz, H – 2), 6.26 (m, 1 H, H – 3), 3.42 – 3.37 (m, 4 H, H – 14; 16), 1.26 – 1.22 (t, 6 H, J = 14.4; 7.2 Hz, H – 15, 17); **^{13}C NMR** (400 MHz, CD_3OD): 153.69, 126.35, 123.97, 121.48, 121.23, 114.60, 106.23, 97.42, 36.97, 13.41; **IR** (FT – IR, cm^{-1}): 3288.30, 2922.65, 1760.52, 1217.09; **MS** (EI, 70 ev) m/z: 232.15 $(M+H)^+$; HR-ESI $[M+H]^+$: calcd. 232.14443, found. 232.1442.

1H-Indol-5-yl-diethylcarbamate (3)

Yield: 81 %; **mp**: 126 ºC; **Rf**: 0.71; **^{1}H NMR**: (400 MHz, CD_3OD) □H: 7.19 – 7.8 (d, 1 H, J = 8.8 Hz, H – 7), 7.14 - 7.13 (d, 1 H, J = 2.8 Hz, H – 4), 6.92 – 6.91 (d, 1 H, J = 4.0 Hz, H – 2), 6.60 – 6.40 (dd, 1 H, J = 8.8; 2.4 Hz, H – 6), 6.27 – 6.25 (dd, 1 H, J = 3.2; 0.8 Hz; H – 3), 3.21 – 3.16 (m, 4 H, H – 14; 16), 1.13 – 1.09 (t, 6 H, J =14.4; 6.8 Hz, H – 15, 17); **^{13}C** NMR (400 MHz, CD_3OD): 158.38, 137.79, 134.52, 126.28, 125.43, 120.71, 116.83, 106.66, 102.06, 42.47, 14.13; **IR** (FT – IR, cm^{-1}): 3298.82, 2971.20, 1210.75; **MS** (EI, 70 ev) m/z: 233.11 $(M+H)^+$; HR-ESI $[M+H]^+$: calcd. 233.1285, found. 233.1289.

1H-Indol-6-yl-diethylcarbamate (4)

Yield: 80 %; **mp**: 159 ºC; **Rf**: 0.67; **^{1}H NMR**: (400 MHz, $CDCl_3$) □H: 7.63 – 7.26 (d, 1 H, J = 1.6 Hz, H – 7), 6.95 – 6.94 (d, 1 H, J = 2.0 Hz, H – 4), 6.68 – 6.65 (dd, 1 H, J = 8.4; 2.0 Hz, H – 5), 6.48 – 6.46 (t, 1 H, J = 6.4; 3.2 Hz, H – 2), 6.38 – 6.36 (m, 1 H, H – 3), 3.43 – 3.37 (m, 4 H, H – 14; 16), 1.26 – 1.22 (t, 6 H, J =14.4; 6.8 Hz, H – 15, 17); **^{13}C NMR** (400 MHz,

CD_3OD): 158.52, 137.78, 134.55, 125.36, 122.75, 120.76, 116.79, 106.73, 101.26, 42.39, 14.08; **IR** (FT – IR, cm^{-1}): 3253.61, 1683.13, 1215.52; **MS** (EI, 70 ev) m/z: 233.13 $(M+H)^+$; HR-ESI $[M+H]^+$: calcd. 233.1285, found. 233.1287.

General procedure for the synthesis of compounds 5-8

Compounds **5 - 8** were synthesized by conjugating the propargyl bromide (1.2 mmol) to position *N*1 of the synthesized compounds, **1** – **4** (1 mmol). This mixture was stirred at room temperature in the presence of NaH (1 mmol) and dimethylformamide (10 ml) and irradiated under microwave conditions (95 °C, 150 W) for 2 to 4 hours. Once the reaction was complete water (30 ml) was added followed by at least five extractions with ethyl acetate (5 x 15 ml). Thereafter the organic phase was washed with brine and water. The ethyl acetate was removed *in vacuo* to render the pure products as amorphous solids.

***N,N*-Diethyl-*N*'-[1-(prop-2-yn-1-yl)-1H-indol-5-yl]urea (5)**

Yield: 95 %; **mp**: 158 ºC; **^{1}H NMR**: (400 MHz, $CDCl_3$) □H: 7.64 – 7.63 (d, 1 H, J = 1.6 Hz, H – 4), 7.29 – 7.27 (d, 1 H, J = 8.8 Hz, H – 7), 7.15 – 7.14 (m, 2 H, J = 10.4 Hz, H – 2, 6), 6.47 – 6.46 (t, 1 H, J = 1.0, 2.0 Hz, H – 3), 4.12 – 4.11 (d, 2 H, J = 4.0 Hz, H – 18), 3.42 – 3.37 (m, 4 H, H – 14; 16), 2.22 – 2.20 (t, 1 H, J = 4.8; 2.4 Hz), H – 20), 1.26 – 1.23 (t, 6 H, J =14.0; 6.8 Hz, H – 15, 17); **^{13}C NMR** (400 MHz, CD_3OD): 157.03, 153.96, 147.94, 139.35, 126.21, 120.56, 114.78, 110.24, 109.63, 105.20, 97.47, 43.55, 11.50; **IR** (FT – IR, cm^{-1}): 3293.69, 2922.34, 1761.13, 1217.23; **MS** (EI, 70 ev) m/z: 270.94, $(M+H)^+$; HR-ESI $[M+H]^+$: calcd. 271.1441, found. 271.1439.

***N,N*-Diethyl-*N*'-[1-(prop-2-yn-1-yl)-1H-indol-6-yl]urea (6)**

Yield: 87 %; **mp**: 166 ºC; **^{1}H NMR**: (400 MHz, CD_3OD) □H: 7.42 – 7.40 (m, 2 H, H – 7, 4), 7.15 – 7.14 (d, 1 H, J = 3.8 Hz, H – 3), 6.94 – 6.92 (d, 1 H, J = 8.4 Hz, H – 5), 6.37 – 6.36 (d, 1 H, J = 3.2 Hz, H – 2), 4.10 – 4.09 (d, 2 H, J = 4.0, H – 18), 3.46 – 3.41 (m, 4 H, H – 14, 16), 2.18 – 2.16 (t, 1 H, J = 8.0; 4.0, H – 20); 1.23 – 1.19 (t, 6 H, J =14.4; 6.8 Hz, H – 15, 17); **^{13}C NMR** (400 MHz, CD_3OD): 157.13, 139.29, 127.18, 126.16, 120.56, 114.69, 110.23, 109.85, 105.26, 102.33, 97.49, 43.46, 11.61; **IR** (FT – IR, cm^{-1}): 3300.95, 3194.06, 2927.43, 1210.50; **MS** (EI, 70 ev) m/z: 271.15 $(M+H)^+$; HR-ESI $[M+H]^+$: calcd. 271.1441, found. 271.1443.

1-(Prop-2-yn-1-yl)-1H-indol-5-yl-diethylcarbamate (7)

Yield: 94 %; **mp**: 187 ºC; **^{1}H NMR**: (400 MHz, CD_3OD) □H: 7.50 – 7.46 (d, 1 H, J = 16.0 Hz, H – 7), 7.24 – 7.19 (dd, 2 H, J = 19.2; 3.2 Hz, H – 4, 6), 7.16 – 7.13 (dd, 1 H, J = 10.4; 1.6 Hz, H – 2), 6.41 – 6.37 (dd, 1 H, J = 15.6; 2.8 Hz, H – 3), 4.96 – 4.95 (d, 2 H, J = 4.0, H – 18); 3.45 – 3.40 (m, 4 H, H – 14; 16), 2.79 – 2.78 (t, 1 H, J = 4.8; 2.4 Hz, H – 20), 1.23 – 1.19 (t, 6 H, J = 14.4; 7.2 Hz, H – 15, 17); **^{13}C NMR** (400 MHz, CD_3OD): 158.52, 135.13, 132.06, 129.38, 125.73, 120.36, 116.34, 114.23, 111.79, 107.90, 102.34, 101.38, 42.32, 14.13; **IR** (FT – IR, cm^{-1}): 3299.52, 3195.74, 1210.83; **MS** (EI, 70 ev) m/z: 270.11 $(M+H)^+$; HR-ESI $[M+H]^+$: calcd. 270.1601, found. 270.1599.

1-(Prop-2-yn-1-yl)-1H-indol-6-yl-diethylcarbamate (8)

Yield: 95 %; **mp**: 168 ºC; **^{1}H NMR**: (400 MHz, CD_3OD) □H: 7.47 – 7.46 (dd, 1 H, J = 4.0, 2.0 Hz, H – 7), 7.39 – 7.36 (d, 1 H, J = 12.0 Hz, H – 4), 7.24 – 7.23 (d, 1 H, J = 4.0 Hz, H – 5), 7.20 – 7.19 (d, 1 H, J = 4.0 Hz, H – 2), 6.43 – 6.33 (m, 1 H, H – 3), 4.96 – 4.95 (d, 2 H, J = 4.0 Hz, H – 18); 3.46 – 3.40 (m, 4 H, H – 14,16), 2.79 – 2.70 (t, 1 H, J = 8.0; 4.0 Hz, H – 20), 1.23 – 1.21 (t, 6 H, J = 8.0; 4.0 Hz, H – 15, 17); **^{13}C NMR** (400 MHz, CD_3OD): 158.76, 135.15, 132.05, 129.32, 126.16, 126.08, 124.58, 119.97, 116.27, 111.79, 102.32, 101.29, 42.52, 14.14; **IR** (FT – IR, cm^{-1}): 3291.83, 2922.52, 1761.08, 1217.03; **MS** (EI, 70 ev) m/z: 270.59 $(M+H)^+$; HR-ESI $[M+H]^+$: calcd. 270.1601, found. 270.1609.

7.1.4.2. Biological evaluation

Recombinant human MAO-A and MAO-B inhibition studies

Stock solutions of the test compounds and controls (clorgiline for MAO-A and selegiline for MAO-B) were prepared by dissolving the test compounds in DMSO and it was kept under refrigeration until use. The solutions were made at 10 mM concentrations and further serial diluted to achieve final concentrations of 100 µM, 10 µM, 1 µM, 0.1 µM and 0.01 µM. The potassium phosphate buffer was prepared in water at a concentration of 100 mM (adjusted to pH 7.4 by 2 N NaOH). It was also refrigerated until use. The stock solution of the substrate kynuramine was made at 750 µM (45 µM final assay concentration) for MAO-A and 500 µM (30 µM final assay concentration) for MAO-B. Using the phosphate buffer, MAO enzyme stock solution was prepared and stored in aliquots at -80 ºC until use. To each vial 207.5 µL of phosphate buffer and 2.5 µL of corresponding test compound or control compound was added. This was followed by 25 µL of the enzyme at 10 second intervals. The mixture was then incubated for 10 minutes at 37 ºC. Thereafter 15 µL of kynuramine was added also at 10

second intervals and it was then further incubated for 20 minutes. 150 µL of 2 N NaOH were used to stop the reaction. Finally, 200 µL of the mixture was added to each well of a black 96 well plate, placed in the fluorescent plate reader and read at excitation/emission wavelength of 310 nm/400 nm. Each assay was run in triplicate and the data was analysed with Graph Pad Prism 7 software (San Diego, CA, USA).

Time-dependent MAO inhibition studies

To investigate whether the observed enzyme inhibition is reversible or irreversible, time-dependant inhibition studies were carried out with the active inhibitors. Recombinant human MAO-A or human MAO-B (0.03 $mg.ml^{-1}$) were preincubated for periods of 0, 15, 30, 60 min at 37 °C. The concentrations of inhibitor in these incubations were twofold the measured IC_{50} values for the inhibition of MAO. The incubations were carried out in potassium phosphate buffer (100 mM, pH 7.4, made isotonic with KCl). A final concentration of 45 µM kynuramine for MAO-A and 30 µM kynuramine for MAO-B were then added to the preincubated enzyme preparations and the resulting reactions were incubated at 37 °C for 15 min. The final volumes of these incubations were 250 µl and the final concentration of the inhibitors were approximately equal to the IC_{50} values for the inhibition of the respective enzyme. The final enzyme concentrations of the MAO preparations were 0.015 $mg.ml^{-1}$. The reactions were terminated with 100 µL NaOH (2 N) and a volume of 600 µL distilled water was added to each reaction. The rates of formation of 4-hydroxyquinoline were measured and quantified as described above. All measurements were carried out in triplicate and are expressed as mean ± SD.

Cholinesterase inhibition studies

AChE from electric eel, BuChE from equine serum, S-butyrylthiocholine iodide (BTCI), acetylthiocholine iodide (ATCI), 5,5′-dithiobis-(2-nitrobenzoic acid) (Ellman's reagent, DTNB), donepezil and tarcine hydrochloride were purchased from Sigma-Aldrich. The inhibitory activities of the test compounds were evaluated by Ellman's method.[36] The compounds were dissolved in DMSO and diluted with the buffer solution (50 mM Tris–HCl, pH = 8.0) to yield the corresponding test concentrations (DMSO less than 0.01%). In each well of the plate, 160 µl of 1.5 mM DTNB, 50 µl of AChE (0.22 U/ml eeAChE) or 50 µl of BuChE (0.12 U/ml eqBuChE) were incubated with 10 µl of different concentrations of test compounds (0.01–100 µM) at 37 °C for 10 min. After this period, ATCI (15 mM) or BDCI (15 mM) as the substrate (30 µl) was added, incubated for a further 10 minutes, and thereafter the absorbance was measured at a wavelength of 405 nm at different time intervals (0, 60,

120, and 180 s). IC_{50} values were calculated as concentration of the compound that produces 50 % enzyme activity inhibition, using the Graph Pad Prism 7 software (San Diego, CA, USA).

SH-SY5Y cell viability assays

Cell line and culture conditions

The human neuroblastoma cell line SH-SY5Y was generously donated by our collaborator at the Division of Molecular Biology and Human Biology, Stellenbosch University, Tygerberg, Cape Town. Cells were cultured in monolayer using Dulbeco Modified Eagles Medium (DMEM, Gibco, Life Technologies Ltd) supplemented with 10% foetal bovine serum (FBS, Gibco, Life Technologies Ltd.) and 1% 100 U/mL penicillin and 100 µg/mL streptomycin (Lonza Group Ltd., Base Switzerland). Cells were grown at 37 °C, in a humidified atmosphere consisting of 5% CO_2 and 95% air. Media was replaced every two to three days and cells were sub-cultured by splitting with trypsin (Lonza Group Ltd., Basel Switzerland).

MTT cytotoxicity assay

The 3-[4,5-dimethylthiazol-2-yl]-2,5-diphenyl tetrazolium bromide (MTT) is a yellow tetrazolium salt that is reduced to purple formazan in the presence of living cells. This assay which measures cell metabolic activity was used to determine cytotoxicity as described by Mosmann, (1983).[53] Briefly, SH-SY5Y cells were plated in flat bottom 96 well plates in growth medium as stated above at a density of 7,500 cells/well. Cells were allowed to adhere to the plate surface for 24 hours and used media were replenished with fresh media containing test compounds at 10 µM, 50 µM and 100 µM. Vehicle control cells were treated with dimethyl sulfoxide (DMSO, solvent for dissolving test compounds) at a concentration similar to the amount contained in the highest concentration of test compounds. After 48 hours, 10 µL of MTT solution (5 mg/mL) was added to each well and incubated for 4 hours and the purple formazan formed was solubilized with 100 µL DMSO and plates were read spectrophotometrically to determine absorbance at 570 nm using a BMG Labtech Omega® POLARStar multimodal plate reader.

MPP$^+$-induced cytotoxicity in SHSY-5Y cells

SH-SY5Y cells were seeded onto a 96-well plate and treated with 1000 μM MPP$^+$ for approximately 48 hours. Different concentrations (1 μM, 5 μM, 10 μM) of test compounds were administrated two hours prior to MPP$^+$ treatment. Afterwards, cell viability was measured by MTT colorimetric assay and performed as stated above

7.1.4.3. Molecular modelling studies

MAO docking studies

Computer-assisted docking was carried out using the CHARMm force field and hMAO-A co-crystallized with clorgiline (PDB ID: 2BXS)[40] and hMAO-B co-crystallized with safinamide (PDB ID: 2V5Z)[41], which were recovered from the Brookhaven Protein Database (www.rcsb.org/pdb). Docking simulations were performed on the test compounds using Molecular Operating Environment (MOE)[43] with the following protocol. (1) Enzyme structures were checked for missing atoms, bonds and contacts. (2) Hydrogens and partial charges were added using the protonate 3D application in MOE. (3) The ligands were constructed using the builder module and were energy minimized. (4) Ligands were docked within the MAO-A or MAO-B active sites using MOEDock application, the poses were generated by the Triangle Matcher placement method. (5) The retained best poses were visually inspected and the interactions with binding pocket residues were analyzed. To determine the accuracy of this docking protocol, the co-crystallised ligand, clorgiline (PDB ID: 2Z5X), was re-docked into the MAO-A active site and the co-crystallised ligand, safinamide (PDB ID: 2V5Z), was re-docked into the MAO-B active site. This procedure was repeated three times and the best ranked solutions of clorgiline and safinamide exhibited RMSD values of less than 2 Å from the position of the co-crystallised ligand for MAO-A and MAO-B, respectively. In general, RMSD values smaller than 2.0 Å, indicate that the docking protocol is capable of accurately predicting the binding orientation of the co-crystallised ligand.[63,64] These protocols were thus deemed to be suitable for the docking of inhibitors into the active site models of MAO-A and MAO-B.

Acetylcholinesterase docking studies

The dock function of MOE[43] was used to predict the interactions and binding modes of the synthesized inhibitors in the *ee*AChE active site. The crystal structure of the *ee*AChE protein co-crystallized with donepezil was acquired from the Protein Data Bank (PDB ID: 1EVE).[42] The docking procedure followed the same protocol as described for the MAO docking. To determine the accuracy of this docking protocol, the co-crystallised ligand, was re-docked into the AChE active site. This procedure was repeated three times and the best ranked solution exhibited an RMSD value of 1.15 Å from the position of the co-crystallised ligand. The RMSD value in this case is smaller than 2.0 Å indicating that the docking protocol is capable of accurately predicting the binding orientation of the co-crystallised ligand.[60,61] This protocol was thus deemed to be suitable for the docking of inhibitors into the active site model of AChE.

Butyrylcholinesterase docking studies

Because no X-ray structure exists for eqBuChE, a homology model was used to rationalize the experimental data. The eqBuChE model was retrieved from the SWISS-MODEL Repository. This is a database of annotated three-dimensional comparative protein structure models generated by the fully automated homology-modeling pipeline SWISS-MODEL. A putative three-dimensional structure of eqBuChE has been created based on the crystal structure of hBuChE (PDB ID: 2PM8), these two enzymes exhibited 89% sequence identity. Proper bonds, bond orders, hybridization and charges were assigned and CHARMm force field was applied using MOE.[43] The prepared protein was directly loaded into AutoDockTools (ADT; version 1.5.4), hydrogens were added and partial charges for proteins and ligands were calculated using Gasteiger charges. Flexible torsions in the ligands were assigned with the AutoTors module, and the acyclic dihedral angles were allowed to rotate freely. Docking calculations were performed with the program Autodock Vina.[46] Because VINA uses rectangular boxes for the binding site, the box center was defined and the docking box was displayed using ADT. All dockings were performed as blind dockings where a cube of 75 Å with grid points separated by 1 Å, was positioned in the middle of the protein (x = 29.885; y = -54.992; z = 58.141). Default parameters were used except num_modes, which was set to 40. The lowest docking-energy conformation was considered as the most stable orientation. Finally, the docking results generated were analysed using MOE.

Acknowledgements

We are grateful to Dr Edith Antunes for assistance with the NMR experiments as well as the University of the Western Cape and the National Research Foundation of South Africa for financial support.

Author Contributions

I.D. and J.J. conceived of the presented idea. I.D. took the lead in writing the manuscript. I.D. performed the ChE and MAO inhibition assays. I.D. and J.J. performed the *in-silico* studies. F.T.Z., S.I.O., A.B.E. and O.E.E. planned and carried out the cytotoxicity and neuroprotection assays. S.F.M. and J.J. supervised the findings of this work. All authors discussed the results and contributed to the final manuscript.

References

1. Goedert, M and Spillantini, M. *Science*. 2006; 5800 (314): 777–781

2. Spencer, PS and Schaumberg, HH. *Experimental and clinical Neurotoxicology*. 2nd ed. United States: Oxford University Press; 2000.

3. Bartus, RT. *Experimental Neurology*. 2000; 1632: 495–529.

4. Christen, Y. *Am. J. Clin. Nutr*. 2000; 712: 621S–9S

5. Hardy, J. *Curr. Alzheimer Res*. 2006; 31: 71–73.

6. Talesa, VN. *Mech. Ageing Dev*. 2001; 122: 1961–1969.

7. Parnetti, L, Senin, U, Mecocci, P. 1997; 53: 752–768.

8. Giacobini, E. *Pharmacol. Res.* 2004; 504: 433–440.

9. Mesulam, M, Guillozet, A, Shaw, P, *et al. Neuroscience*. 2002; 1104: 627–639.

10. Greig N, Utsuki T, Ingram D, Wang Y, *et al. Proc. Natl Acad. U. S. A*. 2005; 102: 17213-17218.

11. Youdim, MBH and Bakhle, YS. *Br. J. Pharmacol*. 2006; 147S1: S287–S296.

12. Youdim, MBH, Edmondson, D and Tipton, KF. *Nat. Rev. Neurosci.* 2006; 74: 295–309.

13. Riederer P, Youdim MB, Rausch WD, *et al. J. Neural. Transm*. 1978; 43: 217–26.

14. Sonsalla PK, Golbe LI. *Clin. Neuropharmacol*. 1988; 11: 500–11.

15. Burke, W, Li, S, Chung, H, Rugiero, D *et al. Neurotoxicology*. 2004; 251 (2): 101–115.

16. Nicotra, A, Pierucci, F, Parvez, H and Parvez, H. *Neurotoxicology*. 2004; 251 (2): 155–165.

17. Zhou G, Miura Y, Shoji H, Yamada S, Matsuishi T. *J. Neurol. Neurosurg. Psychiatry.* 2001; 70: 229– 31.

18. Johnston, J. *Biochem. Pharmacol.* 1968; 17: 1285-1297.

19. Kalaria, RN, Mitchell, MJ and Harik, SI. *Brain.* 1988b; 111 (6): 1441-1451.

20. Collins, G, Sandler, M, Williams, E. and Youdim, M. *Nature*. 1970b; 225: 817-820.

21. Sterling, J, Herzig, Y, Goren, T, Finkelstein, N, *et al. J. Med. Chem*. 2002; 4524: 5260–5279.

22. Bar-Am, O, Weinreb, O, Amit, T and Youdim, MBH. *FASEB J*. 2005; 19(13): 1899-901.

23. Geldenhuys, WJ, Youdim, MBH, Carroll, RT and Van der Schyf, CJ. *Prog. Neurobiol.* 2011; 944: 347–359.

24. Yogev-Falach, M, Bar-Am, O, Amit, T, Weinreb, O and Youdim, MB. *FASEB J*. 2006a; 2012: 2177–9.

25. Avraham Pharma. Ladostigil background. http://www.avphar.com/ladostigil/background/; 2016: Accessed 3 November 2016.

26. Cavalli, A, Bolognesi, ML, Minarini, A, Rosini, M, *et al. J. Med. Chem.* 2008; 513: 347 372.

27. Zhang, H.-Y. *FEBS Letters.* 2005; 57924: 5260–5264.

28. Panarsky, R, Luques, L and Weinstock, M. *Neuroimmune Pharmacology*, 2012; 72: 488-498.

29. Norberto, F, Santos, S, Iley, J, Silva, D and Corte Real, M. *J. Braz. Chem. Soc*. 2007; 181: 171-178.

30. Giacobini, E. *Int. J. Geriatr. Psychiatry*. 2003; 18S1: S1–S5.

31. Fernández García, C, Marco, J and Fernández-Alvarez, E. *Eur. J. Med. Chem.* 1992; 279: 909-918.

32. Buemi, MR, De Luca, L, Chimirri, A, Ferro, S, *et al. Bioorg. Med. Chem*. 2013; 2115: 4575–4580.

33. Bellik, L., Dragoni, S., Pessina, F., Sanz, E., Unzeta, M. and Valoti, M. *Acta Biochim. Pol*. 2010; 572: 235–239.

34. Krajl, M. *Biochem. Pharmacol.* 1965; 1411: 1684–1685.

35. Wang, Y, Sun, Y, Guo, Y, Wang, Z, Huang, L and Li, X. *J. Enzyme Inhib. Med. Chem.* 2016; 30 (3) 389-397.

36. Ellman G, Courtney K, Andres V, Featherstone R. *Biochem. Pharmacol*. 1961; 7: 88-95.

37. Colovic, MB, Krstic, DZ, Lazarevic-Pasti, TD, Bondzic, AM and Vasic, VM. *Curr. Neuropharmacol.* 2013; 113: 315-335.

38. Inestrosa, NC, Alvarez, A, Pérez, CA, Moreno, RD, *et al. Neuron.* 1996; 164: 881–891.

39. Reyes, A, Perez, D, Alvarez, A, Garrido, J, *et al. Biochem. Biophys. Res. Commun.* 1997; 2323: 652-655.

40. De Colibus, L, Li, M, Binda, C, Lustig, A, Edmondson, DE and Mattevi, A, *Proc. Natl Acad. U. S. A.* 2005; 102 (36): 12684-12689.

41. Binda C, Wang J, Pisani L, Caccia C, Carotti A, Salvati P *et al. J. Med. Chem.* 2007; 50: 5848-5852.

42. Kryger G, Silman I, Sussman J. *Structure.* 1999; 7: 297-307.

43. Molecular Operating Environment MOE, Version 2015.10. http//www.chemcomp.com.

44. Arnold K, Bordoli L, Kopp J, Schwede T. *Bioinformatics* 2005; 22: 195-201.

45. Kiefer F, Arnold K, Kunzli M, Bordoli L, Schwede T. *Nucleic Acids Res.* 2009; 37: D387-D392.

46. Trott Olson A. J. *Comput. Chem.* 2009; 31: 455-461.

47. Edmondson, D. *Neurotoxicology*. 2004; 251 (2), 63–72.

48. Tougu, V. *Curr. Med. Chem.: Cent. Nerv. Syst. Agents.* 2001; 12: 155–170.

49. Ordentlich, A, Barak, D, Kronman, C, *et al. J. Biol. Chem.* 1993; 26823: 17083-17095.

50. Bajda, M., Więckowska, A., Hebda, M., *et al. Int. J. Mol. Sci.* 2013; 143: 5608-5632.

51. Blessy, M, Patel, R, Prajapati, P and Agrawal, Y. *J. Pharm. Anal.* 2014; 43: 159-165.

52. Armstrong, V, Farlow, D and Moodie, R. *J. Chem. Soc. B.* 1968; 0: 1099.

53. Mosmann T. *J Immunol Methods.* 1983; 65: 55–63.

54. Cui, W, Zhang, Z, Li, W, Hu, S, *et al. Br. J. Pharmacol*. 2013; 168: 1201-1214.

55. Jantas, D, Greda, A, Golda, S, Korostynski, M, *et al. Neuropharmacology*. 2014; 83: 36 53.

56. Pyszko, J, Strosznajder, JB. *Mol. Neurobiol.* 2014 50: 38-48.

57. Wang, Y, Gao, J, Miao, Y, Cui, Q, *et al. J. Mol. Neurosci*. 2014 53: 537-545.

58. Nakaso, K, Tajima, N, Horikoshi, Y, *et al. Biochim. Biophys. Acta.* 2014 1842: 1303-1312.

59. Tasaki, Y, Omura, T, Yamada, T, Ohkubo, T, *et al. Brain Res*. 2010 1344: 25-33.

60. Zhu, G, Wang, X, Wu, S and Li, Q. *Neurochem. Int.* 2012 60: 400-408.

61. Binda C, Li M, Hubalek F, Restelli N, Edmondson D, Mattevi A. *Proc. Natl. Acad. Sci. U. S. A.* 2003 100: 9750-9755.

62. Boström J, Greenwood J, Gottfries J. *J. Mol. Graphics Modell.* 2003 21: 449-462.

7.2. Versatility of 7-substituted coumarin molecules as antimycobacterial agents, neuronal enzyme inhibitors and neuroprotective agents

Article published on 30 September 2017

Molecules 2017, 22, 1644. DOI: 10.3390/molecules22101644

Versatility of 7-substituted coumarin molecules as antimycobacterial agents, neuronal enzyme inhibitors and neuroprotective agents

Erika Kapp [1], Hanri Visser [2], Samantha L. Sampson [2], Sarel F. Malan [1], Elizabeth M. Streicher [2], Germaine B. Foka [1], Digby F. Warner [3], Sylvester I. Omoruyi [4], Adaze B. Enogieru [4], Okobi E. Ekpo [4], Frank T. Zindo [1] and Jacques Joubert. [1*]

[1]*School of Pharmacy, Faculty of Natural Sciences, University of the Western Cape, Cape Town, Bellville 7550, South Africa;*

[2]*DST/NRF Centre of Excellence in Biomedical Tuberculosis Research, SA MRC Centre for Tuberculosis Research, Division of Molecular Biology and Human Genetics, Faculty of Medicine and Health Sciences, University of Stellenbosch, Cape Town, Tygerberg 7505, South Africa;*

[3]*Medical Research Council/National Health Laboratory Service/University of Cape Town Molecular Mycobacteriology Research Unit, Department of Science and Technology/National Research Foundation Centre of Excellence for Biomedical Tuberculosis Research, Institute of Infectious Disease and Molecular Medicine and Department of Clinical Laboratory Sciences, University of Cape Town, Cape Town, Rondebosch 7700, South Africa;*

[4]*Department of Medical Biosciences, University of the Western Cape, Cape Town, Bellville 7550, South Africa;*

***** *Correspondence: jjoubert@uwc.ac.za; Tel.: +27-21-959-2195*

Graphical Abstract

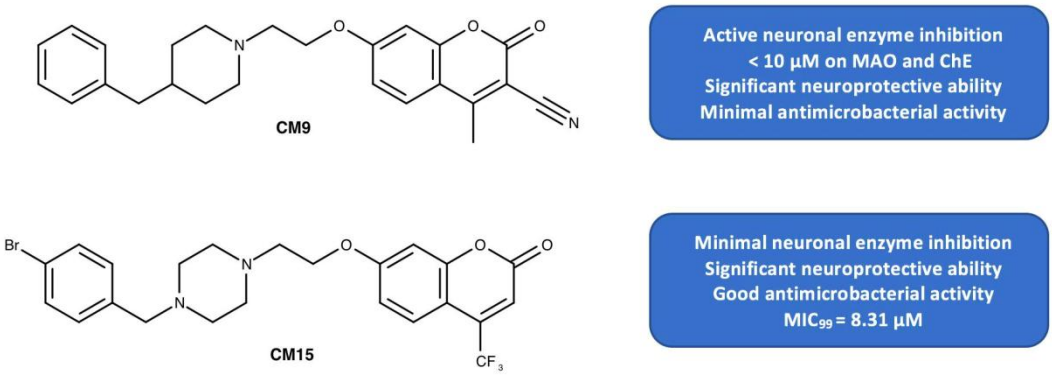

Abstract

An *in vitro* medium-throughput screen using *M. tuberculosis* H37Rv was employed to screen an in-house library of structurally diverse compounds for antimycobacterial activity. From this initial screen, eleven 7-substituted coumarin derivatives with confirmed monoamine oxidase-B and cholinesterase inhibitory activities, demonstrated growth inhibition of more than 50% at a 50 µM concentration. This prompted further exploration of all the 7-substituted coumarins in our library, nineteen in total, as potential antimycobacterial agents. Four derivatives showed promising antimycobacterial activity with MIC_{99} values of 8.31 – 29.70 µM and 44.15 – 57.17 µM on *M. tuberculosis* H37Rv in independent assays using Gaste-Fe and 7H9 + OADC media, respectively. These compounds were found to bind to albumin which may explain the variations in MIC between the two assays. Preliminary antimycobacterial evaluation of moxifloxacin resistant *M. tuberculosis* show that these compounds are able to maintain their activity in fluoroquinolone resistant mycobacteria. Analysis of structure activity relationships for antimycobacterial *versus* neuronal enzyme inhibitory activity indicate that structural modification on position 4 and/or 7 of the coumarin scaffold may be utilized to improve selectivity towards either inhibition of neuronal enzymes or antimycobacterial effect. Cytotoxicity evaluations of the compounds indicate moderate cytotoxicity with slight selectivity towards mycobacteria. Further neuroprotective assays on SH-SY5Y human neuroblastoma cells indicate significant neuroprotection for selected compounds irrespective of their neuronal enzyme inhibitory properties. These coumarin molecules are thus interesting lead compounds that may provide insight into the design of new antimicrobacterial and neuroprotective agents.

Keywords: coumarin; *Mycobacterium tuberculosis*; cholinesterase inhibitor; monoamine oxidase B inhibitor; Structure-activity relationship; albumin binding, neuroprotection

7.2.1. Introduction

Progressive development of resistance to various chemotherapeutic agents used in the management of infectious diseases presents a very serious problem in global public health. Natural products have yielded various classes of effective antimicrobials over the last few decades and continue to play a large role in the identification of novel lead molecules for this purpose [1].

A large variety of coumarin derivatives have been isolated from natural products and an array of pharmacological activities have been described for these, as well as related synthetic coumarins [2, 3]. The ability of the coumarin moiety to form several possible interactions with a particular binding site (including hydrogen bonds, electrostatic, π-π and hydrophobic interactions) likely stabilize target binding and contribute to the versatile pharmacological profile of coumarin derivatives. Both the type and placement of functional groups on the coumarin scaffold determine the specific activity of the given derivative [2-4].

Antibacterial and more specifically, antimycobacterial activity are amongst the pharmacological effects that have been described for a range of structurally diverse coumarin derivatives. One prominent example of a coumarin based antibacterial is novobiocin. Novobiocin, the structurally related chlorobiocin as well as coumermycin A_1 are 3-amino-4,7-dihydroxycoumarin derivatives, alternatively referred to as the classical aminocoumarin antibiotics. Classical aminocoumarins act as competitive inhibitors of bacterial topoisomerase, more precisely DNA gyrase [5, 6]. Competitive inhibition of DNA gyrase by the classical aminocoumarin antibiotics results from an overlap in binding sites between the sugar moiety of the aminocoumarins (Figure 1, numbered in blue) and the adenine ring of ATP which is required for the gyrase activity [7]. The non-classical aminocoumarin, simocyclinone D8 (Figure 1), lacks the 7-aminosugar moiety and inhibits bacterial DNA gyrase through simultaneous binding to two alternate binding pockets *via* interactions with the coumarin moiety and a terminal angucyclinone group. Simocyclinone D8 thus has a unique mechanism of action, despite structural similarities to the standard aminocoumarins [8-10]. Similarly, differences in the binding sites between the fluoroquinolone antibiotics (e.g. moxifloxacin which primarily inhibits topoisomerase IV but also interacts with gyrase) allow fluoroquinolone antibiotics to maintain potency in aminocoumarin resistant bacteria and *vice versa* [5, 6, 11]. Mycobacterial gyrase, which is a validated drug target in *Mycobacterium tuberculosis*, is also the likely target for the fluoroquinolone class antibiotics as *M. tuberculosis* does not express the topoisomerase IV enzyme [12].

Apart from an interaction with gyrase, bacterial DNA helicase is another suggested target of selected coumarin derivatives [13-15]. Similar to other non-classical coumarin antibiotics, the 7-position on these coumarin derivatives does not contain an amino sugar, but rather a moiety able to undergo hydrophobic interactions with the target site [13-15]. Compound **22** (Figure 1), a 4,8–dimethyl-3-propionic acid coumarin derivative with a 2-(4-chloro[1,1-biphenyl]4-yl)ethyl substitution on the 7-position was the most active helicase inhibitor in this series of 7-substituted biphenyl coumarin derivatives [14]. In this series, the methyl

substitution in position 4 of the coumarin structure drastically increased the anti-helicase activity of the compounds.

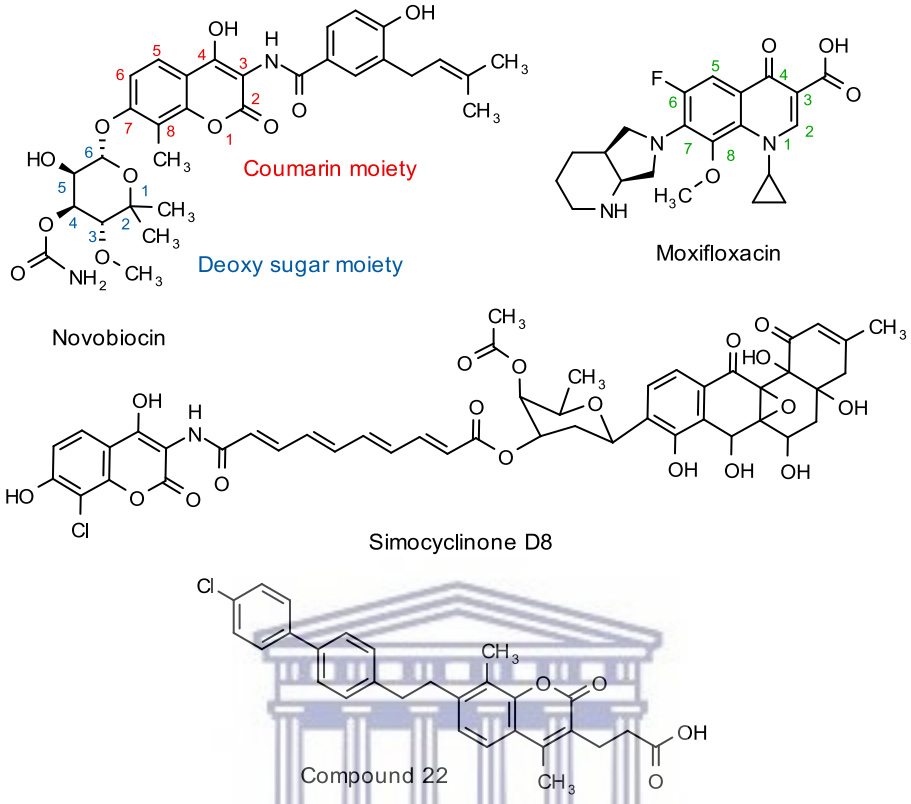

Figure 1: Molecular structure of novobiocin, moxifloxacin, simocyclinone D8 and Compound **22** as examples of antimicrobial coumarin derivatives.

Various reports have been published on coumarin derivatives with antimycobacterial activity. Although most studies adequately describe and quantify the activity for respective series of coumarin derivatives, differences in assay methods prevent a direct comparison of antimycobacterial activity of these molecules. Novobiocin as discussed above, demonstrated a minimum inhibitory concentration (MIC) of approximately 6.5 µM in the standard laboratory strain of *M. tuberculosis*, H37Rv [16]. Figure 2 depicts some of the most active compounds in their particular series as evaluated in *M. tuberculosis*. Compound **3** [17] was identified as a likely mycobacterial gyrase inhibitor whereas inhibition of FadD32, an enzyme involved in mycolic acid biosynthesis, was confirmed as target for compound 6 [4]. Mechanisms of action were not suggested for compounds **1** [18], **2** [19], **4** [20] and **5** [21].

As can be expected for compounds which do not necessarily attain their antimycobacterial effect through interaction with the same target sites, structural features important for activity differ between the respective series of compounds. Ultimately, various types and combinations of substitutions on all but position 1 and 2 of the coumarin scaffold yielded

generally effective antimycobacterials, though possibly through different mechanisms of action. This versatile nature of the coumarin scaffold may promote interaction with unique, or possibly multiple targets within the mycobacterial bacilli.

Unfortunately, structure activity relationships for the activity of various classes of coumarin derivatives (e.g. central nervous system acting, anticoagulant and anti-cancer agents) often overlap with that for potent antimicrobial activity [3, 22]. A number of review papers describe the importance of coumarin compounds in the field of neurodegenerative disorders where they have shown inhibitory properties towards monoamine oxidases, cholinesterases, β- and γ-secretase and other targets involved in the progression of neurodegenerative disorders [23-25]. Similarly, coumarin derivatives described in this article also demonstrated neuronal enzyme inhibitory properties [26]. Therefore, the effective utilization of the coumarin scaffold may essentially be hampered by its versatility unless sufficient selectivity can be ensured. Early identification and structure activity relationship evaluation of alternative pharmacological effects, over-and-above standard cytotoxicity assays, may increase the viability of coumarin-based antimycobacterial and/or neuroprotective agents.

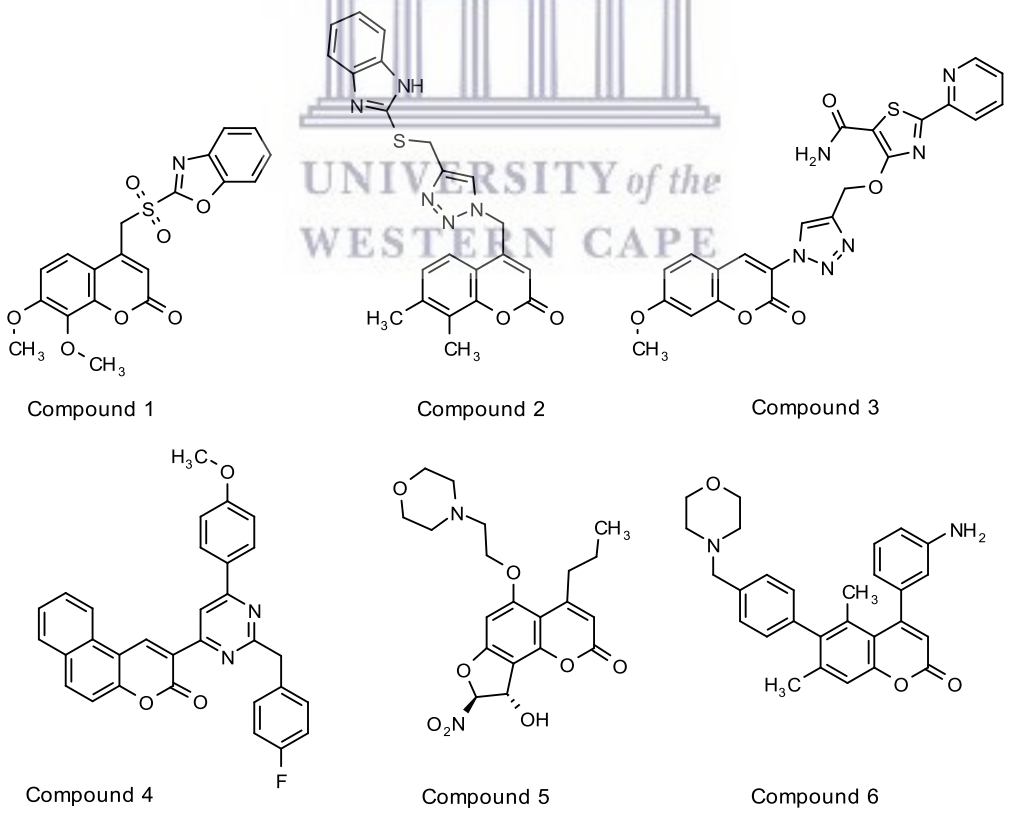

Figure 2: Selected coumarin derivatives demonstrating promising *M. tuberculosis* activity across various assays.

As part of a collaborative project, a number of 7-substituted coumarin derivatives initially designed and synthesized as multifunctional neuronal enzyme inhibitors [26], were found to exhibit promising antimycobacterial activity (see Table 1) The compounds, originally designed to incorporate coumarin structures known to show monoamine oxidase B (MAO-B) inhibition [27] and selected structural elements of donepezil, a selective acetylcholinesterase (AChE) inhibitor [28], were able to selectively inhibit human MAO-B as well as electric eel AChE and equine butyrylcholinesterase (BuChE) [26]. Further evaluation of the structure activity relationships for selectivity and specific characteristics of these compounds were therefore required in order to assess the viability of the compounds as neuronal enzyme inhibitors and/or antimycobacterial clinical agents. This article describes the antimycobacterial activity, plasma protein binding properties, cytotoxicity and neuroprotection data for the series of neuronal enzyme inhibitors. Preliminary evaluations on antimycobacterial activity in drug resistant *M. tuberculosis* are described and structure activity relationships for neuronal enzyme inhibition *versus* antimycobacterial activity as well as a paired analysis of the neuroprotective properties of selected derivatives are discussed.

7.2.2. Results and discussion

7.2.2.1. Medium Throughput Screen

A medium throughput screen (MTS) of various compounds from the University of the Western Cape, School of Pharmacy, drug-design compound library was done to identify novel antimycobacterial agents. A large proportion of the compounds which demonstrated potential antimycobacterial activity in the initial MTS, were coumarin derivatives. A total of 11 coumarin derivatives inhibited more than 50% mycobacterial growth at 50 µM. Table 1 provides the structures and activity of two series of coumarin derivatives **CM1**–**CM19** identified in the MTS, as classified based on the substitution on the 7-position of the coumarin scaffold. The compound numbering from our library was maintained and the derivatives sorted in order of potency within their respective series. Antimycobacterial activity is indicated as the percentage mycobacterial growth on day 5 at 100 µM, 50 µM and 1 µM of the respective derivatives.

Based on this screen, series 1 seems to contain more potent inhibitors of *M. tuberculosis* with the p-bromo-*N*-benzylpiperizine derivatives demonstrating higher activity than the benzyl substituted piperidine derivatives. The exception to this is **CM13** with a chloro substitution on the R^3 position which reduces the antimycobacterial activity of the compound in this

whole cell assay. Interestingly the chloro substitution on R^3 improves the activity in the piperidine type compound, though it should be noted that the simultaneous removal of the bromine substitution may have contributed to the change in activity. The small activity differences between the 6 most active compounds in series 1 do not allow for prediction of structure activity relationships within this range. It would however seem that the p-bromo-*N*-benzylpiperizine derivatives can tolerate various large and small substitutions in position 4 of the coumarin scaffold relatively well. No significant differences in activity were observed between the trifluoromethane, methyl or unsubstituted 4-substituted coumarin derivatives for this series. This is not the case with series 2, where the trifluoromethane group in position 4 of the coumarin scaffold seems to decrease the activity when compared to a methyl substitution in this position. The most active compound in series 2 is the R^2-methyl substituted benzyl-ether (**CM17**) followed by a similar bromobenzyl-ether (**CM2**). Replacement of the hydrogen in position 3 of the coumarin scaffold with a nitrile moiety does not seem to influence activity, but a chloro-substitution in this position decreases activity similar to what was observed for the p-bromo-*N*-benzylpiperizine derivatives in series 1. The combination of halogens in R^1 and R^3 with a methyl substitution on R^2 seems to decrease activity in both series 1 and 2. Comparison of the compounds evaluated in this study with other antimycobacterial coumarin derivatives described in literature (see Figure 2, section 1) highlighted minor similarities and trends. Many of the more active derivatives described in literature only have small groups substituted at positions 5, 6, 7 and 8 of the coumarin scaffold whereas the compounds evaluated in this study carry the larger substitution at 7 position. Bisubstitution on these positions seem to increase activity. Compound **1** [18], a 4-substituted sulfonyl-benzoxazole derivative was more active when substituted with methoxy groups in both the 7 and 8 positions of the coumarin, than single- or unsubstituted derivatives. Compound **2** [19], a 4-substituted, triazole-linked benzimidazole coumarin with methyl groups at the 5, 7 or 7, 8 positions on the coumarin scaffold similarly demonstrated the highest activity in its series. A common trend for most of these derivatives seems to be a large functional group on position 3 or 4 of the coumarin moiety. Compound **3** [17], bearing a triazole ring on the 3 position of the coumarin scaffold, was able to achieve and MIC value of 6.5 µM. Compound **4** [20], also with a large group on position 3, was the most active in a series of 3-substituted benzocoumarin-pyrimidine hybrid molecules. Series 1 derivatives evaluated in this study likewise seem to tolerate large substitutions on position 3 with no significant differences in activity between substituted or unsubstituted derivatives.

Table 1: Molecular structure and activity of coumarin derivatives series 1 and 2

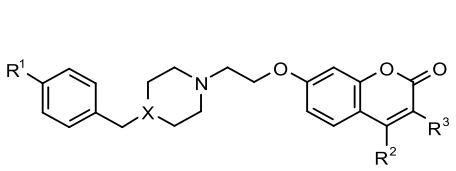

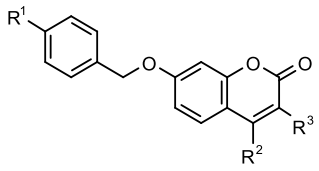

Series 1					Series 2		
					% *M. tuberculosis* Growth, Day 5		
Number	**X**	**R¹**	**R²**	**R³**	**100 μM**	**50 μM**	**1 μM**
Series 1							
CM12**	N	Br	CH_3	H	3.93	4.35	95.23
CM14**	N	Br	CH_3	CN	4.44	4.40	99.53
CM8**	CH	H	CH_3	Cl	4.62	5.69	93.59
CM15**	N	Br	CF_3	H	4.88	6.68	106.71
CM11*	N	Br	H	H	4.46	7.05	95.18
CM9*	CH	H	CH_3	CN	6.19	7.75	92.82
CM7*	CH	H	CH_3	H	8.18	29.50	95.10
CM6	CH	H	H	H	15.43	52.71	98.19
CM13*	N	Br	CH_3	Cl	32.06	42.47	97.03
Series 2							
CM17*		H	CH_3	H	19.81	28.65	97.59
CM2*		Br	CH_3	H	33.16	40.86	89.98
CM4*		Br	CH_3	CN	33.52	44.60	95.27
CM5		Br	CF_3	H	56.09	65.04	106.87
CM19		H	CH_3	CN	55.44	66.92	98.28
CM16		H	H	H	50.66	72.70	97.53
CM1		Br	H	H	63.63	79.77	96.28
CM18		H	CH_3	Cl	75.52	87.91	97.30
CM3		Br	CH_3	Cl	92.86	96.11	97.82

**Compounds that underwent further analysis; **Compounds selected for MIC determination*

In addition to substitutions on position 4, compounds **5** and **6** carries larger morpholine-containing moieties in positions 5 and 6 respectively. Compound **6** [4], bearing a comparatively larger *N*-benzylmorpholine substitution on the 6-position of the coumarin scaffold, was previously shown to inhibit mycobacteria through inhibition of FadD32, a newly validated and promising mycobacterial drug target involved in mycolic acid biosynthesis [29]. Methyl substitutions on positions 5 and 7 were again crucial for activity. The importance of the methyl moieties may be their influence on the geometrical conformation of the adjoining aryl groups, indicating conformation-specific target binding [4]. Similar to the piperidine and piperizine derivatives in series 1 evaluated in this study, compounds **5** and **6** with the larger substitutions on the benzene ring of the coumarin scaffold was substituted with functional groups able to form hydrogen bonds with the target site.

The neuronal enzyme structure activity relationships of the coumarin derivatives in table 1 were discussed in detail in our recently published paper [26]. Briefly, the coumarin derivatives substituted at the 7-position with a *N*-benzylpiperidine or p-bromo-*N*-benzylpiperazine (series 1) showed better multifunctional neuronal inhibitory activities compared to their 7-benzyl only substituted counterparts (series 2). In addition, the substitution of a nitrile group at position 3 of the coumarin scaffold (**CM9** and **CM14**) improved the multifunctional neuronal inhibitory activities of the compounds in series 1 and the MAO-B activity (**CM4** and **CM19**) in series 2. In both series 1 and 2 substitution at position 4 with a large trifluoromethyl group drastically decreased their neuronal enzymatic activities. It was also noted that, in general, the *N*-benzylpiperidine substituted coumarin derivatives showed significantly improved activities over their p-bromo-*N*-benzylpiperazine substituted counterparts. From these studies compound **CM9** was identified as the most promising multifunctional neuronal enzyme inhibitor. It may therefore be possible to increase the selectivity of coumarin derivatives towards either neuronal enzyme inhibitory activity or antimycobacterial property through selective substitution in positions 4- and 7 of the coumarin scaffold.

All derivatives in series 1 and 2 that demonstrated more than 50% mycobacterial growth inhibition at 50 µM were further analysed at narrower concentration ranges using a similar method to the original MTS. Figure 3 depicts the mycobacterial growth inhibition for compounds **CM12** and **CM17**, which were the most active in their respective series in the initial screen. Relative fluorescence of the far-red fluorescent reporter mCHERRY was used as the indicator of growth during this screen which was performed once to validate the activity found during the initial screen. These graphs show the inhibitory effect of the compounds compared to the untreated as well as a known antimycobacterial rifampicin (RIF) at 6 µM. From this activity validation screen **CM8**, **CM12**, **CM14** and **CM15** (all in series 1) were identified as the most potent compounds and evaluated in further studies to gain insight into their antimicrobacterial properties.

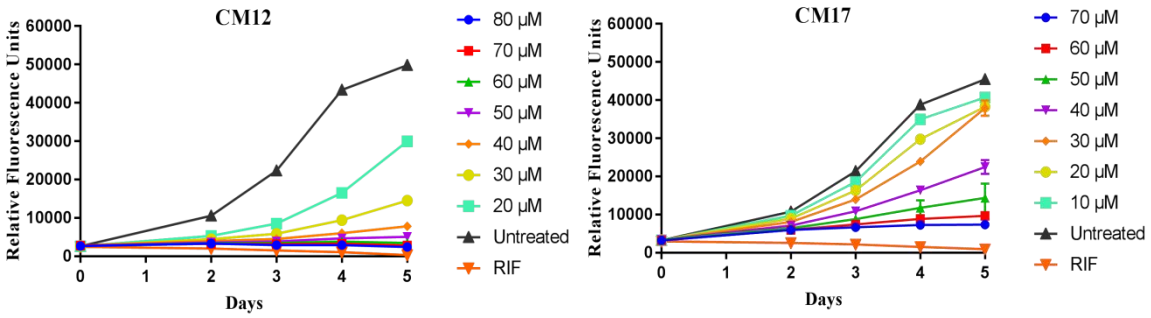

Figure 3: Mycobacterial growth inhibition by compounds **CM12** and **CM17** at narrower concentration intervals. *M. tuberculosis* H37Rv:pCHERRY3 was cultured in 96 well plates as described, with compounds at the concentrations as shown. Experiments were repeated in biological triplicates; each plot shown here shows a representative biological replicate with the mean and standard deviation of 3 technical replicates for each data point.

7.2.2.2. Evaluation of Compound Activity in Quinolone Resistant *Mycobacterium tuberculosis*

Various coumarin based antimicrobials have been shown to target bacterial DNA gyrase, which is also the suggested target of the fluoroquinolone antibiotics in mycobacteria [5, 6, 11, 12]. It was therefore decided to evaluate whether the coumarin derivatives evaluated in this study would be able to maintain potency in fluoroquinolone resistant mycobacteria. The activity of **CM12** and **CM14** were evaluated in three strains (Gly88Cys, Ala90Val and Asp94Gly) of *M. tuberculosis* demonstrating moxifloxacin resistance. Genetic mutations in quinolone-resistance determining regions (QRDR) of DNA gyrase are primarily responsible for conferring resistance to various fluoroquinolone antibiotics. Particularly substitutions in the 94 position are commonly identified in quinolone resistant strains [30]. **CM12** and **CM14** maintained potency in all evaluated strains featuring 3 different mutations in the QRDR region (see Figure 4). Preliminary investigations indicate that it is likely that compounds in series 1 will maintain activity in fluoroquinolone resistant mycobacteria. Additional evaluations are required to determine the true extent of activity in resistant strains for series 1 as well as series 2 derivatives.

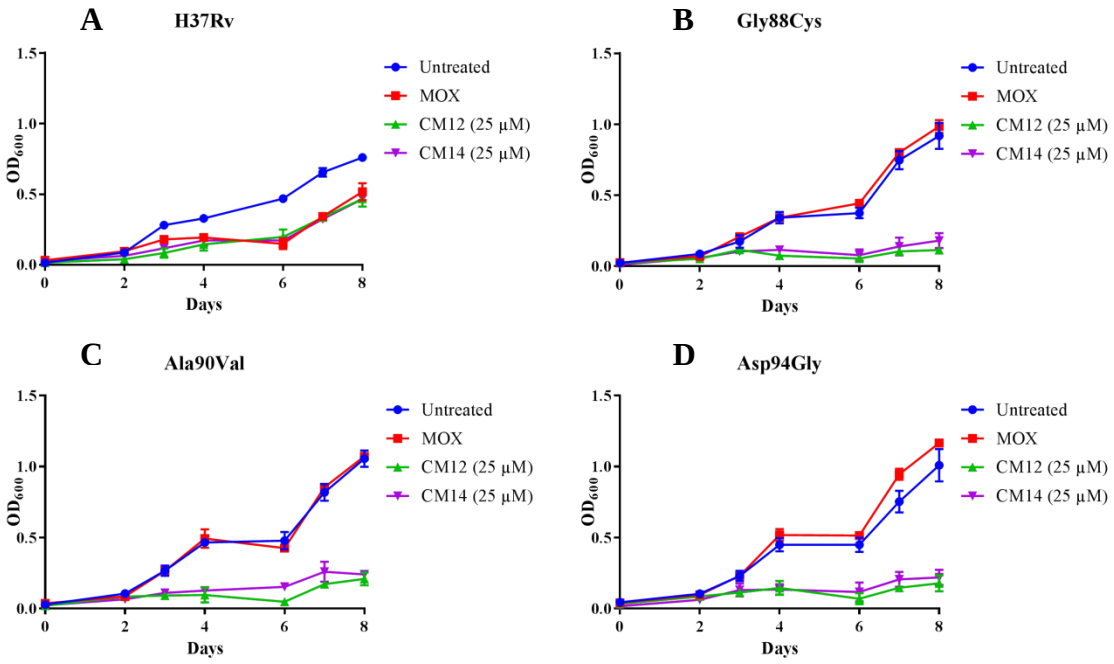

Figure 4: Preliminary evidence of maintained activity of **CM12** and **CM14** in fluoroquinolone sensitive (**A**: H37Rv) and resistant *M. tuberculosis* (**B**, **C**, and **D**: Gly88Cys, Ala90Val, and Asp94Gly, respectively). Moxifloxacin (MOX) was used at a concentration of 1.2 µM. OD_{600}: optical density measured at 600 nm.

7.2.2.3. Minimum Inhibitory Concentration Determination

MICs of the most active compounds from the initial evaluations (**CM8**, **CM12**, **CM14** and **CM15**) were determined independently at the University of Stellenbosch (US) and University of Cape Town (UCT) utilizing different assay methods described in detail in the methodology section. Briefly, the US assay (similar to the assay used for the MTS), utilized a H37Rv strain transformed with a plasmid encoding a red fluorescent reporter (pCHERRY3 [31]), a gift from Tanya Parish (Addgene plasmid # 24659)), in albumin-containing media [Middlebrook 7H9 broth, (Becton, Dickinson and C., USA) enriched with 10% OADC, 0.2% glycerol and 0.05% Tween 80; 7H9+OADC]. The UCT method utilized a standard broth microdilution method with *M. tuberculosis* H37RvMA pMSP12:GFP in glycerol-alanine-salts with 0.05% Tween 80 and iron (GAST-Fe) [32]. Consistently lower MICs were observed in the GFP GAST-Fe assay. **CM8**, **CM12** and **CM14** all showed approximately 2 to 3-fold lower MIC_{90} values in the UCT laboratory assay with **CM15** showing the largest discrepancy with a 14-fold difference between the two methods (Table 2). For the purposes of comparison with standard antimycobacterials under similar conditions, **CM12** and **CM14** at 25 µM was able to achieve growth inhibition in similar ranges to moxifloxacin at 1.2 µM

whereas rifampicin at 6 µM resulted in 100% inhibition of bacterial growth in the pCHERRY3 assay. Rifampicin has a MIC of 0.0274 µM in the GFP assay.

Table 2: Minimum inhibitory concentrations determined using two methods

Compound	GFP GAST-Fe		mCHERRY – 7H9+OADC			
	MIC_{90} (µM)	MIC_{99} (µM)	MIC_{90} (µM)	St. Dev.	MIC_{99} (µM)	St. Dev.
CM8	19.6	25.2	40.55	1.16	44.15	1.37
CM12	14	29.7	40.89	0.06	50.40	8.96
CM14	16.7	28	45.22	3.04	54.46	9.58
CM15	3.2	8.31	43.78	1.46	57.17	10.05

Abbreviations: St. Dev., standard deviation; MIC_{90}, minimum inhibitory concentration required to inihibit 90% of the organism; MIC_{99}, minimum inhibitory concentration required to inhibit 99% of the organism; GFP, green fluorescent protein; GAST-Fe, glycerol-alanine-salts with 0.05% Tween 80 and iron; 7H9+OADC, Middlebrook 7H9 broth, enriched with 10% oleic albumin dextrose catalase (OADC), 0.2% glycerol and 0.05% Tween 80.

Although it is relatively common to see differences in MIC between different media types, the drastic differences in particularly compound **CM15** warranted further investigation. In the assay methods used in this study, differences in the observed MIC could be due to the lack and presence of albumin in GAST-Fe and 7H9+OADC media respectively; the unique reporters used in the two assays; the difference in inoculum size or alternatively, result directly from the mechanism of action of the compounds. The size of the inoculum has been shown to influence the MIC of antimycobacterials. A 10-fold increase in inoculum size resulted in an approximately 4-fold increase in MIC of bedaquiline [33]. The OD_{600} of 0.004 and 0.04 for the GAST-Fe and 7H9+OADC methods respectively, could therefore contribute to the higher MIC observed using the second method.

Another likely contributor to the observed differences in MIC for the coumarin-based derivatives may be binding to albumin. Various coumarin derivatives (e.g. warfarin) are known to bind extensively to blood-soluble proteins. Serum albumins, which are the major soluble protein constituents of the circulatory system (4% w/v), have the ability to reversibly bind a large variety of exogenous compounds including fatty acids, amino acids, drugs and pharmaceuticals [34-36]. Plasma protein binding forms an integral part of distribution and bioavailability for numerous medications currently on the market but might also become problematic where binding is extensive [37, 38]. *In vitro*, binding to albumin would reduce the amount of compound available to exert an effect on the mycobacterial cell and in theory reduce the observed MIC of the derivative. The impact of the albumin binding on *in vivo* MIC of compounds would however depend on the extent and nature of the binding to albumin within the host.

7.2.2.4. Albumin Binding Assay

To better understand the observed differences in MIC between the two assays, we investigated possible albumin binding for the two coumarin derivatives (**CM14** and **CM15**) with the largest differences in MIC between the GAST-Fe and 7H9+OADC media based assays. Albumin enriched media contains approximately 0.5 % w/v bovine serum albumin (BSA). Results of previous studies indicate that human serum albumin (HSA) and BSA are similar proteins in space structure and chemical composition [39-41]. BSA was therefore selected as a protein model to investigate fluorescence quenching as an indicator of the extent of interaction between coumarin derivatives (**CM14** and **CM15**) and albumin, using fluorescence spectroscopy. Fluorescence quenching is the decrease of the quantum yield of fluorescence from a fluorophore induced by a variety of molecular interactions with the quencher molecule. Fluorescence quenching can be dynamic, resulting from collisional encounters between the fluorophore and quencher, or static, resulting from the formation of a ground state complex between the fluorophore and quencher [42-44]. The effects of compounds **CM14** and **CM15** on the fluorescence quenching of BSA, excited at 295 nm are presented in Figure 5.

The emission spectrum of **CM14** showed two maxima, the first one at 335 nm (which is characteristic for tryptophan in BSA [45]) and the second peak at 400 nm (which is assigned to fluorescence of compound **CM14** at concentrations of 5 x 10^{-6} mol L^{-1} and upwards). The emission spectrum of **CM15** only showed one maxima at 335 nm for BSA and a weak emission peak of **CM15** at 415 nm at higher concentrations of the compound. The excitation and emission maxima of **CM14** and **CM15** are shown in Table 3.

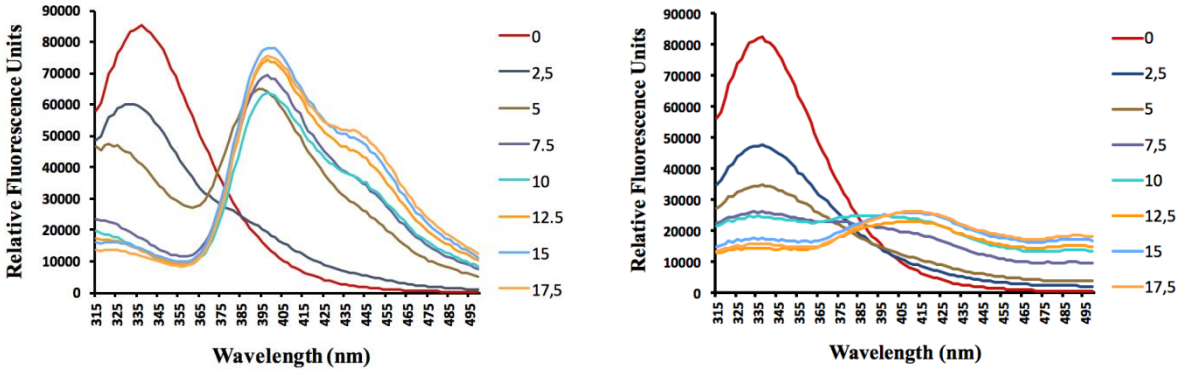

Figure 5: The effects of **CM14** (left) and **CM15** (right) on the fluorescence spectra of BSA at 22 °C. ex = 295 nm; c(BSA) = 1.00 x 10^{-5} mol L^{-1}; c(Q)/(x 10^{-6} mol L^{-1}). Final concentrations of **CM14** and **CM15** = 0, 2.5, 5.0, 7.5, 10, 12.5, 15.0, and 17.5 x 10^{-6} mol L^{-1}, respectively.

The mechanism of the fluorescent quenching of **CM14** and **CM15** to BSA is described using the Stern-Volmer equation:

$$F_0/F = 1 + K_{sv}[Q] = 1 + K_q \tau_0[Q]$$

where F_0 and F are the fluorescence intensities before and after the addition of the quencher, respectively; K_{sv} is the dynamic quenching constant; K_q is the quenching rate constant; [Q] is the concentration of quencher; τ_0 is the average lifetime of the molecule without quencher and its value is considered to be 10^{-8} s [46, 47]. The Stern-Volmer plot of the **CM14** and **CM15** is presented in Figure 6.

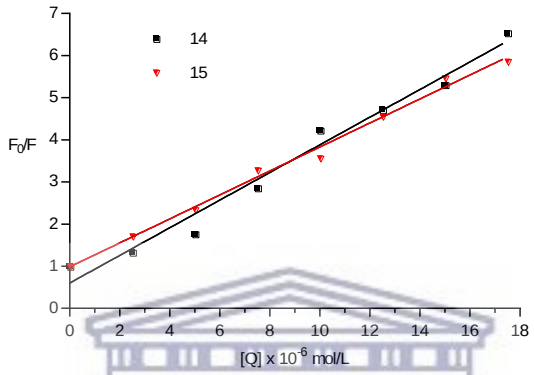

Figure 6: Stern–Volmer plots of BSA (1.00×10^{-5} mol L^{-1}) quenched by **CM14** and **CM15** at 22 °C.

The plots show a good linear relationship within the investigated concentrations of **CM14** and **CM15**.

The results in Table 3 showed that K_q were much greater than the limiting diffusion rate constant of the biomolecule (2.0×10^{10} mol L^{-1} S^{-1}), which indicated that the probable quenching mechanism of BSA–**CM14** and BSA-**CM15** interactions was initiated by complex formation rather than by dynamic collision [48].

It is evident from the results that the fluorescence intensity of BSA decreases with increasing concentrations of compounds **CM14** and **CM15**. It can also be concluded that the fluorescence quenching of tryptophan in BSA as observed for compounds **CM14** and **CM15** results from complex formation between the two compounds and BSA. The more extensive decrease in fluorescence observed at lower concentrations of compound **CM15** likely indicate a higher binding affinity between compound **CM15** and albumin. These results indicate that albumin binding likely plays a large role in the observed differences in activity between the GAST-Fe and 7H9+OADC assays used in this study. The higher albumin binding affinity of **CM15** is likely the reason for the larger MIC variation perceived for this compound**.**

Table 3: Excitation and emission maxima of **CM14** and **CM15**, and the quenching constant of BSA by **CM14** and **CM15**.

Compound	T (°C)	λ_{Ex} (nm)	λ_{Em} (nm)	k_{sv} (mol L^{-1})	k_q (mol L^{-1} S^{-1})	R^2
CM14	22	350[a] 350[b]	395[a] 400[b]	3.80 x 10^5	2.63 x 10^{14}	0.9780
CM15	22	335[a] 335[b]	415[a] 415[b]	4.88 x 10^5	2.00 x 10^{14}	0.9927

[a]Measured in Tris-HCl buffer at 1 x 10^{-6} mol L^{-1}. [b]Measured in BSA (1 x 10^{-5} mol L^{-1}) at 1 x 10^{-6} mol L^{-1}. Abbreviations: λ_{Ex}: excitation; λ_{Em}: emission; k_{sv}: dynamic quenching constant; k_q: quenching rate constant; R^2: coefficient of determination.

In addition to providing more clarity on observed MICs, albumin binding properties may also provide some insight into the possible pharmacokinetic behavior of these drugs. Binding and dissociation of compounds from plasma proteins is a dynamic process with only the unbound fraction of the drug available to exert an effect. In a clinical setting, the dosage of a drug is calculated to ensure that, at any point in time, sufficient free drug is available to have the required pharmacological effect. The same principle would apply to side effects or toxicity and thus, plasma protein binding becomes an important consideration, particularly in highly bound drugs. In light of the divergent albumin binding affinities observed in the evaluated compounds, it would likely be more pertinent to utilize the MIC values obtained in the albumin free GFP-GAST-Fe media for the purposes of determining structure activity relationships for antimycobacterial activity. **CM15**, which seems to be at least 3-fold more active than the other top compounds in the GFP assay, has a large CF_3 substitution on the 4 position of the coumarin scaffold, and a p-bromo-*N*-benzylpiperizine substitution on *C7*. Activity differences between **CM8**, **CM12** and **CM14** are not pronounced enough to draw structure activity relationship conclusions.

7.2.2.5. Cell Viability Assays

Cytotoxicity assays for the compounds showing the lowest MIC_{99} (**CM8**, **CM12**, **CM14**, and **CM15**) were done on Chinese hamster ovary (CHO) epithelial cells using a standard MTT assay method (Table 4) [49]. Data was supplemented with further cytotoxicity analysis of **CM14** and **CM15** as well as **CM9** in a similar assay using the neuronal type SH-SY5Y neuroblastoma cells. The SH-SY5Y cytotoxicity assay results were used to determine the concentration at which the compounds do not affect the viability of the SH-SY5Y cells in

order to determine their neuroprotective effect using the 1-methyl-4-phenyl pyridinium (MPP^+) induced neurotoxicity method [50, 51].

CM9 was included in the neuronal cell viability and MPP^+ induced neurotoxicity assays because it was identified previously as the best multifunctional neuronal enzyme inhibitor (IC_{50}: MAO-B = 0.30 uM; AChE = 9.10 uM; BuChE = 5.90 uM) within the series of coumarin derivatives (Table 4) [23]. **CM9** did not show any significant antimycobacterial activity and was therefore not included in the CHO cytotoxicity assay. **CM14** was included to draw a comparison between the neurotoxicity and potential neuroprotective effect of the 3-nitro-4-methyl-coumarin derivatives substituted at the 7-position with either a *N*-benzylpiperidine (**CM9**) or p-bromo-*N*-piperazine moiety (**CM14**). **CM15**, with a large trifluoromethane substitution on position 4, showed the most promising antimycobacterial activity with minimal multifunctional neuronal enzyme inhibitory activity. It was included in the neurotoxicity assays to study the effect of the neuronal enzyme inhibitory activities, or lack thereof, on the neuroprotective ability of these compounds or if other mechanisms of action are involved. **CM8** and **CM12** were not included in the neurotoxicity assays as their multifunctional neuronal enzyme inhibitory properties were not as pronounced as **CM9** and **CM14**.

Table 4: Cell viability (CC_{50}) and selectivity indices on CHO cells, cell viability on SH-SY5Y cells and enzyme inhibition (IC_{50}) of selected test compounds.

CM	CC_{50} uM CHO	SI GFP[a]	SI mCHERRY[b]	CC 50% SH-SY5Y[c]	MAO-A IC_{50} uM[d]	MAO-B IC_{50} uM[d]	AChE IC_{50} uM[d]	BuChE IC_{50} uM[d]
CM8	33.0	1.31	0.75	ND	n.a.	0.29	31.30	1.27
CM9	ND	ND	ND	10-50	n.a.	0.30	9.10	5.90
CM12	15.5	0.52	0.31	ND	n.a.	3.60	12.8	9.70
CM14	41.2	1.47	0.76	50-100	n.a.	1.41	38.5	13.3
CM15	26.3	3.16	0.46	10-50	n.a.	5.64	>100	>100
Emetine	0.06	ND	ND	ND	ND	ND	ND	ND

[a]Selectivity index (SI) = CC_{50} CHO/MIC_{99} GFP-GAST-Fe. [b]Selectivity index (SI) = CC_{50} CHO/MIC_{99} mCHERRY-7H9 + OADC. [c]Inhibition range (uM) where 50% cell toxicity will be observed. [d]Data taken from Joubert *et al.*, 2017 [23]. ND = not determined. n.a. = no activity.

Cytotoxicity CC_{50} on CHO cells observed for **CM8**, **CM12**, **CM14** and **CM15** was moderate (CC_{50}: 16.5 – 41.2 µM) indicating low toxicity compared to the cytotoxic agent emetine (CC_{50} = 0.06 uM). These compounds however showed low selectivity indices when both the GFP and mCHERRY MIC_{99} assay results are compared to the CC_{50} results (Table 4). The compounds, in general, were slightly more selective towards the mycobacterial strain when using the GFP assay results, with **CM15** showing the best selectivity (SI = 3.16). The slight

selectivity was however not retained when the results from the mCHERRY assay were used in the SI calculations. These poor selectivity indices may limit the further development of these coumarin derivatives. However, the structure activity relationships identified in this paper may enable the design of coumarin structures with improved antimycobacterial activities and subsequently more favourable selectivity indices.

The viability of SHSY-5Y human neuroblastoma cells was assessed at different concentrations of compounds **CM9**, **CM14** or **CM15** (Figure 6, A). Treatment with the compounds at 10 µM did not significantly affect the viability of the SH-SY5Y cells ($p > 0.05$). However, at higher concentrations (50 µM and 100 µM) the viability of the cells were significantly ($p < 0.001$) affected by the test compounds, although to a lesser extent by **CM14**. These results also correlate to the CC_{50} CHO values obtained for **CM14** and **CM15** (Table 4).

Based on the SH-SY5Y cytotoxicity analysis it was decided that the MPP^+ neuroprotection studies would be done at compound concentrations between 1 µM and 10 µM in order maintain the viability of the cells. MPP^+ is highly toxic to neurons and has been widely used to induce neurodegeneration in various *in vitro* and *in vivo* models [50, 51]. Several signaling pathways have been suggested to be responsible for MPP^+-mediated neurotoxicity in SH-SY5Y cells, for instance, trigger of oxidative stress [52], induction of apoptosis [53], and inactivation of pro-survival phosphoinositide 3-kinase (PI3-K)/Akt cascade [54-56]. This assay was deemed appropriate to test for initial neuroprotective ability of **CM9**, **CM14** and **CM15** because of the multitude of pathways involved in MPP^+ mediated neurotoxicity and the multifunctional enzyme inhibitory abilities of the test compounds, especially **CM9**.

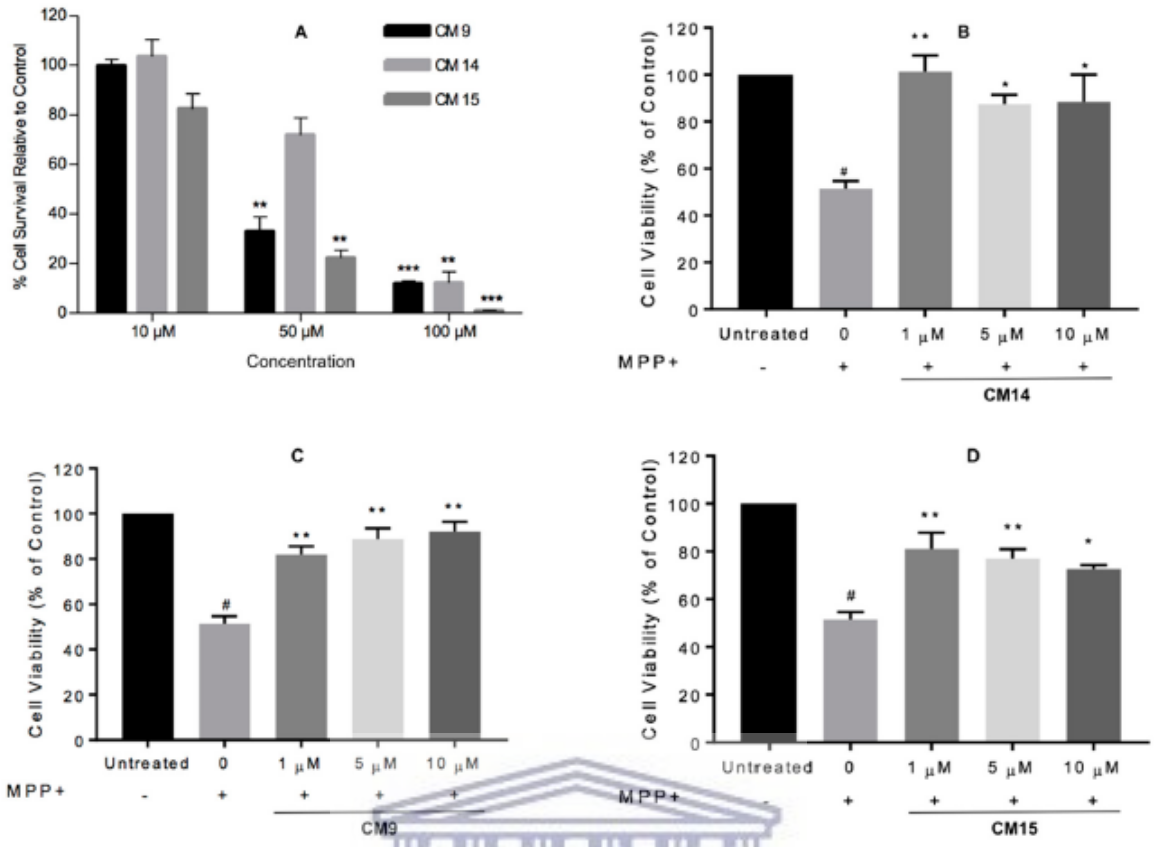

Figure 7: (A) Cellular viability of SH-SY5Y cells treated with compounds CM**9**, **CM14** or **CM15** at 10 µM, 50 µM and 100 µM for 48 hours. Data is presented as mean ± SEM. Significance is set at a level of *p<0.05 compared to vehicle treated control cells (taken as 100 % cell viability). (B-D) The effects of compounds **CM9**, **CM14** or **CM15** on MPP^+-induced (1000 µM) cytotoxicity in SH-SY5Y cells. The viability of the untreated control was defined as 100 %. MPP^+ without test compound showed a significant decrease in cell viability relative to the control (#p<0.05). The level of significance for the test compounds is set at *p<0.05 compared to the MPP^+ only treated control (0). Statistical analysis (Turkey's post hoc test) was performed on all raw data, with asterisks signifying significant inhibitory effect. *p<0.05; **p<0.001; ***P<0.0001.

SH-SY5Y cells were exposed to the neurotoxin MPP^+ with or without test compound, and cell viability was evaluated using the MTT mitochondrial function assay [43]. As illustrated in Figure 7B-D, after the exposure to 1000 µM MPP^+ for 48 hours, the cell viability declined significantly to 51.42 ± 3.18 %. However, its cytotoxic effects were ameliorated in the presence of **CM9**, **CM14** and **CM15** at 1 µM, 5 µM and 10 µM concentrations. The compounds, at a 1 µM concentration, restored cell survival to 81.86 ± 3.72 %, 101.2 ± 6.00 % and 81.05 ± 6.83 %, respectively. **CM9** showed activity in a dose dependent manner exerting maximal cytoprotection of 92.2 ± 4.18 % at 10 µM. At 5 µM and 10 µM a slight decrease in cytoprotection was observed for **CM14** and **CM15**. This may indicate that in the neurotoxin challenged state the SH-SY5Y cells may be more sensitive to the cytotoxic effect of the test compounds. Therefore, **CM14** and **CM15** might have enhanced the toxicity of the neurotoxin which resulted in lower neuroprotection values observed at higher concentrations.

Thus, in general and especially at a 1 µM concentration, these compounds, and particularly **CM14**, exerted highly significant cytoprotection towards MPP^+ insults to the SH-SY5Y neural cells.

The results of the MPP^+ neuroprotection study did not provide any information on structure activity relationships of these compounds as **CM9**, **CM14** and **CM15** showed similar levels of cytoprotection. It was however noted that the neuronal enzyme inhibitory activity of these compounds is not the only factor that play a role in cytoprotection and that other mechanisms of action are involved. For instance, **CM15** showed poor neuronal enzyme inhibitory activities but was still able to significantly protect the cells from MPP^+ induced injury. **CM9** with the best multifunctional enzyme inhibitory profile showed cytoprotection at the same level as **CM15**. As described in the literature coumarin derivatives may possess anti-inflammatory, anti-apoptotic and antioxidant effect [2, 3]. These effects combined with the multifunctional neuronal enzyme inhibitory abilities of the compounds may explain the excellent neuroprotection observed. Therefore, further neuroprotection studies are necessary to elucidate the mechanism(s) of action of these compounds.

7.2.3. Materials and Methods

7.2.3.1. Compound Synthesis

Synthesis methods of the compounds described in this article are described in detail in previous publications by the drug design group at UWC [26].

7.2.3.2. Initial Medium Throughput *In Vitro* Activity Screen

This study was approved by the Stellenbosch University Health Research Ethics Committee (S15/06/135). The M. tuberculosis H37Rv strain used during this study was obtained from the ATCC (ATCC 27294) and whole genome sequencing [57] and virulence confirmation in a murine infection model [58] was used to verify the strain. The episomal plasmid pCHERRY3, a gift from Tanya Parish (Addgene plasmid #24659) [31], which expresses the far-red fluorescent reporter mCHERRY and contains a hygromycin B resistance cassette, was transformed into this electrocompetent M. tuberculosis H37Rv. Growth curve analysis of both M. tuberculosis H37Rv and M tuberculosis H37Rv:pCHERRY was performed twice to ensure that the plasmid did not have any deleterious effects on growth.

The antimycobacterial activity of the synthetic compounds was determined using a medium throughput 96-well plate assay. *M. tuberculosis* H37Rv with and without the reporter was cultured in 7H9+OADC, without and with 50 µg/mL hygromycin B respectively, whereafter the culture was strained (40 µm; Becton, Dickinson, and Co., USA), and the OD_{600} was adjusted to 1.0. Culture was added to each well, resulting in a final OD_{600} of 0.02. White, flat bottom 96-well microtiter plates were prepared, with a final volume of 200 µL, final bacterial OD_{600} of 0.02, and final compound concentration of 100 µM, 50 µM or 1 µM,

Controls included a gain, negative, bacterial growth, dimethyl sulfoxide (DMSO), positive, negative and compound control. The background control, which contains *M. tuberculosis* H37Rv without the fluorescent reporter is subtracted from the fluorescence measurements since it displays the inherent fluorescence of *M. tuberculosis* H37Rv. Negative control is included as an untreated fluorescence control where the DMSO control is included to ensure that the maximum amount of DMSO present in the compound dilutions does not interfere with growth. The positive control wells contained 6 µM rifampicin (RIF) and the compound controls contained 100 µM compound which was used to confirm that the compound does not autofluoresce in the absence of *M. tuberculosis*.

One-hundred microliters of the *M. tuberculosis* H37Rv:pCHERRY3 diluted culture was added to each well except the gain, background and compound control wells. In the gain control wells, 100 µL of the undiluted *M. tuberculosis* H37Rv:pCHERRY3 culture was added and in the background control wells *M. tuberculosis* H37Rv without the fluorescent reporter was added. The plates were sealed with breathable sealing film and incubated at 37°C for 6 days, taking readings on days 0, 2, 3, 4, 5, and 6 using a BMG Labtech POLARstar Omega plate reader (Excitation: 587 nm, Emission: 610 nm). During the readings the breathable seal was removed and an optical sealing film was adhered, whereafter it was removed and replaced by a new breathable sealing film. The average of the background control was subtracted from the fluorescence readings whereafter the data was visualised using GraphPad Prism v7.01, by plotting the relative fluorescence units (as a measure of growth) over time. The percentage inhibition was also calculated on Day 5, by dividing the treated by the untreated values. Compounds that inhibited more than 50% growth at 50 µM were selected for further study and screened at narrower concentration ranges to more accurately ascertain the extent of the compound's antimycobacterial activity. The second round of screening was also performed using relative fluorescence as a proxy for growth. The growth curves were set up similarly to the initial screen. Five compounds which

showed the highest activity during the second screen were selected to undergo further analysis. Of these 5 compounds, 4 were coumarin derivatives.

7.2.3.3. Activity in Moxifloxacin Resistant *M. tuberculosis*

Three *M. tuberculosis* moxifloxacin resistant mutants, carrying G88C, A90V or D94G amino acid changes in gyrase A, were tested for **CM12** and **CM14** cross-resistance. Moxifloxacin stock solutions were prepared at a concentration of 25 µM in DMSO and stored at -80°C. The resistant mutants and an *M. tuberculosis* H37Rv susceptible strain were prepared as described in section 3.2 and subsequently exposed to 1.2 µM moxifloxacin, 25 µM **CM12** and 25 µM **CM14** in technical triplicates in a black, flat, clear-bottom 96 well plate. Each well containing the respective strain was inoculated to an OD_{600} of 0.02 in a final volume of 200 µL. Readings were taken as described in section 3.2 over 8 days and OD_{600} was plotted over time using GraphPad Prism v7.01.

7.2.3.4. Minimum Inhibitory Concentration Determination

MICs were determined for the four most active coumarin derivatives identified in the MTS. **CM8**, **CM12**, **CM14** and **CM15** were screened using two independent methods as described below.

***M. tuberculosis* pMSP12:GFP in GAST-Fe media**

The first MIC determination was performed at the Institute of Infectious Disease & Molecular Medicine, University of Cape Town (UCT) at a screening facility jointly managed by the MRC/NHLS/UCT Molecular Mycobacteriology Research Unit (A/Prof Digby Warner) and the H3D Drug Discovery and Development Unit (Prof Kelly Chibale). Here, the standard broth microdilution method was performed using *M. tuberculosis* H37RvMA pMSP12:GFP [32]. A 10 ml culture was grown in glycerol-alanine-salts with 0.05% Tween 80 and iron (0.05%; GAST-Fe) pH 6.6, to an OD_{600} of 0.6 – 0.7. Thereafter the culture was diluted 1:100 in GSAT-Fe. In a 96-well microtiter plate, two-fold serial dilutions of each compound were prepared in GAST-Fe whereafter 50 µL of the diluted culture was added to each serial dilution well resulting in an OD_{600} of 0.004. The plate layout used was modified from a previously described method [59]. Controls included a bacterial growth control (5% DMSO in GAST-Fe) and a positive control (0.15 µM RIF). The microtiter plate was

incubated at 37°C with 5% CO_2 and humidity, sealed within a secondary container. Using a platereader (FLUOstar OPTIMA, BMG Labtech; Excitation: 485nm; Emission: 520nm) relative fluorescence was measured on day 7 and 14. The CCD Vault from Collaborative Drug Discovery was used to archive and analyse the fluorescence data. Analyses included normalisation to the bacterial growth and antimycobacterial growth control as the maximum and minimum growth representations respectively generating a dose-response curve using the Levenberg-Marquardt damped least-squares method. This dose response curve was used to calculate the MIC_{90} and MIC_{99} which is described as the lowest concentration at which the compound inhibits growth by more than 90% and 99%, respectively (Burlingame, CA, www.collaborativedrug.com).

M. tuberculosis H37Rv:pCHERRY3 in 7H9+OADC

The second technique used a different fluorescent reporter (mCHERRY) and media (7H9+OADC). Dose-response curve analysis was carried out on the same compounds as above. Dose response curves were performed by exposing *M. tuberculosis* H37Rv:pCHERRY3 to increasing concentrations of each compound in white flat bottom 96 well plates. *M. tuberculosis* H37Rv with and without mCHERRY was prepared as described in section 3.2.2. In a white, flat bottom 96 well microtiter plate two-fold serial dilutions of the compounds were prepared with a 100 µL final volume and final bacterial OD_{600} of 0.04. The plate layout is shown in Figure 3.3. This method was adapted from a previously described method [59]. The controls included were a background control (*M. tuberculosis* H37Rv in 7H9+OADC), a negative control (*M. tuberculosis* H37Rv:pCHERRY3 in 7H9+OADC) and a positive control (*M. tuberculosis* H37Rv:pCHERRY3 in 7H9+OADC containing 2 µM RIF). The microtiter plate was sealed with a breathable film, placed in a secondary container and incubated at 37°C for 5 days, after which a relative fluorescence measurement (Excitation: 587 nm; Emission: 610 nm) was taken using a BMG Labtech POLARstar Omega plate reader. To analyse the relative fluorescence data the average of the background control was subtracted from each well, and the subsequent data set was analysed in GraphPad Prism v.7.01. Data was first normalised using built in non-linear dose-response curve analysis. This gave an output of IC_{50} as well as a Hill Slope which was used to determine the IC_{90} and IC_{99} of each compound. IC_{90} and IC_{99} were defined as the concentration where 90% and 99% of growth was inhibited, respectively.

7.2.3.5. Bovine Serum Albumin Binding Assay

The interaction between coumarin derivatives (**CM14** and **CM15**) and BSA were measured by fluorescence spectroscopy. BSA (≥ 98%) was obtained from Sigma Aldrich South Africa and dissolved in a Tris–HCl (0.10 mol L^{-1}, pH = 7.4) buffer to form the BSA solution with a concentration of 1.00 x 10^{-5} mol L^{-1}. A Tris–HCl buffer (0.10 mol L^{-1}, pH = 7.4) containing 0.10 mol L^{-1} NaCl was selected to keep the pH value constant and to maintain the ionic strength of the solution. Coumarin **14** and **15** stock solution (1.00 x 10^{-3} mol L^{-1}) was prepared in MeOH. All other reagents were of analytical grade and double-distilled water was used in the experiments. Fluorescence spectra were recorded on a Biotek Synergy Mx fluorescence plate reader. Black 96 well plates were used in all experiments. The excitation and emission slits were 9 nm. Fluorescence spectra were measured in the range of 315–500 nm at the excitation wavelength of 295 nm. All experiments were done at 22 °C. The assay was conducted using a 200 µL solution containing 1.00 x 10^{-5} mol L^{-1} BSA that was titrated by successive additions of 1.00 x 10^{-3} mol L^{-1} coumarin **CM14** or **CM15** solution. The final concentration of the compounds varied from 0 to 1.75 x 10^{-5} mol L^{-1}. Titrations were done manually using a micro-pipette in 2 minute intervals. Quenching values remained unchanged for more than 10 minutes after individual titrations.

7.2.3.6. Chinese Hamster Ovary Cell Cytotoxicity Assays

Cytotoxicity was evaluated on CHO cells utilizing a standard MTT assay [49]. The 3-[4,5-dimethylthiazol-2-yl]-2,5-diphenyl tetrazolium bromide (MTT) is a yellow tetrazolium salt that is reduced to purple formazan in the presence of living cells. This reduction reaction was used to measure growth and chemosensitivity. The test samples were tested in triplicate on one occasion. Cells were seeded in microtiter plates at a density of 10^5 cells/ml and incubated for 24 hours prior to exposure . The test samples were prepared to a 20 mg/mL stock solution in 10% methanol or 10% DMSO and were tested as a suspension if not properly dissolved. Test compounds were stored at -20˚C until use, and administered in volumes of 100 µL to the plated cells. Emetine was used as the reference drug in all experiments. The highest concentration of each compound was 100 µg/mL, which was serially diluted in complete medium with 10-fold dilutions to give 6 concentrations, the lowest being 0.001 µg/mL. The same dilution technique was applied to the all test samples. The highest concentration of solvent to which the cells were exposed to had no measurable effect on the cell viability (data not shown). Plates were developed after 44 hours of exposure to the drug by the addition of a solution of MTT. After four hours, further incubation at 37 °C the supernatant was removed

from the cells via suction and DMSO was added to each well to dissolve the reduced dye crystals. Plates were analysed at 540 nM wavelength using a spectrophotometer to determine the relative amount of formazan salt in each well. The amount of formazan produced in wells containing untreated cells only and growth medium only represent 100% survival and 0% survival respectively, and the amount in each treatment well was converted to a survival percentage relative to these two extremes. The 50% inhibitory concentration (IC_{50}) values were obtained from full dose-response curves, using a non-linear dose-response curve fitting analysis via GraphPad Prism v.4 software.

7.2.3.7. Human Neuroblastoma SH-SY5Y Cell Viability Assays

Cell line and culture conditions

The human neuroblastoma cell line SH-SY5Y was generously donated by our collaborator at the Division of Molecular Biology and Human Biology, Stellenbosch University, Tygerberg, Cape Town. Cells were cultured in monolayer using Dulbecco Modified Eagles Medium (DMEM, Gibco, Life Technologies Ltd) supplemented with 10% foetal bovine serum (FBS, Gibco, Life Technologies Ltd.) and 1% 100 U/mL penicillin and 100 µg/mL streptomycin (Lonza Group Ltd., Base Switzerland). Cells were grown at 37 °C, in a humidified atmosphere at 5% CO_2. Media was replaced every two to three days and cells were sub-cultured by splitting with trypsin (Lonza Group Ltd., Base Switzerland).

SH-SY5Y cytotoxicity assays

The standard MTT assay which measures cell metabolic activity was used to determine cytotoxicity of CM14, CM15 and CM9 as described by Mosmann [49]. Briefly, SH-SY5Y cells were plated in flat bottom 96 well plates in growth medium as stated in 3.7.1 at a density of 7,500 cells/well. Cells were allowed to adhere to the plate surface for 24 hours and used media were replaced with fresh media containing test compounds at 10 µM, 50 µM and 100 µM. Vehicle control cells were treated with DMSO (solvent for dissolving test compounds) at a concentration similar to the amount contained in the highest concentration of test compounds. After 48 hours, 10 µL of MTT solution (5 mg/mL) was added to each well and incubated for 4 hours and the purple formazan formed was solubilized with 100 µL DMSO and plates were read spectrophotometrically to determine absorbance at 570 nm using a BMG Labtech POLARStar Omega multimodal plate reader.

MPP^+-induced cytotoxicity in SH-SY5Y cells

SH-SY5Y cells were seeded onto a 96-well plate and treated with 1000 μM MPP^+ for approximately 48 hours. Different concentrations (1 μM, 5 μM, 10 μM) of test compounds were administrated two hours prior to MPP^+ treatment. Afterwards, cell viability was measured by MTT colorimetric assay and performed as stated above.

7.2.4. Conclusion

As part of a collaborative project, compounds from the University of the Western Cape, School of Pharmacy drug-design group compound library were screened for antimycobacterial activity. Various coumarin derivatives, originally designed and synthesized as multifunctional neuronal enzyme inhibitors, demonstrated noteworthy antimycobacterial activity.

The coumarins substituted with a *N*-benzylpiperidine containing moiety on the 7-position and a 3-nitrile substitution on the coumarin nucleus (**CM9**) showed the best MAO-B and ChE inhibitory activities. This study identified that structural modification on position 4 and/or 7 of the coumarin scaffold can be utilized to improve selectivity towards either inhibition of neuronal enzymes or antimycobacterial effect. Large substitutions on position 4 (4-trifluoromethyl moiety) and p-bromo-*N*-benzylpiperazine compared to *N*-benzylpiperidine substitutions on position 7 increases activity against *M. tuberculosis* but inversely affects monoamine oxidase and cholinesterase inhibition.

After validation of the antimycobacterial activity observed in the MTS; **CM8, CM12, CM14** (4-metyl substituted) and **CM15** (4-trifluoromethyl substituted) were identified as the most active compounds in the series. In addition to activity in standard *M. tuberculosis* H37Rv, we also described activity of selected coumarin derivatives in fluoroquinolone resistant bacteria. Evaluations on three moxifloxacin resistant strains harboring mutations in the QRDR of DNA gyrase indicate that the compound in series 1 will likely maintain potency in fluoroquinolone resistant mycobacteria.

The MICs of the four most active compounds were evaluated using two methods i.e. *M. tuberculosis* H37RvMA pMSP12:GFP in GAST-Fe media [32], and ***M.*** *tuberculosis* H37Rv:pCHERRY3 [31] in 7H9 + OADC. The MIC values in the GAST-Fe assay were consistently lower (2-3 fold lower for **CM8**, **CM12**, and **CM14** and 14 fold lower for **CM15**). Difference in inoculum size and the lack and presence of albumin in GAST-Fe and

7H9+OADC media respectively was suggested as primary contributing factors to the MIC variations.

As coumarin derivatives are known to bind extensively to blood-soluble proteins, albumin binding properties of **CM15** and **CM14** (with the highest and lowest MIC fold difference between assays respectively) was evaluated. Fluorescence quenching of BSA in response to compound binding was evaluated in the presence of various concentrations of the compounds. Analysis of fluorescence quenching of tryptophan in BSA indicate that both **CM14** and **CM15** form concentration dependant complexes with BSA. These results suggest that albumin binding plays a large role in the observed differences in activity between the GAST-Fe and 7H9+OADC assays used in this study. The more extensive decrease in fluorescence observed with **CM15** likely indicates a higher binding affinity between **CM15** and thus explains the large MIC differences observed for this compound. This report therefore highlights the importance of early consideration of plasma binding properties of coumarin derivatives as it was shown here to influence *in-vitro* evaluations in addition to its more commonly considered effect on *in-vivo*, and future pharmacokinetic behavior of the compounds.

CM8, **CM12**, **CM14** and **CM15** showed moderate (CC_{50}: 16.5 – 41.2 µM) cytotoxicity compared to the cytotoxic agent emetine (CC_{50} = 0.06 uM). These compounds however showed low selectivity indices when both the GFP and mCHERRY MIC_{99} assay results are compared to the CC_{50} results (Table 4). The compounds, in general, were slightly more selective towards the mycobacterial strain when using the GFP assay results, with **CM15** showing the best selectivity (SI = 3.16). The slight selectivity was however not retained when the results from the mCHERRY assay were used in the SI calculations. These poor selectivity indices may limit the further development of these coumarin derivatives. However, the structure activity relationships identified in this paper may enable the design of coumarin structures with improved antimycobacterial activities and subsequently more favourable selectivity indices.

The viability of SHSY-5Y human neuroblastoma cells was also assessed at different concentrations of compounds **CM9**, **CM14** or **CM15**. Treatment with the compounds at 10 µM did not significantly affect the viability of the SH-SY5Y cells ($p > 0.05$). However, at higher concentrations (50 µM and 100 µM) the viability of the cells were significantly ($p < 0.001$) affected. Neuroprotective ability of the three compounds were therefore evaluated atconcentrations between 1 µM and 10 µM. **CM9**, **CM14** and **CM15** all demonstrated significant and comparable cytoprotection towards MPP^+ insults to the SH-SY5Y neural

cells. As these compounds differ significantly in their neuronal enzyme inhibitory activity it can be concluded that enzyme inhibition is not the only factor that plays a role in cytoprotection and that other mechanisms of action are involved in the observed neuroprotection.

This article therefore describes the versatile neuronal enzyme inhibitory, neuroprotective and antimycobacterial nature of a range of coumarin derivatives. Importantly, comparison of corresponding SAR, demonstrates that it is possible to reduce the promiscuous activity of the derivatives through careful modification on the coumarin scaffold. Furthermore the article highlights the importance of broader evaluation of pharmacological effects of coumarin derivatives over and above cytotoxicity assays to identify and afford early limitation of unwanted pharmacological effects. This report also shows that albumin binding properties of coumarin derivatives may impact on *in-vitro* assay results and should therefore be taken into consideration even during early evaluations of coumarin-type compounds.

Acknowledgements

We are grateful to the National Research Foundation of South Africa, the South African Medical Research Council and the University of the Western Cape for financial support. S.L.S is funded by the South African Research Chairs Initiative of the Department of Science and Technology and National Research Foundation (NRF) of South Africa, award number UID 86539. The content is solely the responsibility of the authors and does not necessarily represent the official views of the NRF. Research reported in this publication was supported by the South African Medical Research Council.

Author Contributions

E.K., S.L.S., E.M.S., H.V., D.T.W., S.I.O., A.B.E., S.F.M., F.T.Z., O.E. and J.J. conceived and designed the experiments; G.B.F. and J.J. synthesized the compounds; H.V., J.J., F.T.Z., D.F.W., G.B.F., S.I.O. and A.B.E. performed the experiments and analysis; E.K. and J.J. wrote the paper.

References

1. Brown, D. G.; Lister, T.; May-Dracka, T. L. New natural products as new leads for antibacterial drug discovery. *Bioorg. Med. Chem. Letters* **2014**, *24*, 413-418.

2. Hu, Y. Q.; Xu, Z.; Zhang, S.; Wu, X.; Ding, J. W.; Lv, Z. S.; Feng, L. S. Recent developments of coumarin-containing derivatives and their anti-tubercular activity. *Eur. J. Med. Chem.* **2017**, *136*, 122-130.

3. Keri, R. S.; Sasidhar, B. S.; Nagaraja, B. M.; Santos, M. A. Recent progress in the drug development of coumarin derivatives as potent antituberculosis agents. *Eur. J. Med. Chem.* **2015**, *100*, 257-269.

4. Stanley, S. A.; Kawate, T.; Iwase, N.; Shimizu, M.; Clatworthy, A. E.; Kazyanskaya, E.; Sacchettini, J. C.; Ioerger, T. R.; Siddiqi, N. A.; Minami, S.; Aquadro, J. A.; Grant, S. S.; Rubin, E. J.; Hung, D. T. Diarylcoumarins inhibit mycolic acid biosynthesis and kill Mycobacterium tuberculosis by targeting FadD32. *Proc. Natl. Acad. Sci. U. S. A.* **2013**, *110*, 11565-11570.

5. Heide, L. New aminocoumarin antibiotics as gyrase inhibitors. *International Journal of Medical Microbiology* **2014**, *304*, 31-36.

6. Schroder, W.; Goerke, C.; Wolz, C. Opposing effects of aminocoumarins and fluoroquinolones on the SOS response and adaptability in Staphylococcus aureus. *J. Antimicrob. Chemother.* **2013**, *68*, 529-538.

7. Collin, F.; Karkare, S.; Maxwell, A. Exploiting bacterial DNA gyrase as a drug target: current state and perspectives. *Appl. Microbiol. Biotechnol.* **2011**, *92*, 479-497.

8. Flatman, R. H.; Howells, A. J.; Heide, L.; Fiedler, H.; Maxwell, A. Simocyclinone D8, an Inhibitor of DNA Gyrase with a Novel Mode of Action. *Antimicrobial Agents and Chemotherapy* **2005**, *49*, 1093-1100.

9. Edwards, M. J.; Williams, M. A.; Maxwell, A.; McKay, A. R. Mass Spectrometry Reveals That the Antibiotic Simocyclinone D8 Binds to DNA Gyrase in a "Bent-Over" • Conformation: Evidence of Positive Cooperativity in Binding. *Biochemistry* **2011**, *50*, 3432-3440.

10. Hearnshaw, S. J.; Edwards, M. J.; Stevenson, C. E.; Lawson, D. M.; Maxwell, A. A New Crystal Structure of the Bifunctional Antibiotic Simocyclinone D8 Bound to DNA Gyrase Gives Fresh Insight into the Mechanism of Inhibition. *J. Mol. Biol.* **2014**, *426*, 2023-2033.

11. Cheng, G.; Hao, H.; Dai, M.; Liu, Z.; Yuan, Z. Antibacterial action of quinolones: From target to network. *Eur. J. Med. Chem.* **2013**, *66*, 555-562.

12. Aldred, K. J.; Blower, T. R.; Kerns, R. J.; Berger, J. M.; Osheroff, N. Fluoroquinolone interactions with Mycobacterium tuberculosis gyrase: Enhancing drug activity against wild-type and resistant gyrase. *Proc. Natl. Acad. Sci. U. S. A.* **2016**, *113*, E839-46.

13. Shadrick, W. R.; Ndjomou, J.; Kolli, R.; Mukherjee, S.; Hanson, A. M.; Frick, D. N. Discovering new medicines targeting helicases: challenges and recent progress. *J. Biomol. Screen.* **2013**, *18*, 761-781.

14. Li, B.; Pai, R.; Di, M.; Aiello, D.; Barnes, M. H.; Butler, M. M.; Tashjian, T. F.; Peet, N. P.; Bowlin, T. L.; Moir, D. T. Coumarin-based Inhibitors of Bacillus anthracis and Staphylococcus aureus Replicative DNA Helicase: Chemical Optimization, Biological Evaluation, and Antibacterial Activities. *J. Med. Chem.* **2012**, *55*, 10896-10908.

15. Aiello, D.; Barnes, M. H.; Biswas, E. E.; Biswas, S. B.; Gu, S.; Williams, J. D.; Bowlin, T. L.; Moir, D. T. Discovery, Characterization and Comparison of Inhibitors of Bacillus anthracis and Staphylococcus aureus Replicative DNA Helicases. *Bioorg. Med. Chem.* **2009**, *17*, 4466-4476.

16. Chopra, S.; Matsuyama, K.; Tran, T.; Malerich, J. P.; Wan, B.; Franzblau, S. G.; Lun, S.; Guo, H.; Maiga, M. C.; Bishai, W. R.; Madrid, P. B. Evaluation of gyrase B as a drug target in Mycobacterium tuberculosis. *J. Antimicrob. Chemother.* **2011**, *67*, 415-421.

17. Jeankumar, V. U.; Reshma, R. S.; Janupally, R.; Saxena, S.; Sridevi, J. P.; Medapi, B.; Kulkarni, P.; Yogeeswari, P.; Sriram, D. Enabling the (3 + 2) cycloaddition reaction in assembling newer anti-tubercular lead acting through the inhibition of the gyrase ATPase domain: lead optimization and structure activity profiling. *Org. Biomol. Chem.* **2015**, *13*, 2423-2431.

18. Jeyachandran, M.; Ramesh, P.; Sriram, D.; Senthilkumar, P.; Yogeeswari, P. Synthesis and *in vitro* antitubercular activity of 4-aryl/alkylsulfonylmethylcoumarins as inhibitors of Mycobacterium tuberculosis. *Bioorg. Med. Chem. Lett.* **2012**, *22*, 4807-4809.

19. Anand, A.; Kulkarni, M. V.; Joshi, S. D.; Dixit, S. R. One pot Click chemistry: A three component reaction for the synthesis of 2-mercaptobenzimidazole linked coumarinyl triazoles as anti-tubercular agents. *Bioorg. Med. Chem. Lett.* **2016**, *26*, 4709-4713.

20. Reddy, D. S.; Hosamani, K. M.; Devarajegowda, H. C. Design, synthesis of benzocoumarin-pyrimidine hybrids as novel class of antitubercular agents, their DNA cleavage and X-ray studies. *Eur. J. Med. Chem.* **2015**, *101*, 705-715.

21. Zheng, P.; Somersan-Karakaya, S.; Lu, S.; Roberts, J.; Pingle, M.; Warrier, T.; Little, D.; Guo, X.; Brickner, S. J.; Nathan, C. F.; Gold, B.; Liu, G. Synthetic Calanolides with Bactericidal Activity against Replicating and Nonreplicating Mycobacterium tuberculosis. *J. Med. Chem.* **2014**, *57*, 3755-3772.

22. Basanagouda, M.; Jambagi, V. B.; Barigidad, N. N.; Laxmeshwar, S. S.; Devaru, V.; Narayanachar Synthesis, structure-activity relationship of iodinated-4-aryloxymethyl-coumarins as potential anti-cancer and anti-mycobacterial agents. *Eur. J. Med. Chem.* **2014**, *74*, 225-233.

23. Skalicka-Woźniak, K.; Orhan, I. E.; Cordell, G. A.; Nabavi, S. M.; BudzyÅ„ska, B. Implication of coumarins towards central nervous system disorders. *Pharmacological Research* **2016**, *103*, 188-203.

24. Epifano, F.; Curini, M.; Menghini, L.; Genovese, S. Natural coumarins as a novel class of neuroprotective agents. *Mini Rev. Med. Chem.* **2009**, *9*, 1262-1271.

25. de Souza, L. G.; RennÃ³, M. N.; Figueroa-Villar, J. Coumarins as cholinesterase inhibitors: A review. *Chem. Biol. Interact.* **2016**, *254*, 11-23.

26. Joubert, J.; Foka, G. B.; Repsold, B. P.; Oliver, D. W.; Kapp, E.; Malan, S. F. Synthesis and evaluation of 7-substituted coumarin derivatives as multimodal monoamine oxidase-B and cholinesterase inhibitors for the treatment of Alzheimer's disease. *Eur. J. Med. Chem.* **2017**, *125*, 853-864.

27. Patil, P. O.; Bari, S. B.; Firke, S. D.; Deshmukh, P. K.; Donda, S. T.; Patil, D. A. A comprehensive review on synthesis and designing aspects of coumarin derivatives as monoamine oxidase inhibitors for depression and Alzheimer's disease. *Bioorg. Med. Chem.* **2013**, *21*, 2434-2450.

28. Birks, J.; Harvey, R. J. Donepezil for dementia due to Alzheimer's disease. *Cochrane Database Syst. Rev.* **2006**, *(1)*, CD001190.

29. Kuhn, M. L.; Alexander, E.; Minasov, G.; Page, H. J.; Warwrzak, Z.; Shuvalova, L.; Flores, K. J.; Wilson, D. J.; Shi, C.; Aldrich, C. C.; Anderson, W. F. Structure of the Essential Mtb FadD32 Enzyme: A Promising Drug Target for Treating Tuberculosis. *ACS Infect. Dis.* **2016**, *2*, 579-591.

30. Maruri, F.; Sterling, T. R.; Kaiga, A. W.; Blackman, A.; van, d. H.; Mayer, C.; Cambau, E.; Aubry, A. A systematic review of gyrase mutations associated with fluoroquinolone-resistant Mycobacterium tuberculosis and a proposed gyrase numbering system. *J. Antimicrob. Chemother.* **2012**, *67*, 819-831.

31. Carroll, P.; Schreuder, L. J.; Muwanguzi-Karugaba, J.; Wiles, S.; Robertson, B. D.; Ripoll, J.; Ward, T. H.; Bancroft, G. J.; Schaible, U. E.; Parish, T. Sensitive detection of gene expression in mycobacteria under replicating and non-replicating conditions using optimized far-red reporters. *PLoS One* **2010**, *5*, e9823.

32. Abrahams, G. L.; Kumar, A.; Savvi, S.; Hung, A. W.; Wen, S.; Abell, C.; Barry, C. E.,3rd; Sherman, D. R.; Boshoff, H. I.; Mizrahi, V. Pathway-selective sensitization of Mycobacterium tuberculosis for target-based whole-cell screening. *Chem. Biol.* **2012**, *19*, 844-854.

33. Lounis, N.; Vranckx, L.; Gevers, T.; Kaniga, K.; Andries, K. *In vitro* culture conditions affecting minimal inhibitory concentration of bedaquiline against M. tuberculosis. *Med. Mal. Infect.* **2016**, *46*, 220-225.

34. Dockal, M.; Carter, D. C.; Ruker, F. Conformational transitions of the three recombinant domains of human serum albumin depending on pH. *J. Biol. Chem.* **2000**, *275*, 3042-3050.

35. Ran, D.; Wu, X.; Zheng, J.; Yang, J.; Zhou, H.; Zhang, M.; Tang, Y. Study on the Interaction between Florasulam and Bovine Serum Albumin. *J. Fluoresc.* **2007**, *17*, 721-726.

36. Tian, J.; Liu, J.; Zhang, J.; Hu, Z.; Chen, X. Fluorescence Studies on the Interactions of Barbaloin with Bovine Serum Albumin. *Chemical and Pharmaceutical Bulletin* **2003**, *51*, 579-582.

37. Seetharamappa, J.; Kamat, B. P. Spectroscopic studies on the mode of interaction of an anticancer drug with bovine serum albumin. *Chem. Pharm. Bull. (Tokyo)* **2004**, *52*, 1053-1057.

38. Sulkowska, A.; Rownicka, J.; Bojko, B.; Sulkowski, W. Interaction of anticancer drugs with human and bovine serum albumin. *J. Mol. Struct.* **2003**, *651*, 133-140.

39. Kun, R.; Kis, L.; Dekany, I. Hydrophobization of bovine serum albumin with cationic surfactants with different hydrophobic chain length. *Colloids and Surfaces B: Biointerfaces* **2010**, *79*, 61-68.

40. Liu, B.; Guo, Y.; Wang, J.; Xu, R.; Wang, X.; Wang, D.; Zhang, L.; Xu, Y. Spectroscopic studies on the interaction and sonodynamic damage of neutral red (NR) to bovine serum albumin (BSA). *J Lumin* **2010**, *130*, 1036-1043.

41. Xiang, G.; Tong, C.; Lin, H. Nitroaniline Isomers Interaction with Bovine Serum Albumin and Toxicological Implications. *J. Fluoresc.* **2007**, *17*, 512-521.

42. Hu, Y.; Liu, Y.; Zhang, L.; Zhao, R.; Qu, S. Studies of interaction between colchicine and bovine serum albumin by fluorescence quenching method. *J. Mol. Struct.* **2005**, *750*, 174-178.

43. Gök, E.; Öztürk, C.; Akbay, N. Interaction of Thyroxine with 7 Hydroxycoumarin: A Fluorescence Quenching Study. *J. Fluoresc.* **2008**, *18*, 781-785.

44. Xu, H.; Gao, S.; Lv, J.; Liu, Q.; Zuo, Y.; Wang, X. Spectroscopic investigations on the mechanism of interaction of crystal violet with bovine serum albumin. *J. Mol. Struct.* **2009**, *919*, 334-338.

45. Shaikh, S. M. T.; Seetharamappa, J.; Kandagal, P. B.; Manjunatha, D. H.; Ashoka, S. Spectroscopic investigations on the mechanism of interaction of bioactive dye with bovine serum albumin. *Dyes and Pigments* **2007**, *74*, 665-671.

46. Papadopoulou, A.; Green, R. J.; Frazier, R. A. Interaction of flavonoids with bovine serum albumin: a fluorescence quenching study. *J. Agric. Food Chem.* **2005**, *53*, 158-163.

47. Shi, X.; Li, X.; Gui, M.; Zhou, H.; Yang, R.; Zhang, H.; Jin, Y. Studies on interaction between flavonoids and bovine serum albumin by spectral methods. *J Lumin* **2010**, *130*, 637-644.

48. Ware, W. R. Oxygen quenching of fluorescence in solution: An experimental study of the diffusion process. *J. Phys. Chem.* **1962**, *66*, 455-458.

49. Mosmann, T. Rapid colorimetric assay for cellular growth and survival: application to proliferation and cytotoxicity assays. *J. Immunol. Methods* **1983**, *65*, 55-63.

50. Cui, W.; Zhang, Z.; Li, W.; Hu, S.; Mak, S.; Zhang, H.; Han, R.; Yuan, S.; Li, S.; Sa, F.; Xu, D.; Lin, Z.; Zuo, Z.; Rong, J.; Ma, E. D. L.; Choi, T. C.; Lee, S. M. Y.; Han, Y. The anti-cancer agent SU4312 unexpectedly protects against MPP(+)-induced neurotoxicity via selective and direct inhibition of neuronal NOS. *Br. J. Pharmacol.* **2013**, *168*, 1201-1214.

51. Jantas, D.; Greda, A.; Golda, S.; Korostynski, M.; Grygier, B.; Roman, A.; Pilc, A.; Lason, W. Neuroprotective effects of metabotropic glutamate receptor group II and III

activators against MPP(+)-induced cell death in human neuroblastoma SH-SY5Y cells: the impact of cell differentiation state. *Neuropharmacology* **2014**, *83*, 36-53.

52. Pyszko, J.; Strosznajder, J. B. Sphingosine kinase 1 and sphingosine-1-phosphate in oxidative stress evoked by 1-methyl-4-phenylpyridinium (MPP+) in human dopaminergic neuronal cells. *Mol. Neurobiol.* **2014**, *50*, 38-48.

53. Wang, Y.; Gao, J.; Miao, Y.; Cui, Q.; Zhao, W.; Zhang, J.; Wang, H. Pinocembrin Protects SH-SY5Y Cells Against MPP+-Induced Neurotoxicity Through the Mitochondrial Apoptotic Pathway. *Journal of Molecular Neuroscience* **2014**, *53*, 537-545.

54. Nakaso, K.; Tajima, N.; Horikoshi, Y.; Nakasone, M.; Hanaki, T.; Kamizaki, K.; Matsura, T. The estrogen receptor beta-PI3K/Akt pathway mediates the cytoprotective effects of tocotrienol in a cellular Parkinson's disease model. *Biochim. Biophys. Acta* **2014**, *1842*, 1303-1312.

55. Tasaki, Y.; Omura, T.; Yamada, T.; Ohkubo, T.; Suno, M.; Iida, S.; Sakaguchi, T.; Asari, M.; Shimizu, K.; Matsubara, K. Meloxicam protects cell damage from 1-methyl-4-phenyl pyridinium toxicity via the phosphatidylinositol 3-kinase/Akt pathway in human dopaminergic neuroblastoma SH-SY5Y cells. *Brain Res.* **2010**, *1344*, 25-33.

56. Zhu, G.; Wang, X.; Wu, S.; Li, Q. Involvement of activation of PI3K/Akt pathway in the protective effects of puerarin against MPP+-induced human neuroblastoma SH-SY5Y cell death. *Neurochem. Int.* **2012**, *60*, 400-408.

57. Ioerger, T. R.; Feng, Y.; Ganesula, K.; Chen, X.; Dobos, K. M.; Fortune, S.; Jacobs, W. R.,Jr; Mizrahi, V.; Parish, T.; Rubin, E.; Sassetti, C.; Sacchettini, J. C. Variation among genome sequences of H37Rv strains of Mycobacterium tuberculosis from multiple laboratories. *J. Bacteriol.* **2010**, *192*, 3645-3653.

58. Goldstone, R. M.; Goonesekera, S. D.; Bloom, B. R.; Sampson, S. L. The transcriptional regulator Rv0485 modulates the expression of a pe and ppe gene pair and is required for Mycobacterium tuberculosis virulence. *Infect. Immun.* **2009**, *77*, 4654-4667.

59. Ollinger, J.; Bailey, M. A.; Moraski, G. C.; Casey, A.; Florio, S.; Alling, T.; Miller, M. J.; Parish, T. A dual read-out assay to evaluate the potency of compounds active against Mycobacterium tuberculosis. *PLoS One* **2013**, *8*, e60531.

7.3 Letters, posters and presentations

The following chapter is a depiction of additional research outputs directly pertaining to previous chapters that serves to further illustrate the potential of polycyclic propargylamine compounds in the study of neurodegeneration. The chapter comprises several poster and podium presentations presented at the various academic conferences attended during the course of the study.

List of letters, posters and presentations

- Poster: Zindo, F.T., Joubert, J., Malan, S.F. 3's Company Pharmacy Conference, Lagoon Beach, Cape Town (Poster session, October 2013).
- Podium presentation 1: Zindo, F.T., Joubert, J., Malan, S.F. 35th Conference of the Academy of Pharmaceutical Sciences, Summerstrand Hotel, Port Elizabeth (August 2014).
- Letter: Zindo, F.T., Joubert, J., Malan, S.F. *S Afr Pharm J*, 82, (2), March 2015.
- Podium presentation 2- 1st Conference of Biomedical and Natural Sciences and Therapeutics, Spier Wine Farm, Stellenbosch (October 2018).

The poster: Summarises the biological activities of evaluations conducted on a previous series of polycyclic propargylamine and acetylene compounds. (expansion of Article 1, Chapter 3). Additional synthetic routes summarised in this poster, include the design and synthesis of additional pentacycloundacane propargylamine derivatives (scheme 1) which were later evaluated and reported in Article 2, Chapter 4.

Podium presentation 1: Highlights the various structure-activity relationships of the series of polycyclic propargylamine and acetylene compounds described in Article 1, Chapter 3. The presentation also summarises the molecular modelling studies that led to the development of the new series of compounds described in Article 2, Chapter 4. This presentation received the Boehringer Ingelheim Young Scientist Award for Laboratory-based research.

The letter: Is a summary article published in the South African Pharmaceutical Journal. It highlights the work published in Article 1, Chapter 3.

Podium presentation 2: Summarises all the work conducted in this PhD project. It highlights the design synthesis and evaluation of various polycyclcic propargylamine derivatives that show multifunctional activity which include MAO-B inhibition, VGCC blockade, NMDAR antagonism as well as general neuroprotective ability (expansion of Article 2, Chapter 4)

Polycyclic propargylamine derivatives as multifunctional neuroprotective agents

Frank T. Zindo, Jacques Joubert and Sarel F. Malan

School of Pharmacy, University of the Western Cape, Private Bag X17, Bellville, 7535, Cape Town, South Africa

Introduction

The abnormal death of neuronal cells in the CNS, which leads to neurodegeneration, takes place by an intrinsic cell suicide program known as apoptosis. Apoptosis is triggered by several stimuli, and consists of numerous pathways and cascades which ultimately lead to cell death.[1] Treatment options can thus be designed to target one or more of the many pathways involved in this cascade. These drug target sites include; but are not limited to *N*-methyl-D-aspartate (NMDA) receptors, *L*-type voltage sensitive calcium channels (VGCC), monoamine oxidase-B (MAO-B) enzymes and dopamine transporters.

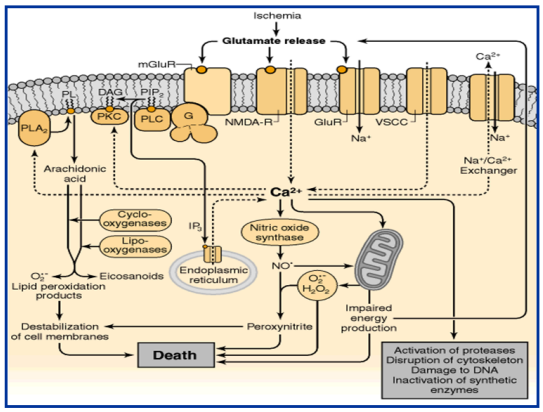

Figure 1: Diagram depicting ischemic events leading to neurodegeneration in a neuronal cell. (Adapted from Siegel, G.J., et al 1999)[2]

Several compounds containing the propargylamine functional group, including rasagiline and selegiline (Figure 2), are known to inhibit the activity of MAO-B enzymes while polycyclic cage amines such as NGP1-01 and MK-801 (Figure 2) have been reported to show antagonistic activity on NMDA receptors and calcium channels.[3] Incorporating the polycyclic cage moiety and the propargylamine functional group in a single compound is believed to result in a multimechanistic compound with inherent activity on NMDA receptors, calcium channels and the MAO-B enzyme. This school of thought inspired the synthesis of a series of polycyclic propargylamine and acetylene derivatives (**1-8**) (Figure 2). In a previous study by our group, these compounds showed excellent anti-apoptotic activity but little to no activity on the MAO-B enzyme.

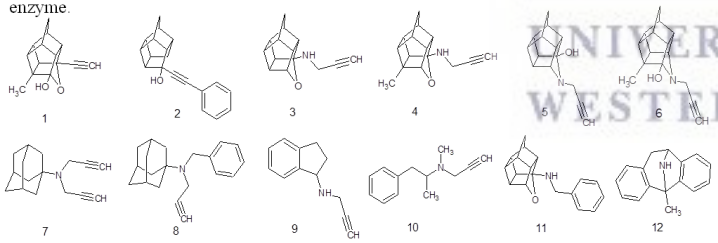

Figure 2: Novel polycyclic propargylamine and acetylene derivatives (**1-8**) and the structures of rasagiline (**9**), selegiline (**10**) , NGP1-01 (**11**) and MK-801 (**12**).

The current study was thus aimed at establishing the potential activity of these polycyclic propargylamine and acetylene derivatives on NMDA receptors and VGCC's. Findings from these assays inspired the design of a new series (Scheme 1) of multifunctional propargylamine derivatives which will potentially exhibit improved activity on the MAO-B enzyme and retain or improve NMDA modulatory effects, VGCC modulatory effects and anti-apoptotic activity.

Proposed Series Design

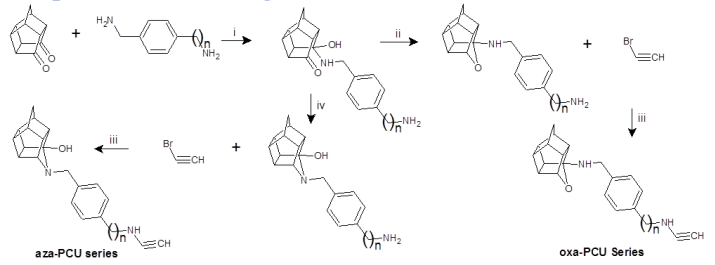

Scheme 1: Reagents and conditions: (i) THF, 0 °C, 1hr; (ii) THF/MeOH, $NaBH_4$ rt, 24 h; (iii) DMF, rt, 24 h ; (iv) MeOH, acetic acid, $NaCNBH_3$, 2 h.

Biological activities

Table 1: Biological activities of test compounds as indication of potential neuroprotectictive activity.

Compound	% Viable Cells – apoptosis induced [10 µM][a]	% VGCC inhibition [100 µM][b]	% NMDA receptor inhibition [100 µM][c]	% MAO-B enzyme inhibition [300 µM][d]
Selegiline	77%	n/a	n/a	93%
NGP1-01	67%	27%	18%	15%
MK801	n/a	n/a	100%	n/a
Nimodipine	n/a	100%	n/a	n/a
1	100%	10%	Inactive	Inactive
2	98%	19%	23%	73%
3	88%	Inactive	Inactive	Inactive
4	97%	26%	38%	12%
5	93%	18%	4%	6%
6	67%	11%	11%	11%
7	68%	18%	52%	20%
8	70%	45%	59%	14%

[a]Anti-apoptotic activity in SK-NBE(2) neuroblastosoma cells using a DesphiperTM® kit, which marks changes in mitochondrial membrane potential that takes place during apoptosis. [b]KCl induced calcium influx inhibition into synaptoneurosomes using Fura-2-AM. [c]NMDA/Glycine induced calcium influx inhibition into synaptoneurosomes using Fura-2-AM. [d]MAO-B inhibitory activity using a spectrophotometric assay that utilized the neurotoxin MMTP as substrate, with baboon liver mitochondria serving as enzyme source. n/a = not available.

Molecular Modeling

To develop a new series of compounds with improved MAO-B activity, when compared to the existing series (Table 1), computer-assisted simulated docking of proposed structures of propargylamine derivatives was conducted using Molecular Operating Environment (MOE). This resulted in a series of compounds (aza-PCU and oxa-PCU in scheme 1) with the ability to traverse deeper into the enzyme cavity of the MAO-B enzyme (PDB ID:2V5Z) compared to compounds **1-8**, which merely occupy the entrance cavity and remain distant from the flavin adenine dinucleotide (FAD) cofactor hence failing to form the necessary interactions required for activity. (Figure 3)[4]

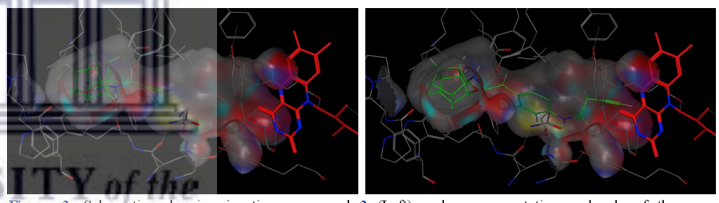

Figure 3: Schematics showing inactive compound **3** (Left) and a representative molecule of the new propargylamine series (Right) in a computer simulated MAO-B enzyme cavity. The compounds are shown in green and the FAD co-factor in red. Note that compound **3** merely occupies the entrance cavity of the enzyme and remains distant from the FAD co-factor rendering it inactive, while the new series traverses deeper into the enzyme cavity to proximate the FAD co-factor allowing for potential binding interactions which may result in improved MAO-B activity.

Conclusion

The previous series of eight polycyclic propargylamine and acetylene derivatives (compounds **1-8**) were assayed for calcium modulatory effect. Compunds **2, 4, 7** and **8** showed the best VGCC and NMDA activity ranging from 18% to 59% and compared favourably to reference compounds. In an attempt to retain or improve all activities established from the previous series of compounds, a new series of polycyclic propargylamine derivatives has been designed. Based on the preliminary findings from the molecular modeling study (Figure 3), the new series show potential interaction with the FAD co-factor of the MAO-B enzyme, suggesting the series to potentially exhibit improved MAO-B activity. Compounds that render such multimechanistic activity have great potential to serve as future analogues for the treatment and management of neurodegenerative disorders.

References

1) Fulda, S., Adrienne, M.G., Hori, O., & Samali, A., 2010, *International Journal of Cell Biology*, **2010(1)**, 1-23.
2) Siegel, G.J., Agranoff, B.W., Albers, R.W., 1999, '*Basic Neurochemistry*: Molecular, Cellular and Medical Aspects'. 6th edition.
3) Joubert, J., Gledenhuys, W.J., Van der Schyf, C.J., Oliver, D.W., Kruger, H.G., Govender, T., Malan, S.F., 2012, *ChemMedChem*, **7(3)**, 375-384.
4) Mitchell, D.J., Nikolic, D., Rivera, E., Sablin, S.O., Choi, S., van Breemen, R.B., Singer, T.P., Silverman, R.B., 2001, *Biochemistry*, **40(18)**,5447-56.

Acknowledgement

We are grateful to the University of the Western Cape and the National Research Foundation of South Africa for their financial support.

Podium presentation 1

Polycyclic propargylamine derivatives as multifunctional neuroprotective agents

Presented by : Mr. Frank Zindo
Supervisor : Dr. Jacques Joubert
Co-supervisor : Prof. Sarel Malan

UNIVERSITY of the WESTERN CAPE

Overview

- Neurodegenerative disorders
  - Disease burden
  - Etiology
- Treatment concepts
- Our concept
- Reported 'preliminary' findings
- Development of improved analogues
- Conclusion

Background

Neurodegeneration

- Umbrella term for the progressive loss of structure or function of neurons.
- Examples: Parkinson's, Alzheimer's, and Huntington's diseases

Parkinson's Disease (PD)

Primary PD:
Neurodegenerative disease characterized by a decrease in Dopamine in the brain
Secondary PD:
Caused by drugs such as antipsychotics and toxins such as CO and CS.

Symptoms:
Muscle rigidity, trembling, reduced arm movements and shuffling walk

Etiology

- Known pathogenesis?
  - Not yet fully understood
  - Scientific consensus is quite firm in describing them as multifactorial diseases caused by genetic, environmental and endogenous factors.
    - The excessive protein misfolding and aggregation (Terry et al. 1964; Grundke-Iqbal et al. 1986)
    - The cholinergic dysfunction, oxidative stress (Coyle and Puttfarcken 1993; Perry et al. 2000; Gella and Durany 2009)
    - Mitochondrial dysfunction (Swerdlow and Khan 2009)
    - Metal dyshomeostasis (Huang et al. 2004)
    - Excitotoxic and neuroinflammatory processes (Mishizen- Eberz et al. 2004)
    - Disturbances in other neurotransmitter systems such as the noradrenergic system

Ischemic events leading to neurodegeneration

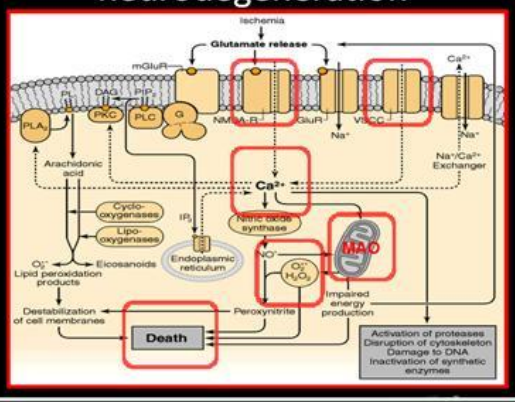

Treatment concept

- Currently available
  - MAO inhibitors
    - Rasagiline, Selegiline
- Shortfalls
  - Symptomatic treatment
  - Single target site
  - Lack of neuroprotective/restorative ability
- Need for Multimodal Drug Ligands (MTDL)
  - Selegiline + L-DOPA

Rasagiline

Selegiline

Lead compounds

Compound 1		Compound 5	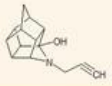
Compound 2	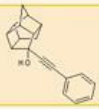	Compound 6	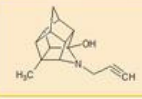
Compound 3		Compound 7	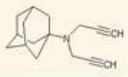
Compound 4	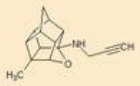	Compound 8	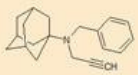

Anti-apoptosis activity

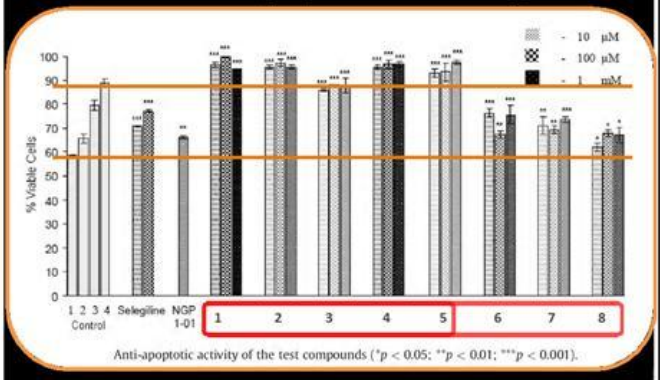

Anti-apoptotic activity of the test compounds (*$p < 0.05$; **$p < 0.01$; ***$p < 0.001$).

MAO-B inhibition

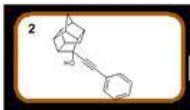

Compound	Molecular formula	Molecular weight (g/mol)	% MAO-B inhibition [300 µM]
Propagylamine	C_3H_5N	55.079	19.93*
Selegiline	$C_{13}H_{17}N$	187.281	93.33***
NGP1-01	$C_{18}H_{19}NO$	265.350	14.57*
1	$C_{14}H_{14}O_2$	214.260	Inactive
2	$C_{19}H_{18}O$	262.346	73.32***
3	$C_{14}H_{15}NO$	212.275	Inactive
4	$C_{15}H_{17}NO$	226.302	11.67*
5	$C_{14}H_{15}NO$	213.275	5.83
6	$C_{15}H_{17}NO$	227.302	10.83*
7	$C_{16}H_{21}N$	227.345	14.00*
8	$C_{20}H_{25}N$	279.419	20.13*
Nimodipine	$C_{21}H_{26}N_2O_7$	418.440	n.d.
MK-801	$C_{16}H_{15}N$	221.297	n.d.

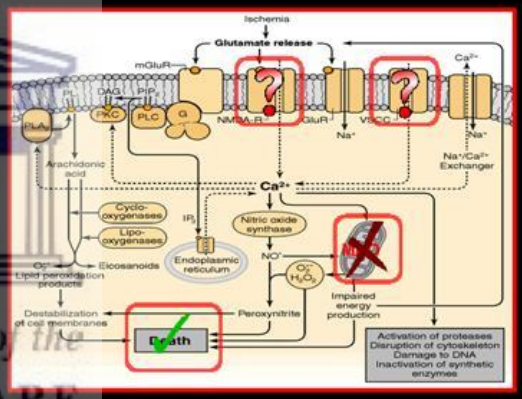

Contributing moieties

- Pentacycloundecane

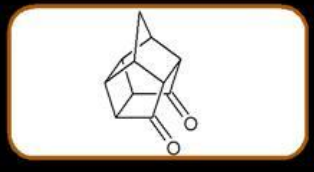

Polycyclic cage useful as a scaffold for side-chain attachment as well as for improving a drug's lipophilicity, pharmacokinetic & pharmacodynamic properties:

- Blood-brain barrier permeability
- Increases affinity for lipophilic regions in target proteins

Contributing moieties

- Amantadine

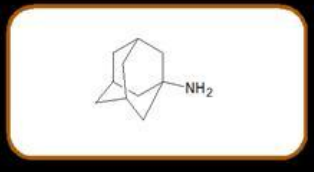

FDA approved antiparkinsonian agent:

- Weak antagonist of the NMDA type glutamate receptor
- Increases dopamine release and blocks dopamine reuptake

Symptomatic treatment of neurodegenerative diseases

Resemblance

- NGP1-01

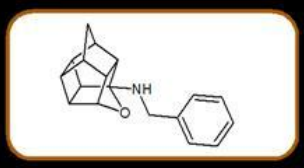

Brain-permeable dual blocker of neuronal VGCC and ligand-operated calcium channels (NMDAr)

VGCC and NMDAr channel assay

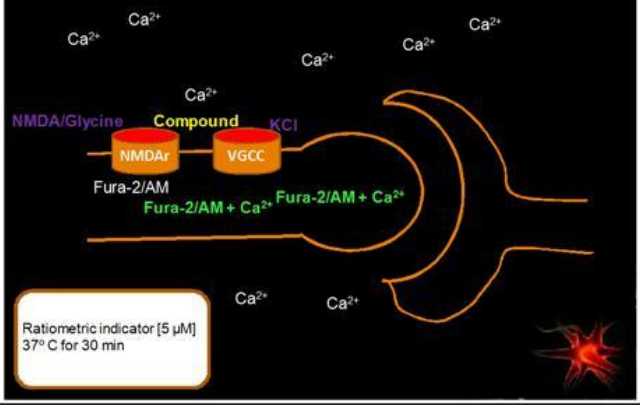

Ca^{2+}- regulation: VGCC and NMDAr channel activity

Compound	Molecular formula	Molecular weight (g/mol)	% VGCC inhibition [100 µM]	% NMDA receptor inhibition [100 µM]
Propagylamine	C_5H_5N	55.079	n.d.	n.d.
Selegiline	$C_{13}H_{17}N$	187.281	n.d.	n.d.
NGP1-01	$C_{18}H_{19}NO$	265.350	27**	18*
1	$C_{14}H_{14}O_2$	214.260	10	Inactive
2	$C_{19}H_{18}O$	262.346	19	23
3	$C_{14}H_{15}NO$	212.275	Inactive	Inactive
4	$C_{15}H_{17}NO$	226.302	26	38**
5	$C_{14}H_{15}NO$	213.275	18*	4
6	$C_{14}H_{17}NO$	227.302	11	11
7	$C_{16}H_{21}N$	227.345	18*	52***
8	$C_{20}H_{25}N$	279.419	45*	59*
Nimodipine	$C_{21}H_{26}N_2O_7$	418.440	100***	n.d.
MK-801	$C_{16}H_{15}N$	221.297	Inactive	100***

[Statistical significance (*) $p < 0.05$, (**) $p < 0.001$, (***) $p < 0.0001$]. n.d. = not determined.

Ca^{2+}- regulation: VGCC and NMDAr channel activity

Summary Activity

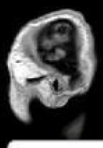

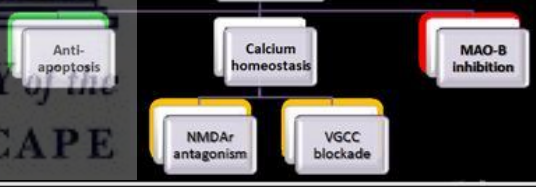

Other target sites

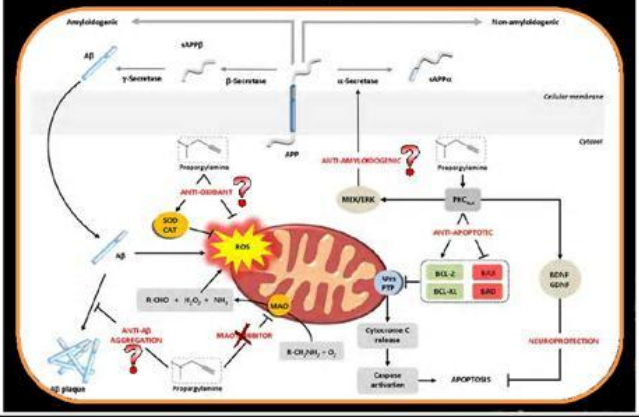

Designing improved analogues (Series 2)

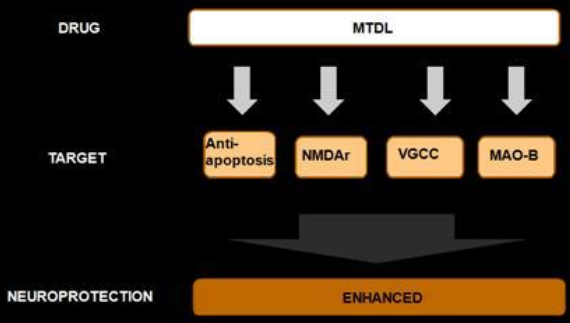

Molecular Modelling

Safinamide: Reversible and selective monoamine oxidase B inhibitor

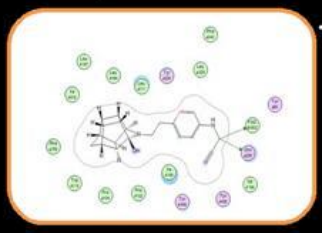

- Main features:
  - Entrance cavity
  - Substrate cavity
  - Flavin adenine dinucleotide co-factor (FAD)
  - Amino acid residues

Molecular Operating Environment (MOE) generated images of compound docking in MAO-B enzyme (PDB ID: 2V5Z)

Synthesis

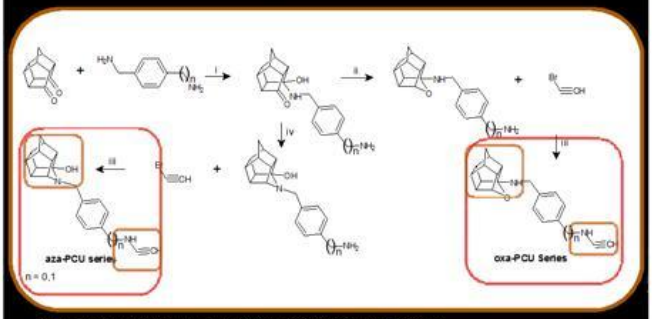

Schematic for the synthesis of a new series of aza-PCU and oxa-PCU compounds. Reagents and conditions: (i) THF, 0 °C, 1hr; (ii) THF/MeOH, $NaBH_4$, rt, 24 h; (iii) DMF, rt, 24 h ; (iv) MeOH, acetic acid, $NaCNBH_3$, 2 h.

Concluding remarks

- Establishing the site of action
- Computer simulated software's (MOE) afford great foresight
- Propargylamine derivatives: great drug candidates for neuroprotection

Acknowledgements

- Dr Jacques Joubert, Professor Sarel Malan and fellow research colleagues
- National Research Fund (NRF)

Questions?

Cum Laude
Academy of Pharmaceutical Sciences

Polycyclic propargylamine derivatives as multifunctional neuroprotective agents

Frank Zindo, Jaques Joubert, Sarel Malan
Pharmaceutical Chemistry, School of Pharmacy, University of the Western Cape, Bellville
Correspondence to: Sarel Malan, e-mail: sfmalan@uwc.ac.za
Keywords: polycyclic propargylamine derivatives, multifunctional neuroprotective agents
Frank Zindo is the winner of the 2014 Boehringer Ingelheim Young Scientist Award (Pharmaceutical Sciences category)


Frank Zindo

Introduction

The abnormal death of neurons in the central nervous system of individuals suffering from neurodegenerative diseases, which include Parkinson's disease, Alzheimer's disease, Huntington's disease and amyotrophic lateral sclerosis, takes place by an intrinsic cell suicide programme, known as apoptosis.[1,2] This process is triggered by several stimuli, and consists of numerous pathways and cascades which lead to apoptosis. One such pathway is the excitotoxic process, which results from the activation of postsynaptic receptors including N-methyl-D-aspartate (NMDA) receptors, and 2-amino-3-(3-hydroxy-5-methylisoxazol-4-yl)proprionate and kainate receptors. Upon their activation, these receptors open their associated ion channel to allow the influx of Ca^{2+} and Na^{+} ions. The excessive influx of calcium, together with any calcium release from the intracellular compartments, can overwhelm Ca^{2+} regulatory mechanisms and lead to cell death.[3,4] This mechanism of cell death suggests that the receptors and their associated calcium channels serve as drug target sites to curb neurodegeneration. It has also been shown that there are age-related elevated levels of monoamine oxidase B (MAO-B), which not only act indirectly as a trigger to the apoptotic process, but also give rise to some of the signs and symptoms associated with these disorders.[5,6] Therefore, compounds that exhibit MAO-B inhibition are more advantageous as neuroprotective agents than agents with little or no activity on this enzyme. However, it is important to note that the pathogenesis of these complex neurodegenerative conditions is not yet fully understood, and other ascribed theories of causation include mitochondrial dysfunction,[7] cholinergic dysfunction,[8] oxidative stress[8] and metal dyshomeostasis.[3]

Aim

Eight lead compounds, in the form polycyclic propargylamine or derivatives thereof, selected from our compound library, were reported to exhibit anti-apoptotic activity as they improved cell viability by values ranging from 9-41%.[9] The reported anti-apoptotic activity of these compounds seems to result from some mechanism apart from MAO-B inhibition, as these compounds showed little to no activity when assayed for MAO-B inhibition at 300 µM.

Thus, the study aimed to assess the lead compounds 1-8 (Figure 1), which were developed to serve as multifunctional drugs, for potential calcium flux modulatory activity, and to design a new series of compounds, based on the findings from calcium flux assays and computer modelling studies, with the aim of affording novel compounds with improved multifunctional properties.

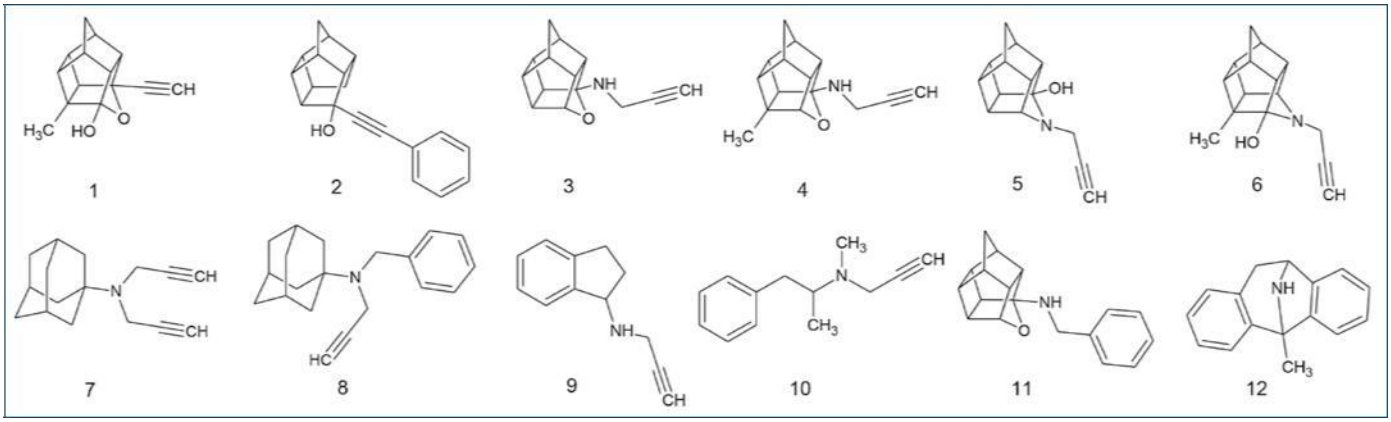

Figure 1: Novel polycyclic propargylamine and acetylene derivatives (1-8) and the structures of rasagiline (9), selegiline (10), NGP1-01 (11) and MK-801 (12)

This new series was designed to halt the apoptotic process and eliminate some of the signs and symptoms of neurodegenerative disorders by:

• Modulating the calcium influx by antagonising the NMDA receptors and blocking the *L*-type voltage-gated calcium channels (VGCC)

• Inhibiting the MAO-B enzyme, thus allowing an increase in the depleted neurotransmitter levels in the central nervous system, and reducing the concomitant production of hydrogen peroxide and other neuronal cell-damaging free radicals[10,11]

• Halting the apoptotic process.

Method

Synthesis

Considering the structures of rasagiline (9) and selegiline (10), two well known MAO-B inhibitors with anti-apoptotic activity,12 the lead series of neuroprotective agents all contained the propargylamine functional group or a derivative thereof, conjugated to various polycyclic cage moieties.

To synthesize compounds 1-8 (Figure 1), propargylamine, propargylbromide or ethynyl magnesium bromide was made to react with the pentacycloundecane (PCU) or amantadine to give the final compounds. Each compound was synthesized to evaluate the activity and benefit of a certain group of atoms in the molecule. The structural characterisation of these compounds was performed using mass, fourier transform mass, and nuclear magnetic resonance, spectroscopy, in combination with single crystal X-ray diffraction analysis.[10]

Calcium modulation assays

All derivatives (1-8) were screened at 100 µM for their potential inhibitory activity on the VGCC and NMDA receptor channels. They were assessed using the fluorescent ratiometric indicator, Mag-Fura-2/AM™, and a fluorescent plate reader. KCl- and NMDA/ glycine-mediated calcium influx in murine synaptoneurosomes was used to evaluate the influence of the test compounds on the calcium influx via the VGCC and NMDA receptor channels, respectively. Both assays were carried out with reference to standard positive controls, i.e. nimodipine, a dihydropyridine *L*-type calcium-channel blocker; NGP1-01 (11), a prototype pentacycloundecane compound with neuroprotective ability;[13-16] and MK-801, a potent high-affinity NMDA receptor channel blocker.

Results and discussion

Voltage-gated calcium channel blockade

The adamantine-propargylamine derivative 8 showed the best VGCC inhibitory activity (45%); higher than that of NGP1-01 (11) (27%). Although structurally similar to 8, the substitution of the aromatic moiety of 8 with a propargyl moiety to give the disubstituted propargylamine adamantane compound 7, led to a significant decrease in VGCC activity (18%). This observation

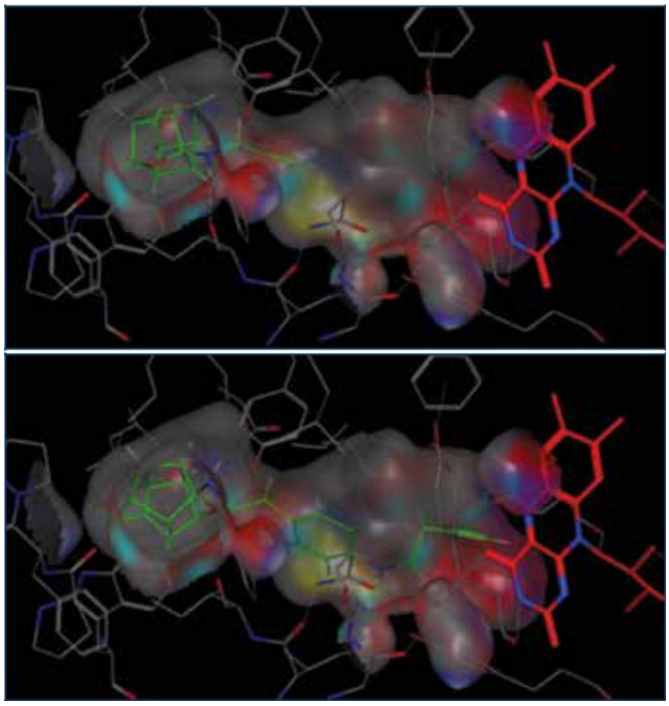

Figure 2 a and b: Schematic generated from the Molecular Operating Environment® software, showing inactive compound 3 (Figure 2 a), and a representative molecule of the new pentacycloundecylamine-propargylamine series (Figure 2 b), in a monoamine oxidase B enzyme active site cavity

indicates the importance of including the benzylamine moiety within these structures for optimal VGCC activity.

N-methyl-D-aspartate receptor antagonism

The best inhibitory activities were observed for compounds 7 and 8, of 52% and 59%, respectively. This high activity might be attributed to the inclusion of the adamantane moiety, which has known NMDA receptor inhibitory activity.[17]

It is important to note that the concentration at which these lead compounds show calcium modulation is too high to ascribe the anti-apoptotic activity of these compounds to NMDA receptor antagonism and VGCC blockade. Therefore, it is postulated that these derivatives exert their effect by acting on one or more other mechanisms implicated in neurodegeneration, and unexplored in this study. Further studies to elucidate the possible anti-apoptotic mechanism of these compounds are underway.

Monoamine oxidase B molecular modelling

The realisation of minimal MAO-B inhibitory activity in the initial series led to the development and synthesis of a new series of compounds which may potentially exhibit improved MAO-B activity when compared to the lead series. Computer-assisted simulated docking of the proposed propargylamine derivatives was conducted using Molecular Operating Environment® software,18 and allowed the design of a series of aza-PCU and oxa-PCU compounds (Figure 2a and b and Figure 3), with the ability to traverse deeper into the enzyme cavity of the MAO-B enzyme (PDB ID: 2V5Z) compared to compounds 1-8.

The compounds are shown in green and the flavin adenine dinucleotide co-factor in red. Note that compound 3 merely

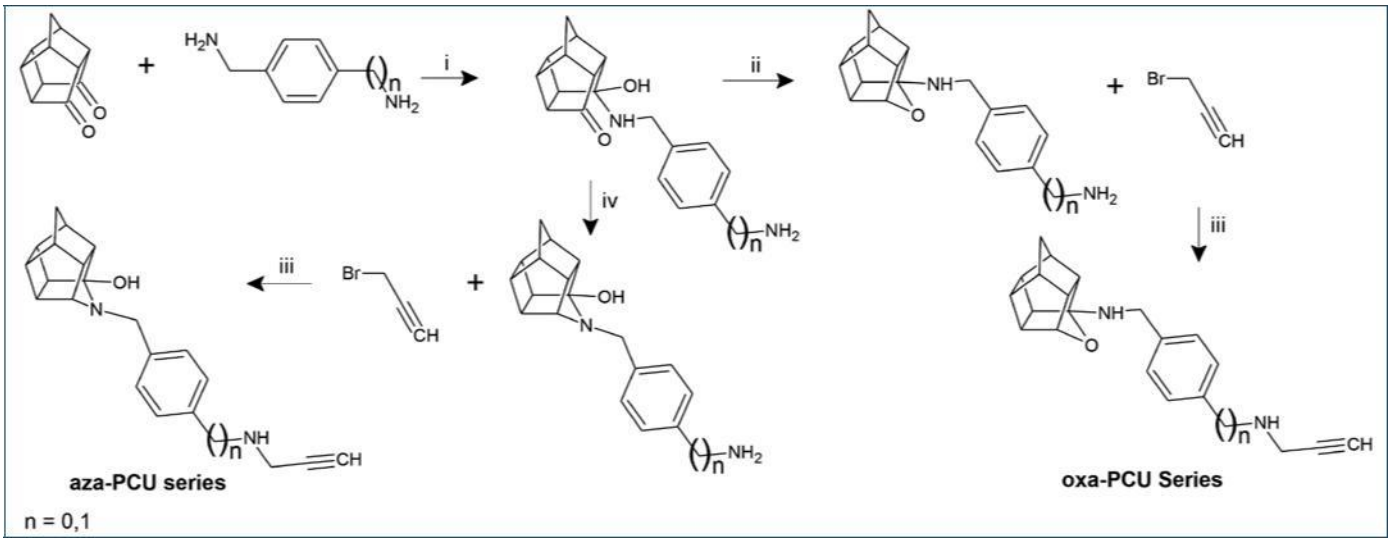

PCU: pentacycloundecylamine

Figure 3: Schematic for the synthesis of a new series of aza-pentacycloundecylamine and oxa-pentacycloundecylamine compounds. Reagents and conditions: (i) THF 0°C 1 hour, (ii) THF/MeOH and $NaBH_4$ rt 24 hours, (iii) DMF rt 24 hours, (iv) MeOH, acetic acid and $NaCNBH_3$ 2 hours

occupies the entrance cavity of the enzyme, and remains distant from the flavin adenine dinucleotide co-factor, rendering it inactive, while the new series traverses deeper into the enzyme cavity to proximate the flavin adenine dinucleotide co-factor, allowing for potential binding interactions which may result in improved monoamine oxidase B activity.

Synthesis of new analogues

Using the PCU moiety as a scaffold, the new compounds were synthesized by virtue of SN2 nucleophilic substitution reactions to afford the two series of propargylamine-derived compounds (Figure 3).

Biological evaluation of the new series will include calcium modulation, MAO-B inhibition and anti-apoptotic assays. The findings thereof will allow for further derivation of structural activity relationships pertinent to these types of compounds in serving as neuroprotective agents.

Conclusion

The compounds in the lead series all had significant anti-apoptotic activity (6-8) comparable to and better than selegiline (1-5). This activity could not be ascribed to MAO-B inhibition as these compounds showed little to no activity on the MAO-B enzyme, except for two which inhibited the MAO-B enzyme by 73% at 300 µM. It could also not be ascribed to calcium modulation as the best results reported for compounds 2, 4, 7 and 8 were at a significantly high concentration of 100 µM. The initial series of compounds, which had significant anti-apoptotic activity, presented interesting leads for the design and development of more potent inhibitors. Findings from the bioassays performed in the lead series and molecular modelling have lead to the design of a new series of PCU-propargylamine analogues, which might potentially exhibit a broader spectrum of activities, which most importantly might include significant MAO-B activity. Compounds that render such multimechanistic activity have great potential to serve as future analogues for the treatment and management of neurodegenerative disorders.

Acknowledgements

Quinton Barber is thanked for providing the lead compounds obtained from his MSc.

References

1. Schweichel JU, Merker HJ. The morphology of various types of cell death in prenatal tissues. Teratology. 1973;7(3):253-266.
2. Mattson MP. Apoptosis in neurodegenerative disorders. Nat Rev Mol Cell Biol. 2000;1(2):120-129.
3. Arundine M, Tymianski M. Molecular mechanisms of calcium-dependent neurodegeneration in excitotoxicity. Cell Calcium. 2013;34(4-5):325-337.
4. Arundine M, Tymianski M. Molecular mechanisms of glutamate-dependent neuro-degeneration in ischemia and traumatic brain injury. Cell Mol Life Sci. 2004;61(6):657-668.
5. Fowler JS, Volkow ND, Wang GJ, et al. Age-related increases in brain monoamine oxidase B in living healthy human subjects. Neurobiol Aging. 1997;18(4):431-435.
6. Karolewicz B, Klimek V, Zhu H, et al. Effects of depression, cigarette smoking, and age on monoamine oxidase B in amygdaloid nuclei. Brain Res. 2005;1043(1-2):57-64.
7. Holbrook NJ, Martin GR, Lockshin RA, editors. Cellular aging and cell death. New York: Wiley-Liss, 1996.
8. Wylie AH, Kerr JFR, Currie AR. Cell death: the significance of apoptosis. Int Rev Cytol. 1980;68:251-306.
9. Zindo FT, Barber QR, Joubert J, et al. Polycyclic proparglamine and acetylene deriviatives as multifunctional neuroprotective agents. Eur J Med Chem. 2014;80:122-134.
10. Joubert J, Samsodien H, Baber QR, et al. J Chem Crystall. 2014;44(4):194-204.
11. Hollingsworth EB, McNeal ET, Burton JL, et al. Biochemical characterization of a filtered synaptoneurosome preparation from guinea pig cerebral cortex: cyclic adenosine 3':5'-monophosphate-generating systems, receptors and enzymes. J Neurosci. 1985;5(8):2240-2253.
12. Maruyama W, Akao Y, Carrillo MC, et al. Neuroprotection by propargylamines in Parkinson's disease: suppression of apoptosis and induction of prosurvival genes. Neurotoxicol Teratol. 2002;24(5):675-682.
13. Geldenhuys WJ, Terre'Blanche G, van der Schyf CJ, Malan SF. Screening of novel pentacyclo-undecylamines for neuroprotective activity. Eur J Pharmacol. 2003;458(1-2):73-79.
13b. Geldenhuys WJ, Malan SF, Murugesan T, et al. Synthesis and biological evaluation of pentacyclo[5.4.0.0(2,6).0(3,10).0(5,9)]undecane derivatives as potential therapeutic agents in Parkinson's disease. Bioorg Med Chem. 2004;12(7):1799-1806.
13c. Mdzinarishvili A, Geldenhuys WJ, Abbruscato TJ, et al. NGP1-01, a lipophilic polycyclic cage amine, is neuroprotective in focal ischemia. Neurosci Lett. 2005;383(1-2):49-53.
13d. Geldenhuys WJ, Malan SF, Bloomquist JR, et al. Pharmacology and structure-activity relationships of bioactive polycyclic cage compounds: a focus on pentacycloundecane derivatives. Med Res Rev. 2005;25(1):21-48.
14. Parsons CG, Danysz W, Quack G. Memantine is a clinically well tolerated N-methyl-D-aspartate (NMDA) receptor antagonist--a review of preclinical data. Neuropharmacology. 1999;38(6):735-767.
15. Molecular Operating Environment®, version 2011. Chemical Computing Group [homepage on the4 Internet]. c2015. Available from: http://www.chemcomp.co

Podium presentation 2

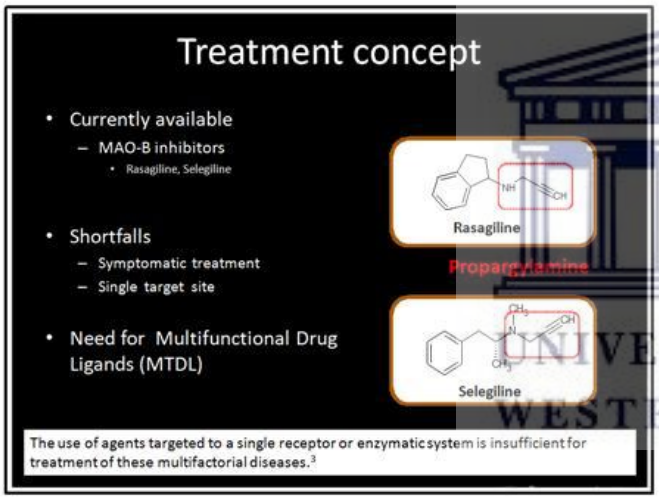

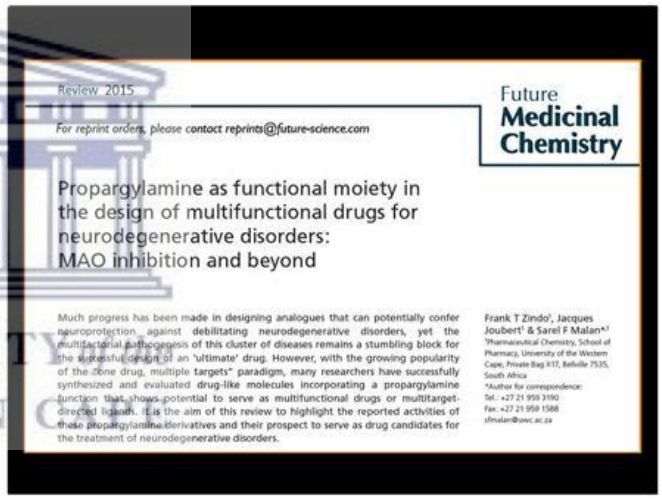

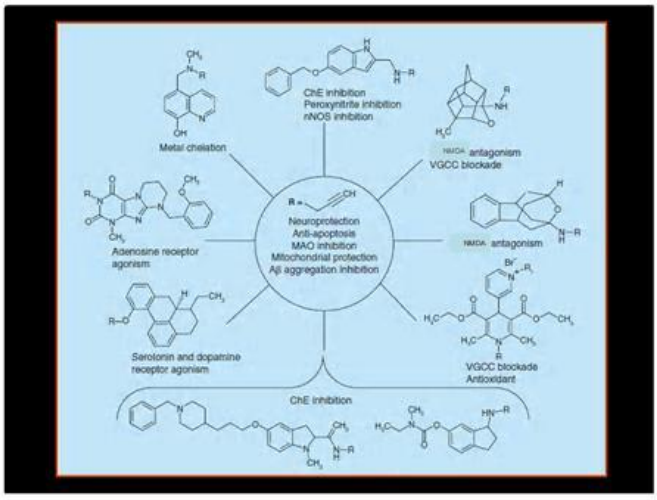

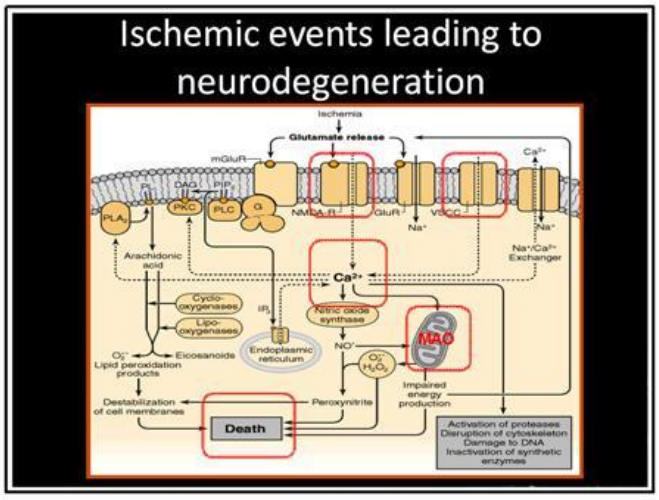

Previous analogues[2]

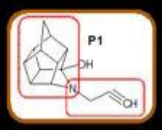

Neroprotection[a] [10 μM]	VGCC I[b] [100 μM]	NMDAr I[b] [100 μM]	MAO-B I[c] [300 μM]
98% ✓	18%	4%	5% ✗

a = SKNBE (2) neuroblastoma cells, b = rat brain homogenate synaptoneurosomes, c = baboon liver mitochondria

[4] Polycyclic propargylamine and acetylene derivatives as multifunctional neuroprotective agents. *Eur. J. Med. Chem.* 80, 122-134 (2014) – **Zindo, F.T. *et al.* (2014)**

Molecular Modelling

Molecular Operating Environment (MOE) generated images of compound docking in MAO-B enzyme (PDB ID: 2V5Z)

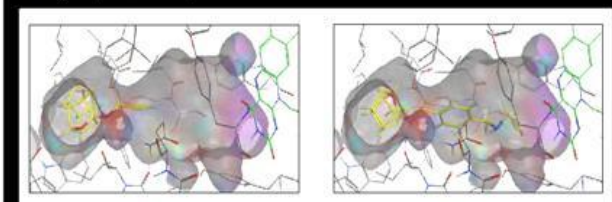

P1 C12

Note that compound P1 merely occupies the entrance cavity of the enzyme pocket and remains distant from the FAD co-factor rendering it inactive, while the new series traverses deeper into the enzyme cavity to proximate the FAD co-factor allowing for potential binding interactions which may result in improved MAO-B activity.

New Series

- NGP1-01 resemblance
  - Calcium homeostasis
    - VGCC
    - NMDA
- Propargylamine
  - Neuroprotection
  - MAO-B inhibition

[5] NGP1-01 - Brain-permeable dual blocker of neuronal VGCC and ligand-operated calcium channels (NMDAr) – **Geldenhuys, W.J. *et al.* (2004)**

Synthesis of Ketal Derivatives

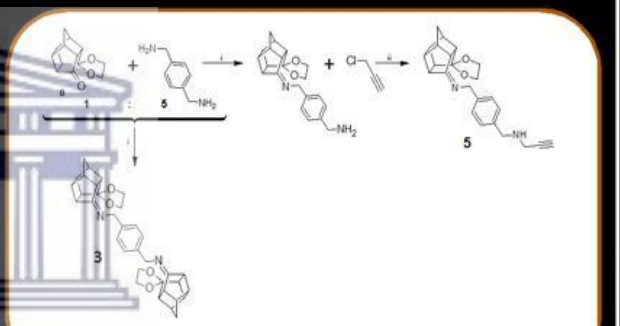

Scheme 2: (i) ethanol, rt 1 h, then MW, 60W, 80 psi, 100 °C, 3 h; (ii) acetonitrile, K_2CO_3, 60 °C, 4 h.

New Series (12 Compounds)

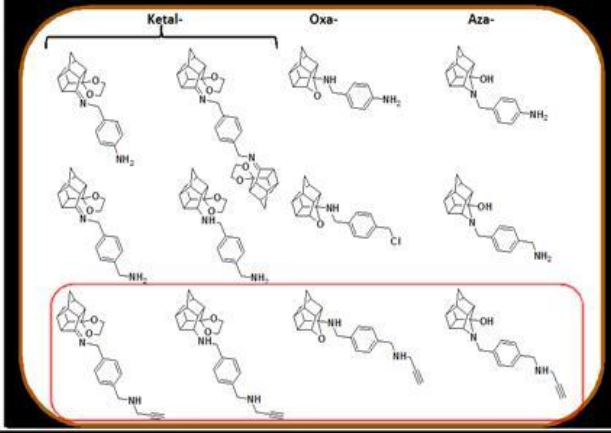

Bioassays

- Performed on human neuroblastoma cell line (SH-SY5Y)[6]
  - MTT cytotoxicity assay
  - MPP^+ Neuroprotection assay
  - VGCC blockade
  - NMDAr antagonism
- rHuman MAO isoenzymes
  - MAO-A & -B inhibition

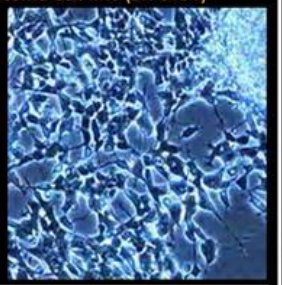

[6] Expresses dopaminergic markers and is suitable for ND studies (Parkinson's Disease). - **Pyszko, J. *et al.* (2014)**

Cytotoxicity

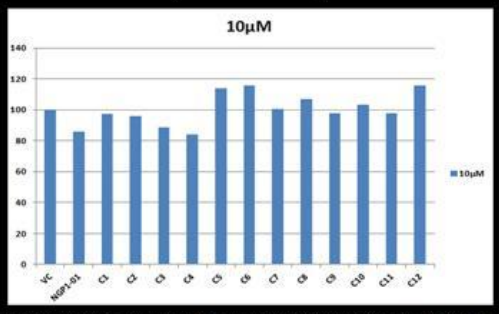

Percentage cell viability of compounds **1**-**12** assessed by means of measuring the metabolic activity of SH-SY5Y neuroblatoma cells, **after 48 h exposure to test compound,** relative to a control of untreated viable cells. Data are mean ± SEM (n = 3, four fields per repeat). Data were subjected to an ANOVA statistical analysis and significance was defined as [(*) $p < 0.05$, (**) $p < 0.001$, (***) $p < 0.0001$].

Cytotoxicity

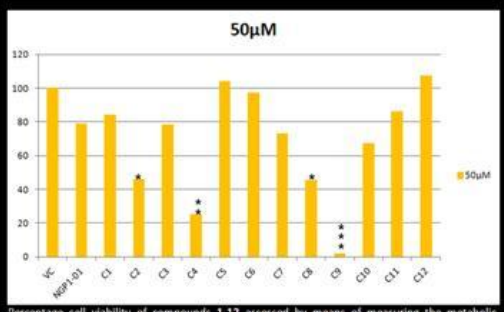

Percentage cell viability of compounds **1**-**12** assessed by means of measuring the metabolic activity of SH-SY5Y neuroblatoma cells, **after 48 h exposure to test compound,** relative to a control of untreated viable cells. Data are mean ± SEM (n = 3, four fields per repeat). Data were subjected to an ANOVA statistical analysis and significance was defined as [(*) $p < 0.05$, (**) $p < 0.001$, (***) $p < 0.0001$].

Cytotoxicity

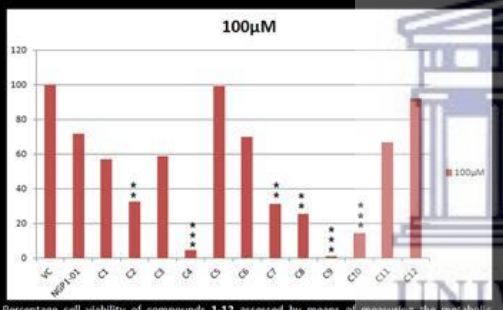

Percentage cell viability of compounds **1**-**12** assessed by means of measuring the metabolic activity of SH-SY5Y neuroblatoma cells, **after 48 h exposure to test compound,** relative to a control of untreated viable cells. Data are mean ± SEM (n = 3, four fields per repeat). Data were subjected to an ANOVA statistical analysis and significance was defined as [(*) $p < 0.05$, (**) $p < 0.001$, (***) $p < 0.0001$].

MPP+ Neuroprotection assay

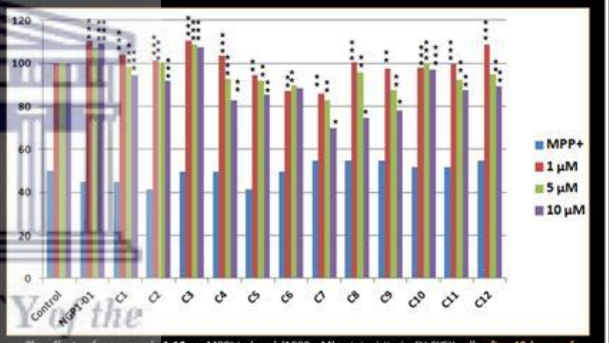

The effects of compounds **1**-**12** on MPP+-induced (1000 µM) cytotoxicity in SH-SY5Y cells **after 48 hours of exposure.** The viability of the untreated control was defined as 100%. MPP+ without test compound showed a significant decrease in cell viability relative to the control (#, $p < 0.05$). Data are mean ± SEM (n = 3, four fields per repeat).

Ca2+ modulation assays
VGCC & NMDAr

- Ratiometric fluorescent calcium indicator
  - Fura-2/AM

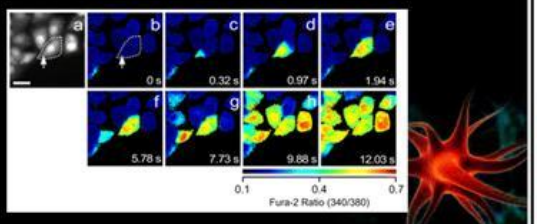

Ca2+ modulation assays

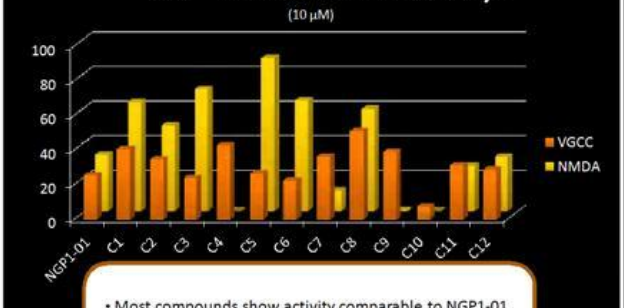

- Most compounds show activity comparable to NGP1-01.
- Compounds appear to be more active as NMDAr antagonists.
- Compounds **1**, **3**, **5** & **6** showed the best NMDAr antagonism.

MAO-A & -B assays

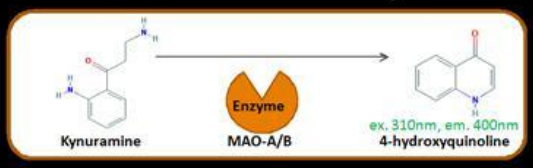

IC_{50} (μM)	1	2	3	4	5	6	7	8	9	10	11	12
MAO-A	>100	>100	>100	>100	>100	>100	>100	>100	56.2 ✓	2.37 ✓	>100	>100
MAO-B	1.91 ✓	13.8 ✓	100	>100	1.70 ✓	36.3 ✓	>100	>100	3.80 ✓	100	14.1 ✓	28.1 ✓
SI	>52	>7.2	-	-	>58	>2.8	-	-	14.8	0.02	7.08	3.55

Molecular Modeling: MAO-B

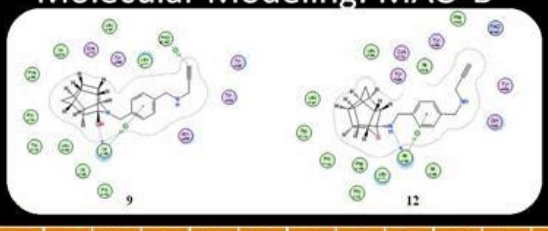

IC_{50} (μM)	1	2	3	4	5	6	7	8	9	10	11	12
MAO-A	>100	>100	>100	>100	>100	>100	>100	>100	56.2	2.37	>100	>100
MAO-B	1.91 ✓	13.8 ✓	100	>100	1.70 ✓	36.3 ✓	>100	>100	3.80 ✓	100	14.1	28.1 ✓
SI	>52	>7.2	-	-	>58	>2.8	-	-	14.8	0.02	7.08	3.55

Reversibility Study

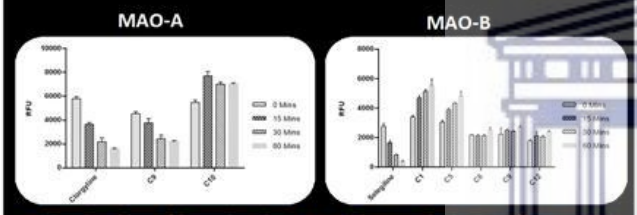

Time-dependent inhibition of the recombinant human MAO-A and MAO-B catalysed oxidation of kynuramine by the selected active compounds. The enzymes were preincubated for various periods of time (0–60 min; x-axis). Data are expressed as the mean RFU (relative fluorescent units) ± SEM of three independent experiments.

- **C9** shows an irreversible type of inhibition on MAO-A
- **C1, C5, C6, C9** and **C12** may be described as reversible MAO-B inhibitors

Concluding remarks

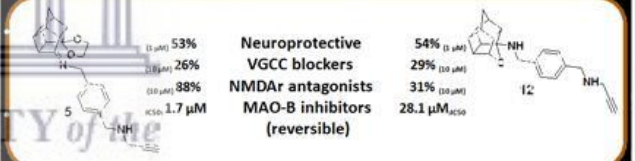

neurodegeneration.

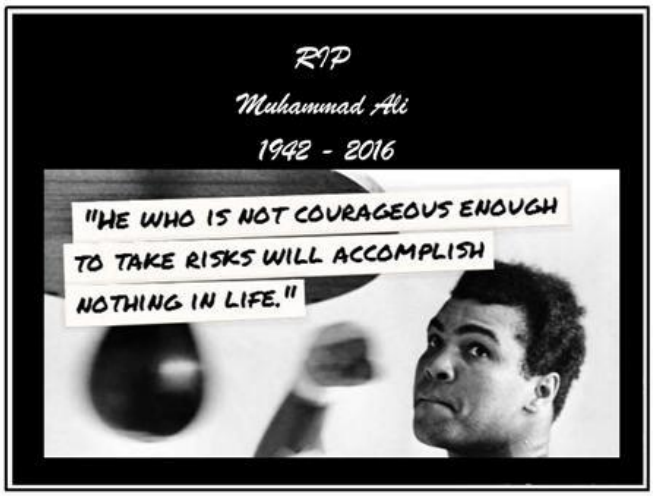

Supplementay Material

Polycyclic propagylamine and acetylene derivatives as multifunctional neuroprotective agents

Quinton R. Baber[a], Jacques Joubert[b], Frank T. Zindo[b], Jacobus J. Bergh[a], Jacobus P. Petzer[a] and Sarel F. Malan[a,b,*]

[a]*Pharmaceutical Chemistry, North-West University, Private Bag 6001, Potchefstroom, 2520 , South Africa.*
[b]*School of Pharmacy, University of the Western Cape, Bellville, South Africa, Private Bag X17, Bellville 7535, South Africa.*

1. **Pseudo colour graphs of the apoptosis detection - DePsipher™ assay**
2. **Representative ^{1}H nuclear magnetic resonance spectra**

1. Pseudo colour graphs of the apoptosis detection - DePsipher™ assay

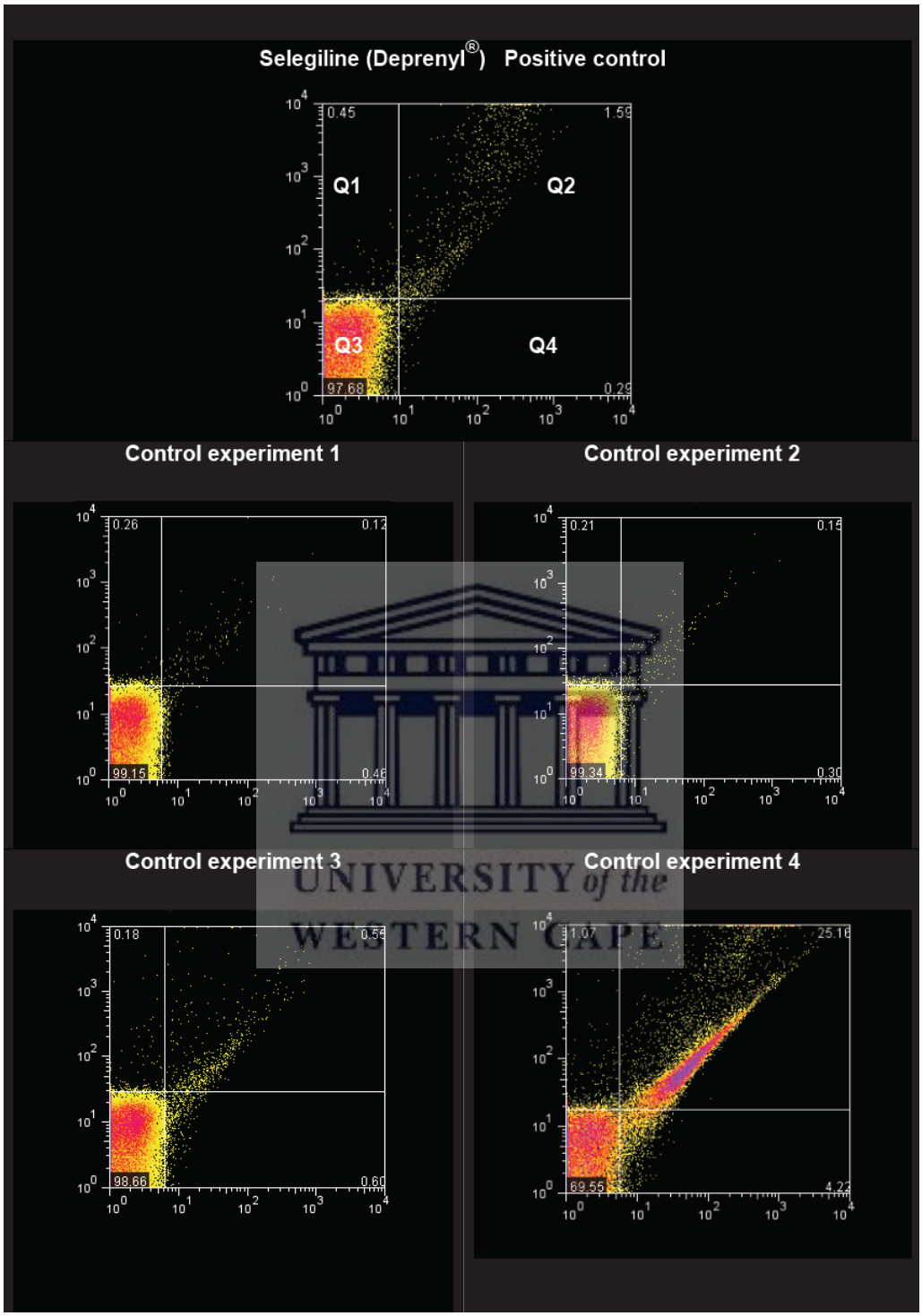

Figure 1: Pseudo-colour graphs of the control experiments

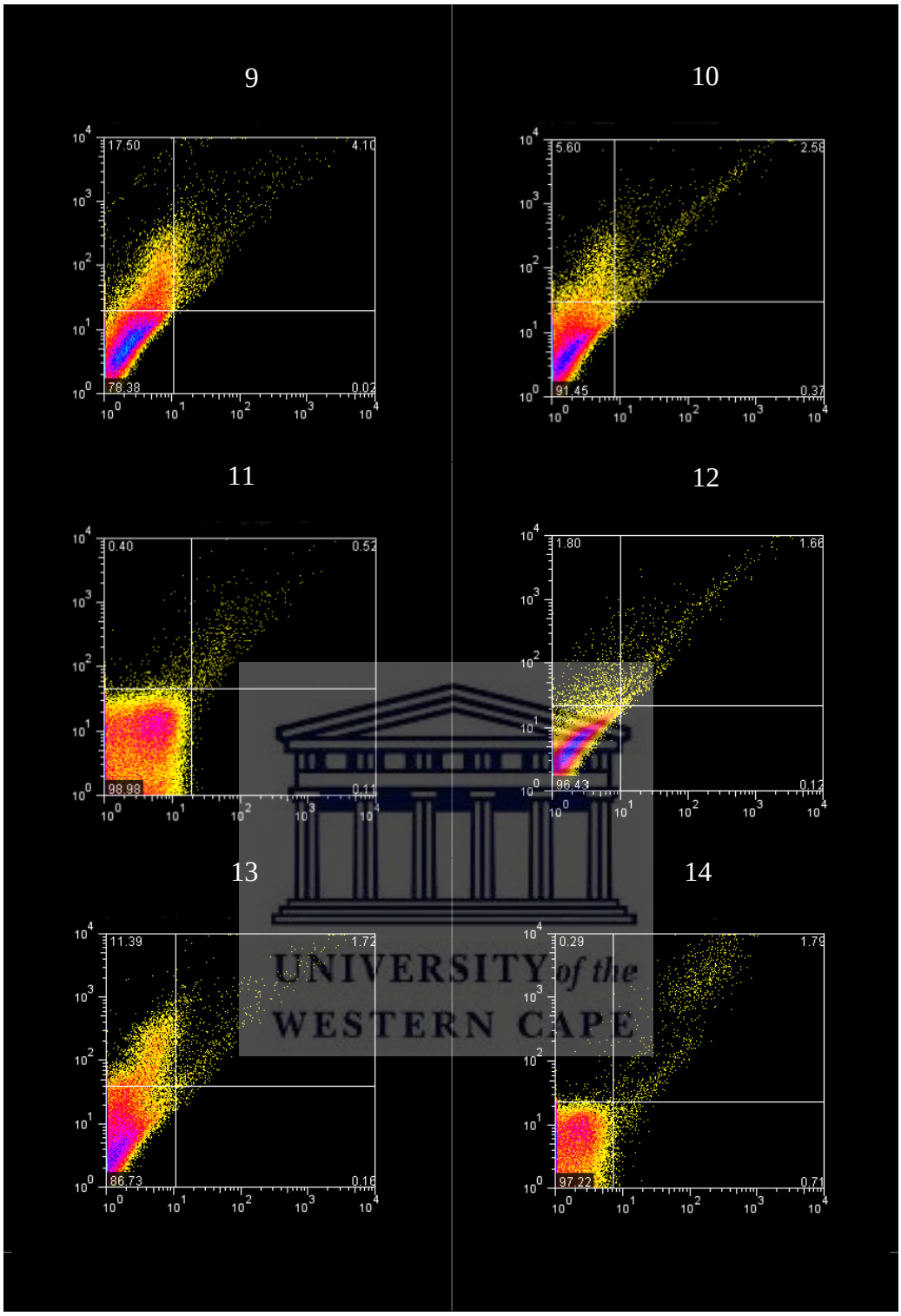

Figure 2: Pseudo-colour graphs of compounds 9 - 14

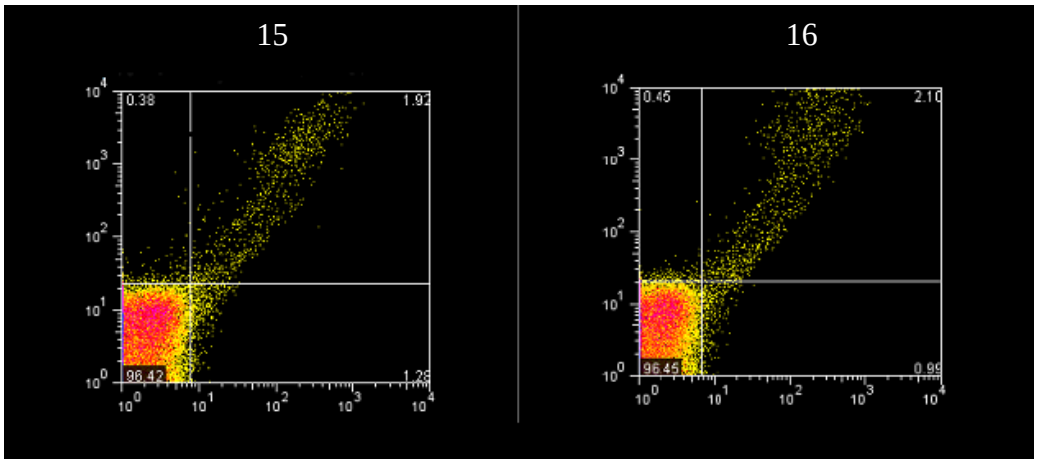

Figure 3: Pseudo-colour graphs of compounds 15 and 16

2. Representative ^{1}H nuclear magnetic resonance spectra

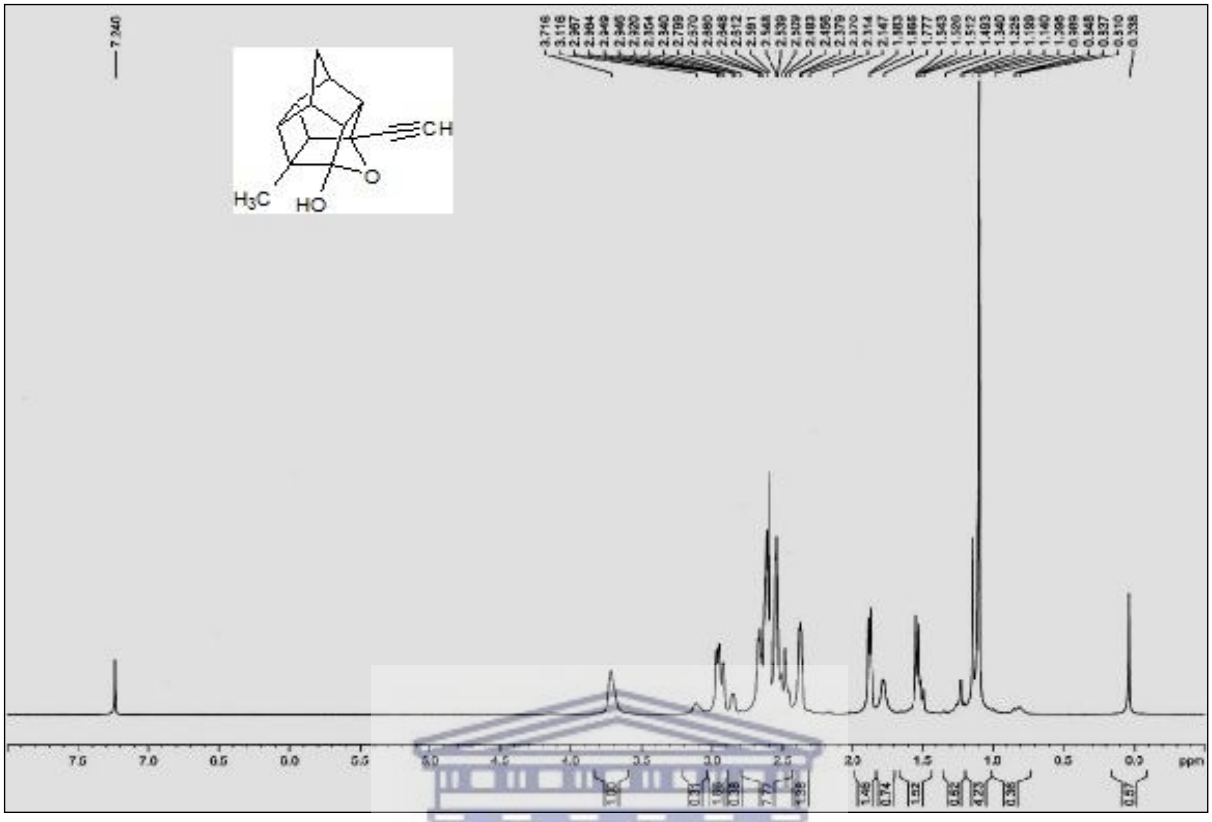

Spectrum 1: Compound **9**

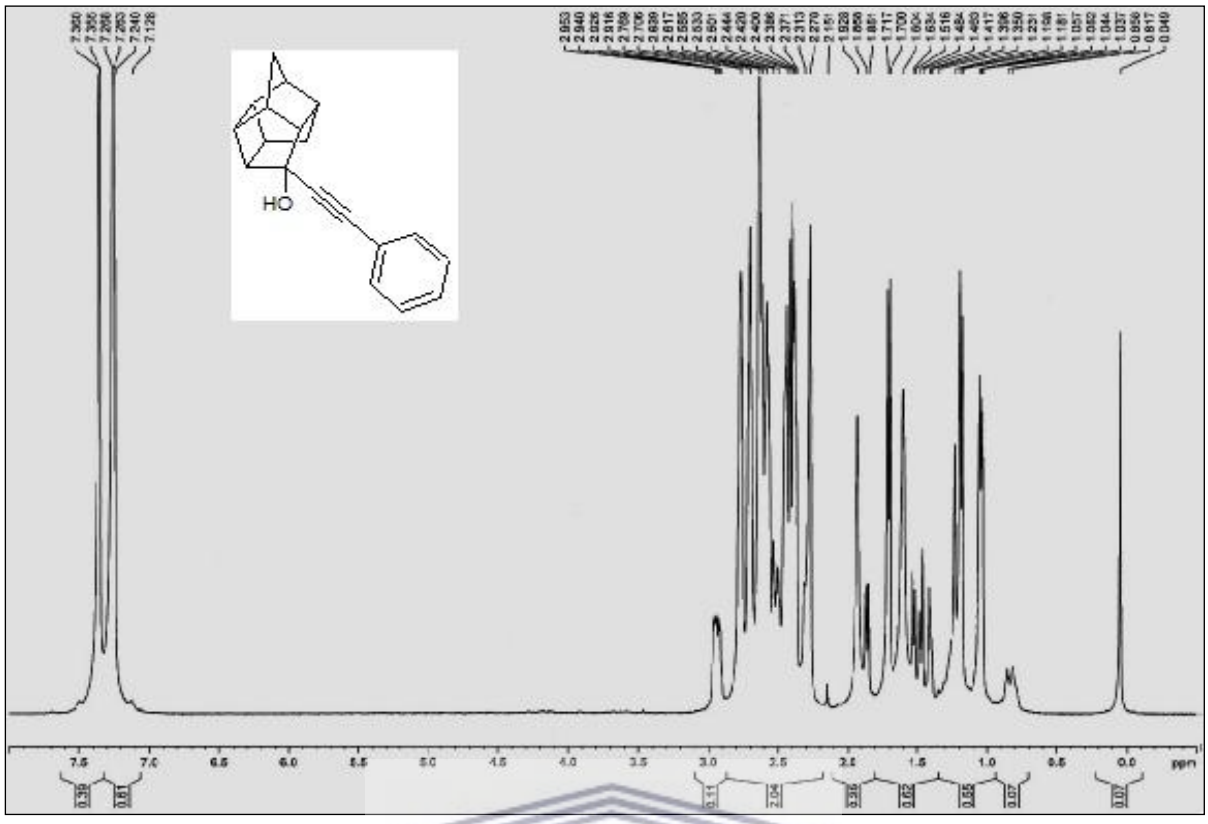

Spectrum 2: Compound **10**

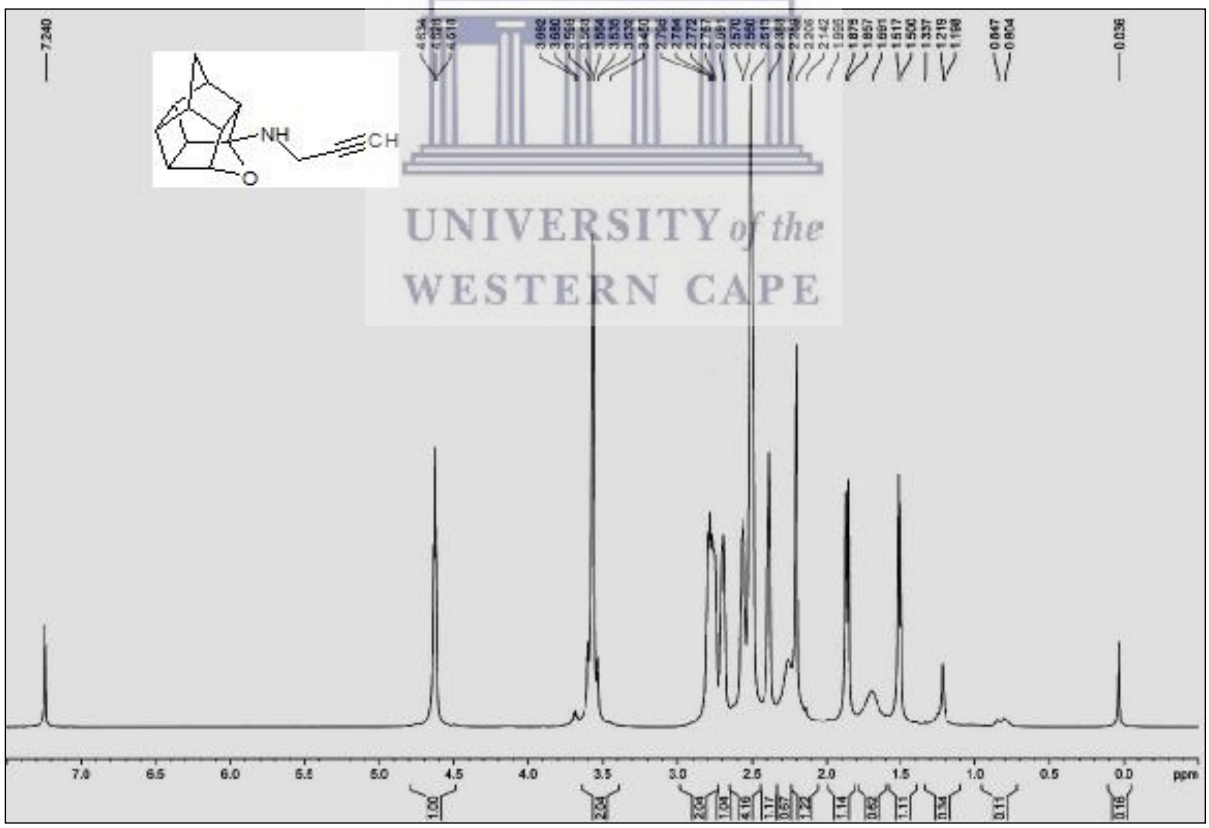

Spectrum 3: Compound **11**

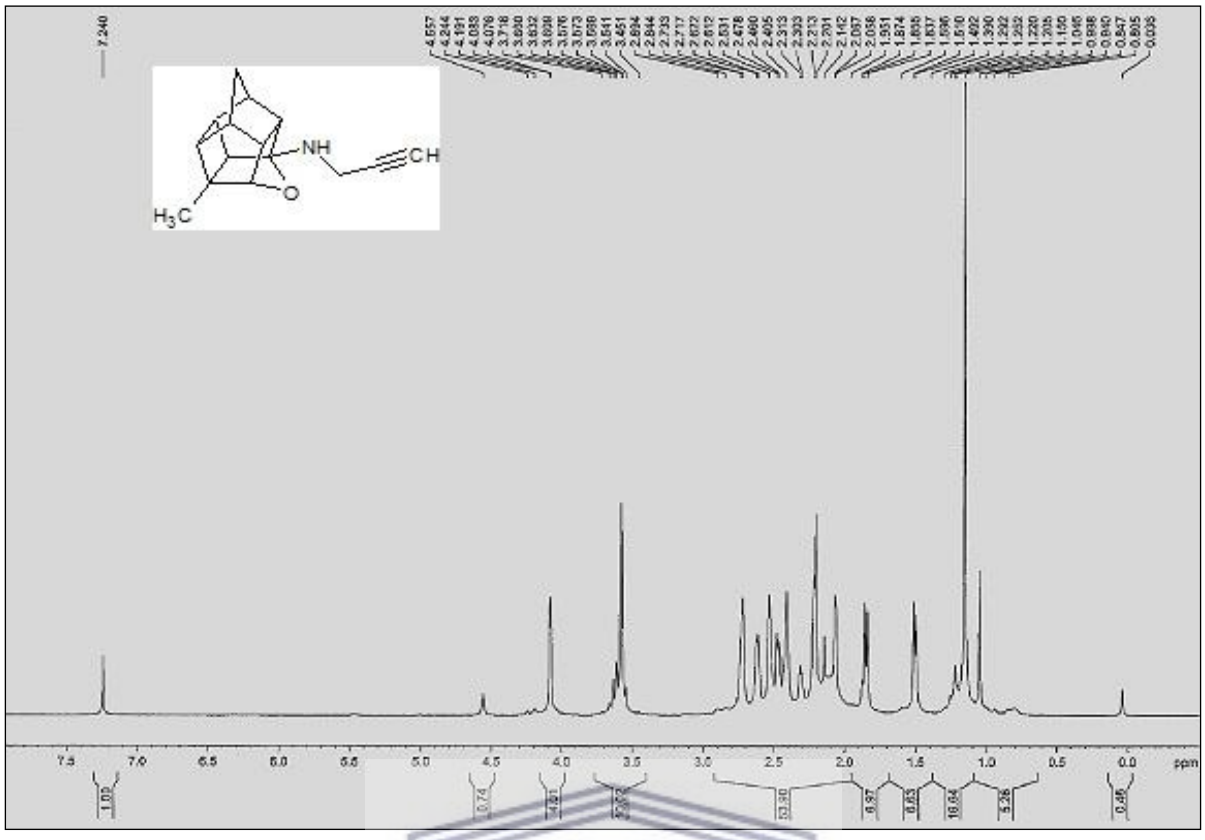

Spectrum 4: Compound **12**

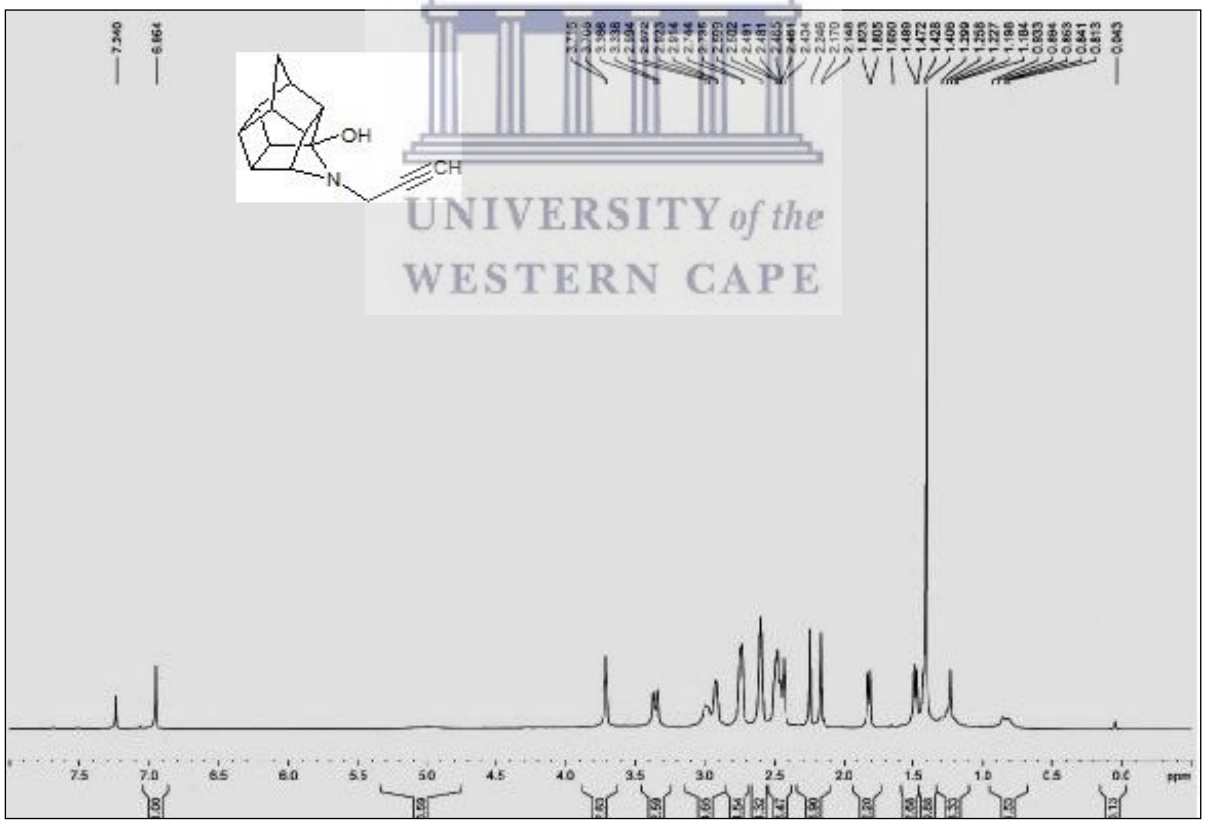

Spectrum 5: Compound **13**

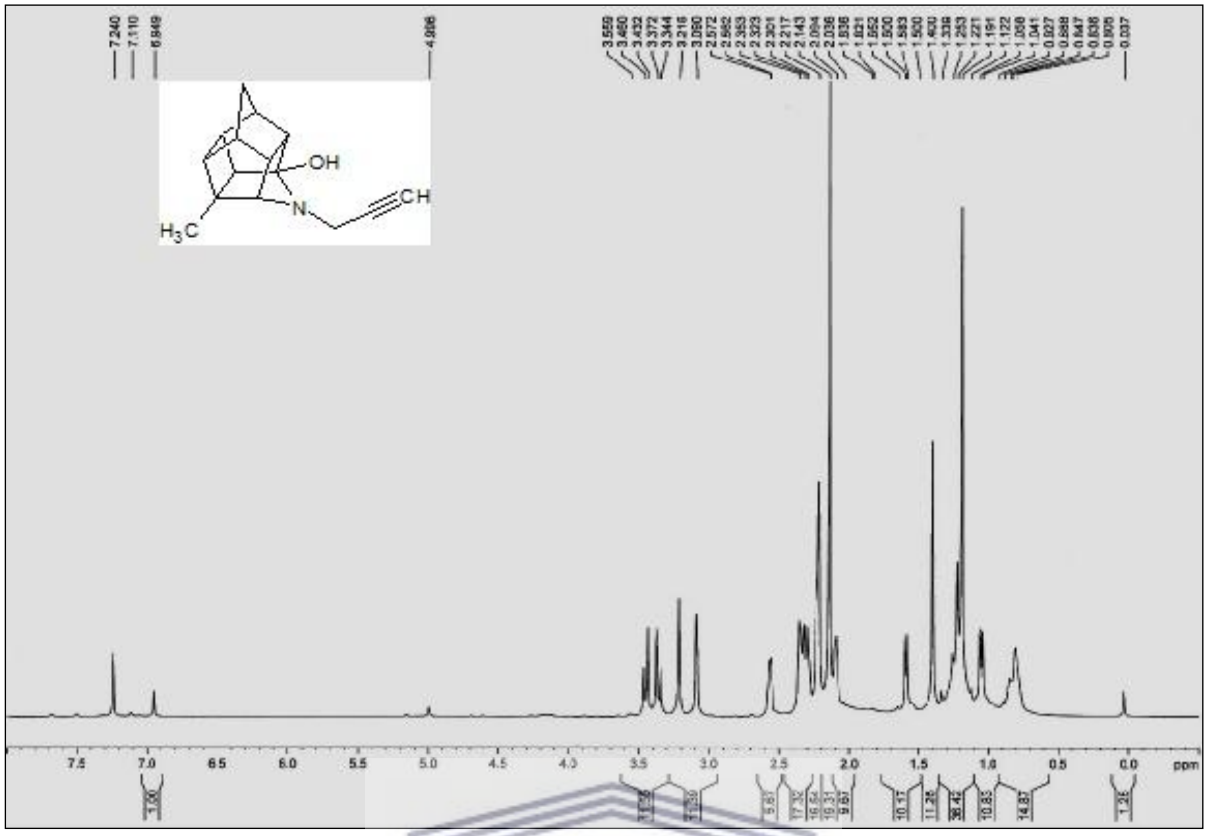

Spectrum 6: Compound **14**

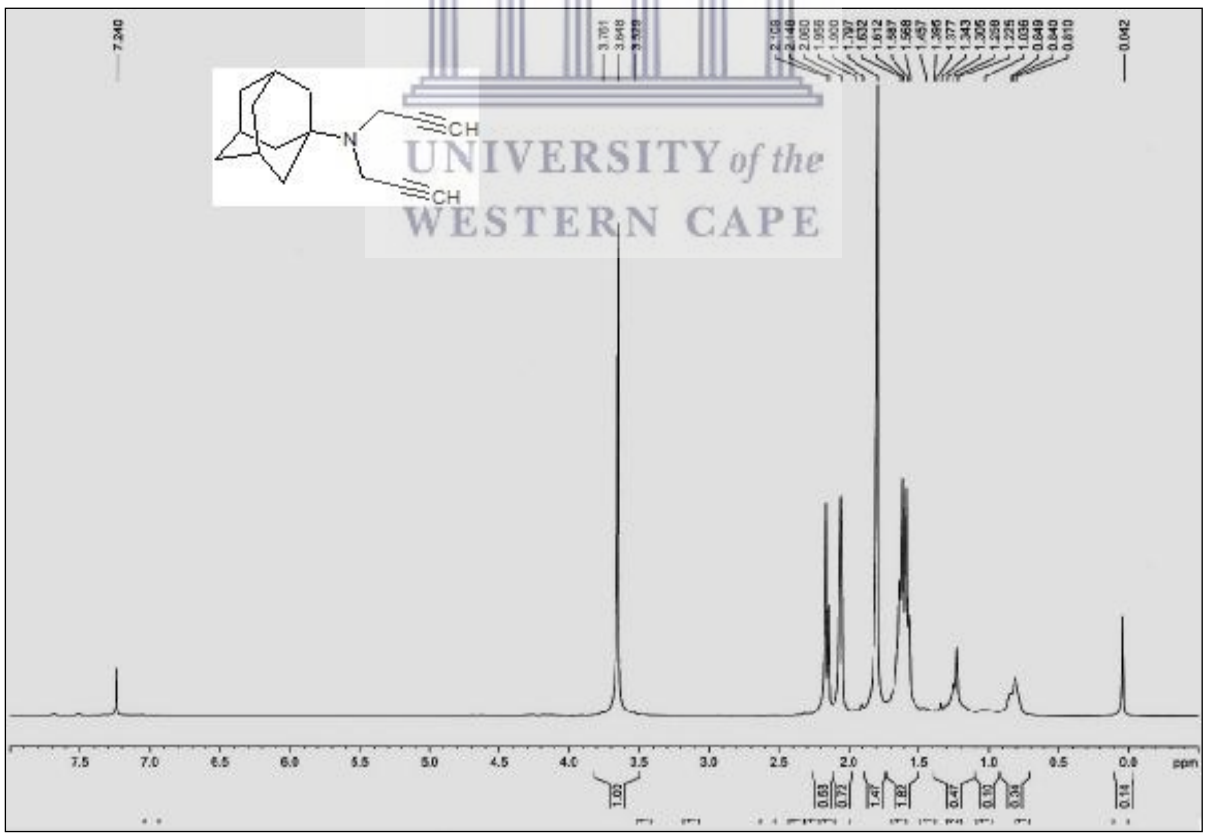

Spectrum 7: Compound **15**

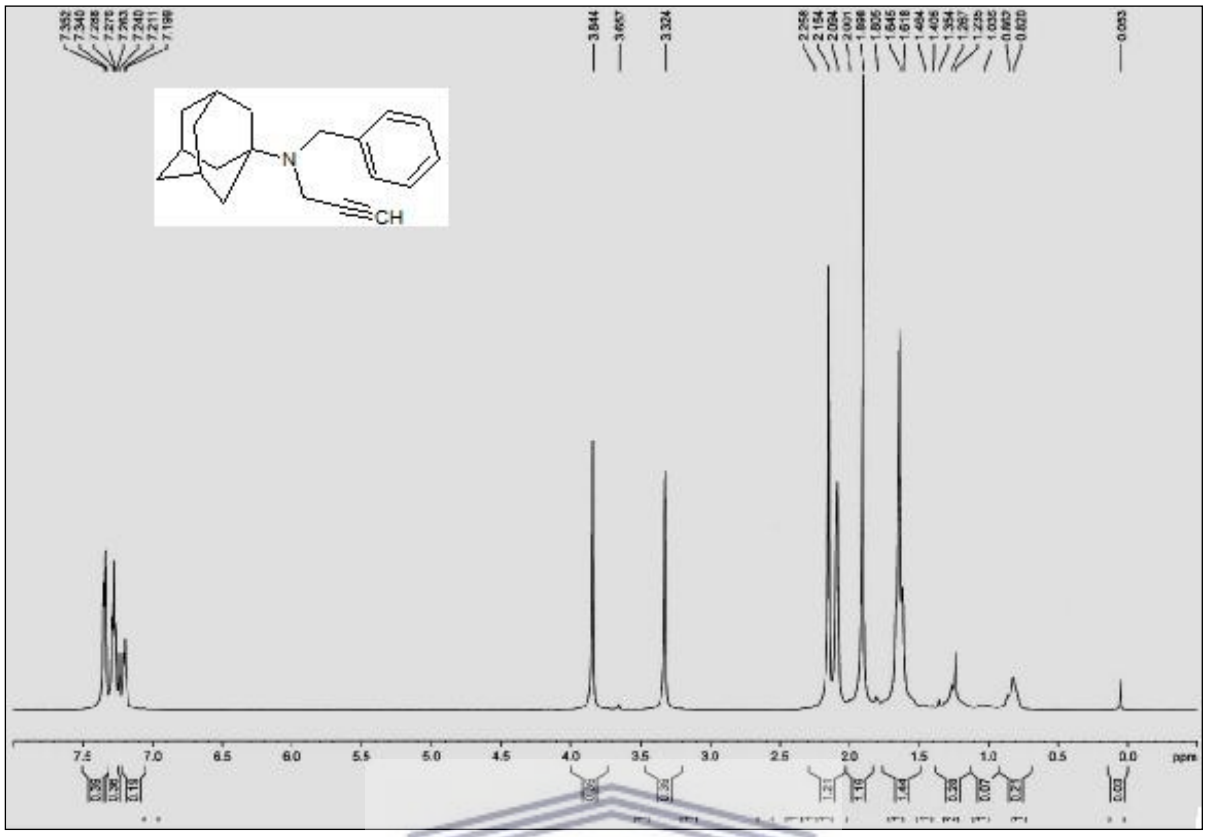

Spectrum 8: Compound **16**

Supplementay Material

Design, synthesis and evaluation of pentacycloundecane and hexacycloundecane propargylamine derivatives as multifunctional neuroprotective agents.

Frank T. Zindo[a], Sarel F. Malan[a], Sylvester I. Omoruyi[b], Adaze B. Enogieru[b], Okobi E. Ekpo[b], Jacques Joubert[a]*

[a]*Pharmaceutical Chemistry, School of Pharmacy, University of The Western Cape, Private Bag X17, Bellville 7535, South Africa*
[b]*Department of Medical Biosciences, University of the Western Cape, Private Bag X17, Cape Town, Bellville 7535, South Africa*

1. **MAO-B molecular modelling results of compounds 1-12**
2. **Representative ^{1}H nuclear magnetic resonance spectra**

.

1. MAO-B molecular modelling results of all test compounds

Table 1: MOE generated docking simulations of compounds **1-12** within the human MAO-B enzyme active site. The compounds and FAD cofactor in is indicated in yellow and green respectively. The binding interactions with the amino acid residues is shown on the right.

Compound ($MAO\text{-}B\ IC_{50}$)	**Docking simulation**	**Ligand interactions**
1 (1.91 µM)	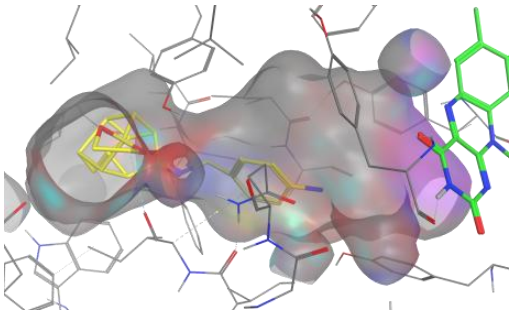	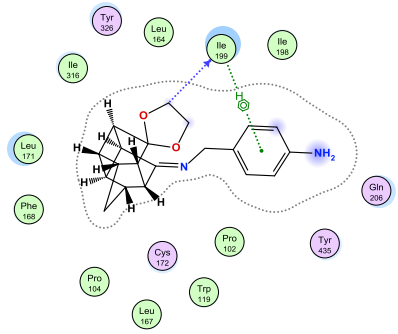
2 (13.80 µM)	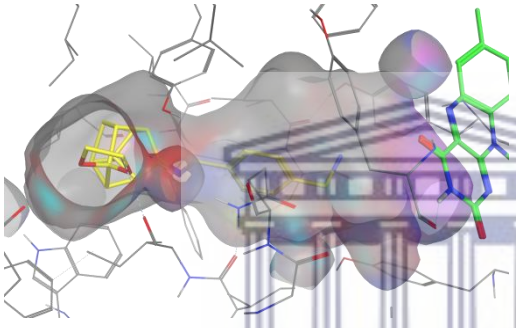	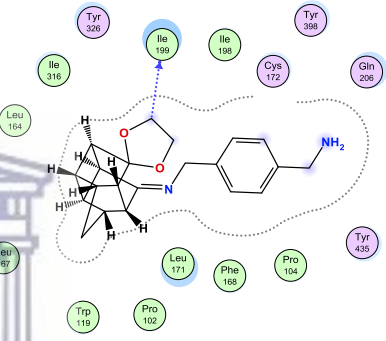
3 (100 µM)	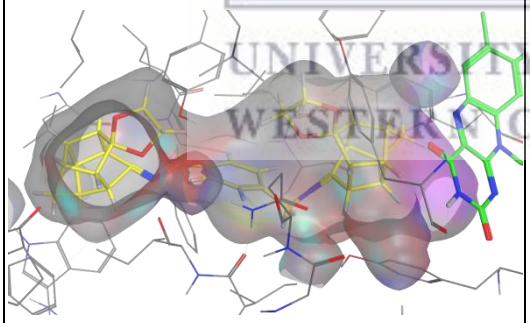	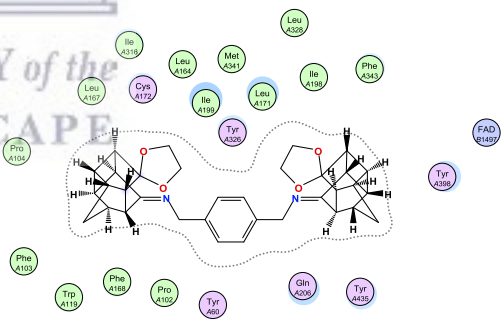
4 (>100 µM)	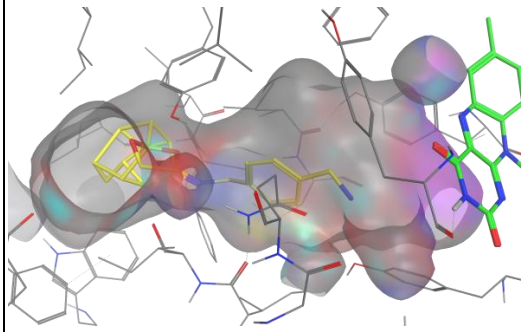	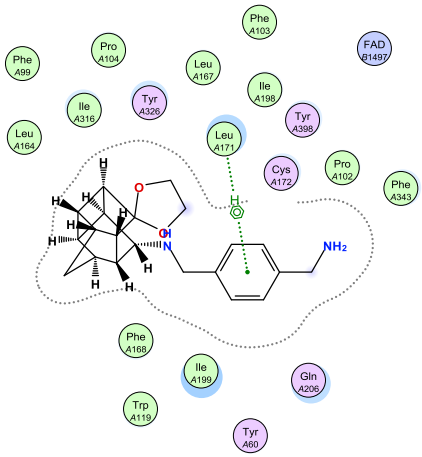

5 (1.70 µM)	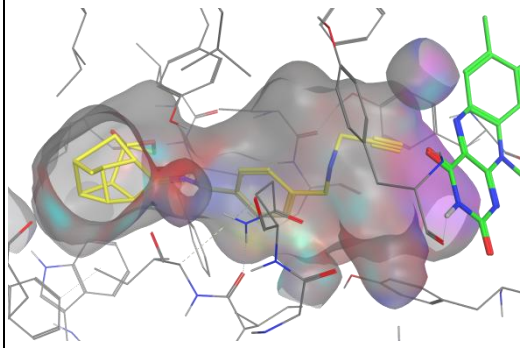	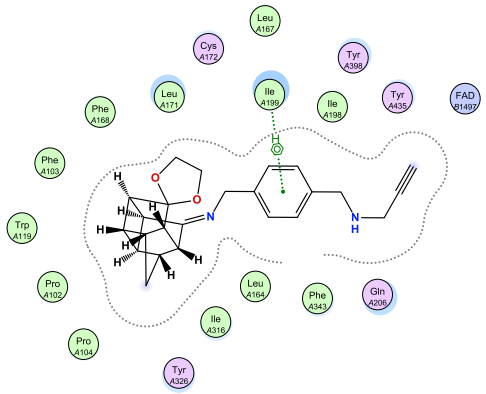
6 (36.31 µM)	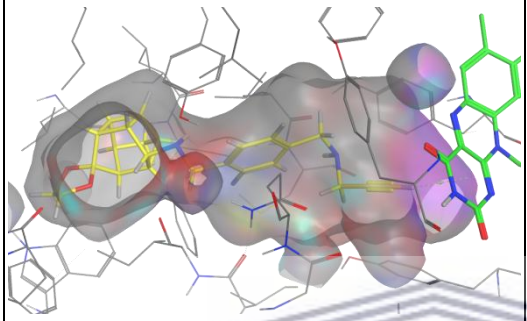	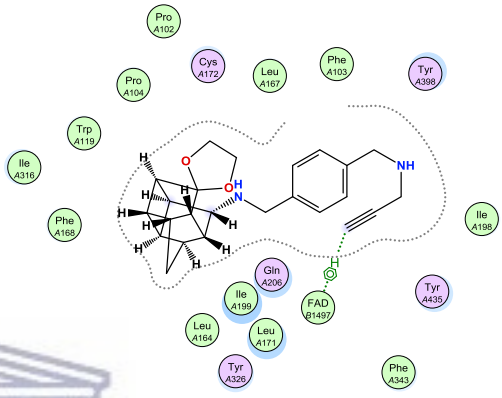
7 (>100 µM)	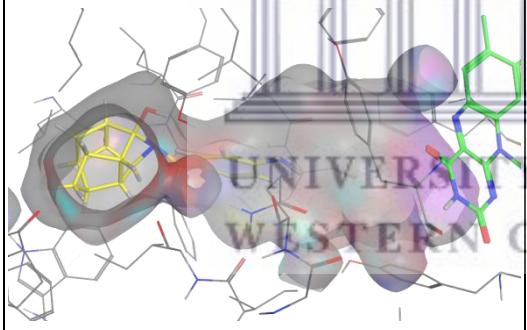	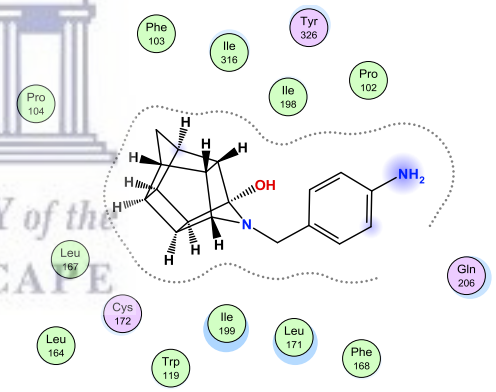
8 (>100 µM)	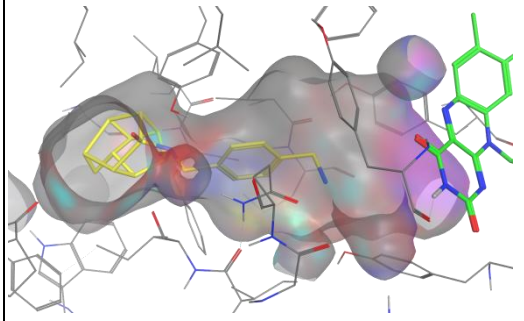	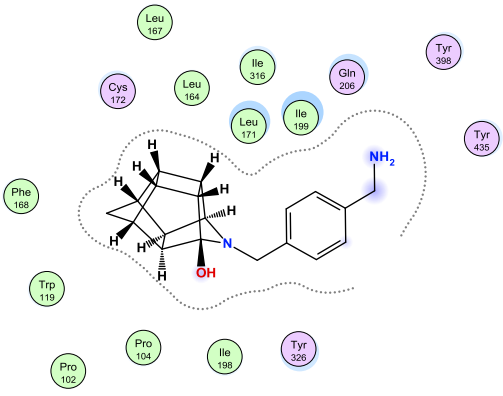

9 (3.80 µM)	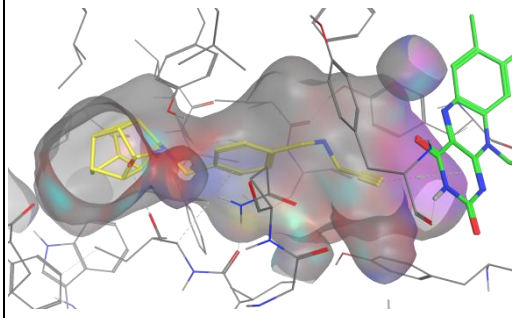	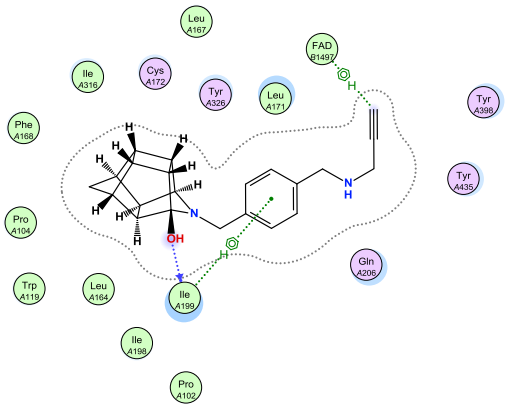
10 (100 µM)	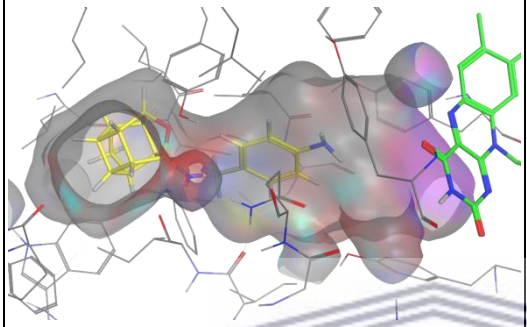	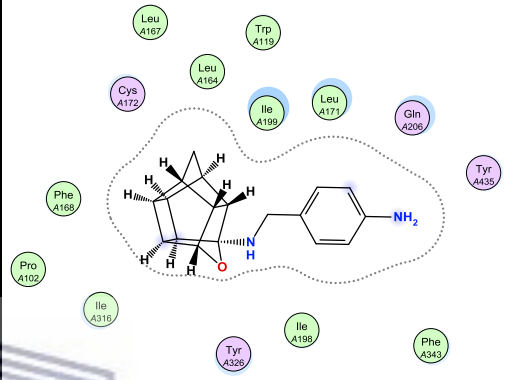
11 (14.13 µM)	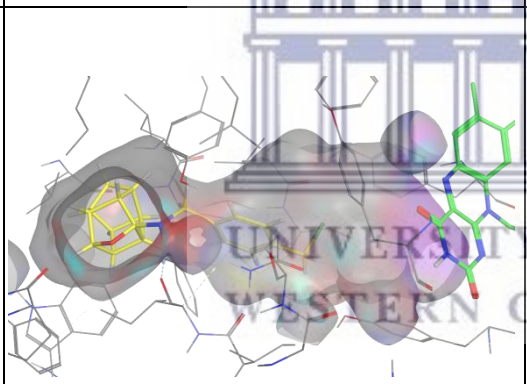	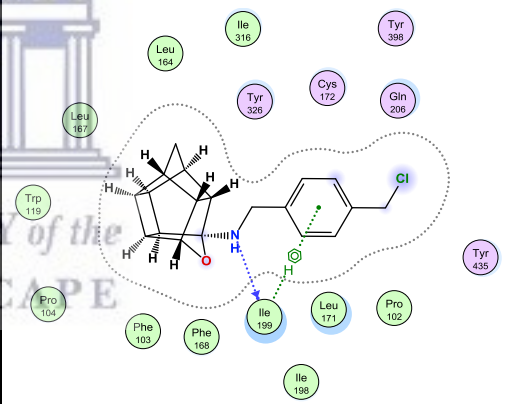
12 (28.18 µM)	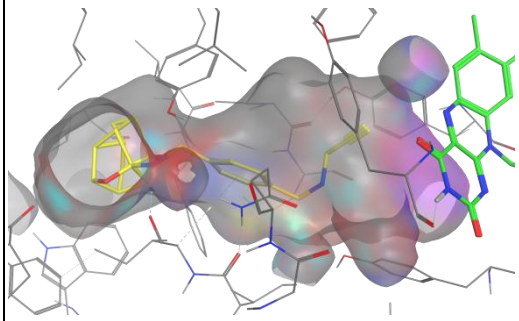	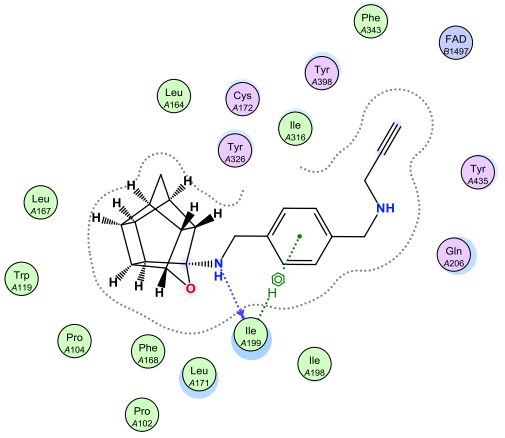

2. ^{1}H NMR spectra of compounds 1-12.

SpinWorks 4: **Compound 1**

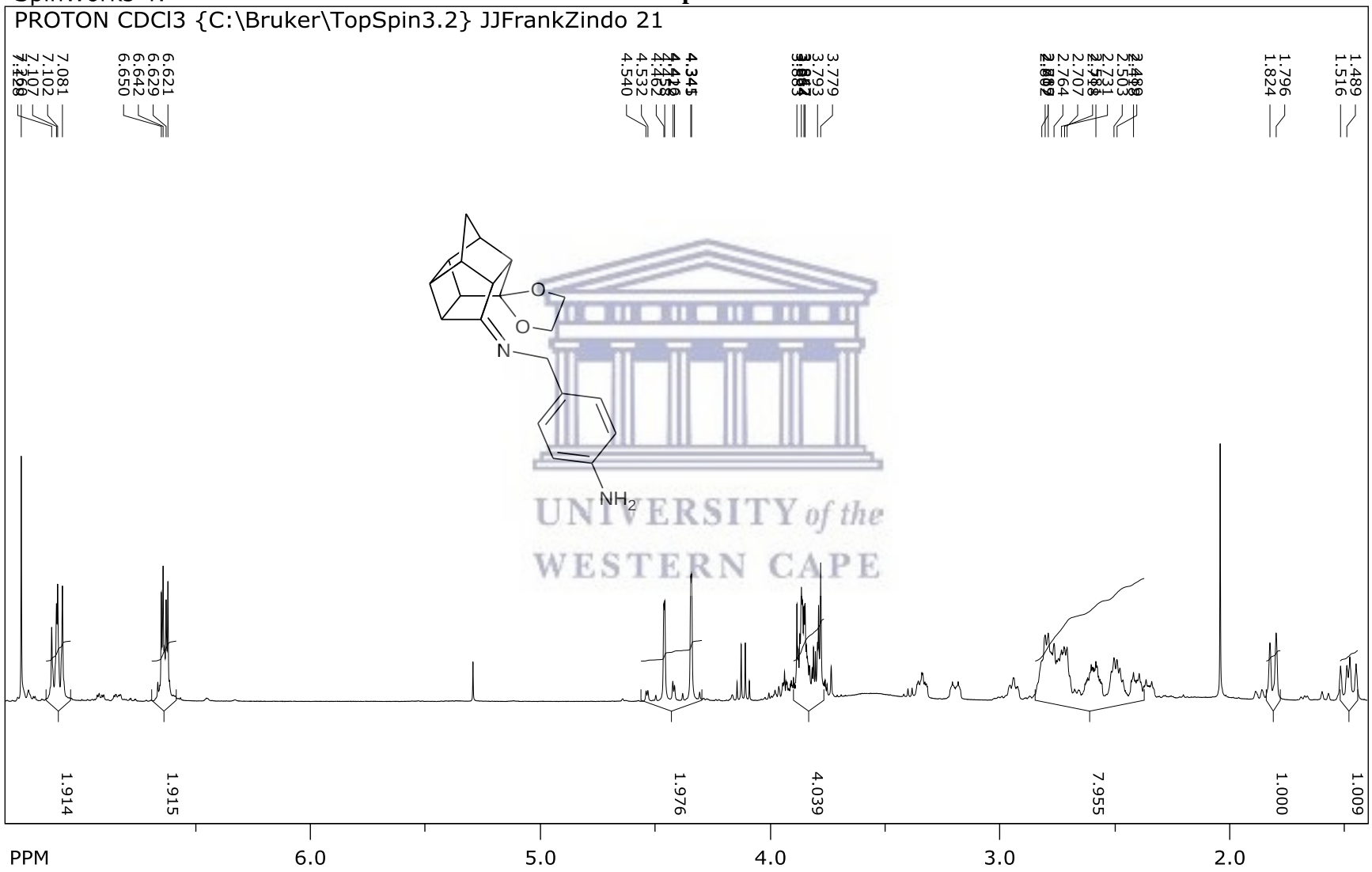

file: ...o - NMR\H-NMR - Select\AB16A\1\fid expt: <zg30>
transmitter freq.: 400.122471 MHz
time domain size: 65536 points
width: 8012.82 Hz = 20.0259 ppm = 0.122266 Hz/pt
number of scans: 16

freq. of 0 ppm: 400.120010 MHz
processed size: 65536 complex points
LB: 0.300 GF: 0.0000

Compound 2

SpinWorks 4:

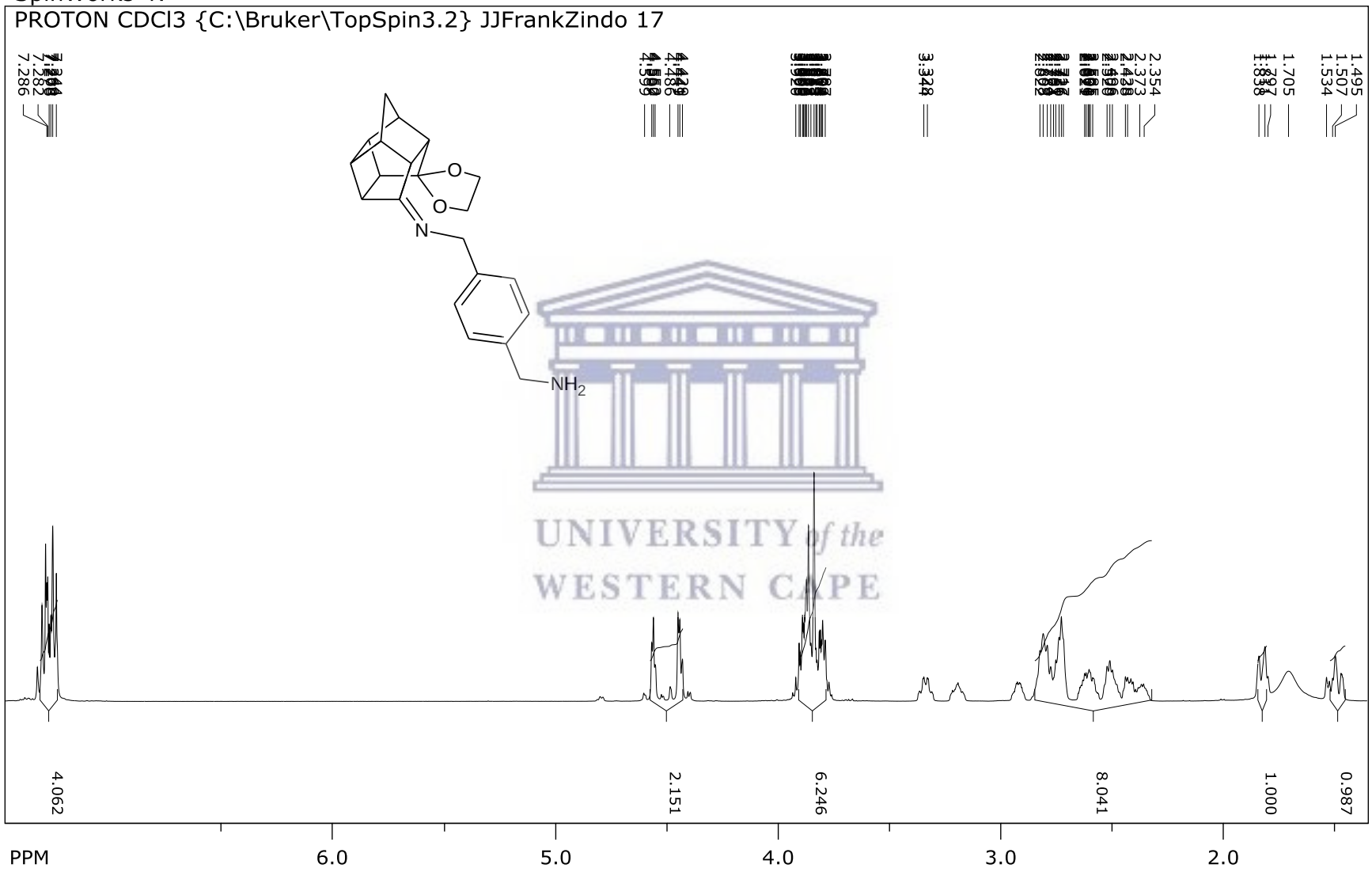

file: ...do - NMR\H-NMR - Select\16B2\1\fid expt: <zg30>
transmitter freq.: 400.122471 MHz
time domain size: 65536 points
width: 8012.82 Hz = 20.0259 ppm = 0.122266 Hz/pt
number of scans: 16

freq. of 0 ppm: 400.120001 MHz
processed size: 65536 complex points
LB: 0.300 GF: 0.0000

Compound 3

SpinWorks 4:

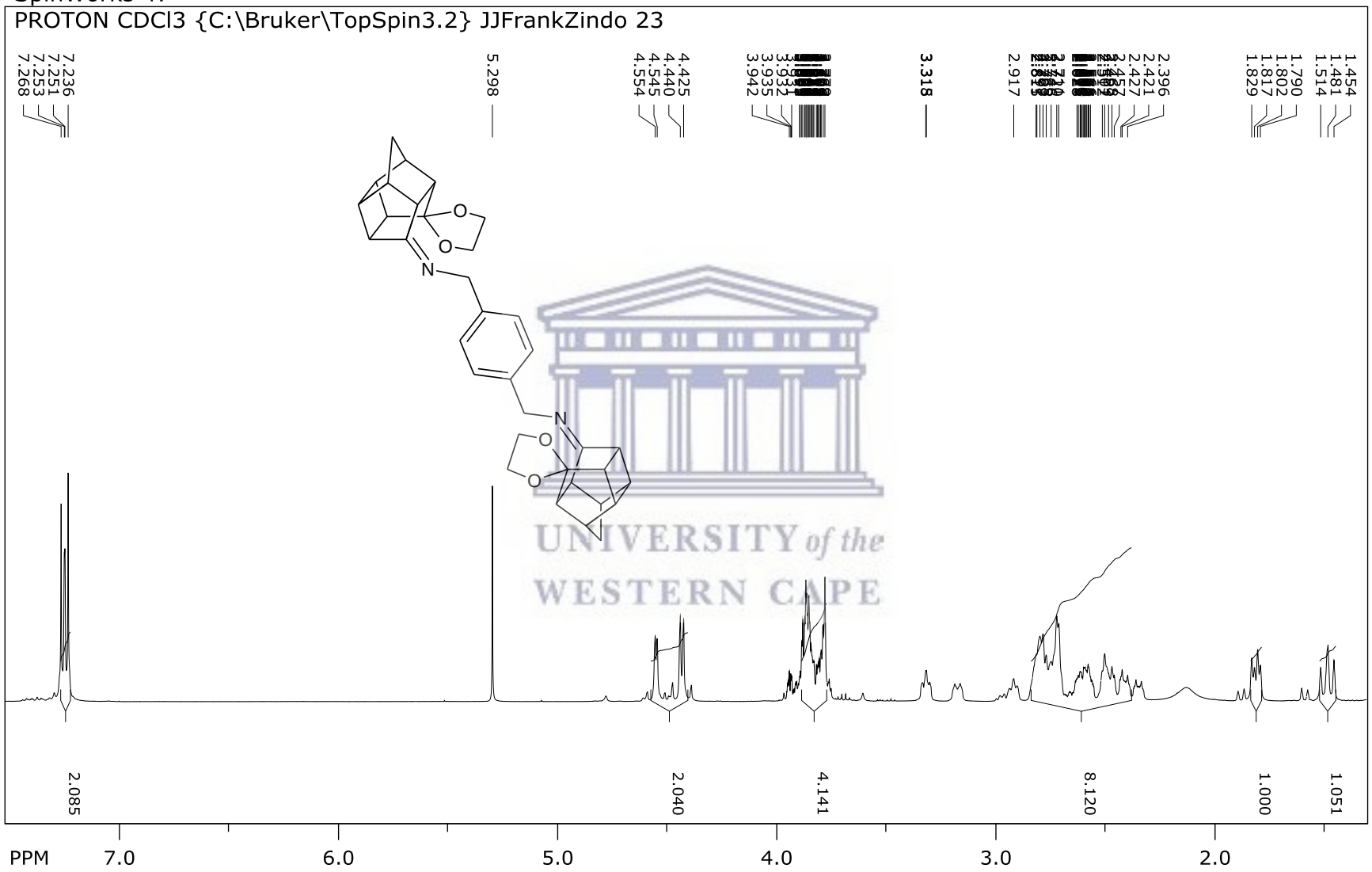

file: ... - NMR\H-NMR - Select\KAM 1A\1\fid expt: <zg30>
transmitter freq.: 400.122471 MHz
time domain size: 65536 points
width: 8012.82 Hz = 20.0259 ppm = 0.122266 Hz/pt
number of scans: 16

freq. of 0 ppm: 400.120007 MHz
processed size: 65536 complex points
LB: 0.300 GF: 0.0000

Compound 4

SpinWorks 4:

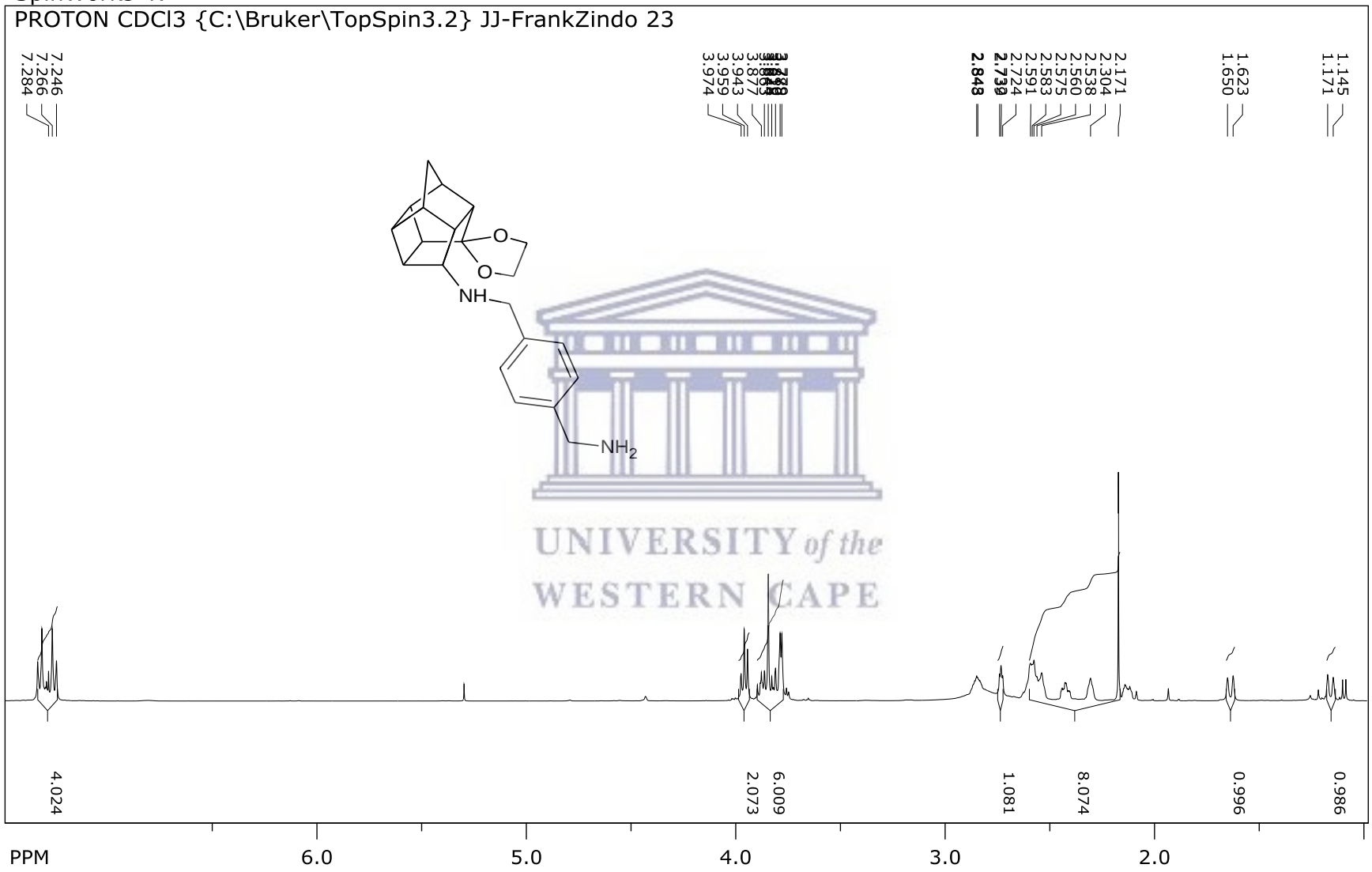

file: ...o - NMR\H-NMR - Select\4RKAM\1\fid expt: <zg30>
transmitter freq.: 400.122471 MHz
time domain size: 65536 points
width: 8012.82 Hz = 20.0259 ppm = 0.122266 Hz/pt
number of scans: 16

freq. of 0 ppm: 400.120001 MHz
processed size: 65536 complex points
LB: 0.300 GF: 0.0000

Compound 5

SpinWorks 4:

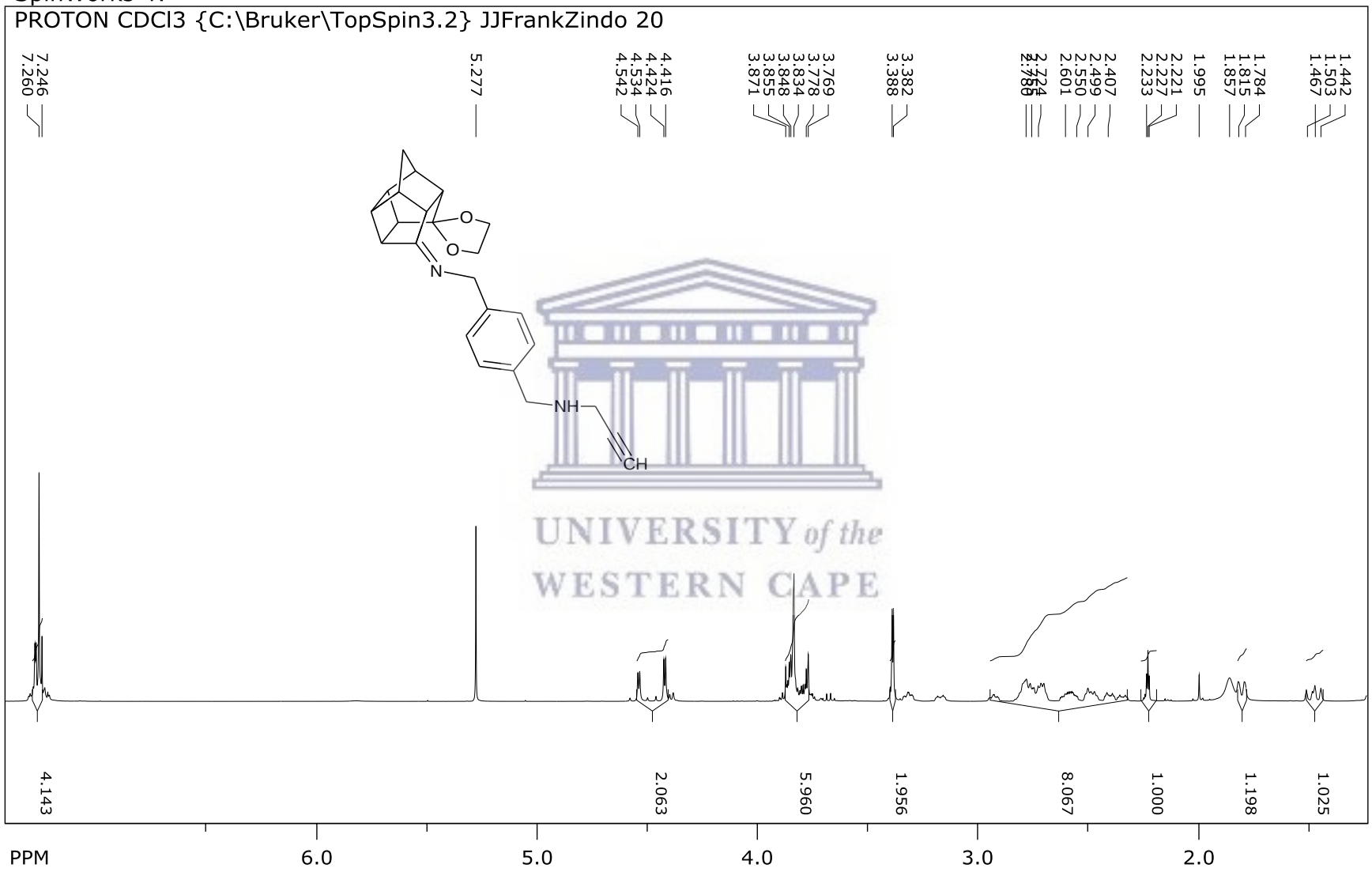

file: ...ndo - NMR\H-NMR - Select\16C\1\fid expt: <zg30>
transmitter freq.: 400.122471 MHz
time domain size: 65536 points
width: 8012.82 Hz = 20.0259 ppm = 0.122266 Hz/pt
number of scans: 16

freq. of 0 ppm: 400.120015 MHz
processed size: 65536 complex points
LB: 0.300 GF: 0.0000

Compound 6

SpinWorks 4:

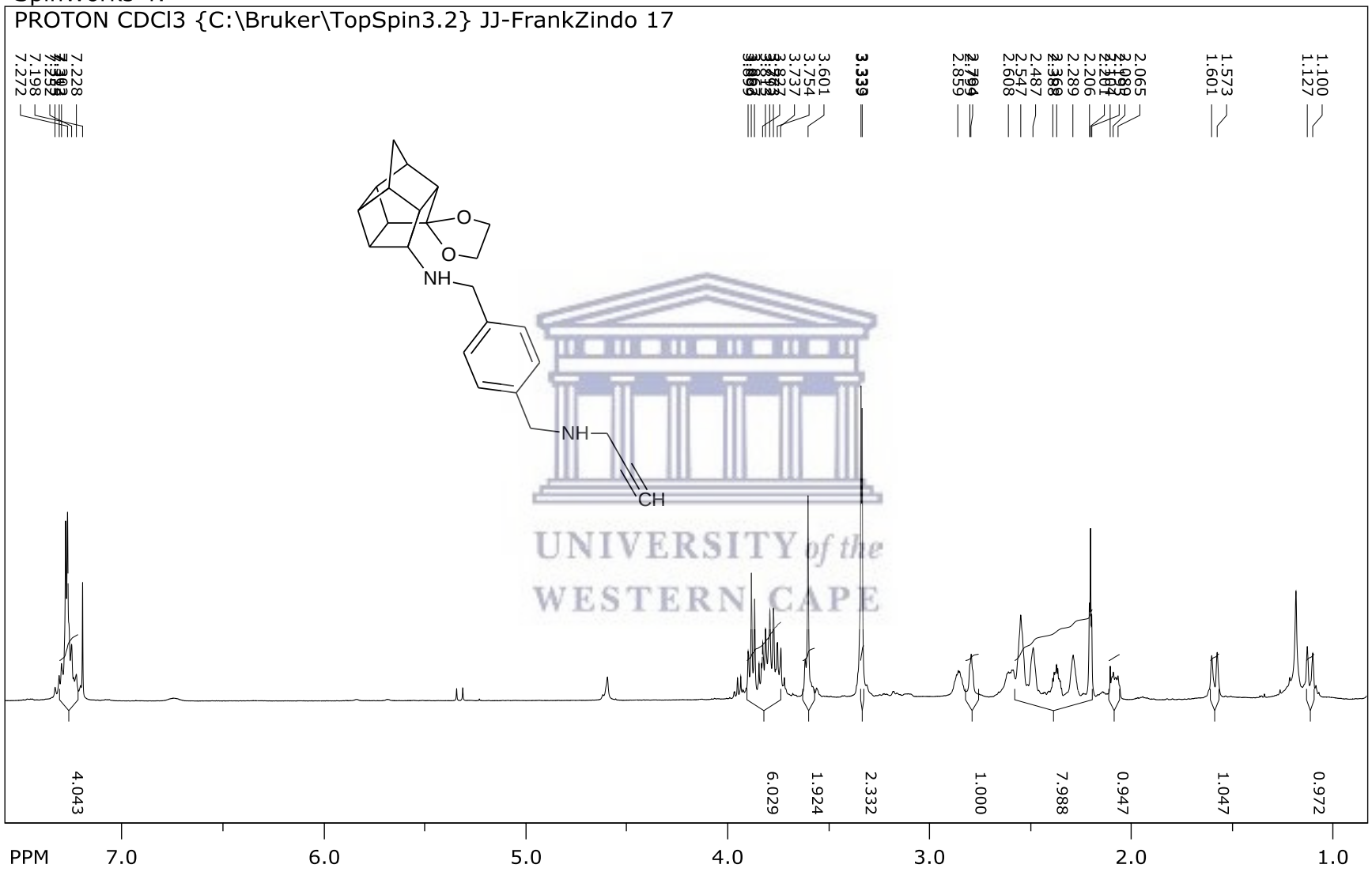

file: ... - NMR\H-NMR - Select\RKPAM2\1\fid expt: <zg30>
transmitter freq.: 400.122471 MHz
time domain size: 65536 points
width: 8012.82 Hz = 20.0259 ppm = 0.122266 Hz/pt
number of scans: 16

freq. of 0 ppm: 400.120035 MHz
processed size: 65536 complex points
LB: 0.300 GF: 0.0000

Compound 7

SpinWorks 4:

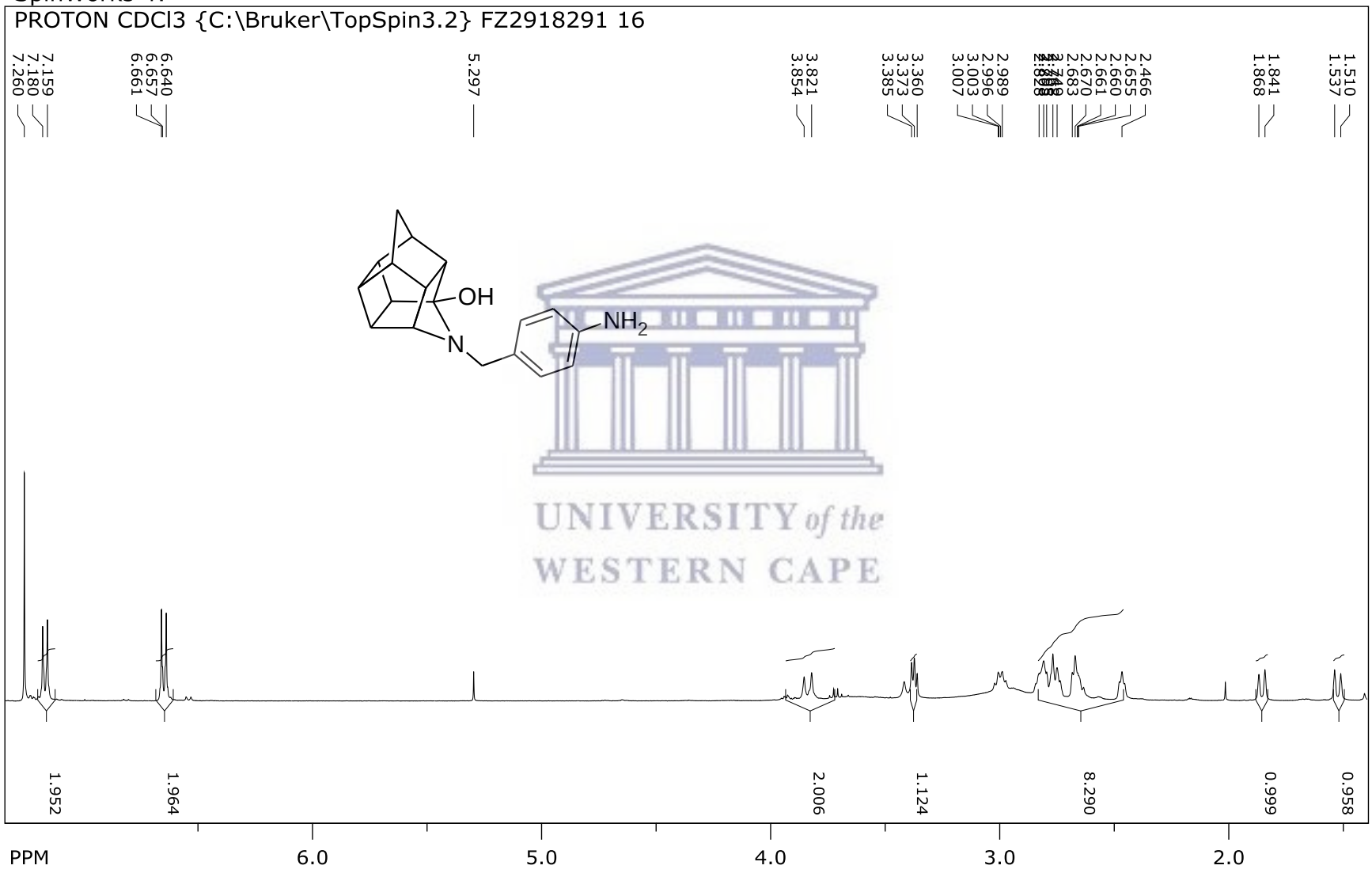

file: ...- NMR\H-NMR - Select\AZA 2.5\1\fid expt: <zg30>
transmitter freq.: 400.122471 MHz
time domain size: 65536 points
width: 8012.82 Hz = 20.0259 ppm = 0.122266 Hz/pt
number of scans: 16

freq. of 0 ppm: 400.120010 MHz
processed size: 65536 complex points
LB: 0.300 GF: 0.0000

Compound 8

SpinWorks 4:

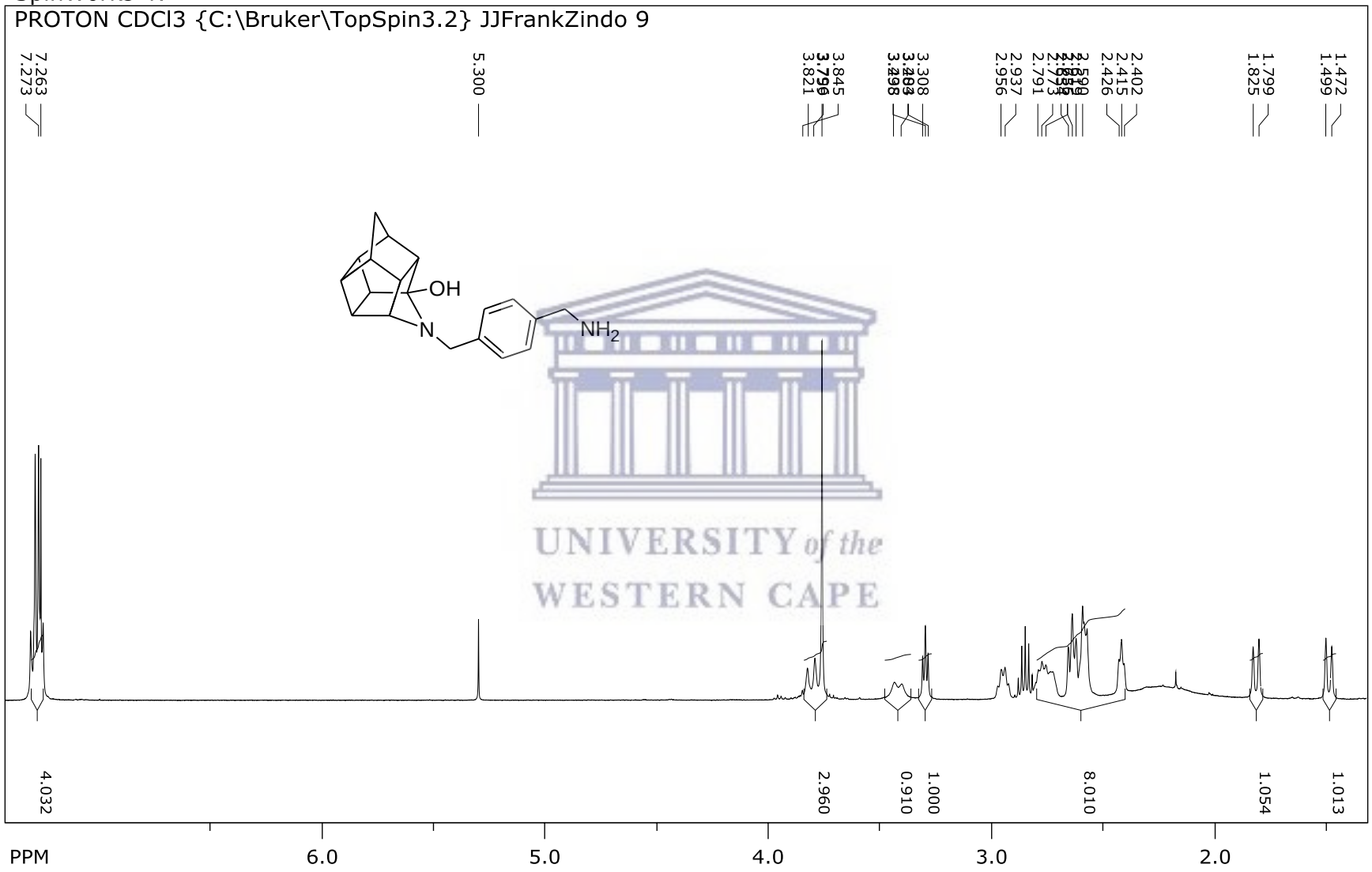

file: ...o - NMR\H-NMR - Select\3AAM1\1\fid expt: <zg30>
transmitter freq.: 400.122471 MHz
time domain size: 65536 points
width: 8012.82 Hz = 20.0259 ppm = 0.122266 Hz/pt
number of scans: 16

freq. of 0 ppm: 400.120009 MHz
processed size: 65536 complex points
LB: 0.300 GF: 0.0000

Compound 9

SpinWorks 4:

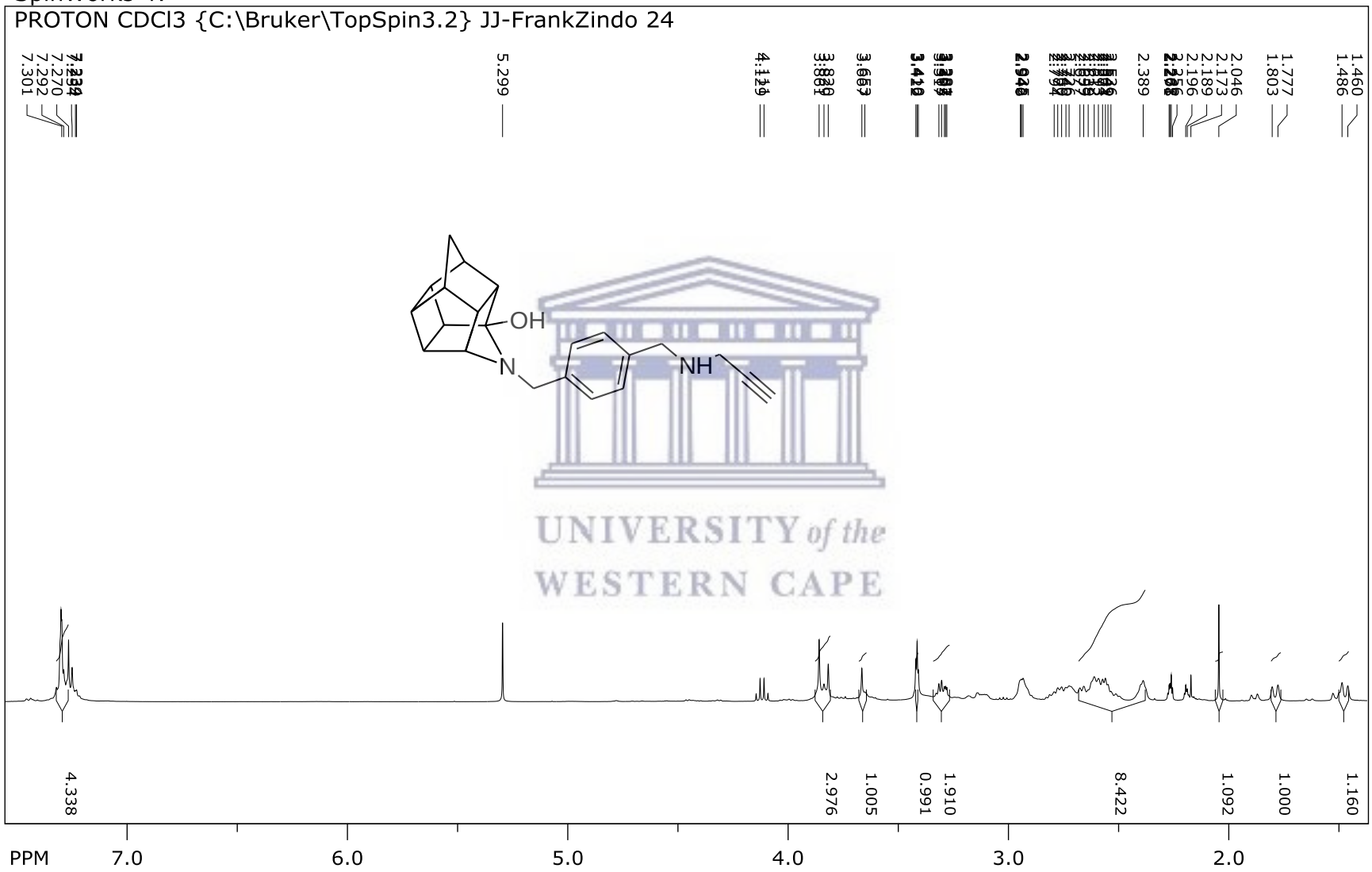

file: ...o - NMR\H-NMR - Select\4APAM\1\fid expt: <zg30>
transmitter freq.: 400.122471 MHz
time domain size: 65536 points
width: 8012.82 Hz = 20.0259 ppm = 0.122266 Hz/pt
number of scans: 16

freq. of 0 ppm: 400.120006 MHz
processed size: 65536 complex points
LB: 0.300 GF: 0.0000

Compound 10

SpinWorks 4:

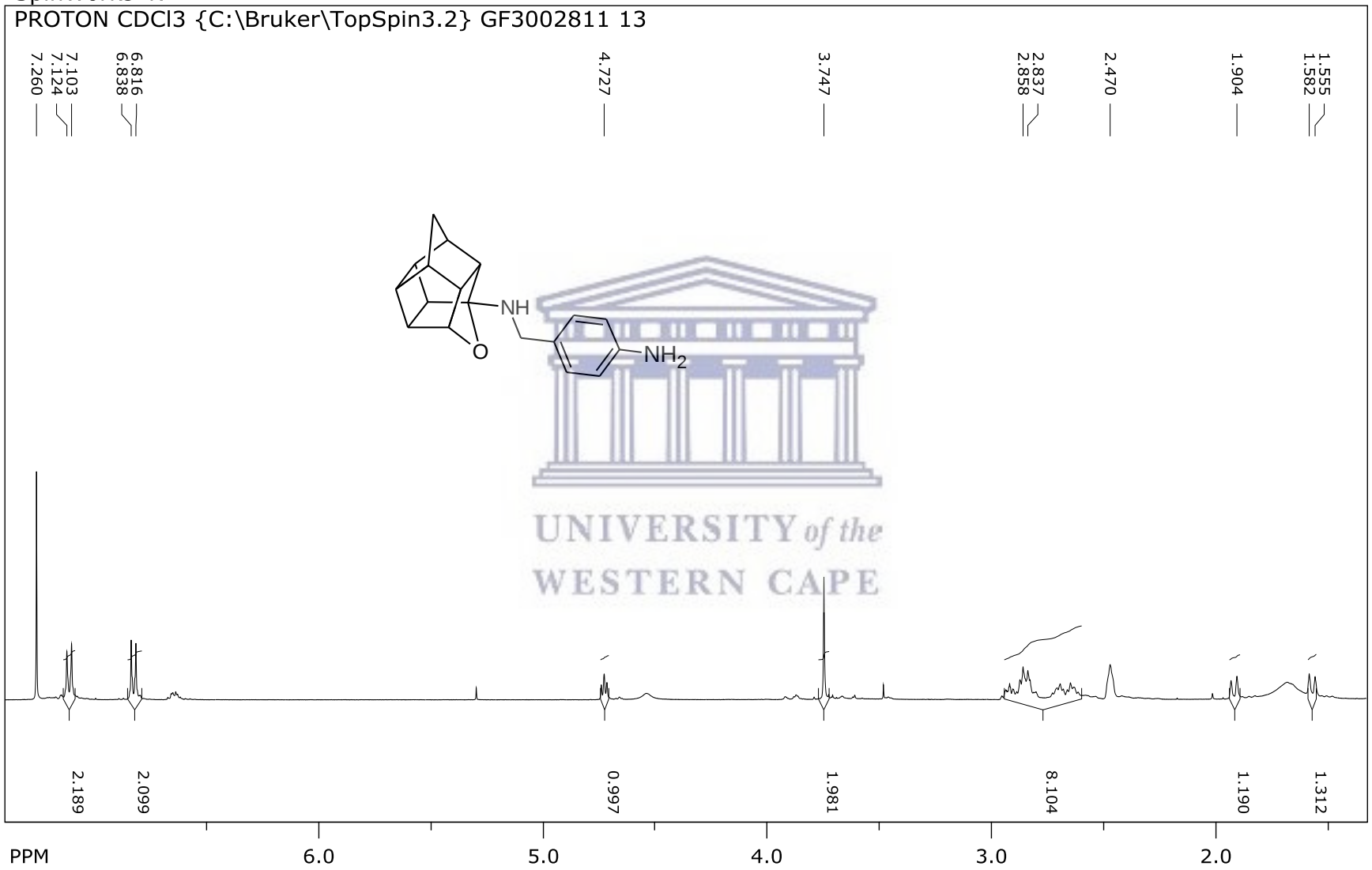

file: ... - NMR\H-NMR - Select\INT1.5\1\fid expt: <zg30>
transmitter freq.: 400.122471 MHz
time domain size: 65536 points
width: 8012.82 Hz = 20.0259 ppm = 0.122266 Hz/pt
number of scans: 16

freq. of 0 ppm: 400.120010 MHz
processed size: 65536 complex points
LB: 0.300 GF: 0.0000

Compound 11

SpinWorks 4:

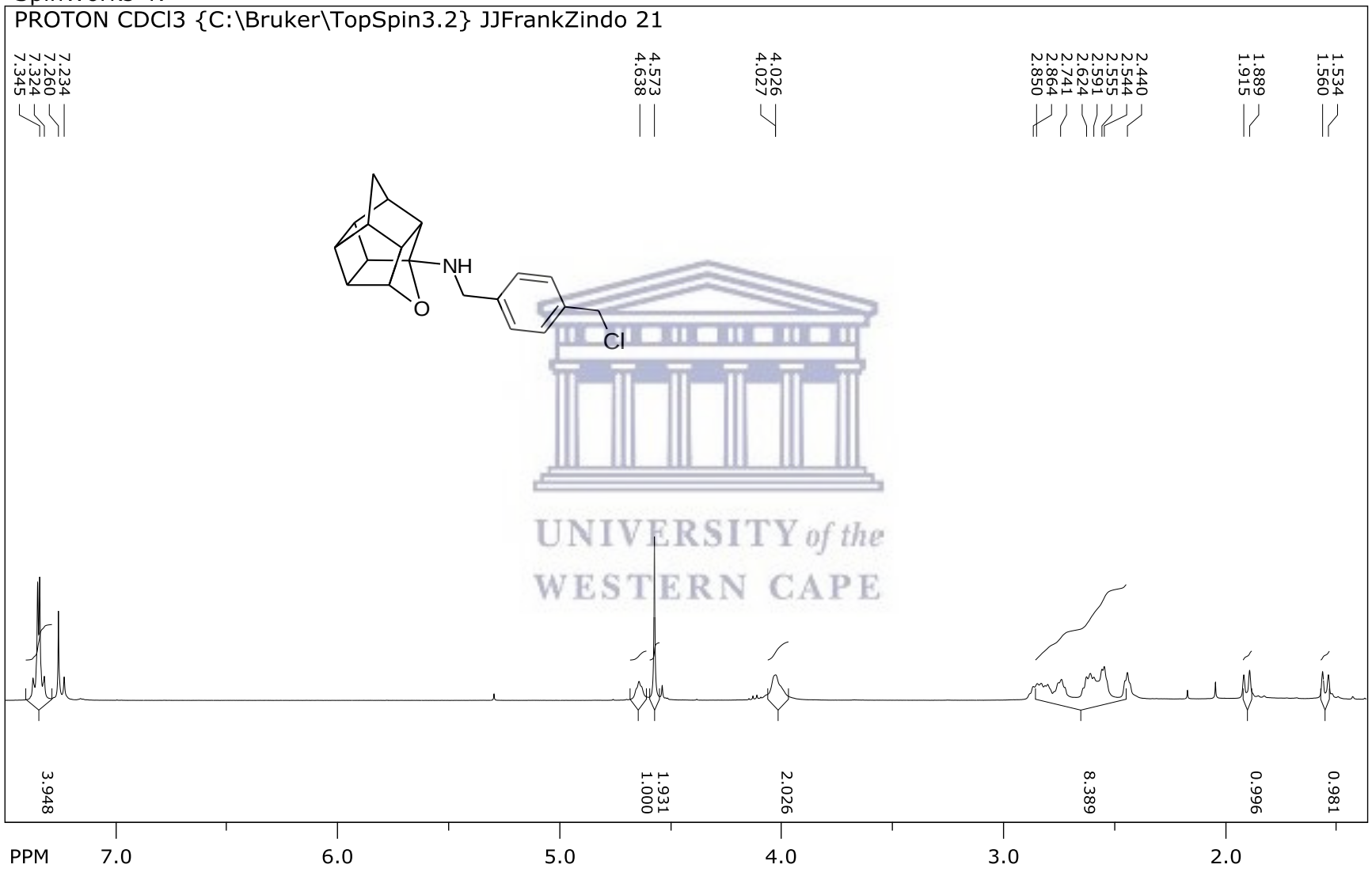

file: ...- NMR\H-NMR - Select\NGP-CL2\1\fid expt: <zg30>
transmitter freq.: 400.122471 MHz
time domain size: 65536 points
width: 8012.82 Hz = 20.0259 ppm = 0.122266 Hz/pt
number of scans: 16

freq. of 0 ppm: 400.120010 MHz
processed size: 65536 complex points
LB: 0.300 GF: 0.0000

Compound 12

SpinWorks 4:

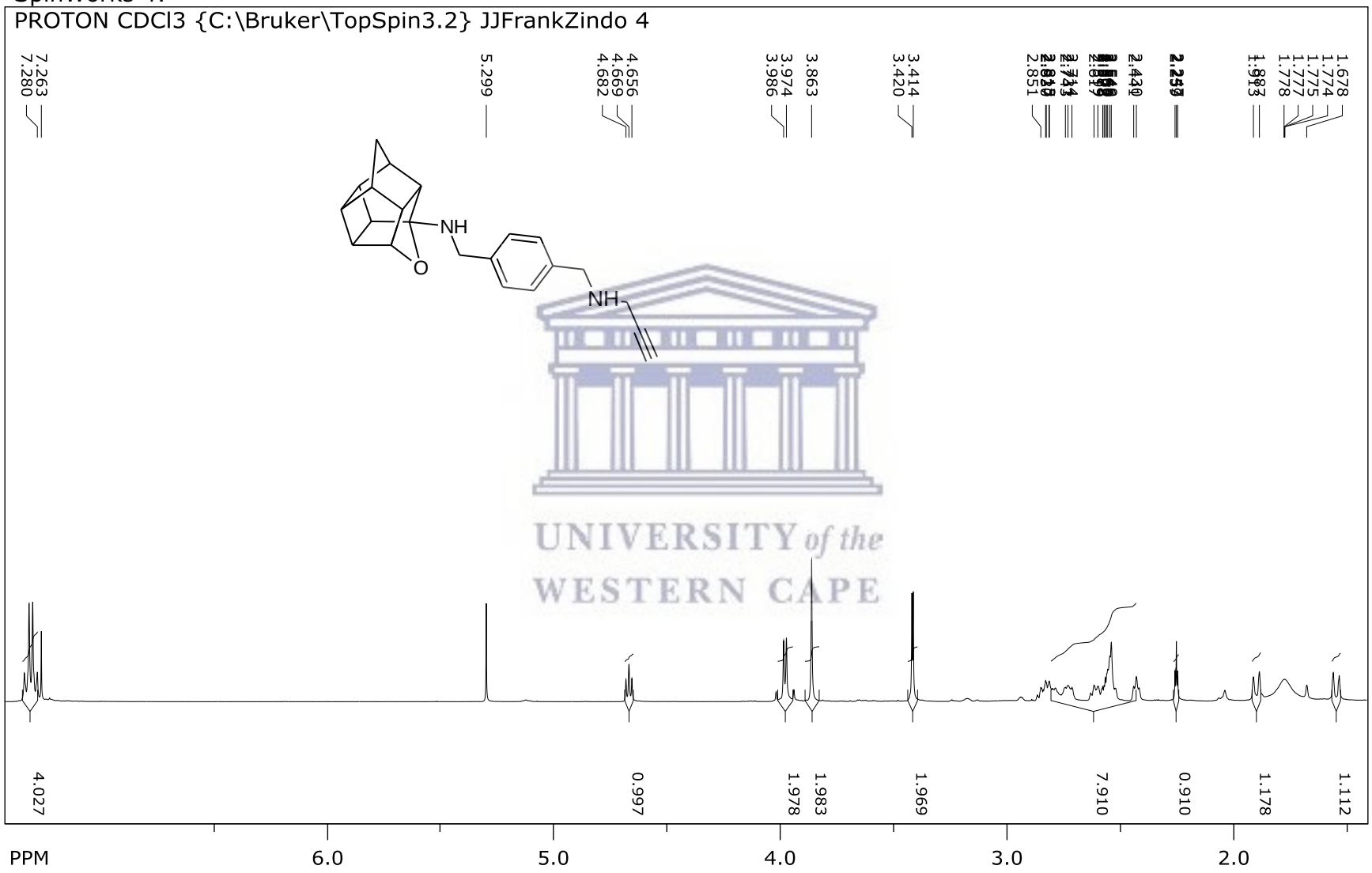

file: ...ndo - NMR\H-NMR - Select\PA4\1\fid expt: <zg30>
transmitter freq.: 400.122471 MHz
time domain size: 65536 points
width: 8012.82 Hz = 20.0259 ppm = 0.122266 Hz/pt
number of scans: 16

freq. of 0 ppm: 400.120009 MHz
processed size: 65536 complex points
LB: 0.300 GF: 0.0000

Copyrights

Review Article: Propargylamine as functional moiety in the design of multifunctional drugs for neurodegenerative disorders: MAO inhibition and beyond

Newlands Press Ltd LICENSE
TERMS AND CONDITIONS

Feb 27, 2018

This is a License Agreement between University of the Western Cape -- Frank Zindo ("You") and Newlands Press Ltd ("Newlands Press Ltd") provided by Copyright Clearance Center ("CCC"). The license consists of your order details, the terms and conditions provided by Newlands Press Ltd, and the payment terms and conditions.

All payments must be made in full to CCC. For payment instructions, please see information listed at the bottom of this form.

License Number	4296300446733
License date	Feb 06, 2018
Licensed content publisher	Newlands Press Ltd
Licensed content title	Future medicinal chemistry
Licensed content date	Jan 1, 2009
Type of Use	Thesis/Dissertation
Requestor type	Academic institution
Format	Print, Electronic
Portion	chapter/article
The requesting person/organization is:	University of the Western Cape
Title or numeric reference of the portion(s)	Propargylamine as functional moiety in the design of multifunctional drugs for neurodegenerative disorders: MAO inhibition and beyond
Title of the article or chapter the portion is from	Propargylamine as functional moiety in the design of multifunctional drugs for neurodegenerative disorders: MAO inhibition and beyond
Editor of portion(s)	N/A
Author of portion(s)	Frank T Zindo, Jacques Joubert and Sarel F Malan
Volume of serial or monograph.	7
Issue, if republishing an article from a serial	5
Page range of the portion	
Publication date of portion	2015

Rights for	Main product
Duration of use	Life of current edition
Creation of copies for the disabled	no
With minor editing privileges	yes
For distribution to	Other territories and/or countries
In the following language(s)	Original language of publication
With incidental promotional use	no
The lifetime unit quantity of new product	Up to 499
Title	Polycyclic propargylamine derivatives as multifunctional neuroprotective agents.
Instructor name	Jacques Joubert
Institution name	University of the Western Cape
Expected presentation date	Apr 2018
Billing Type	Invoice
Billing Address	University of the Western Cape Robert Sobukwe Road P.Bag X17 Cape Town, South Africa 7530 Attn: Frank T Zindo
Total (may include CCC user fee)	0.00 USD
Terms and Conditions	

TERMS AND CONDITIONS

The following terms are individual to this publisher:

None

Other Terms and Conditions:

STANDARD TERMS AND CONDITIONS

1. Description of Service; Defined Terms. This Republication License enables the User to obtain licenses for republication of one or more copyrighted works as described in detail on the relevant Order Confirmation (the "Work(s)"). Copyright Clearance Center, Inc. ("CCC") grants licenses through the Service on behalf of the rightsholder identified on the Order Confirmation (the "Rightsholder"). "Republication", as used herein, generally means the inclusion of a Work, in whole or in part, in a new work or works, also as described on the Order Confirmation. "User", as used herein, means the person or entity making such republication.

2. The terms set forth in the relevant Order Confirmation, and any terms set by the Rightsholder with respect to a particular Work, govern the terms of use of Works in connection with the Service. By using the Service, the person transacting for a republication license on behalf of the User represents and warrants that he/she/it (a) has been duly authorized by the User to accept, and hereby does accept, all such terms and conditions on behalf of User, and (b) shall inform User of all such terms and conditions. In the event such person is a "freelancer" or other third party independent of User and CCC, such party shall be deemed jointly a "User" for purposes of these terms and conditions. In any event, User shall be deemed to have accepted and agreed to all such terms and conditions if User republishes the Work in any fashion.

3. Scope of License; Limitations and Obligations.

3.1 All Works and all rights therein, including copyright rights, remain the sole and

exclusive property of the Rightsholder. The license created by the exchange of an Order Confirmation (and/or any invoice) and payment by User of the full amount set forth on that document includes only those rights expressly set forth in the Order Confirmation and in these terms and conditions, and conveys no other rights in the Work(s) to User. All rights not expressly granted are hereby reserved.

3.2 General Payment Terms: You may pay by credit card or through an account with us payable at the end of the month. If you and we agree that you may establish a standing account with CCC, then the following terms apply: Remit Payment to: Copyright Clearance Center, 29118 Network Place, Chicago, IL 60673-1291. Payments Due: Invoices are payable upon their delivery to you (or upon our notice to you that they are available to you for downloading). After 30 days, outstanding amounts will be subject to a service charge of 1-1/2% per month or, if less, the maximum rate allowed by applicable law. Unless otherwise specifically set forth in the Order Confirmation or in a separate written agreement signed by CCC, invoices are due and payable on "net 30" terms. While User may exercise the rights licensed immediately upon issuance of the Order Confirmation, the license is automatically revoked and is null and void, as if it had never been issued, if complete payment for the license is not received on a timely basis either from User directly or through a payment agent, such as a credit card company.

3.3 Unless otherwise provided in the Order Confirmation, any grant of rights to User (i) is "one-time" (including the editions and product family specified in the license), (ii) is non-exclusive and non-transferable and (iii) is subject to any and all limitations and restrictions (such as, but not limited to, limitations on duration of use or circulation) included in the Order Confirmation or invoice and/or in these terms and conditions. Upon completion of the licensed use, User shall either secure a new permission for further use of the Work(s) or immediately cease any new use of the Work(s) and shall render inaccessible (such as by deleting or by removing or severing links or other locators) any further copies of the Work (except for copies printed on paper in accordance with this license and still in User's stock at the end of such period).

3.4 In the event that the material for which a republication license is sought includes third party materials (such as photographs, illustrations, graphs, inserts and similar materials) which are identified in such material as having been used by permission, User is responsible for identifying, and seeking separate licenses (under this Service or otherwise) for, any of such third party materials; without a separate license, such third party materials may not be used.

3.5 Use of proper copyright notice for a Work is required as a condition of any license granted under the Service. Unless otherwise provided in the Order Confirmation, a proper copyright notice will read substantially as follows: "Republished with permission of [Rightsholder's name], from [Work's title, author, volume, edition number and year of copyright]; permission conveyed through Copyright Clearance Center, Inc. " Such notice must be provided in a reasonably legible font size and must be placed either immediately adjacent to the Work as used (for example, as part of a by-line or footnote but not as a separate electronic link) or in the place where substantially all other credits or notices for the new work containing the republished Work are located. Failure to include the required notice results in loss to the Rightsholder and CCC, and the User shall be liable to pay liquidated damages for each such failure equal to twice the use fee specified in the Order Confirmation, in addition to the use fee itself and any other fees and charges specified.

3.6 User may only make alterations to the Work if and as expressly set forth in the Order Confirmation. No Work may be used in any way that is defamatory, violates the rights of third parties (including such third parties' rights of copyright, privacy, publicity, or other tangible or intangible property), or is otherwise illegal, sexually explicit or obscene. In

addition, User may not conjoin a Work with any other material that may result in damage to the reputation of the Rightsholder. User agrees to inform CCC if it becomes aware of any infringement of any rights in a Work and to cooperate with any reasonable request of CCC or the Rightsholder in connection therewith.

4. Indemnity. User hereby indemnifies and agrees to defend the Rightsholder and CCC, and their respective employees and directors, against all claims, liability, damages, costs and expenses, including legal fees and expenses, arising out of any use of a Work beyond the scope of the rights granted herein, or any use of a Work which has been altered in any unauthorized way by User, including claims of defamation or infringement of rights of copyright, publicity, privacy or other tangible or intangible property.

5. Limitation of Liability. UNDER NO CIRCUMSTANCES WILL CCC OR THE RIGHTSHOLDER BE LIABLE FOR ANY DIRECT, INDIRECT, CONSEQUENTIAL OR INCIDENTAL DAMAGES (INCLUDING WITHOUT LIMITATION DAMAGES FOR LOSS OF BUSINESS PROFITS OR INFORMATION, OR FOR BUSINESS INTERRUPTION) ARISING OUT OF THE USE OR INABILITY TO USE A WORK, EVEN IF ONE OF THEM HAS BEEN ADVISED OF THE POSSIBILITY OF SUCH DAMAGES. In any event, the total liability of the Rightsholder and CCC (including their respective employees and directors) shall not exceed the total amount actually paid by User for this license. User assumes full liability for the actions and omissions of its principals, employees, agents, affiliates, successors and assigns.

6. Limited Warranties. THE WORK(S) AND RIGHT(S) ARE PROVIDED "AS IS". CCC HAS THE RIGHT TO GRANT TO USER THE RIGHTS GRANTED IN THE ORDER CONFIRMATION DOCUMENT. CCC AND THE RIGHTSHOLDER DISCLAIM ALL OTHER WARRANTIES RELATING TO THE WORK(S) AND RIGHT(S), EITHER EXPRESS OR IMPLIED, INCLUDING WITHOUT LIMITATION IMPLIED WARRANTIES OF MERCHANTABILITY OR FITNESS FOR A PARTICULAR PURPOSE. ADDITIONAL RIGHTS MAY BE REQUIRED TO USE ILLUSTRATIONS, GRAPHS, PHOTOGRAPHS, ABSTRACTS, INSERTS OR OTHER PORTIONS OF THE WORK (AS OPPOSED TO THE ENTIRE WORK) IN A MANNER CONTEMPLATED BY USER; USER UNDERSTANDS AND AGREES THAT NEITHER CCC NOR THE RIGHTSHOLDER MAY HAVE SUCH ADDITIONAL RIGHTS TO GRANT.

7. Effect of Breach. Any failure by User to pay any amount when due, or any use by User of a Work beyond the scope of the license set forth in the Order Confirmation and/or these terms and conditions, shall be a material breach of the license created by the Order Confirmation and these terms and conditions. Any breach not cured within 30 days of written notice thereof shall result in immediate termination of such license without further notice. Any unauthorized (but licensable) use of a Work that is terminated immediately upon notice thereof may be liquidated by payment of the Rightsholder's ordinary license price therefor; any unauthorized (and unlicensable) use that is not terminated immediately for any reason (including, for example, because materials containing the Work cannot reasonably be recalled) will be subject to all remedies available at law or in equity, but in no event to a payment of less than three times the Rightsholder's ordinary license price for the most closely analogous licensable use plus Rightsholder's and/or CCC's costs and expenses incurred in collecting such payment.

8. **Miscellaneous.**

8.1 User acknowledges that CCC may, from time to time, make changes or additions to the Service or to these terms and conditions, and CCC reserves the right to send notice to the User by electronic mail or otherwise for the purposes of notifying User of such changes or additions; provided that any such changes or additions shall not apply to permissions already secured and paid for.

8.2 Use of User-related information collected through the Service is governed by CCC's privacy policy, available online here:http://www.copyright.com/content/cc3/en/tools/footer/privacypolicy.html.
8.3 The licensing transaction described in the Order Confirmation is personal to User. Therefore, User may not assign or transfer to any other person (whether a natural person or an organization of any kind) the license created by the Order Confirmation and these terms and conditions or any rights granted hereunder; provided, however, that User may assign such license in its entirety on written notice to CCC in the event of a transfer of all or substantially all of User's rights in the new material which includes the Work(s) licensed under this Service.
8.4 No amendment or waiver of any terms is binding unless set forth in writing and signed by the parties. The Rightsholder and CCC hereby object to any terms contained in any writing prepared by the User or its principals, employees, agents or affiliates and purporting to govern or otherwise relate to the licensing transaction described in the Order Confirmation, which terms are in any way inconsistent with any terms set forth in the Order Confirmation and/or in these terms and conditions or CCC's standard operating procedures, whether such writing is prepared prior to, simultaneously with or subsequent to the Order Confirmation, and whether such writing appears on a copy of the Order Confirmation or in a separate instrument.
8.5 The licensing transaction described in the Order Confirmation document shall be governed by and construed under the law of the State of New York, USA, without regard to the principles thereof of conflicts of law. Any case, controversy, suit, action, or proceeding arising out of, in connection with, or related to such licensing transaction shall be brought, at CCC's sole discretion, in any federal or state court located in the County of New York, State of New York, USA, or in any federal or state court whose geographical jurisdiction covers the location of the Rightsholder set forth in the Order Confirmation. The parties expressly submit to the personal jurisdiction and venue of each such federal or state court.If you have any comments or questions about the Service or Copyright Clearance Center, please contact us at 978-750-8400 or send an e-mail to info@copyright.com.
v 1.1

Questions? customercare@copyright.com or +1-855-239-3415 (toll free in the US) or +1-978-646-2777.

Copyrights

Research Article 1: Polycyclic propargylamine and acetylene derivatives as multifunctional neuroprotective agents

UNIVERSITY of the WESTERN CAPE

FRANK TAPIWA ZINDO <2918291@myuwc.ac.za>

Rights to Published Article - ISSN: 0223-5234

PermissionsFrance <permissionsfrance@elsevier.com>
To: FRANK TAPIWA ZINDO <2918291@myuwc.ac.za>

Tue, Mar 27, 2018 at 1:30 PM

Issy-Les-Moulineaux, 27-March-2018

To the attention of Frank T Zindo

Dear Sir,

As per your request below, we hereby grant you permission to reprint the material detailed in your request at no charge **in your thesis** subject to the following conditions:

1. If any part of the material to be used (for example, Figures) has appeared in our publication with credit or acknowledgement to another source, permission must also be sought from that source. If such permissions are not obtained then that materials may not be included in your publication.

2. Any modification of the material is likely to harm the moral right of the authors and therefore should be first submitted and approved by the authors who are the sole owner of the moral right.

3. Suitable and visible acknowledgement to the source must be made, either as a footnote or in a reference list at the end of your publication, as follows:

   "Reproduced from *Authors name. Article title. Journal title year; volume number(issue number):first page-last page.* Copyright © *year [if applicable: name of learned society,* published by*]* Elsevier Masson SAS. All rights reserved."

4. Your thesis may be submitted to your institution in either print or electronic form.

5. Reproduction of this material is confined to the purpose for which permission is hereby given.

6. This permission is granted for non-exclusive world **English** rights only. For other languages please reapply separately for each one required. Permission excludes use in an electronic form other than submission. Should you have a specific electronic project in mind please reapply for permission.

7. Should your thesis be published commercially, please reapply for permission.

Yours sincerely,

Best Regards

Regina

Regina Lavanya Remigius

Senior Copyrights Coordinator, GR - Copyrights

ELSEVIER | Global Book Production

+91 44 4299 4670 office

r.remigius@elsevier.com

www.elsevier.com

From: FRANK TAPIWA ZINDO [mailto:2918291@myuwc.ac.za]
Sent: Tuesday, February 27, 2018 11:35 AM
To: PermissionsFrance <permissionsfrance@elsevier.com>
Subject: Rights to Published Article - ISSN: 0223-5234

[Quoted text hidden]

Copyrights

Research Article 2: Design, synthesis and evaluation of pentacycloundecane and hexacycloundecane propargylamine derivatives as multifunctional neuroprotective agents.

This article was accepted for publication in the European Journal Of Medicinal Chemistry on the 9th of November 2018 and is yet to be published online. The rights to this article could therefore not be obtained at the time of submission of this thesis. Rights will be obtained before the final submission to the university library.

Copyrights

Research Article 3: Adamantane amine derivatives as dual acting NMDA receptor and voltage-gated calcium channel inhibitors for neuroprotection.

Adamantane amine derivatives as dual acting NMDA receptor and voltage-gated calcium channel inhibitors for neuroprotection

Y. E. Kadernani, F. T. Zindo, E. Kapp, S. F. Malan and J. Joubert, *Med. Chem. Commun.*, 2014, **5**, 1678
DOI: 10.1039/C4MD00244J

- For reproduction of material from NJC:
  [Original citation] - Reproduced by permission of The Royal Society of Chemistry (RSC) on behalf of the Centre National de la Recherche Scientifique (CNRS) and the RSC
- For reproduction of material from PCCP:
  [Original citation] - Reproduced by permission of the PCCP Owner Societies
- For reproduction of material from PPS:
  [Original citation] - Reproduced by permission of The Royal Society of Chemistry (RSC) on behalf of the European Society for Photobiology, the European Photochemistry Association, and RSC
- For reproduction of material from all other RSC journals:
  [Original citation] - Reproduced by permission of The Royal Society of Chemistry

If you are the author of this article you still need to obtain permission to reproduce the whole article in a third party publication with the exception of reproduction of the whole article in a thesis or dissertation.

Information about reproducing material from RSC articles with different licences is available on our Permission Requests page.

Copyrights

Research Article 4: Design, synthesis and evaluation of indole derivatives as multifunctional agents against Alzheimer's disease.

Design, synthesis and evaluation of indole derivatives as multifunctional agents against Alzheimer's disease

I. Denya, S. F. Malan, A. B. Enogieru, S. I. Omoruyi, O. E. Ekpo, E. Kapp, F. T. Zindo and J. Joubert, *Med. Chem. Commun.*, 2018, **9**, 357
DOI: 10.1039/C7MD00569E

- For reproduction of material from NJC:
  [Original citation] - Reproduced by permission of The Royal Society of Chemistry (RSC) on behalf of the Centre National de la Recherche Scientifique (CNRS) and the RSC
- For reproduction of material from PCCP:
  [Original citation] - Reproduced by permission of the PCCP Owner Societies
- For reproduction of material from PPS:
  [Original citation] - Reproduced by permission of The Royal Society of Chemistry (RSC) on behalf of the European Society for Photobiology, the European Photochemistry Association, and RSC
- For reproduction of material from all other RSC journals:
  [Original citation] - Reproduced by permission of The Royal Society of Chemistry

If you are the author of this article you still need to obtain permission to reproduce the whole article in a third party publication with the exception of reproduction of the whole article in a thesis or dissertation.

Information about reproducing material from RSC articles with different licences is available on our Permission Requests page.

Copyrights

Research Article 5: Versatility of 7-Substituted Coumarin Molecules as Antimycobacterial Agents, Neuronal Enzyme Inhibitors and Neuroprotective Agents.

Versatility of 7-Substituted Coumarin Molecules as Antimycobacterial Agents, Neuronal Enzyme Inhibitors and Neuroprotective Agents.

Erika Kapp, Hanri Visser, Samantha L. Sampson, Sarel F. Malan, Elizabeth M. Streicher, Germaine B. Foka, Digby F. Warner, Sylvester I. Omoruyi, Adaze B. Enogieru, Okobi E. Ekpo, Frank T. Zindo and Jacques Joubert, *Molecules.*, 2017, **22**, 1644
DOI: 10.3990/ molecules22101644

Reproduced material should be attributed as follows:

- For reproduction of material from NJC:
  [Original citation] - Reproduced by permission of The Royal Society of Chemistry (RSC) on behalf of the Centre National de la Recherche Scientifique (CNRS) and the RSC
- For reproduction of material from PCCP:
  [Original citation] - Reproduced by permission of the PCCP Owner Societies
- For reproduction of material from PPS:
  [Original citation] - Reproduced by permission of The Royal Society of Chemistry (RSC) on behalf of the European Society for Photobiology, the European Photochemistry Association, and RSC
- For reproduction of material from all other RSC journals:
  [Original citation] - Reproduced by permission of The Royal Society of Chemistry

If you are the author of this article you still need to obtain permission to reproduce the whole article in a third party publication with the exception of reproduction of the whole article in a thesis or dissertation.

Information about reproducing material from RSC articles with different licences is available on our Permission Requests page.